Fibrocytes, γ-Herpesvirus and Periostin Augment Bleomycin-induced Lung Fibrosis

By

Shanna Leonie Ashley

A dissertation submitted in partial fulfillment
of the requirements for the degree of
Doctor of Philosophy
(Immunology)
in the University of Michigan
2016

Doctoral Committee:

Professor Bethany B. Moore, Chair
Professor Colin D. Duckett
Professor Marc B. Hershenson
Assistant Professor Kevin K. Kim
Associate Professor Christiane E. Wobus

To my family and friends

Acknowledgments

It has been a great pleasure to be offered the opportunity to study in the Department of internal medicine at the University of Michigan. I want to take this opportunity to acknowledge the many people who have contributed to this work and helped to build me as a scientist. To my mentor, Bethany Moore; thank you for believing in me and granting me the opportunity to work in your laboratory. Thank you for your guidance and patience with me. Thank you for the countless hours of helping me with my papers, working on presentations, just to talk about life or to offer comfort and support to all the many catastrophes of life that I experienced during my tenure as a graduate student. I feel truly blessed to have chosen you as my mentor and I look forward to maintaining this relationship for years to come.

I would also like to thank all of my committee members. Each of them has been very supportive; I thank you for all your advice and suggestions to help push my experiments forward.

Additionally, I would like to thank the members of the Moore laboratory, both past and present for making the lab an enjoyable place to work. A special thank you to Carol, for all her help with my numerous intratracheal and tail vein injections for my bone marrow transplantation experiments. Thank you for always making me laugh. Also, I would like to thank members of the Pulmonary Division both past and present for always having their office doors open to answer my many questions and to offer different reagents. Thank you to the members of the Seagal lab, especially Amanda and Patrick. I am very grateful for the valuable suggestions you gave me and for your help with flow cytometry. Special thanks to Amanda Huber for all her help

with editing my manuscripts as well as technical support. Special thanks to our student coordinator Zarinah Aquil, I would not have been able to survive in the Immunology program had it not been for all your hard work. Thank you for caring so much about us as students and always keeping me positive and smiling. I really appreciate all that you do for the Immunology program.

To my friends and everyone who supported me throughout my time here, I am very fortunate to have had the opportunity to discuss science with such elite scientists. Thank you for making this journey so phenomenal, I am very grateful for the networking and the discussions I had with all of you. Special thanks to Swanne Gordon and Kerry-Ann Rodenberg for always being there to listen, support and motivate me throughout this journey. I love you both!

To the beneficence that enabled my own research to be reported in this dissertation, I am grateful to the Immunology Program staff for the support on the Immunology Training grant and to the United Negro College Fund/MERCK for my graduate dissertation fellowship award.

Lastly, I have been blessed to have an extremely supportive family who has played an essential role throughout my life. Thank you for taking this journey with me and keeping me motivated even when everything seemed so dismal. The early morning inspirational quotes, the late night conversations to comfort me as I walked home from lab has kept me going through the years even when distance and time separated us. To mom and dad, thank you for giving me a good foundation with which to meet life. Thank you for teaching me how to work hard, how to be persistent and independent. I am very grateful for your continued support and motivation. You guys are awesome and I love you!

Table of Contents

List of Figures

List of Tables

List of Abbreviations

AECs	Type II Alveolar Epithelial Cells
AMs	Alveolar Macrophages
AP-1	Activation Protein 1
αSMA	Alpha Smooth Muscle Actin
AUC	Area Under Curve
BALF	Bronchoalveolar Lavage Fluid
BM	Bone Marrow
BMP-1	Bone Morphogenic Protein 1
c-IAP-2	Cellular inhibitor of Apoptosis 2
Cath-S	Cathepsin S
CCL12	Monocyte Chemoattractant protein 5
CCL2	Monocyte Chemoattractant protein 1
CCR2	Chemokine (C-C) Motif Receptor 2
CD45	Common Leukocyte Antigen
cIAP-1	Cellular inhibitor of Apoptosis 1
CMV	Cytomegalovirus
Col I	Collagen I
CTGF	Connective Tissue Growth Factor
CXCR4	Chemokine (C-X-C) Motif receptor 4
DLCO	Diffusion Capacity for Carbon Monoxide
DTR	Diptheria Toxin Receptor
EBV	Epstein-Barr Virus
ECM	Extracellular Matrix
EMT	Epithelial to Mesenchymal Transition
ET-1	Endothelin- 1
FCN2	Ficolin 2
FITC	Fluorescein Isothiocyanate
FVC	Force Vital Capacity
γHV-68	Murine gammaherpes Virus-68
H1N1	Influenza A
HCV	Hepatitis C Virus
HHV	Human Herpes Virus
HRCT	High-resolution Computed Tomography
HSV-1	Herpes Simplex Virus 1
i.p	Intraperitoneal

i.t	Intratracheal
i.v	Intravenous
ICOS	Inducible T cell costimulator
IFNγ	Interferon Gamma
IL-12	Interleukin 12
IL-13	Interleukin 13
IL-1β	Interleukin 1 beta
IL-6	Interleukin 6
ILD	Interstitial Lung Disease
IPF	Idiopathic Pulmonary Fibrosis
LAP	Latent associated Peptide
LGMN	Legumain
LOX	Lysyl Oxidase
LTBP	Latent TGFB Binding Protein
MMP	Matrix Mettalloproteinases
MSC	Mesenchymal Stem Cells
NAC	N-Acetylcysteine
NFKB	Nuclear Factor Kappa B
OPN	Osteopontin
PDGF	Platelet Derived Growth Factor
PGE2	Prostaglandin E2
RGD	Arginine-Glycine-Aspartic
ROC	Receiver Operating Score
sc	Subcutaneous
SMAC	Second mitochondria-derived activator of caspases
SOMAmer	Slow Off-rate Modified Aptamer
SPARC	Secreted Protein Acid Rich in Cysteine
SPC	Surfactant Protein C
TGFβ	Transforming Growth Factor Beta
Th1	T helper cell 1
Th2	T helper cell 2
TIMP	Tissue inhibitor metalloproteinase proteins
TLR	Toll-like Receptor
TNFα	Tumor Necrosis Factor alpha
TRY3	Trypsin 3
TSP-1	Thrombospndin-1
UIP	Usual Interstitial Pneumonia
VEGFsR2	Soluble Vascular Endothelial Growth Factor receptor 2
WT	Wild Type
XIAP	X-linked inhibitor of Apoptosis

Abstract

This dissertation is comprised of 4 distinct projects, all of which related to the pathogenesis of lung fibrosis in mice or humans. We tested whether *Pseudomonas aeruginosa*, or Influenza A, (H1N1) could augment bleomycin-induced fibrosis, yet found neither of these agents had the exacerbating effects of murine gamma-herpesvirus (γHV-68). γHV-68 augmented fibrosis by uniquely causing epithelial cell apoptosis.

We also explored the role the matricellular protein, periostin, played in augmenting lung fibrosis when produced in circulating fibrocytes. We demonstrated fibrocytes act via paracrine actions rather than differentiation to lung fibroblasts. Wild-type (WT) fibroblasts were treated with conditioned medium from fibrocytes from bleomycin-treated WT or periostin$^{-/-}$ mice. We saw less α-smooth muscle actin expression in cells treated with medium from periostin$^{-/-}$ fibrocytes. *In vitro* analysis demonstrated co-regulation of mesenchymal activation by TGFβ and periostin and indicated beta 1 integrin as a potential receptor for periostin on fibrocytes. Furthermore, periostin influenced production of connective tissue growth factor from fibrocytes.

Treatment of WT lung mesenchymal cells with periostin led to increased X-linked inhibitor of apoptosis (XIAP) protein expression. TGF-β1 and bleomycin treatments increased XIAP and cellular IAP (cIAP) 1 and 2 in murine lungs and mesenchymal cells. Functional blockade of XIAP and the cIAPs with AT-406, an orally bioavailable, inhibitor of apoptosis (IAP) antagonist abrogated bleomycin-induced lung fibrosis when given both prophylactically and therapeutically. Surprisingly, we compared fibrosis in XIAP deficient mice (XIAP$^{-/y}$) and

littermate controls but found no difference. XIAP$^{-/y}$ mesenchymal cells had increased resistance to Fas-mediated apoptosis, but AT-406 treatment restored sensitivity to Fas-mediated apoptosis in XIAP$^{-/y}$ mesenchymal cells *in vitro* and increased apoptosis of mesenchymal cells *in vivo* indicating that the increased apoptosis resistance in XIAP$^{-/y}$ mesenchymal cells was the result of increased cIAP expression. These results highlight the potential usefulness of AT-406 as a treatment for lung fibrosis *in vivo*.

Biomarkers in human idiopathic pulmonary fibrosis (IPF) would be clinically valuable. We used an unbiased proteomic approach to identify a six-analyte index, scaled 0 to 11, based on markers of immune function, proteolysis and angiogenesis [high levels of ficolin-2 (FCN2), cathepsin-S (Cath-S), legumain (LGMN) and soluble vascular endothelial growth factor receptor 2 (VEGFsR2), but low levels of inducible T cell costimulator (ICOS) or trypsin 3 (TRY3)] that predicted better progression-free survival over 80 weeks in IPF when measured using aptamers in plasma near time of diagnosis. This index could be useful for clinical decision making in IPF.

Chapter 1: Background and Introduction

The work reported in this dissertation covered four distinct projects which all related to the pathogenesis of lung fibrosis. In particular, this work explored bacterial and viral infections for their ability to exacerbate murine models of lung fibrosis, the ability of the matricellular protein, periostin, to influence fibrosis, particularly when secreted from circulating fibrocytes, and determined that therapeutic targeting of inhibitor of apoptosis proteins can have benefit in the murine model of bleomycin-induced fibrosis. Finally, biomarkers in patients with IPF were studied in an attempt to define pathological pathways for further exploration. The following sections briefly outline the background material related to all of these projects, and highlight much of what is known and not known about the pathogenesis of lung fibrosis**.**

General Background on Pulmonary Fibrosis

Idiopathic Pulmonary Fibrosis (IPF): Epidemiology, Diagnosis, Pathogenesis and Treatment

IPF is a chronic and progressive lung disorder characterized by aberrant deposition of extracellular matrix (ECM) leading to extensive lung remodeling (1). IPF accounts for about 20% of all cases of interstitial lung disease (ILD) and is the most frequent and severe disease among the idiopathic interstitial pneumonias. It has no known cause and currently has no cure but is characterized by inflammation and fibrosis (2).

Epidemiology

IPF has a poor prognosis with a 20% 5 year survival rate (3). The available registry data suggests IPF accounts for 17-37% of all ILD diagnoses (4, 5). Understanding IPF epidemiology is hindered by the diverse definition of IPF including cases diagnosed before the 2000 consensus statement on IPF(6). Past studies have used both diagnostic and death registries as well as surveys of clinicians with varying degree of specialties and the results are not easily comparable.

Research thus far shows that prevalence and incidence of IPF is increasing worldwide, and is now similar to other conditions such as stomach, liver, testicular, and cervical cancer (7). For example, a study collecting data from US Medicare beneficiaries 65 years or older between 2001 and 2011 showed the overall range and incidence of IPF to be between 200 and 500 cases per 100,000 in the population, with incidence remaining stable at 93.7 cases per 100,000/year but the prevalence appeared to be on the rise (8). In the United Kingdom, a study retrieving cases from a longitudinal primary care database first reported incidence of the disease as 4.6 per 100,000/year between 1993 and 2003 (9). However, a higher incidence of 7.4 per 100,000/year was reported in a follow-up study using data between 2000 and 2009 (10). There have also been some epidemiologic studies in Asian communities. A Japanese study reported prevalence and incidence of IPF to be 10.0 and 2.23 per 100,000/year respectively (11). Most of the data reported was done predominantly in males and the increased frequency with increasing age was also confirmed in these studies.

Overall, the data summarized here suggest an increasing prevalence and stable or increasing incidence of IPF in western countries. Further analysis of the data analyzing sex and age showed higher prevalence and incidence rates among men, increasing with age and shorter survival time after diagnosis (8).

Diagnosis

IPF mainly occurs in adults 60 years or older and is more prevalent in men (12). The predominant symptom early in the disease is shortness of breath during activity; however, during advanced disease this also occurs at rest. The prognosis of IPF is poor, with median survival rate of 3-5 years from the time of diagnosis (13). The diagnosis of IPF requires the presence of a typical radiologic and pathologic pattern called usual interstitial pneumonia (UIP) (12). Radiographically, UIP is characterized by subplueral, basal-predominant, reticular abnormalities and the histology shows patchy involvement of the lung parenchyma showing fibrosis and honeycombing in a predominantly subplueral/paraseptal distribution as well as the presence of fibroblastic foci (12).

In the absence of a definite UIP pattern on high-resolution computed tomography (HRCT), **(Figure 1)** and after exclusion of systemic disease causing fibrosis, a diagnosis of IPF is possible with a surgical lung biospsy. Bronchoalveolar lavage can also be a useful tool to exclude other fibrotic lung diseases presenting with UIP pattern, such a hypersensitivity pneumonitis (14). A major challenge in achieving an accurate diagnosis of IPF involves cases where a surgical lung biopsy is needed, because the risk sometimes outweighs the benefits, especially when the disease is more advanced or in older persons.

In recent years, a new technique using flexible cryoprobes has been developed to use in bronchoscopic lung biopsy. In patients with suspected diffuse parenchymal lung disease, bronchoscopy cryobiopsy is a minimally invasive approach to obtain lung tissue with high diagnostic yield (15, 16). It has been demonstrated that the accuracy of the diagnosis of IPF increases with multidisciplinary discussion among pulmonologists, radiologists and pathologists experienced in the diagnosis of ILD (12). Undoubtedly, the definition of radiological UIP as

reported in the current guidelines is not without flaws but as new and more targeted therapies are being developed, tools for stratification of patients are necessary to be able to personalize treatments to those patients who could benefit the most as well as help with better diagnosis.

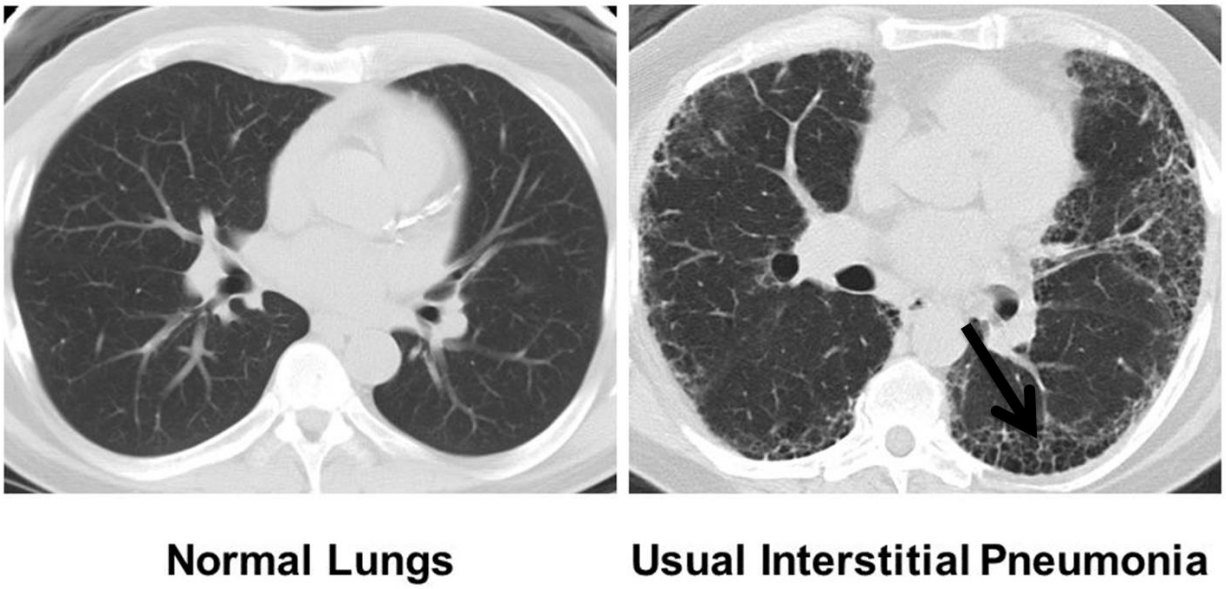

Figure 1: High Resolution Axial CT images of Normal and IPF lungs
Arrow indicates UIP predominant basal abnormalities with sub-pleural honeycombing **(adapted from www.PILOTforIPF.org)**

Pathogenesis and Treatment

IPF is a fatal lung disease. The natural history is variable and unpredictable. Most patients with IPF demonstrate a gradual worsening of lung function over several years; however, some patients remain relatively stable or decline rapidly. Patients may also experience episodes of acute respiratory worsening despite previous stability (17, 18) **(Figure 2).** The paradigm about disease pathogenesis has shifted from the idea that IPF is a result of chronic inflammation to a paradigm of disordered fibroblast proliferation and alveolar epithelial cell dysfunction (19). The inflammatory response in IPF is thought to closely resemble a Th2-type immune response. There

are eosinophils, mast cells and increased amounts of the Th2 cytokines, interleukin 4 and interleukin-13 (20-24).

In murine models of lung disease, animals with a Th2 response were more prone to pulmonary fibrosis following lung injury than those with a predominantly Th1 response (22, 25, 26). However, the current model regarding the pathogenesis of IPF implies aberrant fibrosis as a consequence of recurrent injury to alveolar epithelial cells in a susceptible host (27, 28). The excessive deposition of ECM with irreversible lung remodeling and honeycombing is likely to be the result of many processes.

Gene polymorphisms and transcriptional changes are linked to the inability of epithelial cells to respond appropriately to repetitive insults such as infections, chronic aspiration, tobacco, or mechanical stress (29). Abnormal telomere shortening, as well as epigenetic mechanisms involving DNA methylation, histone tail modification, and dysregulation of microRNA expression take place in aging lungs leading to loss of epithelial integrity and epithelial senescence (27). In an attempt to restore functional integrity, the injured Type II alveolar epithelial cells (AECs) aberrantly release cytokines and growth factors, matrix metalloproteinases (MMPs), matricellular proteins and pro-coagulant mediators, which promote the recruitment and activation of apoptosis-resistant fibroblasts, the key players in fibrotic tissue remodeling (27, 30).

There is no proven pharmacologic cure for IPF. The results of the PANTHER-IPF trial, a randomized, three-arm trial of prednisone, azathioprine, and N-acetylcysteine (NAC) in combination, NAC alone or placebo, showed no effect of NAC monotherapy on the rate of change in forced vital capacity (FVC) in patients with IPF over a 60-week period (31). Sadly, the triple arm therapy actually showed worse outcomes for patients and the triple-arm therapy

was stopped early(32). The efficacy of two approved anti-fibrotic therapies, pirfenidone (Esbriet) and nintedanib (OFEV), in slowing progression of IPF was confirmed by the Phase III ASCEND trial (33) and the twin Phase III INPULSIS-1 and -2 trials (34), respectively. Based on the results from these trials, in patients with IPF and mild or moderate impairment in FVC, both pirfenidone and nintedanib improved FVC by approximately 50% in 1 year, with acceptable safety profiles. This led to the approval of both medications for treatment for IPF in the United States in 2014 and to approval of nintedanib in Europe at the beginning of 2015.

The recently updated ATS/ERS/JRS/ALAT clinical practice guideline gives conditional recommendations for use of nintedanib and pirfenidone in the majority of patients with IPF (35). However, neither of these treatments can actually halt IPF progression, and to do that, we need a better understanding of the disease pathogenesis. The following sections will describe some of the different cell types, cytokines and chemokines that contribute to the pathogenesis and progression of the disease.

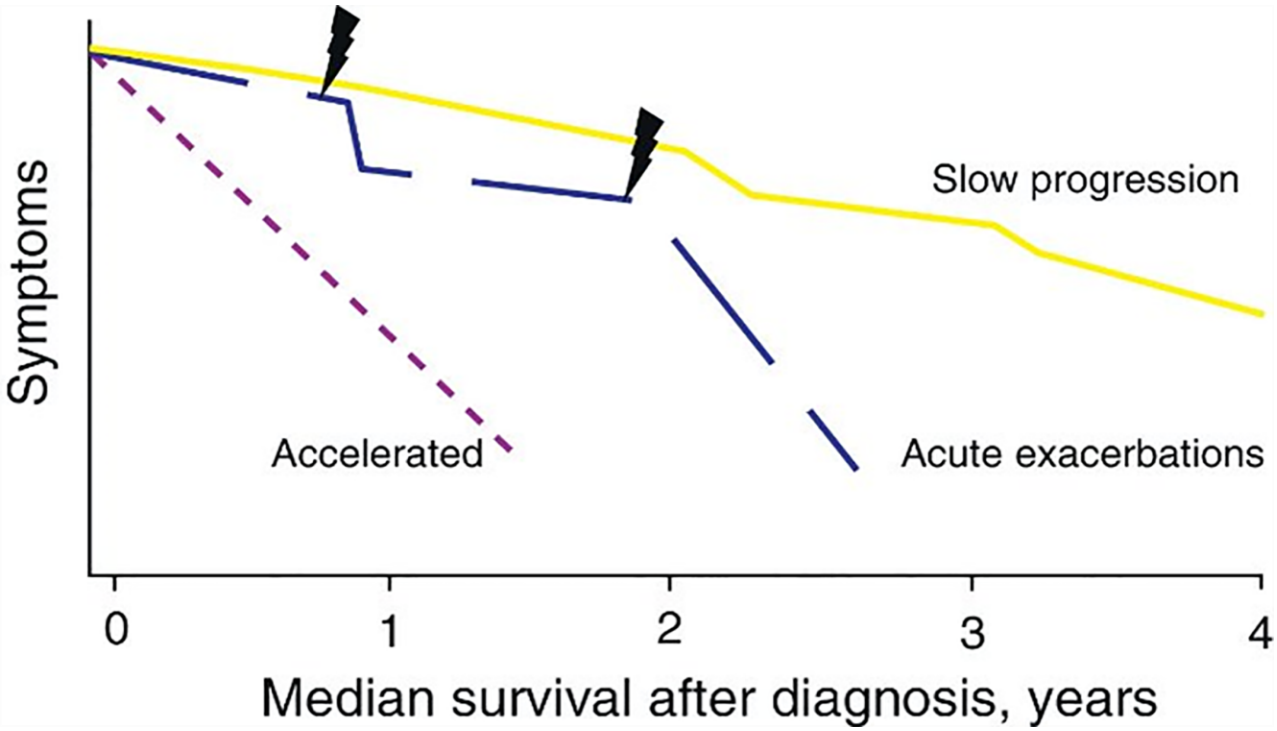

Figure 2: The natural history of IPF. (Adapted from (36)).
The disease is very rapid is some patients (Accelerated), some patients show relative stability with episodes of acute worsening (acute exacerbations) and most patients present with a slow progression that eventually results in chronic respiratory failure. Patients who develop infections generally have a disease course that mimics acute exacerbations of unknown cause.

Immune Responses in the Elderly

Changes in the immune response during aging include predisposition for increased production of proinflammatory mediators by macrophages (37). Preclinical studies in mice have shown that aged animals have an exaggerated lung inflammatory response to inhaled particles and ozone compared to young mice (38). Bronchoalveolar lavage fluid (BALF) from young and old healthy patients showed increased numbers of neutrophils in the lungs of older individuals suggesting that low-grade inflammation exists in the airspaces of normal, healthy older adults (39, 40). Shrinking T cell repertoire is a well-recognized phenomenon in humans and animals (39). Normal aging is associated with a shift in T lymphocytes from a predominantly Th1

phenotype to a Th2 phenotype that is evident in sickly older individuals. The well recognized increased susceptibility to respiratory infection and decreased efficacy of vaccination in older people are consequences of the aging immune system (41). Th2 cytokines promote expression of profibrotic factors and Th2-biased animals are susceptible to lung injury and fibrosis (42). Humans with chronic fibrotic lung disease also demonstrate a Th2-biased phenotype (43, 44).

Aging and Lung Fibrosis

IPF is an age-related disease. The incidence and prevalence of IPF increases almost exponentially with each decade of life with the majority of patients older than 60 years with a mean age of 66 years at the time of diagnosis (45). Aging is characterized by progressive loss of functional integrity leading to increased susceptibility to diseases and death. Recently nine pivotal hallmarks of aging were described; genomic instability, telomere shortening, epigenetic alterations, loss of proteastasis, mitochondrial dysfunction, cellular senescence, stem cell exhaustion and altered intercellular communication (46). How these pathways contribute to the development of IPF is still unclear. The aging process is normally accompanied by accumulation of nuclear and mitochondrial DNA damage (47, 48). There is strong evidence supporting microsatellite DNA instability and loss of heterozygosity in IPF (49). Similarly, abnormal shortening of telomeres, which are highly susceptible to age-related deterioration, impaired autophagy, dysfunctional mitochondria, excessive reactive oxygen species (ROS) production and mitochondrial-mediated AEC apoptosis have all been described in IPF (50-52). Cell cycle arrest coupled to a variety of phenotypic changes is common in the alveolar epithelium of IPF lungs as well (51).

Likewise, immunosenescence, an age-related decline of immunocompetence characterized by expansion of CD4+CD8- T cells and the presence of autoantibodies was observed in some IPF patients (53, 54). Based on these data, one concept regarding the pathogenesis of IPF suggests that the following changes are critical for the development of disease: 1) excessive and unresolved ER stress and mitochondrial dysfunction enhance an apoptotic response in the AECs and 2) abnormal changes in the telomeres result in an inability to regenerate normal epithelium. It is also possible that immunosenescence increases the likelihood of infection-related exacerbation in aged individuals.

Most of the preclinical animal models of lung fibrosis use young mice, however in an age-related model of persistent fibrosis, data suggest that in response to lung injury, myofibroblasts from young mice manifest transient senescence and apoptosis susceptibility that permits fibrosis resolution. Alternatively, in the context of aging, myofibroblasts acquire a sustained senescent and apoptosis resistant phenotype that impairs the resolution of fibrosis (55). The authors also demonstrated that established fibrosis in the lungs of aged mice was at least partially reversed by administration of GKT137831, a small molecule NOx1/NOx4 dual inhibitor similar to the effects of NOx4-targeted siRNA (55).

A more recent study compared the development of lung pathology in both young and aged mice (2 months and 18 months of age, respectively) after pulmonary injury and proposed a mechanism to explain the increased prevalence of IPF and persistent fibrosis in older patients (55). Both groups of mice showed similar levels of collagen deposition 3 weeks after injury, which demonstrated that the initial fibrogenic healing response was intact and of similar magnitude for the young and aged mice. After the primary fibrotic response, the older mice presented an impaired capacity for fibrosis resolution as they failed to return to normal body

weight and still had myofibroblasts present in the fibrotic regions 2 months after the initial injury. Tissue samples from mice with pulmonary fibrosis expressed higher levels of NOx4, an enzyme involved in producing hydrogen peroxide. Additionally, the antioxidant transcription factor Nrf2 was only present at low levels in the fibroblastic foci, but most of the protein was localized in the cytoplasm and was deficient in the nucleus of senescent cells suggesting that an imbalance in the expression of NOx4 and Nrf2 was promoting the production and maintenance of ROS-mediated damage in the aged mice (55).

Overall these results indicated that with increased age, myofibroblasts that developed in response to an injury persist for an excessive amount of time because they do not undergo apoptosis. Instead the altered homeostasis of NOx4/Nrf2 allows oxidative damage to induce the persistence of myofibroblasts and prevent the clearance of these cells and their associated ECM proteins.

ECM changes have important implications in the aging lung. In aging, the collagen content of the ECM increases (56), along with decreases in elastin fibers (57). The exact mechanism of how the age-dependent changes in ECM components affect lung repair is still unclear, but it is known that the expression of fibronectin is increased in clinical and experimental models of fibrosis (58, 59) which in turn suggests an association with the repair process. Fibronectin production increases early in the injured lung and this augmentation coincides with fibroblast proliferation. The activation and proliferation of fibroblasts are responsible for the excessive synthesis and deposition of collagen proteins (60), and in this regard, it is interesting that our data suggest periostin production is enhanced in aged mice **(see Chapter 3)**. Changes in cell-fibronectin interactions may also contribute to the abnormal tissue remodeling by stimulating the proliferation of fibroblasts (61), myofibroblast differentiation (59)

and epithelial to mesenchymal transition (EMT), or by simply just facilitating the deposition of other ECM components such as collagens (60).

Other components of the ECM that might have implications in the aging lung are the expression of matrix metalloproteinases (MMPs) and their inhibitors, tissue inhibitor of metalloproteinases (TIMPs). Studies comparing young and old mice showed a significant increase in MMP2, MMP9 and Timp2 mRNA expression in old lungs. MMP9 activity was enhanced in the old lungs with low expression of Timp-1, its inhibitor (62). The increase in MMP expression could lead to increased susceptibility to injury, leading to increased leukocyte migration and more tissue damage in the injured lung. Overall these observations indicate that aging leads to changes in the composition of the ECM that might play a role in the lung repair process.

Relevant Background Information for Chapters 2 and 3:

Murine Models of Fibrosis

A number of murine models of fibrosis have been developed. No current model replicates all the manifestations of the human disease; however, investigations using murine models of fibrosis have led to the identification of many potential therapeutic targets that are believed to be important.

Bleomycin

The most common and best-characterized animal model of fibrosis involves a single intratracheal (i.t.) or intranasal (i.n.) administration of bleomycin to the lung. Bleomycin was originally isolated from the fungus *Streptomyces verticillatus (63).* Bleomycin has been shown to

induce lung injury and fibrosis in a number of experimental animals including mice, rat, hamster, rabbits, guinea pigs, dogs and primates over a range of doses via intraperitoneal (i.p.), intravenous (i.v.), subcutaneous (s.c.) or i.t. delivery (64). A single i.t. administration of bleomycin causes lung injury and resultant fibrosis in rodents (65-68). I.t. delivery of bleomycin results in direct damage to AECs, followed by inflammatory cell infiltration, collagen deposition and parenchymal consolidation (69-72).

In this model, the development of fibrosis can be seen both histologically and biochemically by 14 days post-bleomycin administration. Peak responses are observed around days 21-28 (72-76). By 30 days post bleomycin, the changes were more heterogeneous (72) (67, 68, 75). Collagen deposition post-bleomycin treatment is measured by both histological and biochemical techniques **(Figure 3)**. Most notably thru the accumulation of hydroxyproline, a component of collagen in the lung that serves as a read-out for whole lung collagen content (77). The mechanism of bleomycin-induced lung fibrosis is not entirely clear but likely involves oxidative damage, deficiency of the deactivating enzyme bleomycin hydrolase, genetic susceptibility and elaboration of inflammatory cytokines (78). The fibrotic response is strain-dependent; C57BL/6 mice are more susceptible to bleomycin compared to Balb/c mice (76, 79). Cytokines such as interleukin-1 (IL-1), chemoattractant protein-1(MCP-1), platelet-derived growth factor (PDGF) and transforming growth factor beta (TGFβ) are released from alveolar macrophages in animal models of bleomycin toxicity, resulting in fibrosis(80). Damage and activation of AECs may result in the release of cytokines and growth factors that stimulate proliferation of myofibroblasts and secretion of ECM proteins leading to fibrosis. Specifically, TGFβ, PDGF receptor alpha (PDGFRα) and tumor necrosis factor alpha (TNFα) are believed to stimulate the transformation, proliferation and accumulation of fibroblasts, which leads to the deposition of ECM (81-83).

There was increased PDGFRα in epithelial cells and macrophages in the lungs of patients with IPF (84). Studies in bleomycin-induced lung fibrosis indicate that some fibroblasts in fibrosis may be formed from bone marrow progenitors as well as from epithelial cells through EMT (85). Given the heterogeneity of the human disease among patients, investigating whether the bleomycin model accurately reflects disease mechanisms for all IPF patients or specific subsets will be important for translating findings from this model to the appropriate patient population. The bleomycin model is well characterized and has clinical relevance but a clear disadvantage is that it is self-limiting in mice as reflected in the temporal and spatial heterogeneity (86). Bleomycin treatment was shown to provide symptomatic relief to patients with craniofacial venous malformations and lymphangiomas (87). However, as a therapy, bleomycin treatment is limited because of the potential for life threatening interstitial pulmonary fibrosis or pneumonia and hypersensitivity pneumonitis (78, 88, 89). BALF studies in patients with bleomycin-induced pneumonitis have the presence of polymorphonuclear alveolitis (90).

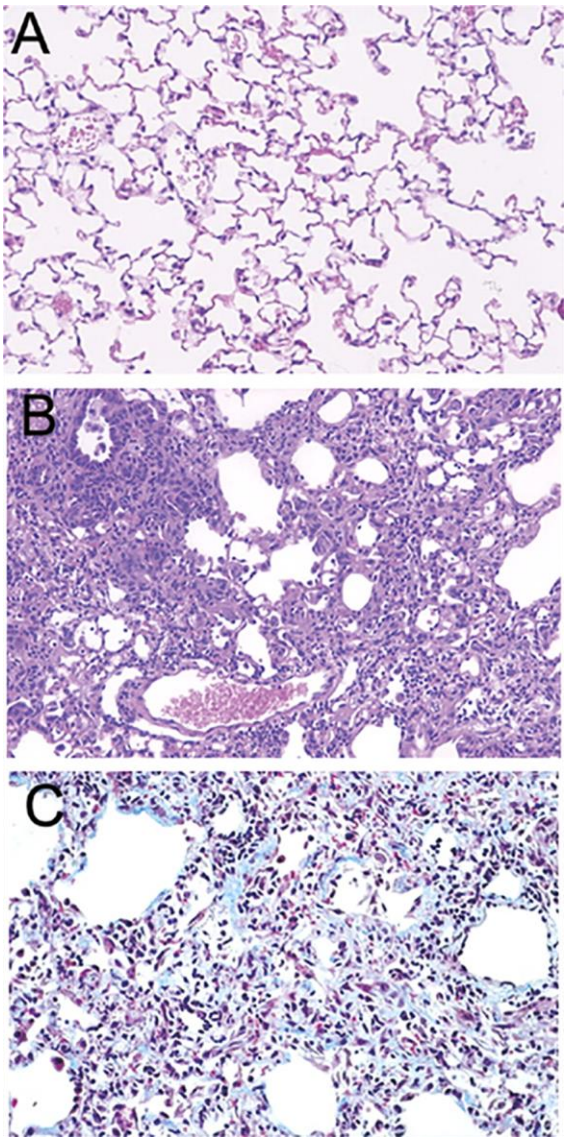

Figure 3: Characteristic pathology seen with bleomycin.
A: hematoxylin and eosin (H&E) staining of a paraffin-embedded section of untreated lung. B: H&E section prepared from a CBA/J mouse on day 14 post-intratracheal injection of bleomycin sulfate (0.02 U). Interstitial thickening, inflammation, alveolar collapse, and cystic air spaces are all noted. C: Trichrome staining of a lung section from a C57Bl/6 mouse on day 21 post-0.025 units of bleomycin sulfate. The blue staining represents collagen deposition. (Adapted from (86))

Fluorescein isothiocyanate (FITC)

Roberts and colleagues originally described this model of pulmonary fibrosis in Balb/c mice in 1995 (91). Intratracheal administration of FITC at 0.007mg per gram body weight/mice

dissolved in phosphate buffered saline (PBS) resulted in infiltration of mononuclear cells and neutrophils in the lung interstitium. The response to FITC is persistent; anti-FITC specific antibodies were detected in FITC treated mice from day 7 to 6 week's post-FITC treatment. By 5 months post-FITC, patchy focal destruction of normal lung architecture with interstitial fibrosis was noted (91).

Christensen and colleagues further characterized this model and demonstrated that both C57BL/6 and Balb/c mice were susceptible to FITC-induced fibrosis, with Balb/c mice showing a greater degree of fibrosis to the dose tested (92). Similar to findings in the bleomycin model, FITC was demonstrated to induce fibrosis by day 21 in a number of wild type and transgenic strains of mice (92). Further investigations with the FITC model of fibrosis demonstrated that like bleomycin, the fibrotic response to FITC is chemokine receptor 2 (CCR2)-dependent (93). Production of chemokine (C-C motif) ligand 12 (CCL12) and CCL2 (94) in the injured lung resulted in the recruitment of CCR2 expressing circulating fibrocytes (25) augmenting the fibrosis. IL-13 was also produced in response to FITC, which was essential for the fibrotic response (95). One clear advantage of the FITC model is the ability to visualize the areas of lung deposition by immunofluorescence (91, 92) (**Figure 4**). Another advantage of this model is that the fibrotic response lasts for at least 6 months and is not self-limiting like the bleomycin model (96), making it more suitable for long-term studies.

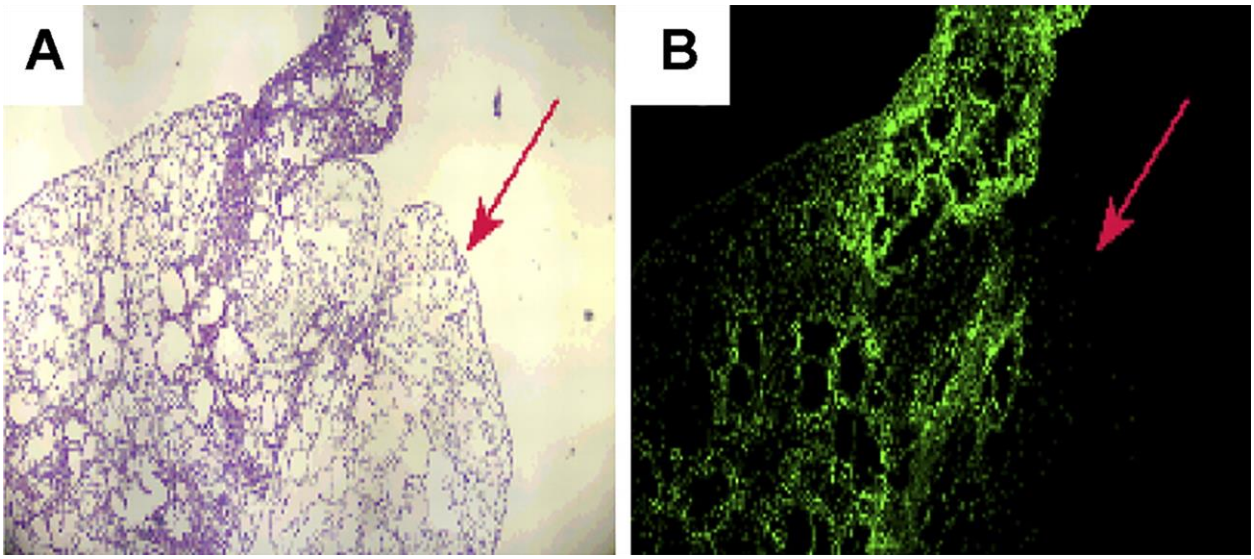

Figure 4: Fibrosis develops in areas of FITC deposition.
FITC was instilled intratracheally into C57Bl/6 mice on day 0. On day 21, lungs were harvested for histology. A: H&E stain at 4X magnification showing areas of consolidation, inflammation, and fibrosis. B: serial section of A at 4X magnification and viewed under UV light to show areas of FITC deposition. Note that areas of fibrosis in A correspond to areas of FITC fibrosis in B. The red arrows represent areas of the lung with normal architecture, which correspond to areas where FITC did not deposit. Patterns of both central and subpleural fibrosis are noted. (Adapted from (86))

Adoptive Transfer Models

A prominent feature of pulmonary fibrosis is constant fibroblast proliferation, which is mediated by a number fibroblast subtypes. These subtypes include fibrocytes, epithelial-derived mesenchymal cells, tissue resident progenitor cells, pericytes and resident fibroblasts. Bone-marrow derived collagen producing cells known as fibrocytes respond to chemotactic stimuli in response to injury and contribute to the wound healing process (97). It was shown that i.v. injection of human fibrocytes results in migration into the mouse lung following bleomycin challenge and these recruited cells appeared to contribute to the injury (98). In addition, adoptive transfer of murine lung fibrocytes to FITC-challenged mice exacerbated the fibrotic response (94). The transfer of human fibroblasts into immunodeficient mice also showed pathology by day

21(99). Overall these data suggest that bone marrow-derived mesenchymal cells or tissue resident mesenchymal cells can contribute to the pathogenesis of lung fibrosis.

Pericytes are specialized mesenchymal cells that share basement membrane with endothelial cells (100) (101). Pericytes frequently express the markers PDGFRβ aSMA, angiopoietin 1, CD146 and glial fibrillary acidic protein (GFAP) (102). Pericytes have been studied extensively in the eye, brain, kidneys and have been shown to regulate angiogenesis and vascular permeability (102). This cell type has been implicated as a source of myofibroblasts differentiation but the data available in the literature is controversial. Rock et al showed that pericytes are not a source of origin for myofibroblasts (103). However, recent studies by Hung and colleagues showed an expansion of Foxd1 progenitor-derived pericytes post-bleomycin lung injury and illustrated that these cells express collagen I and αSMA, a marker for myofibroblast differentiation (102), suggesting that pericytes are precursor cells in lung myofibroblast differentiation.

Infections and Pathogenesis of Fibrosis

Some patients with pulmonary fibrosis experience a slow progressive disease course over months to years while others experience rapid worsening of symptoms over a month or less. The rapid deteriorations are idiopathic in nature and are termed acute exacerbation [reviewed in (104)]. There is no animal model for the development of idiopathic acute exacerbations, but several studies have suggested that viral infections; mainly infections with herpesviruses, may augment fibrotic responses when given before the fibrotic challenge. In a bleomycin-induced model of lung fibrosis, gammaherpesvirus was shown to augments the fibrotic response (105, 106).

Infections can also cause rapid deterioration of symptoms with enhanced morbidity and mortality in fibrosis patients (18). Viruses have long been suspected of playing a role in the pathogenesis of IPF and it is well recognized that many patients report viral-type symptoms following initial diagnosis (107). However, the evidence supporting a role for viruses in IPF is limited/inadequate and often conflicting.

Hepatitis C virus (HCV) is a positive sense RNA virus that frequently causes fibrosis in the liver resulting in cirrhosis. In a Japanese study with 66 IPF patients and 9646 controls, Ueda and colleagues found that 28.8% of IPF subjects and 3.66% of controls had evidence of prior HCV infection (108). Multivariate analysis suggested that age, smoking and liver cirrhosis were all independent risk factors for the development of IPF. A number of studies have failed to replicate this association (109) and others have only shown an association of HCV with a range of non-fibrotic respiratory conditions (110). The lack of coherent signal across studies suggests that HCV is unlikely to be an important trigger for the development of IPF at least globally.

The human herpes viruses (HHVs) are a large family of DNA viruses, including the common pathogens, herpes simplex virus type 1 (HSV-1), Epstein-Barr virus (EBV), cytomegalovirus (CMV), and HHV-7 and-8. In the first study to suggest an association between HHV and IPF, it was reported that 12 out 13 IPF patients were seropositive for EBV compared to none of the 12 patients with other forms of interstitial lung disease (111). Several other studies have since reported similar findings of increased incidence of EBV in lung biopsy and BALF specimens from IPF patients when compared to controls (112-115). The most frequently studied of the HHVs is EBV; however Tang and colleagues (116) looked broadly at HHV family members and found evidence of past infection with at least one HHV in 97% of patients with IPF compared to 36% of healthy controls (116). It has been suggested that reactivation of this virus

acts as a second hit to the epithelium following exposure to a first injurious insult (117). These studies, however, only demonstrate an association of HHV and IPF, not a causal relationship. Given the limitations of *in vivo* human studies most researchers have focused on animal models of fibrosis for what has been learned.

Murine gamma herpesvirus type 68 (-γHV-68) is closely related to HHV and like its human counterpart, infects respiratory epithelium (118). Infection of young healthy mice does not result in pulmonary fibrosis. However, when γ-HV-68 is given in conjunction with known fibrotic stimuli; bleomyicn or FITC, it dramatically enhances lung fibrosis (119, 120). In further support of the human data, Stoolman and colleagues demonstrated that mice latently infected with γ-HV68 produce abundant TGFβ, which may promote the fibrotic response. (121). Other observations in mice that may be relevant to IPF include the finding that interferon gamma (IFNγ) knockout mice develop fibrosis when infected with γ-HV-68 alone (120). These mice mimic the Th2-dependent cytokine environment found in the lungs of patients with IPF. Similarly, aged mice (15-18months), but not young mice also develop pulmonary fibrosis when infected with γ-HV-68 (122)(123).

The mechanisms by which viruses might predispose patients to the development of IPF are beginning to be elucidated. HHV induces endoplasmic reticulum (ER) stress and apoptosis in vitro in epithelial cells (124). In human IPF biopsy samples, data showed co-localization of latent HHV and markers for ER stress and apoptosis (125). In the murine bleomycin model, chronic γHV-68 infection results in deposition of collagen, increased TGFβ expression and the altered synthesis of surfactant proteins (121). Likewise, γHV-68-induced pulmonary fibrosis in aged mice is associated with upregulation of TGFβ (122). Interestingly, stabilization of IPF, through

the administration of antiviral therapy, has been described in case reports, though generally in individuals with evidence of infection on either BAL or biopsy (116).

Another study in patients with severe IPF and positive EBV-serology showed that following a 2 week course of ganciclovir, 9 out of 14 patients, at week 8 showed improvements in 3 out of 4 of the composites measured (126). The small study size and short duration of the study makes it difficult to draw conclusions about antiviral therapy in IPF. However, it provides a rationale to have larger future studies involving antiviral therapy in treating IPF.

Acute exacerbations are devastating episodes of rapidly progressive respiratory compromise that occur in individuals with IPF (104). Histologically, acute exacerbations are characterized by the finding of diffuse alveolar damage; which has been shown in clinical trials to affect between 4-15% of individuals with IPF per year and are the main cause of IPF related mortality with a 3-month survival of less than 50% (127). In patients with IPF, respiratory tract infections that result in hospitalization confer a mortality risk indistinguishable from that seen with acute exacerbations (128). In animal models there is now good evidence to show that viral infection can exacerbate established fibrosis and give rise to a lesion resembling diffuse alveolar damage (129). However, Wootton et al failed to clearly identify a viral or other infectious trigger as the cause for acute exacerbation in the majority of IPF patients included in their study (130). It is possible that by the time of presentation, the triggering viruses may no longer be detectable.

Role of Bacteria in the Pathogenesis of IPF

While there is some evidence to suggest a role for viruses in the pathogenesis of IPF, the role of bacteria is much less well established. The only observational evidence demonstrated positive BAL cultures for *Haemphilus, Streptococcus* and *Psuedomonas* in 8 of 22 stable IPF

patients (131). A large multicenter, randomized, placebo-controlled study evaluated the prophylactic use of 12 months of septrin in treatment of IPF (132), and the authors reported that there was no difference in the primary end-point of change in vital capacity when comparing septrin and placebo. However, post-hoc analysis suggested that in subjects that adhered to the treatment, septrin led to a reduction in infections and mortality. Together with high mortality associated with bacterial respiratory tract infections in IPF, this suggests that bacteria may play a role in driving IPF disease progression.

In a small study looking at the potential role of *Pneumocystis jiroveci* infection in IPF, it was demonstrated that a number of uncultured bacteria were in the BAL of IPF patients using basic, culture-independent techniques (133). A recent study investigating the role of bacteria in the pathogenesis and progression of IPF showed increased bacterial burden in BAL, which predicted decline in lung function and death (134). Patients with increased bacterial load at the time of diagnosis were identified as patients with more rapidly progressive IPF and higher risk mortality (134).

Environmental triggers are integral to the pathogenesis and progression of IPF. Both bacteria and viruses have the potential to cause airway epithelial cell injury and apoptosis and both have the capacity to modulate the host response to injury. Han and colleagues showed in a patient cohort consisting of IPF patients within 4 years of diagnosis that the presence of *Staphylococcus* and *Streptococcus* genera was associated with the progression of IPF (135). Active infection in IPF is known to carry a high morbidity and mortality; the effect of latent viral infection or changes in lung microbiome remains unknown, but additional studies are necessary to determine if this is causal as well as to identify specific bacterial species. Interestingly, one of

the next multi-center clinical trials to be conducted in IPF will involve an investigation of antibiotic therapy.

Mechanisms involved in Pulmonary Fibrosis

The work discussed in this dissertation will explore different areas in the pathobiology of pulmonary fibrosis with a major focus on using the bleomycin-induced model of fibrosis to demonstrate how viruses, bacteria, recruited inflammatory cells (fibrocytes) and matricellular proteins such as periostin cause damage to the epithelial cells. The effects of apoptosis in the epithelial cells as well as how secreted profibrotic mediators contributed to myofibroblast differentiation leading to an exacerbated fibrotic response was also explored. As outlined in the model below; a number of steps are involved in fibrogenesis but this process can be differentiated into 4 distinct phases (**Figure 5**).

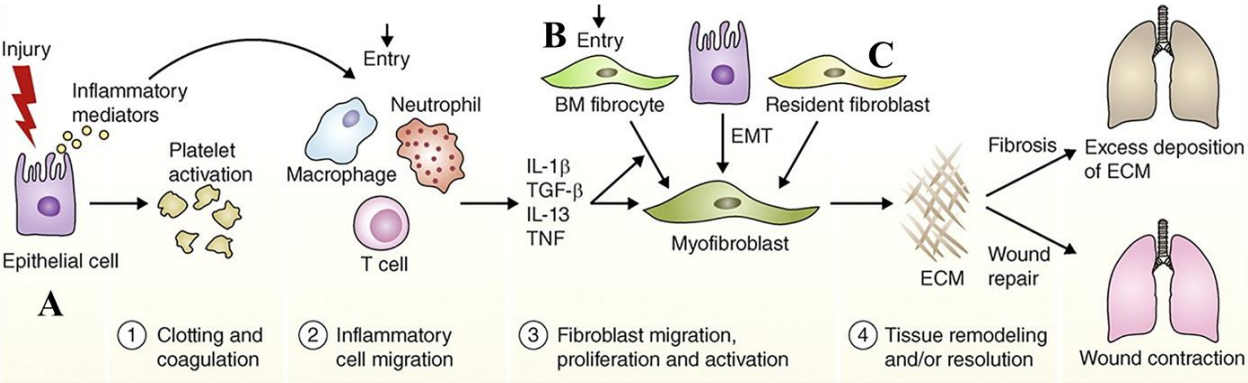

Figure 5: Changes in normal wound healing contribute to the development of pulmonary fibrosis.
Lung injury causes damage to the endothelial and epithelial cells eliciting an immune cascade that involves (1) coagulation, (2) inflammatory cell recruitment, (3) fibroblast proliferation and activation. (4) In the final remodeling and resolution phase, myofibroblasts can promote wound repair, leading to wound contraction and restoration of blood vessels. However, fibrosis often develops if the tissue repair program is dysregulated leading to fibrosis. (Adapted from (136))

The work discussed in this dissertation will focus on areas outlined on figure 5. (**A)** Understanding how different insults to lung epithelial cells contributed to the exacerbation of the other three phases; **(B)** Following lung injury and epithelial cell damage how the recruitment of hematopoietic bone-marrow derived fibrocytes contributed to myofibroblast differentiation; and **(C)** How the production of profibrotic mediators from structural or hematopoietic cells affected resident fibroblasts leading to lung fibrosis. The remainder of this chapter will outline background and preliminary data that led to the hypothesis for this project.

Inflammatory Cells

IPF is a progressive and irreversible disease that destroys the lung architecture in a series of steps that are poorly understood. Chronic inflammation can lead to an imbalance in the production of chemokines, cytokines and growth factors, and can disrupt cellular recruitment. Alveolar macrophages can both promote and limit pulmonary fibrosis through secretion of TNF-α, TGF-β1, interleukin-13 (IL-13)(94, 137, 138) and the production of the pro-inflammatory chemokines, CCL2 and CCL12 (94, 139).

In the earliest stages of tissue damage, epithelial cells and endothelial cells release inflammatory mediators initiating a coagulation cascade that triggers clotting and the development of ECM. Platelet aggregation and degranulation in turn promotes blood vessel dilation and increased permeability, allowing efficient recruitment of inflammatory cells such as neutrophils, macrophages, lymphocytes and eosinophils to the site of injury (136). Neutrophils are the most abundant inflammatory cells at the early stages of wound repair but are quickly replaced by macrophages that produce a variety of cytokines and chemokines that

amplify the inflammatory response and trigger fibroblast proliferation and recruitment [reviewed in, (136)] **(Figure 5).**

Fibrotic lung diseases including IPF are associated with a distinct type of macrophage activation called M2 or alternative activation (140, 141). Classical/M1 macrophage activation by microbial agents and or Th1 cytokines, in particular by interferon gamma (IFN-γ), induces the production of IL-12. On the other hand, macrophages stimulated by Th2 cytokines display a different activation pathway called alternative activation or M2, which plays a critical role in wound healing (142). A profibrotic role of alternatively activated alveolar macrophages (AMs) was demonstrated in IPF (143), as well as in mouse models (143-146).

Several animal models of pulmonary fibrosis have demonstrated that AMs display a phenotype with alternative activation. In the silica-induced model, mRNA expression of Ym1 increased significantly in the lungs of wild type mice but did not increase in the silica-treated IL-4R null mice, indicating the importance of a Th2 environment for M2 polarization (147). In the herpes virus-induced and transgenic TGFβ models of fibrosis, AMs accumulated in the lungs and expressed alternative activation markers Ym1/2, Fizz1 and arginase-1 (140, 146, 148). AMs collected from IPF patients showed increased expression of CD206 and generated higher levels of CCL17, CCL18 and CCL22 compared to healthy controls (143, 149). Levels of arginase-1 were also higher in AMs and lung tissue of IPF patients (148). Clearly, alternative activation can alter the profile of mediators secreted by macrophages. The following section will describe profibrotic mediators and how they affect pulmonary fibrosis.

Profibrotic Mediators

TGFβ1

Nearly two decades of research have suggested that TGFβ1 plays a central role in the pathogenesis of pulmonary fibrosis by regulating the proliferation, activation and differentiation of epithelial cells and collagen-producing myofibroblasts (150). TGFβ1 signals through activation of its downstream effectors, the SMAD proteins. TGFβ/Smad signaling induces EMT and fibrosis in a variety of organs (151-153). It was shown that TGFβ1 was able to induce alveolar epithelial cells to undergo EMT in vivo and in vitro via Smad2 activation (154).

TGFβ1 is synthesized and secreted into small and large latent complexes. TGFβ1 genes encode a N-terminal latency-associated peptide (LAP) and a C-terminal mature cytokine that forms dimeric structures. In the LAP of TGFβ1 and TGFβ 3, but not TGFβ2, there is an arginine-glycine-aspartic acid (RGD) site that facilitates the binding of integrins. In some cells, the small latent complex can associate with latent TGFβ binding protein (LTBP) via interactions with LAP, forming the large latent complex (155).

Two integrins, alphaVbeta6 and alphaVbeta8, appear to jointly regulate much of the TGFβ1 activation relevant to adaptive immunity, given that combined inhibition of these integrins largely mimics the immune dysregulation seen in mice with complete loss of TGFβ1 signaling in T cells (155). Which integrins mediate TGFβ1 activation in other cells is an area of active study.

In the lungs, TGFβ is produced by a wide variety of cell types, including AMs neutrophils, activated alveolar epithelial cells, endothelial cells, fibroblasts, and myofibroblasts (156). When activated, TGFβ is a pleiotropic growth factor with chemotactic and proliferative properties. TGFβ induces macrophage and fibroblast recruitment as well as fibroblast

proliferation via PDGF expression. In these cells, TGFβ also stimulates expression of a number of proinflammatory and fibrogenic cytokines, such as TNFα, PDGF, IL-1β, or IL-13, thereby further enhancing and perpetuating the fibrotic response (156).

TNF-α

TNF-α is the most widely studied cytokine member of the TNF super family. In pathophysiological conditions, generation of TNF-α at high levels leads to the development of inflammatory responses that are hallmarks of many diseases. Of the various pulmonary diseases, TNFα is implicated in asthma (157-161), chronic bronchitis, chronic obstructive pulmonary disease (162-165), acute lung injury, acute respiratory distress syndrome (166-169), and pulmonary fibrosis (170, 171). Its role in fibrosis is controversial, but in vivo studies indicate that TNFα is predominantly a pro-fibrotic effector (172).

Induction of TNFα overexpression causes fibrosis in rat lungs resulting in severe infiltration of the lungs by neutrophils, macrophages and lymphocytes (173). These data were supported by the analysis of peripheral CD4+ T cells from patients with IPF where CD4+ T cells from IPF patients synthesized higher levels of TNFα compared to normal subjects (174). Studies in bleomycin-induced TNF-α receptor knockout and wild type mice treated with anti-TNFα antibodies initially suggested that TNFα receptor signaling was required for the development of pulmonary fibrosis (175, 176). However, a more recent study demonstrated that TNFα is involved in the resolution of established fibrosis by reducing numbers of profibrotic macrophages, suggesting an anti-fibrotic role for TNFα (171).

CCL2 and CCL12

Monocyte chemoattractant protein-1(CCL2) and monocyte chemoattractant protein-5(CCL12) are potent chemotactic ligands for chemokine (C-C motif) receptor 2 (CCR2)

mediating recruitment of inflammatory cells and fibrocytes during pulmonary fibrosis (25, 177). Both bleomycin and FITC-induced murine models of lung fibrosis showed elevated levels of CCL2 in response to fibrotic injury (25, 93, 94). Patients with interstitial lung disease also have elevated CCL2 in their bronchoalveolar lavage fluid (BALF) (178-180) and high levels of CCL2 correlated with poor survival (181). Fibrotic fibroblasts overexpress CCL2 (44, 182, 183), and respond to CCR2 stimulation by increasing TGFβ and limiting apoptosis (184).

Fibrocytes are recruited by CCL12 in mice via CCR2 (94) and CCR2 stimulation of fibrocytes increased expression of collagen I (25); these findings were also confirmed in human studies (185). Mice deficient in CCR2 are protected from pulmonary fibrosis suggesting that CCL2 and CCL12 are crucial for the development of pulmonary fibrosis in mice (93). Recent work from Deng and colleagues demonstrated that CCL2 expression is transcriptionally regulated by thrombin via the nuclear factor kappa B (NF-κB) and activation protein-1 (AP-1) pathways resulting in an overexpression of CCL2 in pulmonary fibrosis (182).

Fibrocytes

Originating in the BM, fibrocytes comprise a small subset (0.1%) of mononuclear cells and were first described as common leukocyte antigen (CD45) and type-I-collagen (Col I) expressing leukocytes that mediate tissue repair and are capable of antigen presentation to naïve T cells (97). Human fibrocytes isolated from peripheral blood have a spindle-like shape but obtain a myofibroblastic phenotype upon differentiation on plastic in response to TGFβ1 (186-189). Fibrocytes express leukocyte-associated antigens including CD45, a myeloid antigen CD13, hematopoietic stem cell antigen CD34, and major histocompatibility complex antigens class II (MHCII), CD80, CD54 and other antigens (186, 190).

Cultured fibrocytes have been shown to express collagen I, collagen III, and fibronectin (97, 189, 191-193). Under normal conditions, few fibrocytes can be detected in the peripheral blood or tissues. It is believed that fibrocytes contribute to wound healing and maintenance of tissue integrity thus playing a vital role in matrix remodeling and cellular homeostasis (194). Egress of fibrocytes from the BM and homing to peripheral organs is regulated by profibrotic mediators such as TGFβ1 and chemokines (CCL2, CCL3, and CCL12) (195). Importantly, fibrocytes express a number of chemokine receptors including CXCR4, CCR7 and CCR2, which likely mediate recruitment, and activation of fibrocytes to areas of tissue damage (25, 94, 98). In a bleomycin-induced model of pulmonary fibrosis in mice, the number of bone marrow (BM)-derived fibrocytes recruited to the injured lung constituted up to 25% of the collagen producing cells (196), suggesting that fibrocytes play an important role in the development of pulmonary fibrosis (188).

In patients with IPF, elevated numbers of circulating fibrocytes in the blood correlated with the severity of the disease and may serve as a prognostic marker (197). In addition, fibrocytes and monocytes have been shown to be the major producers of the matricellular protein, periostin, in the blood of IPF patients (198). In a murine model of lung injury, adoptive transfer of Tregs was shown to decrease CXCL12 expression and fibrocyte recruitment resulting in improvement in fibroproliferation (199). Conversely, adoptive transfer of fibrocytes has been shown to worsen fibrotic outcomes (94). Even though fibrocytes have been shown to contribute to the pathogenesis of pulmonary fibrosis and have been shown to express Col I, these cells are not an essential source of collagen during pulmonary fibrosis (200). Another study suggested that increased levels of the protein lumican; secreted by fibroblasts in

the presence of TNF-α, causes monocytes to differentiate into fibrocytes, providing another mechanism to account for accumulation of fibrocytes in fibrotic lesions (201).

Fibrocytes are different from bone marrow-derived mesenchymal stem cells. Both fibrocytes and mesenchymal stem cells (MSCs) are derived from the bone marrow, but the cellular markers and functions are different. While fibrocytes, contribute to the ECM deposition and secrete pro-inflammatory cytokines like IL-1β, IL-6, TNF-α and TGF-β1, MSCs are derived from the stroma of the bone marrow and are believed to attenuate scar tissue formation and suppress inflammation in fibrotic lesions (202).

Myofibroblasts and Fibroblasts

Fibroblasts are present in virtually all tissues and organs, albeit in limited numbers under normal conditions (203). Quiescent resident fibroblasts can be activated in response to extracellular triggers such as transforming growth factor beta (TGFβ1) (152, 204, 205), WNT (206), Jagged/NOTCH (207, 208), Fizz1 (208, 209), and hedgehog. In response to specific stimuli, epithelial cells can give rise to fibroblasts or myofibroblasts in the lung through a process of epithelial to mesenchymal transition EMT. In addition, myofibroblasts can also be derived from resident fibroblasts.

Myofibroblasts are characterized in part, by the presence of alpha smooth muscle actin (αSMA) and their ability to produce ECM proteins including type-I-collagen. Lung tissue from patients with pulmonary fibrosis contains myofibroblasts (210-212), which are responsible for the deposition of collagen and other ECM components during development and progression of pulmonary fibrosis (213). Data suggest that myofibroblasts are derived from at least three sources; resident lung fibroblasts may expand, alveolar epithelial cells may undergo EMT or

circulating bone marrow-derived stromal cells/fibrocytes may enter the lungs and differentiate into fibroblasts (214-216). During EMT, the expression of the epithelial marker E-cadherin is lost while the expression of mesenchymal markers including αSMA and MMPs are increased; resulting in the loss of cell-cell and cell-matrix interactions, increased cell-migratory behavior and excess ECM production (217).

TGFβ1 is a potent inducer of myofibroblast differentiation (218). TGFβ1 not only induces synthesis of ECM proteins, particularly collagens and fibronectin but it also reduces MMP activity by promoting tissue inhibitor metalloproteinase proteins (Timp) expression (219, 220). IPF is characterized by the accumulation of fibroblasts and myofibroblasts, which aggregate in clusters termed "fibroblastic foci", the number of which correlates with patient mortality (221, 222). The myofibroblasts has been identified as a key mediator of IPF and other profibrotic conditions (223-225). The distinct myofibroblast phenotype is TGFβ-dependent and arises secondary to chronic epithelial injury or inflammation.

Additionally, myofibroblasts accumulate because they are resistant to apoptosis. TGF-β1 and endothelin-1(ET-1) have been found to promote resistance to apoptotic stimuli in fibroblasts while prostaglandin E_2 (PGE_2) has been shown to inhibit apoptotic resistance induced by TGF-β1 (226-229). Fibrotic disease can reduce the ability of lung fibroblasts to produce PGE_2 due to a decrease in the upregulation of cyclooxygenase 2, an important enzyme for PGE_2 synthesis (229). Additionally, fibroblasts in fibrotic lungs often lose the ability to respond to PGE_2 (230, 231). While resident fibroblasts can differentiate into myofibroblasts and epithelial cells can undergo EMT, circulating cells can also contribute to progression of the disease.

Matricellular Proteins

The concept of a matricellular protein was first proposed by Paul Bornstein in the mid-1990's to account for the non-lethal phenotypes of mice with inactivated genes encoding thrompbospondin-1(TSP-1), tenascin-C or secreted protein acidic and rich in cysteine (SPARC)(232). Matricellular proteins are a family of structurally unrelated extracellular molecules that do not play a primary role in tissue architecture but are induced following injury and modulate cell-cell and cell-matrix interactions (232, 233). With the rapid expansion in our understanding of cell-matrix interactions several additional proteins were later included such as TSP-2 and -4, tenascin X, osteopontin (OPN), periostin, and the members of the CCN family of matricellular proteins which will be discussed.

Matricellular proteins bind to various ECM proteins and to cell surface receptors, while associating with cytokines, growth factors, and proteases. These interactions allow them to serve as key integrators. TSP-1 is a major constituent of platelet alpha granules but can also be synthesized by many other cell types including endothelial cells, vascular smooth muscle cells, fibroblasts, keratinocytes, and macrophages (234). TSP-1 plays a key role in TGFβ activation through a cell and protease mechanism thus contributing to the exacerbation of fibrotic diseases (235, 236); in contrast, the other TSPs do not activate TGFβ. Studies in TSP-1 null mice demonstrated that TSP-1 was important for the activation of TGFβ, as these mice exhibited inflammatory changes in the lung and pancreas. Treatment of TSP null mice with a TSP-1 derived peptide that activates TGFβ showed partial reversion of the lung and pancreatic abnormalities towards the wild type phenotype (237). The significance of TSP-1 mediated TGFβ activation has been further supported by findings in a wide range of biological processes including tissue repair, fibrosis and neoplasia (238).

Tenascins

The expression of tenascin C and –X is regulated by micro-environmental factors (239). Tenascin C is induced by a number of growth factors such as PDGF, fibroblast growth factor and TGFβ. Tenascin-C expression is associated with the development of fibrosis both in experimental models (240) and in patients with fibrotic conditions (241, 242). Loss of tenascin-C attenuated bleomycin-induced lung fibrosis (243). Decreased extracellular matrix deposition in the absence of tenascin C was associated with decreased TGFβ signaling.

SPARC

SPARC regulates cell function and tissue remodeling by modulating growth factor signaling and affecting cell cycle arrest (244). In bleomycin-induced lung fibrosis, SPARC null mice showed decreased collagen deposition in the lungs (245). A more recent article showed that SPARC exerts different functions in pulmonary fibrosis depending on the cell of origin (246). Bone marrow chimera experiments demonstrated that SPARC produced by BM-derived leukocytes limits fibrosis by decreasing inflammation whereas, SPARC from fibroblasts or fibrocytes sustain fibrosis promoting collagen deposition. The anti-inflammatory activity of SPARC was dependent on its regulation of TGFβ signaling in macrophages (246). SPARC has also been shown to suppress apoptosis in fibroblasts from patients with IPF (247).

Osteopontin

Osteopontin (OPN) is expressed as a 33kDa protein, but can also be seen as a 44kDa protein due to posttranslational modification. OPN interacts with a number of integrins alphaVbeta1, alphaVbeta3, alphaVbeta5, alphaVbeta6, and alpha5beta1 integrins through its

RGD motif (248, 249). OPN is expressed by numerous immune cells and is upregulated in response to tissue injury and inflammation in a number of different organs (250). In dystrophic skeletal fibrosis, these findings were associated with alterations in the profile of immune cell infiltration and decreased TGFβ expression (251).

Periostin

Periostin was originally named osteoblast specific factor-2 (OSF-2) (252) and was suggested to play a role in bone metabolism. The name was later changed to "periostin" because of its intense expression in the periosteum and periodontal ligament (253). Increased periostin expression in tissue repair, remodeling and fibrosis may be due to activation of TGFβ and bone morphogenic protein (BMP) signaling. In vitro, TGFβ and BMP-2 are potent inducers of periostin in a variety of cell types including fibroblasts (254). In subepithelial fibrosis associated with asthma, periostin appears to play an important role by enhancing profibrotic TGFβ signaling (255). In asthma, the periostin gene is upregulated in epithelial cells by IL-4 and IL-13. Persiotin is also recognized as a biomarker of type 2 inflammation and has been examined in the serum of asthma patients as a surrogate for clinical efficacy regarding anti-IL-13 therapy (256).

Evidence supporting a role of periostin in lung fibrosis comes from studies using mouse models of experimental lung fibrosis, as well as data showing that periostin expression was upregulated in the lung tissue of IPF patients (198, 257). In patients with IPF, periostin is highly expressed in the lung tissue in areas of active fibrosis (198). Periostin was also detected in the circulation of IPF patients with significantly higher levels of serum periostin in IPF patients compared to healthy individuals or patients with other interstitial lung pneumonias (258). Periostin-deficient mice are protected from bleomycin-induced fibrosis, which is suggested to be

a result of impaired recruitment of inflammatory cells due to decreases in chemokine production by fibroblasts in mice on the Balb/c background (257). In periostin-deficient mice on the C57BL/6 background, periostin seemed to be playing a role in the fibroproliferation because no difference was found in inflammation in these knockout mice when compared to WT controls (198); however, there was still less collagen content in the lungs of these mice post-bleomycin treatment.

Cross-linking of collagen is catalyzed by lysyl oxidases (LOX). Periostin has been shown to activate BMP-1 to cleave LOX, promoting its activation on the ECM and increasing cross-linking between collagen fibrils (259). The subsequent stiffening of the matrix is thought to promote fibroblast activation, which may further promote a fibrotic environment in IPF. Periostin has also been shown to interact with a number of integrins. OC-20, an antibody that blocks periostin interaction with integrins, limited lung fibrosis and improved survival in a murine bleomycin-induced model of fibrosis (198).

CCN Family of Matricellular Proteins

The CCN gene family (Cyr61/CTGF/NOV) consists of six members; CCN1(cyr61), CCN2(CTGF), CCN3(NOV), CCN4, (WISP1), CCN5(WISP2) and CCN6(WISP3)(260, 261). The mechanisms of regulation have been characterized in detail for CCN2, because of its mitogenic activity in connective tissue; CCN2 was named connective tissue growth factor (CTGF) (262). CCN3 was cloned as a gene that is overexpressed in nephroblastoma, CCN4 and 5 were identified as genes that were upregulated in response to Wnt-1 and were named wnt-1 inducible signal pathway protein 1 (WISP1) and WISP2 (263). Finally CCN6 was identified as a WISP1 homolog and named WISP3. The CCNs interact with a number of ECM proteins and

growth factors, and in some cases specific domains have been identified to be responsible for this interaction (264). CCNs bind and signal through a number of receptors several of which are integrins, transmembrane receptors that bridge cell-cell and cell-ECM interactions (265). The binding of CCNs to co-receptors such as heparin sulfate proteoglycans, the TrkA receptor, or low-density receptor proteins (LRP) are thought to help provide for unique signaling (266, 267).

CCN2/CTGF has been shown to be a downstream profibrotic mediator of TGFβ (268). However, this paradigm is complicated by observations that CCN2 activates or co-activates TGFβ-mediated profibrotic responses and appears in itself to play a primary role in fibrosis (268). CCN2 induces the expression of a variety of cytokines such as VEGF and TGFβ (269) which induces even more expression of CCN2/CTGF. There are multiple positive feedback loops involving CCN2/CTGF expression that can contribute to the progressive nature of fibrosis. Breaking this loop should enable organs to restore normal wound healing response and normal function. In terms of mechanism, CCN2/CTGF acts to initiate and extend fibrosis by directly increasing the production and accumulation of ECM proteins (270). Its presence induces the formation of myofibroblasts through transdifferentiation of other cells including epithelial cells via epithelial to mesenchymal transition (EMT) (271) or resident fibroblasts (272) or fibrocytes that have been recruited to organs through chemokines (273). It was shown that AECs undergoing TGFβ-mediated EMT in vitro were able to activate lung fibroblasts in a CCN2/CTGF-dependent manner (274). In a radiation-induced model of pulmonary fibrosis, inhibition of CCN2/CTGF with small molecule inhibitor (FG-3019) attenuated lung fibrosis and showed an increase in tissue remodeling (275).

CCN3 is a negative regulator of CCN2 and an inhibitor of renal fibrosis (276). CCN3 has been shown to counter the profibrotic effects of CCN2/CTGF by inhibiting the upregulation and

accumulation of ECM proteins such as collagen, ultimately limiting or reversing the progression of fibrosis (277). CCN4 has also been implicated in fibrotic diseases (278). It has important roles in inflammation and tissue injury. There is significant upregulation of CCN4 expression as well as other proinflammatory and profibrotic mediators such as nuclear factor- kB (NFkB) in carbon tetrachloride (CCL4)-induced liver fibrosis (279). Blocking CCN4 in vivo, with a monoclonal antibody significantly attenuated CCL4-induced liver injury and progression of liver fibrosis (279). Similar results were observed in pulmonary fibrosis where treatment with a neutralizing antibody specific for CCN4 reduced pulmonary fibrosis in mouse models (280). CCN4 is also upregulated in patients with IPF (280).

CCN5 has been suggested to play an inhibitory role in some fibrotic diseases such as cardiac fibrosis (281). CCN5 is expressed at low levels in fibroblasts and was shown to exert inhibitory effects on the fibrotic phenotypes of pulmonary fibroblasts both *in vitro* and *in vivo* (282). CCN6 was shown to cause proliferation of lung fibroblasts by binding to integrin beta 1, leading to the phosphorylation of focal adhesion kinase (Y397). CCN6 was highly expressed in the lung tissues of bleomycin-treated mice suggesting that CCN6 may play a role in fibrogenesis (283). Based on the evidence available for the CCN family of proteins and their role in fibrosis, these proteins could be potential targets for the treatment of pulmonary fibrosis.

Integrins

Integrins are a large family of heterodimeric transmembrane glycoprotein receptors, shown to mediate cell adhesion to ECM proteins and mediate cell surface counter-receptors including members of the immunoglobulin and cadherin families (284). Integrins also regulate other families of proteins including growth factors (285) and proteases (286). They can serve as scaffolds for the assembly of signaling complexes and are composed of a single alpha and a

single beta subunit. In mammals, there are 18 human alpha subunit and 8 beta subunits forming a total of 24 integrin heterodimers (287)**(Figure 1)**. A number of specific integrins have been shown to play a role in pulmonary fibrosis in various animal models or have been shown to have an important role in mechanisms that might contribute to pulmonary fibrosis. Integrins have been shown to associate with TGFβ (288). Most tissues including the lung contain significant amounts of latent TGFβ. Early evidence for the mechanism behind latent TGFβ activation suggested that TGFβ1 and -3 might interact with integrins because they contain a RGD peptide sequence (289). It is now known that this RGD sequence in TGFβ 1 and 3 is recognized by 6 different integrins, two of which perform the function of activating the latent TGFβ complex based on *in vivo* data (288).

AlphaVbeta6 is expressed at low levels in the alveolar epithelium; associates with latent TGFβ thru interaction with the RGD sequence of LTBP and is also a receptor for the ECM proteins, fibronectin (290) and tenascin C (291). Data suggest that alphaVbeta6 is not important in development because mice lacking this integrin develop normally (292). The expression of alphaVbeta6 was dramatically upregulated in patients with scleroderma who had UIP, the pathologic correlate of IPF or in patients with IPF (293).

A second integrin, alphaVbeta8 also binds the same RGD sequence in latent TGFβ but appears to activate TGFβ in a different manner. The cytoplasmic domain of the beta 8 subunit is not required for the activation of TGFβ. AlphaVbeta8 appears to activate TGFβ by presenting the latent TGFβ complex to metalloproteases that cleave the LAP and release free TGFβ (294). AlphaVbeta8 has not been shown to be important for development of alveolar fibrosis, suggesting that it is likely alphaVbeta6, which plays a role in the activation of TGFβ-associated pathogenesis of pulmonary fibrosis. However, alphaVbeta8 has been shown to play a role in

airway fibrosis; conditional deletion of alphavbeta8 in lung fibroblasts attenuated airway fibrosis (295). The integrins alphavbeta3 and alphavbeta5 have also been shown to bind the RGD sequence in LAP of TGFβ but only alphaVbeta3 has the potential to activate latent TGFβ (285, 294, 296-298).

Alpha3beta1, an epithelial integrin has been shown to colocalize with E-cadherin and beta-catenin at adherens junctions (299). In a mouse model of pulmonary fibrosis, conditional epithelial cell-specific deletion of alpha3 integrin expression showed normal response to acute bleomycin-induced lung injury, but these mice had reductions in lung myofibroblasts and type I collagen and did not progress to fibrosis (300). Alphavbeta1, which is highly expressed on fibroblasts, directly binds to the LAP of TGFβ and mediates TGFβ activation. A novel alphaVbeta1 inhibitor (C8) was recently shown to attenuate bleomycin-induced pulmonary fibrosis and CCL4-induced liver fibrosis (301). In mouse models of pathological hepatic or pulmonary fibrosis, subcutaneous administration of C8 after the establishment of fibrosis led to significant reduction in fibrosis by downregulating TGFβ signaling (301). Based on the data to date, integrins are suggested to be involved in activating one of the key profibrotic mediators, TGFβ. Since, TGFβ deletion results in autoimmunity targeting signaling pathways that activate TGFβ maybe the path to identifying novel therapeutics for IPF, but they will have to be carefully balanced to avoid autoimmunity.

Therapeutic targeting of Integrins

Blocking antibodies to alphavbeta6 have shown therapeutic promise in a wide range of preclinical models of fibrosis including lung fibrosis (293, 302) and renal fibrosis (303, 304). Furthermore in the lung, low doses of alphavbeta6 blocking antibodies can prevent bleomycin-induced or radiation-induced pulmonary fibrosis in mice without causing inflammation (293,

302). A monoclonal antibody targeting alphavbeta6 (clone6.3G9) has been humanized as STX-100 and is currently being evaluated in phase 2 clinical trials for the treatment of patients with IPF. In addition, recent preclinical data suggests that targeting alphavbeta1 integrin on fibroblasts shows potential therapeutic application in fibrotic diseases (301).

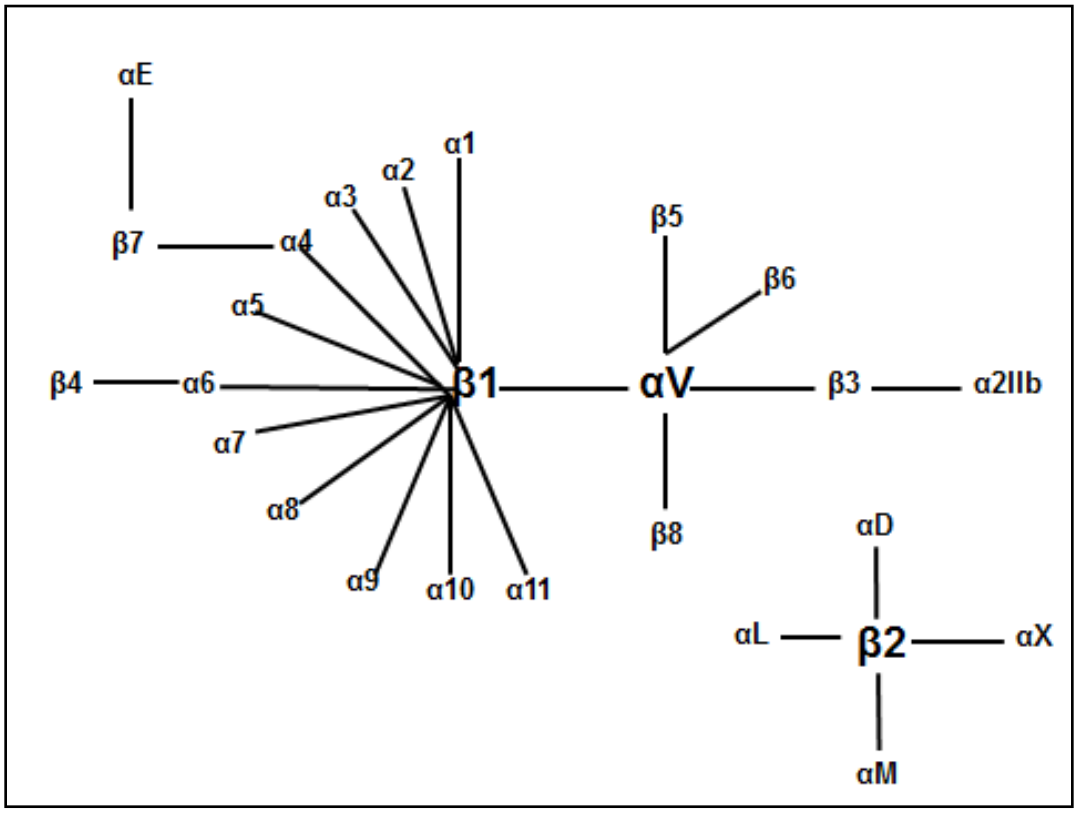

Figure 6: The members of the human integrin superfamily and how they combine to form heterodimeric integrins.
There are 18 alpha subunits and 8 beta subunits that have been identified in humans, which are able to form 24 different integrins. Solid lines as indicated above connect Integrin subunits that bind to each other to form a heterodimer. Each integrin has distinct ligand-binding specificity, tissue and cell distribution (305).

Background Information for Chapter 5:

Apoptosis, Wound Healing and Aging

The late phase of normal wound repair coincides with a decrease in fibroblast numbers by apoptosis, a mechanism that is still not clearly understood (306, 307). However, research has shown that a member of the IAP family of proteins, X-linked inhibitor of apoptosis (XIAP) localizes to fibroblastic foci in IPF tissue and that PGE_2 suppresses XIAP expression while increasing fibroblast susceptibility to apoptosis (308). Ajayi *et al* further demonstrated that inhibition or silencing of XIAP enhanced the sensitivity of lung fibroblasts to Fas-mediated apoptosis (308). Overall these data suggest that XIAP and/or other IAPs were regulating or contributing to the apoptosis-resistant phenotype in IPF fibroblasts. In this study we further assess how targeting IAPs would affect bleomycin-induced fibrosis.

Regardless of the activation pathway, apoptosis plays a role during injury and wound healing. Rapid apoptotic responses increase the magnitude of injury and the possibility of forming scar tissue. Apoptosis is necessary for the removal of inflammatory cells during wound healing. In IPF, with enhanced apoptosis of AECs in combination with resistance to apoptosis in fibroblasts and myofibroblast, these differing cell-specific sensitivities to apoptosis are believed to be critical to the pathogenesis of lung fibrosis (307).

Aging in human lungs show loss of epithelial cells and homogeneous enlargement of the alveolar spaces. During injury, enhanced apoptosis of AECs may result in a defect in the regeneration of the damaged alveolar wall, thus promoting fibrotic tissue repair response (309). Studies have shown that type II lung epithelial cells from aging lungs of mice are highly susceptible to apoptosis during injury and that increased apoptosis was associated with

expression of ER stress proteins; BiP and Xbp1 that are not expressed in the lungs of young mice (123).

Defective wound healing in the aging lung can also be associated with increased apoptosis of epithelial cells by a pro-apoptotic pathway. Data from animal models showed activation of Fas-mediated apoptosis as well as TGFβ overexpression causing apoptosis of lung epithelial cells (310, 311). Mitochondrial dysfunction has been shown to promote apoptosis and may be the central mechanism during mammalian aging (312). The maintenance of mitochondrial function during stress conditions is established by the balance between pro-apoptotic and anti-apoptotic members of the B-cell lymphoma 2 (BCL2) family of proteins, as well as levels of heat shock proteins (HSP) which are up-regulated following exposure to environmental stress and help to stabilize or facilitate the degradation of mediators BAX, Bak, cytochrome C and caspase-3 (313). Mice over-expressing heat shock protein (HSP)-70 showed attenuated bleomycin-induced fibrosis (314), possibly associated with protection against apoptosis of lung epithelial cells. In IPF, low levels of BCL2 were observed in lung epithelial cells, but fibroblasts had high levels of HSP and BCL2.

In conclusion, the association of apoptosis with age-related susceptibility to lung injury and the cell/tissue specificity of this process demands further investigation. However, it is clear that changes in the lung environment or the immune response during aging could cause older adults to be more susceptible to fibrotic lung diseases or other diseases that causes damage to the lung epithelium.

Background Information for Chapter 6:

Biomarkers in IPF

Currently there are no molecular biomarkers available for clinical use in IPF and the search for potential markers remains in its infancy. Despite improvements in the clinical classification of patients with IPF, there is still no cure for the disease. The FDA recently approved two new drugs; Nintedanib and Pirfinedone but these drugs only offer mean progression free survival of 13 months (33). Identifying biomarkers in IPF would be beneficial in many ways. It would improve the ability to identify patients at risk for developing IPF leading to earlier diagnosis, could determine patient's baseline prognosis, could stage disease severity or allow for monitoring for progression (Prognostic biomarkers). Biomarkers could also be useful for identifying target engagement with a specific mechanistic response or predicting response or toxicity to therapy, either by identifying subgroups that are most likely to respond to therapy or serving as a measurable substitute for a clinically meaningful outcome (315, 316).

There are two fundamentally different approaches for biomarker discovery: a hypothesis-based approach where a candidate biomarker is selected based on preexisting evidence or an unbiased approach. The candidate biomarker has been the approach taken by the majority of the biomarker studies in IPF. The advantage of this approach is that it is supported by strong biological evidence and preliminary data but lacks efficiency in the discovery process. Next is the unbiased or hypothesis-free approach that explores systems biology methods whether genomic, transcriptomic, or proteomic to screen a large number of candidate markers for their association with the disease, greatly increasing efficiency and scope of the discovery process but also increasing the risk of false discovery. For biomarker studies, measurements from easily accessible body fluids or tissues are preferred (e.g. blood/serum and urine). Molecular markers

require a wide range of validation across gender, ages, ethnicities and disease severity to create generalization across the study (317, 318). Over the past decade, the pathogenic paradigm of IPF has shifted to alveolar epithelial stress and dysfunction resulting in activation of profibrotic signaling pathways, fibroblast proliferation and continuous ECM deposition (1, 319). The resulting epithelium destruction leads to organ dysfunction, shortness of breath and exercise limitation and ultimately death from respiratory failure.

Genetic changes that contribute to AEC dysfunction involve mutations in genes encoding surfactant proteins (SP) A and D and mucin1/krebs von den Lugen-6 (KL-6). These polymorphisms or the respective proteins have been evaluated as both diagnostic and prognostic biomarkers for IPF (320-322). Short telomeres have been associated with the risk of developing IPF, (323); with further validation telomere length holds promise as a mechanistic biomarker to help predict disease prognosis. Further studies will also be necessary to determine whether the cytoskeletal protein, cytokeratin 18 that's upregulated in the serum of IPF patients could serve as an efficient marker for drugs intended to target ER-stress or AEC apoptotic pathways.

Additionally, proteins involved in innate immunity such as toll-like receptor 3 (TLR3) (324), ELMOD2 (325, 326), toll-interacting protein (TOLLIP) (327), alpha defensin (328), CCL18 expression (143), and YKL40 which is elevated in serum and BALF (329, 330) have all been studied as potential biomarkers of IPF. Changes in the adaptive immune response that affect T cells, chemokines and autoantibodies have also been evaluated. Anti-HSP70 antibodies were identified in IPF patients (331), as were high levels of CXCL13 in the blood and lung tissue of IPF patients (332). IPF patients also had lower percentages of CD28+CD4+ T cells in the peripheral blood (53) suggesting a defect in T cell activation. Quantification of the genes CD28, ICOS, LCK and ITK that are involved in T cell activation correlated with the percentage of

peripheral blood CD4+CD28+ T cells (333). Finally, proteins that play a role in fibroproliferation and ECM remodeling have also been examined as potential biomarkers of IPF. These proteins include metalloproteinases (MMPs), matricellular proteins and circulating fibrocytes. Several MMPs are of interest in the pathobiology of IPF because of their role in the ECM as well as tissue remodeling. In a recent multi-center observational study, it was reported that concentrations of protein fragments generated by MMP activity were increased in the serum of IPF patients compared to controls (334). Matricellular proteins, OPN and periostin are highly expressed in the lung tissue of IPF patients who had progressive disease (198, 258, 320). Serum levels of periostin were also elevated in IPF patients and correlated to disease progression. Finally, fibrocytes were assessed as potential biomarkers for activity and progression of IPF (197). It was reported that fibrocytes were present in IPF but not control lung tissues, along with higher numbers of fibrocytes in circulation of IPF patients compared to controls (197). These data suggest that fibrocytes in circulation may allow for early prediction of mortality in IPF patients since the presence of fibrocytes was associated with worse survival.

Integrins have been studied extensively for their role in TGFβ activation. In a study phenotyping tissue biopsies from ILD patients, Saini and colleagues used immunostaining to show that there were high levels of αSMA, alphaVbeta6, Pro-surfactant protein-C (SPC), human growth factor, tenascin-C and fibroblastic foci present in the tissue of ILD patients (335). The relationship of all the proteins to survival was also analyzed but only alphaVbeta6 showed an association with mortality (335).

There is still a need to identify pivotal mediators that may contribute to fibrosis and serve as clinically relevant biomarkers; in this study we used an unbiased hypothesis-free approach to explore potential biomarkers in plasma from IPF patients compared to controls. We utilized

novel reagents (Slow Off-rate Modified Aptamers, or SOMAmer reagents) (336, 337), in an assay that uses modified nucleotide bases to offer expanded diversity for interactions, in particular hydrophobic groups similar to amino acid residues. Modifications on nucleotides also significantly improve the ability to select SOMAmers for various protein targets with excellent affinity. Plasma from IPF patients was assayed using this technology and samples were analyzed for proteins that predicted progression free survival in IPF. Serum biomarkers in IPF may provide deeper insights into the disease pathogenesis suggesting new therapeutic approaches; in addition, they could be useful surrogate outcome measures to predict later clinical benefits.

Summary

Despite improvements in the clinical classification of patients with UIP, the pathological lesion of IPF, there is still no cure for this fatal disease. Recent advances have led to more persistent models of experimental fibrosis and have created systems to allow for studies to target specific cell types as well as proteins that may play a role in lung fibrosis. Although these models still don't recapitulate all the features of IPF pathogenesis they allow for specific analyses of signaling pathways and interactions among various cell types. Thus, we have taken advantage of animal models in our investigations.

In the work that is discussed in this dissertation, we expanded our knowledge of how viruses and bacteria may or may not contribute to the exacerbation of established fibrosis and analyzed the cytokine signaling pathways that may regulate pathogen-augmented fibrosis. Our results suggest that the ability of a pathogen to augment fibrosis may be restricted to certain pathogen types. In addition, we utilized novel transgenic and chimeric mouse approaches to address the relevance of fibrocytes and their ability to secrete periostin in the development of fibrosis. We

demonstrated that periostin derived from fibrocytes increased XIAP, leading to apoptosis-resistant myofibroblasts. We also proved that fibrocytes function via these paracrine interactions as opposed to differentiation into myofibroblasts. We showed periostin, CTGF and TGFβ co-regulation pathways lead to the progression of fibrosis. Finally, this work also identified different proteins in the plasma of IPF patients that relate to immune response, protease and angiogenesis as predictors of IPF progression.

The dissertation is outlined in the following manner:

Chapter 1: The background related to all projects relevant to the dissertation.

Chapter 2: The methods utilized in these projects and the reagents, animals and human subject data collected to address the biological questions of relevance to future chapters.

Chapter 3: How do infections whether viral or bacterial exacerbates lung fibrosis? Results of this chapter were published in *Am. J Physiol. Lung Cell Mol. Physiol*.

Chapter 4: How does periostin production by fibrocytes contribute to the pathogenesis of pulmonary fibrosis? Results of this chapter are in revision for *Mucosal Immunology*.

Chapter 5: What is the effect of periostin on the accumulation of apoptosis-resistant myofibroblasts during lung fibrosis? Results of this chapter were published in *Am. J Resp Cell and Mol. Biol*

Chapter 6: Can we use a proteomic approach to identify biomarkers that could play a role in disease progression and provide prognostic information for IPF patients? Results in this chapter have been submitted for publication.

Chapter 7: Conclusions and Future Directions.

Chapter 2:

Materials and Methods

Animals

Male wild type C57BL/6(B6, Ly5.1, and CD45.2) mice were obtained from The Jackson Laboratory (Bar Harbor, ME). A number of different knockout mice were used for these studies. $XIAP^{-/y}$ and wild type littermate control mice were bred at the University of Michigan. Because XIAP is an X-linked gene, male mice carrying a non-functional XIAP allele were designated as $XIAP^{-/y}$ and are devoid of XIAP expression (338). $Periostin^{-/-}$ mice were bred at the University of Michigan. These mice were originally purchased from Jackson laboratory on a 129SvEvbackground but were backcrossed for eight generations onto the C57BL/6 background. For these studies wild-type C57BL/6 (B6) age and sex-matched mice were obtained from The Jackson Laboratory. Collagen-1A2-CRE mice were a generous gift from Paul Noble and were bred in the Unit for Laboratory Animal Medicine (ULAM). ROSA-Floxed-DTR mice were obtained from the Jackson laboratory. Crossing Collagen1a2-Cre mice with ROSA-floxed stop DTR mice generated collagen-1A2-CRE-DTR transgenic mice. These mice were used as bone marrow transplant donors to irradiated C57BL/6 (CD45.2) recipients so that donor vs recipient host cells could be distinguished by staining with CD45.1 and CD45.2 alleles using antibodies that are commercially available from BD PharMingen (San Diego, CA).

Both male and female mice were used in various studies between 6- 10 weeks of age. Mice were housed under pathogen-free conditions and provided food and water ad libitum. All animal experiments complied with the university and federal guidelines for humane use and care. Animals were anesthetized by i.p administration of 200 µl of a sterile solution of ketamine, xyaline and saline when required. All mice were euthanized by CO_2 asphyxiation.

Human Subjects

Plasma samples from 60 IPF patients were used in the SOMAmer high throughput screen studies. Patients were enrolled in the COMET multi-center, observational cohort study of well-defined IPF patients that were followed at 16 week intervals out to approximately 80 weeks (NCT01071707); our subcohort consisted of 60 patients diagnosed by characteristic CT or pathology on lung biopsy with available baseline plasma and known 80-week progression status. Subjects underwent baseline assessment, including demographics, patient-reported descriptors, spirometry, diffusion capacity for carbon monoxide (DL_{CO}), 6-minute walk testing and high resolution CT. Patients remained on their current therapy. The combined endpoint was progression-free survival determined by the time until any of the following: death, acute exacerbation of IPF, lung transplant, or relative decrease in forced vital capacity (FVC, liters) of ≥10% or DL_{CO} ($ml \cdot min^{-1} \cdot mmHg^{-1}$) of 15%. Each site received local Institutional Review Board approval. Studies and consent procedures were performed in accordance with the Declaration of Helsinki at the University of Michigan. All human subjects gave written informed consent. Peripheral blood was collected in EDTA-containing vacutainers at study centers and was shipped cold overnight to University of Michigan. Whole blood was centrifuged at 2500 rpm for 10 minutes and plasma was collected, aliquoted and frozen (-80^{o}C). Samples shipped to

SomaLogics were diluted to 3 different concentrations for analysis at optimal concentrations for each SOMAmer.

Bone Marrow Transplant

Recipient mice were treated with 13 Gy total body irradiation using a cesium 137 irradiator, delivered in two doses separated by 3 hours. Whole bone marrow was harvested from the femur and tibia of collagen1a2-CRE-DTR donor mice and resuspended in serum-free medium (SFM; DMEM, 0.1% BSA, 1% penicillin-streptomycin, 1% L-glutamine and 0.1% Amphotericin B). Donor bone marrow cells ($5x\ 10^6$) were injected via the tail vein into irradiated C57BL/6(CD45.2) recipient mice. Mice were given acid water (ph3.3) for the first 3 weeks after BMT. All experiments with BMT mice were performed 5-6 weeks post-BMT. Total numbers of hematopoietic cells were fully reconstituted in the lungs and spleen at this timepoint, with the percentage of donor-derived cells being 93% (339).

Harvesting Alveolar Macrophages (AMs)

Resident AMs were harvested from mice by *ex vivo* broncheoalveolar lavage using a previously described protocol(340). Briefly, AMs were collected in complete medium (DMEM, 10% fetal-calf serum (FCS), 1% penicillin-streptomycin, 1% $_L$-glutamine, 0.1% Fungizone) and 5mM EDTA. Red blood cells were lysed with 3 mL of RBC lysis buffer for 2 mins on ice, and then diluted in 10 mls of Dulbecco's phosphate buffered saline (PBS). Cells were enumerated on a hemocytometer by trypan blue exclusion before plating.

P.aeruginosa PA01 and FITC Labeling

A culture of *P.aeruginosa* was grown in tryptic soy broth (Difco, Franklin, NJ). The culture concentration was determined using absorbance measurements as previously described

(341). For FITC labeling, *P.aeruginosa* culture was centrifuged and washed two times by resuspending the pellet in 1mL of sterile PBS and transferred to a new tube. The bacteria was heat killed by autoclaving for 20 mins then resuspended at 10^9-10^{10} colony forming units per mL (CFU/mL) in 0.1 mL in 0.1M NAHCO3 (pH 9.2). A total of 0.2mg/mL FITC (Sigma Aldrich, St Louis, MO) in DMSO was added to the heat killed *P.aeruginosa* and allowed to incubate in the dark for 1 hour at room temperature with constant shaking. Following FITC-labeling, heat killed *P aeruginosa* was washed three times and resuspended in sterile PBS at 6 x10^9 CFU/mL.

Infection with P. aeruginosa

As previously described, *P. aeruginosa* PA01 inoculum was prepared for injection into mice. Mice were anesthetized and i.t injected with 50 uL of inoculum equivalent to a sublethal dose of 5 x 10^5 CFU as previously described (340, 342).

Quantification of Bacterial Burden in the Blood and Lung

Mice were euthanized 24h following i.t infection with *P. aeruginosa*. Blood and whole lung samples were collected from each mouse and bacterial burden in whole lung and blood samples were analyzed by CFU assay as previously described (342). Data are expressed as total CFU per lung.

In Vitro Phagocytosis Assay

AMs phagocytosis of FITC-labeled *P. aeruginosa* was measured in vitro as previously described (343). Briefly, AMs were harvested and the ability of AMs from saline (control) and bleomycin-treated mice to phagocytize bacteria was assessed. Cells were plated out at 2 x10^5 cells per well in 100uL of complete media on a 96-well, flat-bottomed, half-area tissue culture plate (Costar) and cultured overnight. The following day the media was aspirated and replaced

with 100 uL of SFM. AMs were incubated at 37° C with FITC-labeled *P. aeruginosa* at 300:1 multiplicity of infection. Two hours post-incubation, 50 μL of trypan blue (250 μg/mL in 0.09 M Citrate buffer solutions, Sigma) was added to each well to quench fluorescence of non-phagocytized FITC labeled *P. aeruginosa*. AMs phagocytosis of FITC-labeled bacteria was measured using a microplate fluorimeter and expressed in arbitrary fluorescence intensity units. For differences in AM cell numbers that adhered to the plate, data were normalized for cell number using a LDH Cytoxicity Detection Kit (Roche Diagnostics) as previously described (342).

Bacterial Killing and Tetrazolium Dye Reduction Assay

AMs were isolated from BALs of saline control and bleomycin-treated mice. The ability of AMs from control and bleomycin-treated mice to kill *P. aeruginosa* was quantified using tetrazolium dye reduction assay as described elsewhere(344). Briefly, AMs from saline or bleomycin-treated mice were plated at $2X10^5$ cells per well on to two 96-well tissue culture plate; one control (4°C) and one experimental (37°C). Cells on both plates were infected with IgG-opsonized *P. aeruginosa* at 50:1 multiplicity of infection for 30 mins at 37°C. Cells on experimental plate were washed and incubated for 2h at 37°C, whereas cells on control plate were washed and lysed in 0.5% saponin in tryptic soy broth (Sigma) and placed at 4°C. After 2h, the experimental plate was washed and lysed in 0.5% saponin in tryptic soy broth. Both plates were then incubated at 37°C for 3 hours. Five mg/mL of MTT (sigma) was added to each plate and incubated for 30 mins or until a purple precipitate was visible. Solubilization solution was added to dissolve the formazan salts and the absorbance was measured at 595nm. Results were expressed as a percentage of survival of ingested bacteria normalized to percentage of control, where A_{595} experiment values were divided by the average of the A_{595} control values. Survival of

ingested bacteria =(A_{595} experimental/ A_{595} control) x 100%. The results were expressed as "percent of control' to indicate the percentage survival of ingested bacteria normalized to the percentage of control.

Viral Infection

Mice were anesthetized and infected intranasally with 50 plaque-forming units (PFU) of Influenza A virus (A/PR/8/34(H1N1), 5 x10^4 PFU of γHV-68 clone WUMS (American Type Culture Collection, Manassas, VA) or 5 x10^4 PFU ΔORF72 (a v-cyclin mutant virus described previously) in 20μL saline. Other mice were mock infected with 20 μL saline.

Viral Plaque Assay

3T12 cells (American Type Culture Collection) were cultured in DMEM with 4% FBS, harvested using trypsin digestion and added to 12-well plates at 8.33 x 10^4 cells per well. The cells were incubated overnight to confirm greater than 70% confluence. Whole lungs from infected mice were homogenized in 2 mLs DMEM with complete® protease inhibitor cocktail (Roche diagnostics) and Triton X-100 (7μL/7mL media; Sigma. St Louis, MO) then centrifuged at 1500 rpm for 5 minutes at 4°C. Dilutions were made in DMEM from the supernatant. 250 μL of each dilution was placed on the 3T12 cells; the plates were then incubated at 37°C and rocked every 15mins for 1 hour. The inoculum was not removed and overlaid with 0.75% carboxymethylcellulose and 2X MEM with 10% FBS was layered onto the cell monolayers. The plates were incubated at 37°C. On day 6, the overlay was removed and the cells were fixed and stained with 70% methanol and 0.35% methylene blue to assess plaque formation.

Total Lung Leukocyte Preparation

Whole lung samples were harvested from mice and collagenase-digested as previously described (343). Briefly, lungs were collected, minced and enzymatically digested for 30 mins using 15 mL/lung of digestion buffer (complete media, 1mg/mL collagenase and 30μg/mL DNase). The undigested tissue fragments were further dispersed by repeated passage through a 10mL syringe. The total cell suspension was pelleted and red blood cells lysed with RBC lysis buffer as described above. Cells were centrifuged and resuspended in 5 mLs SFM, where the cells were again dispersed by passing through a 10 mL syringe 20 times. The dispersed cells were filtered through a Nytex filter (Sefar, Depew, NY) to remove clumps. The final volume was brought up to 10mL with complete media. An equal volume of 40% Percoll (Sigma) in complete media was added, and the cells were centrifuged at 3000 rpm for 20 mins with no brake. The cell pellets were resuspended in complete media and total leukocytes were counted on a hemacytometer by trypan blue exclusion. Differential analysis was done using the BAL cells and total lung cells isolated from the collagenase-digested whole lung samples to determine the percentage of neutrophils, eosinophils, monocytes/macrophages and lymphocytes as previously described (343).

Flow Cytometry

Whole lungs were enzymatically digested using collagenase and DNase(93) and leukocytes were isolated. Leukocytes were incubated with Fc block (1:100) clone 24G2 (BD Pharmingen, San Diego, CA) for 15mins, then stained with CD45-PerCPCy5.5, CD4-PE, CD8-FITC (1:500 dilution, BD Pharmingen) to label cell surface markers. To assess fibrocyte markers, surface-stained cells were then followed by fixation/permeabilization using the BD Pharmingen

Cytofix/cytoperm kit according to manufacturer's instructions. Cells were washed twice and then incubated with rabbit anti-mouse collagen I (1:400, Rockland, Immunochemicals, Gelbertville, PA) or rabbit IgG 1:2000, Jackson ImmunoResearch, West Grove, PA) as an isotype control and secondary antibody Donkey anti-rabbit PE (1:200, Jackson ImmunoResearch). Cells were analyzed on the flow cytometer (FACScan, BD Biosciences, Mountain View, CA). The cells were further analyzed using the Flow Jo software (FlowJo LLC, Ashland, OR).

Bleomycin Injections

For bleomycin experiments, mice were given bleomycin (0.025 U (Sigma) dissolved in sterile saline in a 50-µl volume) intratracheally as described previously(93) or via oropharyngeal aspiration. In some experiments, AT-406, an orally bioactive Smac/Diablo mimetic, which was provided by Dr. Wang's laboratory (345), was administered at a dose of 100 mg/kg by oral gavage daily starting either on day 0 or day 10 post-bleomycin.

Mesenchymal Cell Isolation

Lung mesenchymal cells were grown for two weeks from lung minces. At this time, all cells expressed collagen I and were designated lung mesenchymal cells. In some experiments, mesenchymal cells were magnetically sorted for expression of CD45 to obtain $CD45^+$ collagen I^+ fibrocytes or $CD45^-$ collagen I^+ fibroblasts as previously described (94). Briefly, labeled cells were then sorted using LS-positive selection columns using a SuperMacs apparatus (Miltenyi Biotech) according to manufacturer's instructions. For extra purity, CD45+ cells were sometimes reapplied to a second LS-positive selection column.

Adoptive Transfer

Fibrocytes were purified by magnetic separation from lung mince cultures from untreated wild-type or periostin$^{-/-}$ mice as described above. 5×10^5 fibrocytes were injected via tail vein in a 200-μl volume into mice that had received bleomycin inoculation intratracheally 4 d previously. Mice were harvested and lungs collected on day 21 after bleomycin, and lung collagen content was determined by hydroxyproline assay.

Type II Alveolar Epithelial Cells (AEC) Purification

Type II AECs were isolated using dispase and DNase digestion of the lower lungs as previously described (346). Bone marrow-derived cells were removed via anti-CD45 and anti-CD32 magnetic bead depletion. Mesenchymal cells were removed by overnight adherence to tissue culture plates. After the initial plating, AECS were isolated from the remainder of non-adherent cells by putting the non-adherent cells on fibronectin-coated tissue culture plates. Cells were harvested or treated 3 days after adhering to the fibronectin-coated plates.

Lung Histology

Hematoxylin and eosin (H&E) and Picrosirius Red staining were done as previously reported (93, 347).

Lung Collagen Measurements

Collagen deposition in the lungs of all mice from each treatment group was measured using a hydroxyproline assay as described previously (93). Hydroxyproline is a useful surrogate for measuring collagen content because elastin is the only mammalian protein besides collagen that contains hydroxyproline. Mice were euthanized and perfused via the heart with 5 mLs of PBS. Individual lobes were removed and homogenized in 1mL PBS with protease inhibitor, then 500 μL of the homogenate was hydrolyzed by the addition of 500 μL of 12N hydrochloric acid

(HCL). Samples were then incubated in the oven overnight at 120°C. Aliquots (5 μL) were then assayed by adding Chloramine T solution for 20 mins followed by development with Erlich's reagent at 65°C for 15 mins. Absorbance was measured 540 nm, and the amount of hydroxyproline was determined against a standard curve generated using known concentrations of hydroxyproline standard (Sigma).

In vivo Apoptosis Assessments

To assess total apoptosis in the whole lung lysate, active caspase 3/7 levels were measured using Promega Caspase-Glo 3/7 Assay, according to manufacturer's protocol. Samples were analyzed using a Veritas Microplate Luminometer and results normalized to the PBS treated lungs. Immunostaining for TUNEL and α-smooth muscle actin was done as previously described (347).

In vitro Apoptosis Assay

Mesenchymal cell apoptosis was induced by treatment with activating anti-Fas antibody CH11 (Millipore, Billercia, MA) and assessed through identification of caspase 3/7 activity as previously described (347).

Enzyme-linked Immunoassay/ELISA

Whole lung homogenates were prepared for analysis of cytokines and chemokines as described previously (343). Each ELISA assay was done using a Duoset ELISA kit (R&D systems, Minneapolis, MN) according to manufacturer's instructions. Some of the ELISA measurements for TGFβ and periostin were performed on lung mesenchymal cells supernatants according to manufacturers' instructions. The CTGF ELISA was purchased from NeoBiolab

(Cambridge, Massachusetts) and the levels of CTGF were assessed in fibrocyte supernatants post-bleomycin treatment according to manufacturers' instructions.

Western Blot

4×10^5 AECs, primary fibrocytes or fibroblasts were plated per well on a 6- well tissue culture plates. After treatment cells were washed with cold PBS and lysed in radioimmunoprecipitation assay (RIPA) buffer with protease inhibitor cocktail [Sigma]) for 15 min at 4°C and centrifuged. Total protein concentrations in each sample were determined using the Bicinchoninic acid assay (Thermo Scientific, Rockford, IL). 5 to 10 μg of protein from each lysate was separated on a 4-20% gradient SDS-polyacrylamide gel (Invitrogen, Carlsbad, CA) and transferred to a PVDF membrane (Amersham/GE Healthcare, Pittsburgh, PA). For some experiments PVDF membranes were probed with rabbit polyclonal poly ADP ribose polymerase (PARP), GAPDH, SMAD3 (Cell signaling, Beverly, MA), monoclonal αSMA and β-Actin (Sigma) as a loading control.

Semiquantitative real-time RT-PCR

Semiquantitative real time RT-PCR was performed on an Applied Biosytems StepOne Plus thermocycler (Applied Biosystems, Foster City, CA). Gene specific primers and probes were designed using GeneScript online software (Piscataway, NJ). Sequences for primers and probes used can be found in Table 1. LOX expression was measured using Taqman® Probes based assay (Applied Biosystems, Foster City, CA). RNA was extracted from the BAL cells or left lung or mesenchymal cells using TRIzol reagent (Invitrogen, Carlsbad, CA) then used in the real-time PCR. Gene specific primers and probes were purchased from Sigma-Aldrich (St Louis, MO). Relative expression was calculated using the comparative C_T method with beta actin (β-actin) as an internal standard gene control. Fold change in mRNA was quantified using the $\Delta\Delta C_T$

method**.** Additionally, RNA isolated from bleomycin-treated WT and periostin $^{-/-}$ fibrocytes was analyzed using the Mouse Fibrosis RT^2 Profiler ^{TM} PCR Array (PAM120ZE-4) and then confirmed using gene specific primers and probes as previously described.

Table 1: List of primers and probes used for the real-RT-PCR experiments

Gene Name	Oligo	Sequences (5'- 3')		
Beta Actin	**Forward**	**CCGTGAAAGATGACCCAGATC**		
	Reverse	**CACAGCCTGGATGGCTACGT**		
	Probe	**TTTGAGACCTTCAACACCCCCAGCCA**		
Integrin Alpha1	**Forward**	**ATTTATCATGGCAGTGGCAA**		
	Reverse	**AATTTCAGCGTCTTCCCATC**		
	Probe	**ATGCGCAACGCATTCCCTCA**		
Integrin AlphaV	**Forward**	**TGAGAATCAAGACACCCGAA**		
	Reverse	**TGATTCCTTTCTCCCTGTCC**		
	Probe	**CGCCGCCGCTGTGTCATT**		
Integrin Beta 1	**Forward**	**CTCCAGAAGGTGGCTTTGAT**		
	Reverse	**TGTTACATTCCTCCAGCCAA**		
	Probe	**TCAGCGATCCACAAACCGCA**		
Integrin Beta 3	**Forward**	**AAGTGGGACACAGCAAACAA**		
	Reverse	**CCGGTAGGTGATATTGGTGA**		
	Probe	**CCGCTGTATAAAGAGGCCACCTCCA**		
Integrin Beta 5	**Forward**	**TACAGTAGCATCCGGGCTAA**		
	Reverse	**CAGGTGGCAGTGAAGAAGAG**		
	Probe	**TGGCTGATCCCACACTGACAGC**		
CTGF	**Forward**	**GAGTGTGCACTGCCAAAGAT**		
	Reverse	**GGCAAGTGCATTGGTATTTG**		
	Probe	**CGCAGCGGTGAGTCCTTCCA**		
PDGFα	**Forward**	**CGAAGTCAGATCCACAGCAT**		
	Reverse	**GGGCTCTCAGACTTGTCTCC**		

	Probe	**CCGGGACCTCCAGCGACTCT**		
ET-1	**Forward**	**CGTATGGACTGGGAGGTTCT**		
	Reverse	**TCTAACTGCCTGGTCTGTGG**		
	Probe	**TCCAGGTCCAAGCGTTCCTTGA**		
DNApol	**Forward**	**ACAGCAGCTGGCCATAAAGG**		
	Reverse	**TCCTGCCCTGGAAAGTGATG**		
	Probe	**CCTCTGGAATGTTGCCTTGCCTCCA**		
gB	**Forward**	**CGCTCATTACGGCCCAAA**		
	Reverse	**ACCACGCCCTGGACAACTC**		
	Probe	**TTGCCTATGACAAGCTGACCACCA**		
cIAP1	**Forward**	**AGCACGCCTGTGGTTAAA**		
	Reverse	**CATTGACGGTCCTGTAGTTCTC**		
	Probe	**TCCTACTGAAGCCCATTTCCAAGGC**		
cIAP2	**Forward**	**CGCAGCAATCGTGCATTT**		
	Reverse	**GCTCCTACTGAAGCCCATTT**		
	Probe	**ATCTTCCGAACTTTCTCCAGGGCC**		
mPOSTN	**Forward**	**GGGGTTGTCACTGTGAACTG**		
	Reverse	**CGGCTGCTCTAAATGATGAA**		
	Probe	**CGTGTCCTGACACAAATTGG**		
COL I	**Forward**	**TGACTGGAAGAGCGGAGAGTACT**		
	Reverse	**GGTCTGACCTGTCTCCATGTTG**		
	Probe	**CTGCAACCTGGACGCCATCAAGG**		

Reagents Used

Complete media is DMEM (Lonza, Walkersville, MD) with 10% FBS, 1 % penicillin-streptomycin, 1% L-glutamine, and 0.1% Amphotericin B (Lonza). SFM is DMEM with 0.1% bovine serum albumin (Sigma), 1% penicillin-streptomycin, 1% L-glutamine and 0.1% Amphotericin B.

Statistical Analysis

Statistical analysis was measured by analysis of variance or Student t test using GraphPad Prism 6 software (San Diego, CA). Comparisons between three or more experimental groups were performed with ANOVA. Data shown represents SEM+/-, $P < 0.05$ was considered significant.

For the proteomic studies assessing biomarkers in the plasma from IPF patients; each SOMAmer analyte is reported in relative fluorescent units (RFU) and is directly proportional to the amount of native protein in the sample. Steps in constructing the disease progression index:

1. Ability of each continuous biomarker to predict IPF progression status at 80 weeks was evaluated via ROC curves and a biomarker threshold was chosen to maximize combined sensitivity plus specificity. Estimated AUC > 0.7 from ROC analysis of the biomarker as a binary variable (above versus below its threshold) was required for further consideration.
2. Both unadjusted and adjusted odds ratios for 80-week progression were estimated separately via logistic regression. Adjustment factors included age, gender, smoking status, baseline percent predicted FVC and baseline percent predicted DL_{CO}. Biomarker threshold variables had to maintain statistical significance at the 0.05 level in both unadjusted and adjusted analyses, and odds ratios from these models had to maintain the same direction of association
3. To ensure independent prognostic ability of biomarker threshold variables when used in combination, both multivariable logistic and Cox regression models were investigated. Based on available sample size, a limit of four biomarker threshold variables in each multivariable model was enforced to prevent model instability. Automated model selection via the score method identified the top four binary biomarkers based on (a)

multivariable logistic regression predicting 80-week progression status and (b) multivariable Cox proportional hazard regression predicting time to progression over the 80 week follow-up period. Between the two models, 6 unique biomarker threshold variables were identified with $p < 0.05$ for predicting either 80-week progression status or time-to-progression; these were used to create the IPF progression index.

4. For the 6-biomarker threshold variables used in the index, we estimated the difference in progression-free days during the first 80 weeks of follow-up using area between Kaplan-Meier estimates of progression-free survival for those above and below each biomarker threshold. These differences were used to generate a weighted numeric score.
5. To calculate this score, for each patient, if baseline levels of LGMN were below 5173.33 RFU, then the score got +3; if FCN2 was below 2015.33 RFU, then the score got +2; if VEGFsR2 was below 9559.30 RFU, then the score got +1; if Cath-S was below 1451.44 RFU, then the score got +1; if TRY3 went above 928.22 RFU, then the score got +2; if ICOS went above 8032.61 RFU, then the score got +2. This generates a score for each patient accounting for all 6 biomarkers on a scale of 0 to 11.

Analyses evaluating the IPF progression index were then conducted. Three severity groups based on the index were created and evaluated via Cox regression and ROC analysis. Progression-free Kaplan-Meier survival curves for the 3 severity groups were displayed. We performed boot-strap analysis to determine how this index would perform theoretically in additional patient cohorts. Analyses were performed using SAS 9.4 (SAS Institute, Inc.), with plots created using R 3.2.0 (The R Foundation for Statistical Computing Platform).

Chapter 3:

γ-Herpesvirus-68, but not *Pseudomonas aeruginosa* or Influenza A (H1N1) Exacerbate Established Murine Lung Fibrosis

Background

Fibrosis is a condition characterized by the deposition of extracellular matrix (ECM) proteins such as collagen and fibronectin causing stiffening of interstitial tissue or airways when it occurs in the lung. Fibrosis can be triggered by known agents such as allergens, toxic chemicals and radiation or can occur for unknown reasons such as in the case of idiopathic pulmonary fibrosis (IPF) (348). IPF is a progressive disease eventually causing death from respiratory insufficiency usually within 2-5 years of diagnosis. Lung transplantation is the only proven therapy in the United States and this procedure has a median patient survival rate of 3 years (349). The pathogenesis of IPF remains unknown but key events likely involve continuous cycles of injury and abnormal repair with evidence suggesting that the variation in fibrotic lesions is due to repeated lung injury over the course of the disease (350). Chronic viral infection, mainly herpesviruses have been implicated as one cause of ongoing epithelial injury and therefore have been implicated as a cofactor in either the initiation or exacerbation of the disease [reviewed in (351)].

Previous studies have shown the presence of Epstein-Barr virus (EBV), cytomegalovirus, herpes simplex virus 1, as well as human herpesviruses (HHV)-7 and 8 in lung tissue of human IPF patients (113, 114, 116, 352). However, this is somewhat controversial as other studies found no association between herpesviral infection and IPF (353, 354). There is strong evidence in animal models linking γ herpesvirus infection with development of fibrosis in T helper type 2 (Th2) biased mice (119, 120, 355, 356). In these cases, fibrosis was associated with persistent reactivation of the virus and development of alternatively activated macrophages (120, 140, 356, 357). Additionally, infection of aged mice with murine γ herpesvirus-68 (γHV-68) results in development of lung fibrosis (122, 123) and the pathogenic mechanisms have been shown to include epithelial cell stress and apoptosis and enhanced susceptibility of fibroblasts to viral-induced TGFβ secretion.

We previously showed that γHV-68 infection given prior to stimulation with bleomycin or fluorescein isothiocyanate (FITC) augmented development of lung fibrosis (346). Possible mechanisms involved alterations in alveolar epithelial cells such as increased synthesis of cysteinyl leukotrienes, induction of transforming growth factor beta (TGF)-β and recruitment of circulating fibrocytes (346). Similarly, infection of mice with γHV-68 after the establishment of lung fibrosis worsened deposition of collagen within the lung, and this increased fibrosis correlated with enhanced production of IL-13, IFNγ and TNFα (129). Exacerbation of fibrosis required virus capable of replication as UV-inactivated virus did not exacerbate disease (129).

This study aimed to investigate whether the ability to exacerbate established pulmonary fibrosis in mice was unique to γHV-68 or whether other inflammatory/infectious insults could augment fibrosis. Thus, we sought to determine whether an acute bacterial infection with

Pseudomonas aeruginosa (*P. aeruginosa*) or an acute viral infection that does not establish latency, influenza A (H1N1) could augment fibrotic outcomes.

P. aeruginosa is a Gram-negative opportunistic human pathogen which rarely causes disease in healthy individuals. However, *P. aeruginosa* is responsible for life threatening infections in immunocompromised patients, the elderly and following prolonged hospitalization (358). Clearance of *P. aeruginosa* from the lungs requires a functional innate immune system with the involvement of macrophages and polymorphonuclear leukocytes (PMNs)(359). Influenza A is a RNA virus which replicates in the respiratory epithelium leading to the infiltration of inflammatory cells, mainly mononuclear leukocytes and small numbers of PMNs. Innate defense against influenza A infection involves the production of high levels of type I interferons by infected epithelial cells, AMs, recruited conventional dendritic cells (cDCs), PMNs and NK cells (360-362). DCs lining the airways play key roles in activating effector CD8 T cells mediating viral clearance and protection (363, 364). In contrast, γHV-68 can infect a variety of cells within the lung including epithelial cells, fibroblasts, macrophages and B cells (121, 365). There is low level induction of type I interferon and plasmacytoid DCs are necessary to activate cDCs (366). Production of both IFNγ and perforin are important for viral control (367, 368). In this study, bleomycin was used to establish fibrosis in mice, and then, the ability of *P. aeruginosa*, H1N1 and γHV-68 to exacerbate the fibrotic response was examined.

Results

P. aeruginosa infection had no effect on bleomycin-induced pulmonary fibrosis

To determine the effects of *P. aeruginosa* infection on established pulmonary fibrosis, mice were given intratracheal saline or bleomycin on day 0. On day 14, mice were then given 5 x 10^5 CFU P. *aeruginosa* intratracheally or were mock infected. All lungs were harvested on day

21 and lung collagen content was measured by hydroxyproline assay. As expected, bleomycin-treated mice showed significant increases in collagen content when compared to saline controls. However, subsequent infection of bleomycin-treated mice with *P. aeruginosa* showed no significant increase in collagen content when compared to bleomycin-treated mice that were mock infected **(Figure 7).** Thus, *P. aeruginosa* infection in wild type mice did not exacerbate bleomycin-induced fibrotic response in the lungs. Furthermore, at this dose of infection, there was no difference in the survival of bleomycin-treated mice that were mock infected or infected with *P. aeruginosa*.

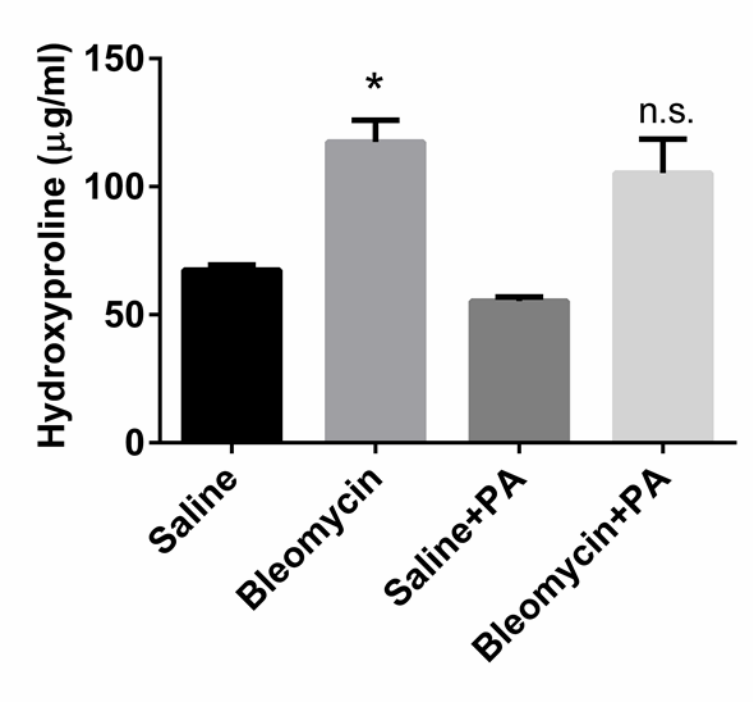

Figure 7: P. aeruginosa infection did not exacerbate bleomycin-induced fibrosis.
Wild-type mice were given bleomycin or saline intratracheally on day 0. On day 14, half of the mice in each group were given *P. aeruginosa* intratracheally or saline as a vehicle control. Lungs were harvested on day 21 for hydroxyproline assay. Data shown represent n= 6-10 mice per group pooled from three independent experiments.

Fibrotic mice did not show increased susceptibility to P. aeruginosa

To determine whether the bleomycin-treated mice were more susceptible to infection with *P. aeruginosa*, mice were treated with saline or bleomycin as previously described. On day 14, both groups of mice were infected with 5 X 10^5 CFU P. *aeruginosa.* Blood and lungs were collected on day 15 (24 h post-infection, a time point noted for maximal bacterial growth post-infection) (342) and plated for CFU assay**.** Mice treated with bleomycin prior to infection with *P. aeruginosa* showed no difference in bacterial load in the lung **(Fig 8A)** or in the blood **(Fig 8B)** compared to mice first treated with saline.

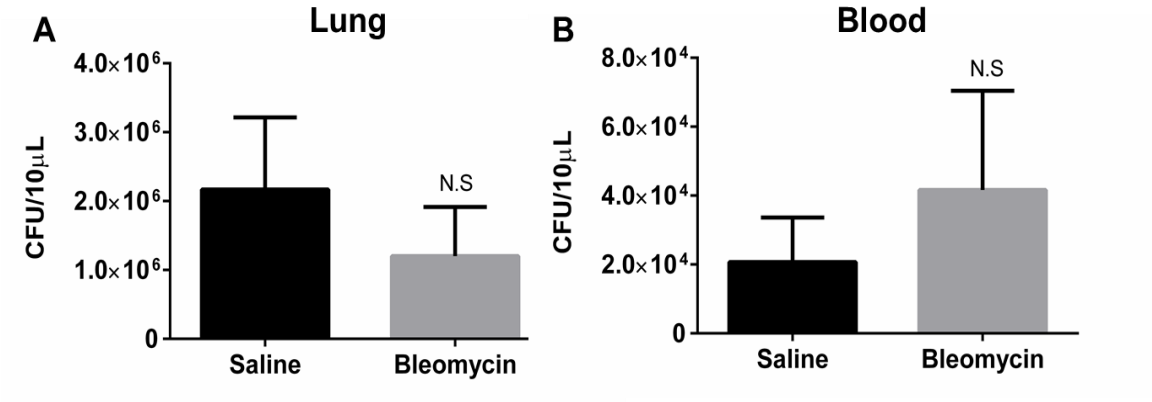

Figure 8: Bleomycin-treated mice showed no defect in the clearance of P. aeruginosa infection.
Mice were first treated with saline or bleomycin on day 0 followed by infection with P. aeruginosa on day 14. On day 15 lungs (A) and blood (B) were collected for CFU analysis. Data represent n=5-8 mice per group from two independent experiments.

H1N1 Influenza A infection did not exacerbate bleomycin-induced fibrosis

To determine whether the exacerbation of established pulmonary fibrosis could occur with an acute viral infection that does not establish latency. Wild type mice were treated with bleomycin or saline on day 0. On day 14, a time of established pulmonary fibrosis, bleomycin-treated mice received 5×10^4 PFU γHV-68 or 50 PFU H1N1 intranasally or were mock infected. These doses were chosen to be non-lethal in control mice. Lungs were harvested on day 21 to

measure lung collagen content by hydroxyproline assay. **Figure 9A** demonstrates that subsequent γHV-68 infection resulted in significantly more collagen deposition in the lungs than did bleomycin treatment followed by mock infection or bleomycin followed by H1N1 infection ($p < 0.05$). These data replicated early findings that γHV-68 can exacerbate established lung fibrosis (129). However, H1N1 was not able to exacerbate fibrosis at day 21.

To see if H1N1 might be able to exacerbate bleomycin-induced fibrosis at an earlier time point that corresponded to expected peak viral replication, mice injected with bleomycin on day 0 were infected with H1N1 on day 18 and lungs were harvested for hydroxyproline content on day 21 **(Figure 9B);** however, no elevations in collagen deposition were noted at this time point either. To determine whether H1N1 or γHV-68 infection altered fibrosis at a later time point, another experiment was set up to harvest lungs at days 21 and 35 following the same initial treatments (**Figure 9C and D**). Levels of fibrosis in γHV-68-infected mice were still the highest of all groups, and the only ones to show significant increases over bleomycin and mock infection. **Figure 10** shows representative histology of lungs from all 3 groups of mice harvested at day 21.

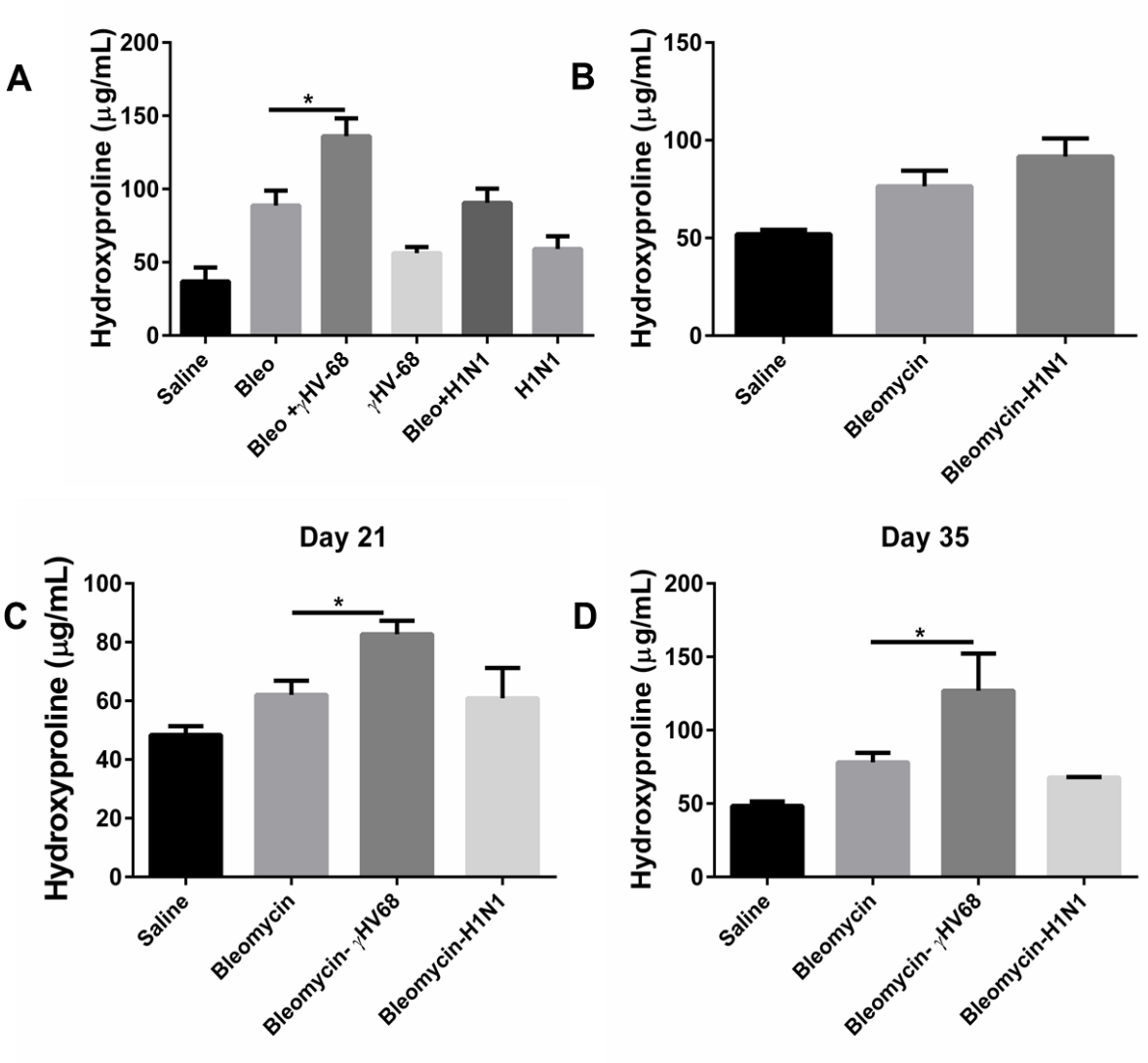

Figure 9: H1N1 infection did not exacerbate bleomycin-induced pulmonary fibrosis. A) Mice were given bleomycin or saline intratracheally on day 0. On day 14, bleomycin or saline-treated mice received γHV-68, H1N1 or saline intranasally. Lungs were harvested for collagen determination on day 21. B) On day 18, bleomycin-treated mice received H1N1 or saline intranasally. Lungs were harvested 3 days post infection to measure collagen content and were compared to mice treated with saline alone. Data represents n=5-8 mice per group collected in two independent experiments. C and D) In a separate experiment, mice were treated with saline or bleomycin on day 0, viral or mock infections occurred at day 14 and lungs were harvested at day 21 or 35; n=3-6 mice per group.

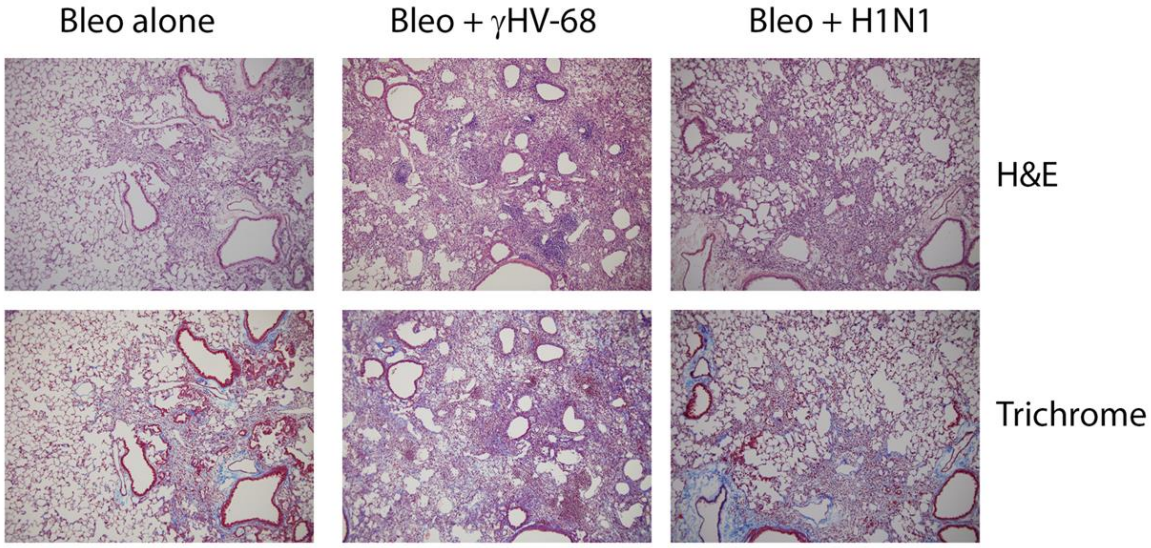

Figure 10: Histologic analyses.
Immunohistochemistry showing representative lungs of mice treated with bleomycin + vehicle control (saline), bleomycin + γHV-68 infection or bleomycin + H1N1 infection. Shown are hematoxylin and eosin or Masson's trichrome staining. Magnification is 200x. Left panels) Mice treated with bleomycin were harvested on day 21 post-injection and show diffuse mononuclear infiltrates and collagen deposition noted as blue coloration in the bottom panel. Middle panels) Mice were infected with bleomycin on day 0 and infected with γHV-68 on day 14. Lungs were harvested on day 21 and show both focal areas of dense mononuclear inflammatory cells as well as diffuse inflammation. Collagen deposition was noted within the interstitium. Right panels) Mice were injected with bleomycin on day 0 and H1N1 on day 14. Lungs were harvested on day 21 and showed diffuse mononuclear infiltration. While collagen deposition was seen within the interstitium, it is similar to that noted in mice treated with bleomycin alone. Overall, the mice treated with bleomycin + γHV-68 showed the greatest degree of lung involvement. Representative of n=4 lungs in each group

γHV-68 replication was enhanced post-bleomycin and the ability to reactivate from latency was required for exacerbation of fibrotic response

To determine the levels of viral replication which were present in the lungs on day 21, total lung RNA was subjected to RT-PCR analysis for expression of the influenza M1 gene **(Figure 11A)** or for the lytic γHV-68 DNA polymerase (DNA pol)**(Figure 11B).** These levels were compared to animals that had been given saline prior to viral infection. Regarding H1N1

infection, expression of M1 was significantly decreased 7 days post-infection (dpi) between mice that were pretreated with saline or pretreated with bleomycin. This suggested that bleomycin administration did not make the mice more susceptible to H1N1 replication measured at 7 dpi. Because of the low level inoculum of H1N1 (50 PFU) or perhaps due to viral clearance, we could not detect virus by plaque assay in the lungs at either day 3 or day 7 post-infection in saline or bleomycin-pretreated mice (data not shown). In contrast, the γHV-68 DNA pol gene was significantly elevated 7 dpi in bleomycin-treated mice when compared to saline-treated mice confirming earlier observations (129). In addition, we were able to demonstrate virus by plaque assay following γHV-68 infection **(Figure 11C)**.

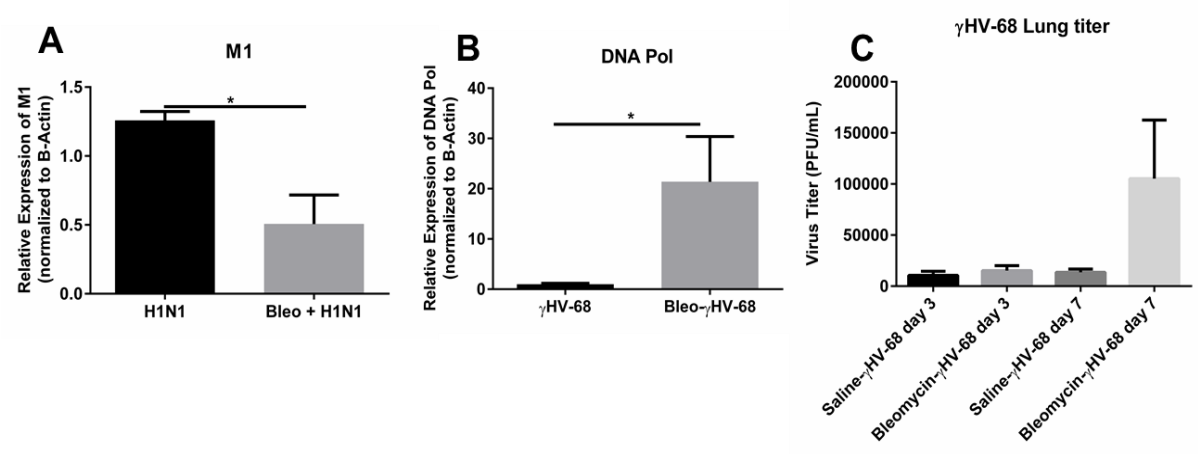

Figure 11: γHV-68 replicated to a greater extent than did H1N1 post-bleomycin.
Mice were injected on day 0 with saline or bleomycin. On day 14 mice were infected with γHV-68 or H1N1. On day 21, lungs were collected and levels of H1N1 viral M1 (A) or γHV-68 DNA polymerase (DNA pol) (B) gene expression were measured by real-time RT-PCR. C) Similarly lungs were collected from mice infected with γHV-68 on days 17 and 21 and virus titers in the lungs were measured by plaque assay. Data shown are from n=3-5 lungs/group representative of 2 experiments.

Exacerbation of lung fibrosis by γHV-68 required the ability to reactivate from latency and was not a property shared by cytomegalovirus (CMV)

A v-cyclin mutant γHV-68 (ΔORF72) is 100-fold decreased in its ability to reactivate from latency (369). In our hands, mice infected with ΔORF72 display decreased replication

within the lung compared to wild-type marker rescue virus by day 3 post-infection (data not shown). To see if on-going viral replication was required to promote fibrosis, we infected bleomycin-treated mice with mock control, marker-rescue virus or ΔORF72 mutant virus and analyzed collagen deposition at day 21 **(Figure 12A).** Wild-type (marker rescue) virus significantly enhanced fibrosis whereas ΔORF72 did not. Surprisingly, infection with a β herpesvirus, CMV did not exacerbate bleomycin-induced fibrosis either **(Figure 12B)**. There was no plaque formation of infectious CMV from the lungs of these C57Bl/6 mice, but the expressions of viral E1 and envelope gB proteins were detectable by real-time RT-PCR (Figure 13).

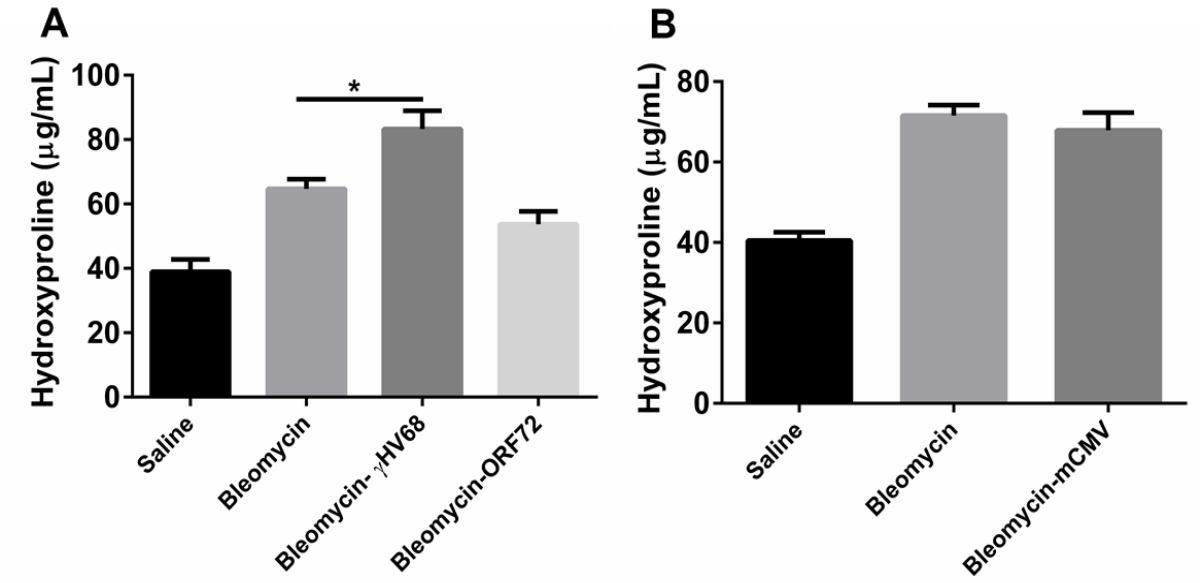

Figure 12: Exacerbation of bleomycin-induced fibrosis was specific to γHV-68 and dependent on viral replication.
Mice were first treated with saline or bleomycin on day 0. On day 14 mice were infected with A) $5x10^4$ PFU of γHV-68 containing a mutation in the v-cyclin gene (ΔORF72) or marker rescue (essentially wild-type) virus or B) 5×10^4 murine cytomegalovirus (CMV) or were mock infected. On day 21, lungs were harvested for collagen determination. Data shown represents n= 5-8 mice per group collected in two independent experiments; *$p<0.05$.

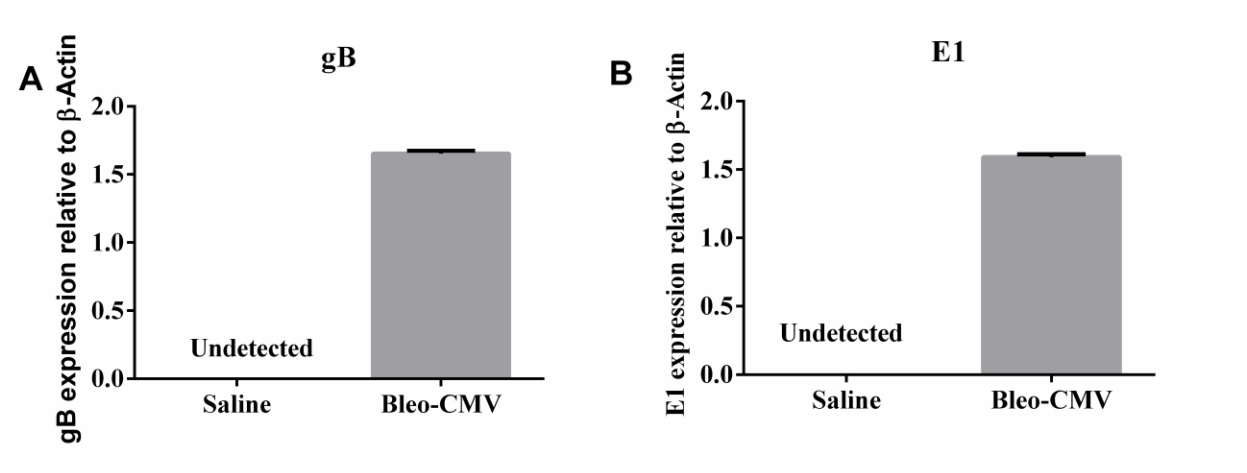

Figure 13: Detection of CMV viral genes in mice post-bleomycin and CMV infection. Mice were injected on day 0 with saline or bleomycin. On day 14 mice were infected with 5 x 10^4 murine cytomegalovirus (CMV) or were mock infected. On day 21, lungs were collected and levels of CMV viral (A) gB and (B) Early 1 (E1) gene expression were measured by real-time RT-PCR. Data shown are from n=3-5 lungs/group representative of 2 experiments.

The profibrotic effects of γHV-68 compared to H1N1 and P. aeruginosa infection were not explained by inflammatory cell recruitment.

To determine whether the inflammatory cell composition was different following the various infections, mice were treated with bleomycin on day 0. Next, bleomycin-treated mice were infected with *P. aeruginosa*, H1N1 or γHV-68 on day 14. Lungs were harvested on days 15 or 21 which represent 1 and 7 dpi respectively. Single cell suspensions were isolated, counted and analyzed by flow cytometry to assess leukocyte populations. As demonstrated in **Figure 14A**, total cells were not different between groups at day 15, but there was a noticeable increase in the percentage of CD45+ leukocytes in the *P. aeruginosa* infected mice at this time point **(Figure 14B)**. This increased percentage of leukocytes in the *P. aeruginosa* group was not maintained at day 21, consistent with rapid clearance of the organism from the lungs **(Figure 14C)**. In contrast, the viral infected mice showed increased percentages of CD45+ leukocytes on

day 21, consistent with the recruitment of leukocytes in response to viral infection. Both H1N1 and γHV-68 infected mice showed similar increases in leukocyte accumulation in the lung **(Figure 14D)**, although histologic evidence in Figure 10 suggests that γHV-68-infected mice showed both diffuse and focal inflammatory infiltrates.

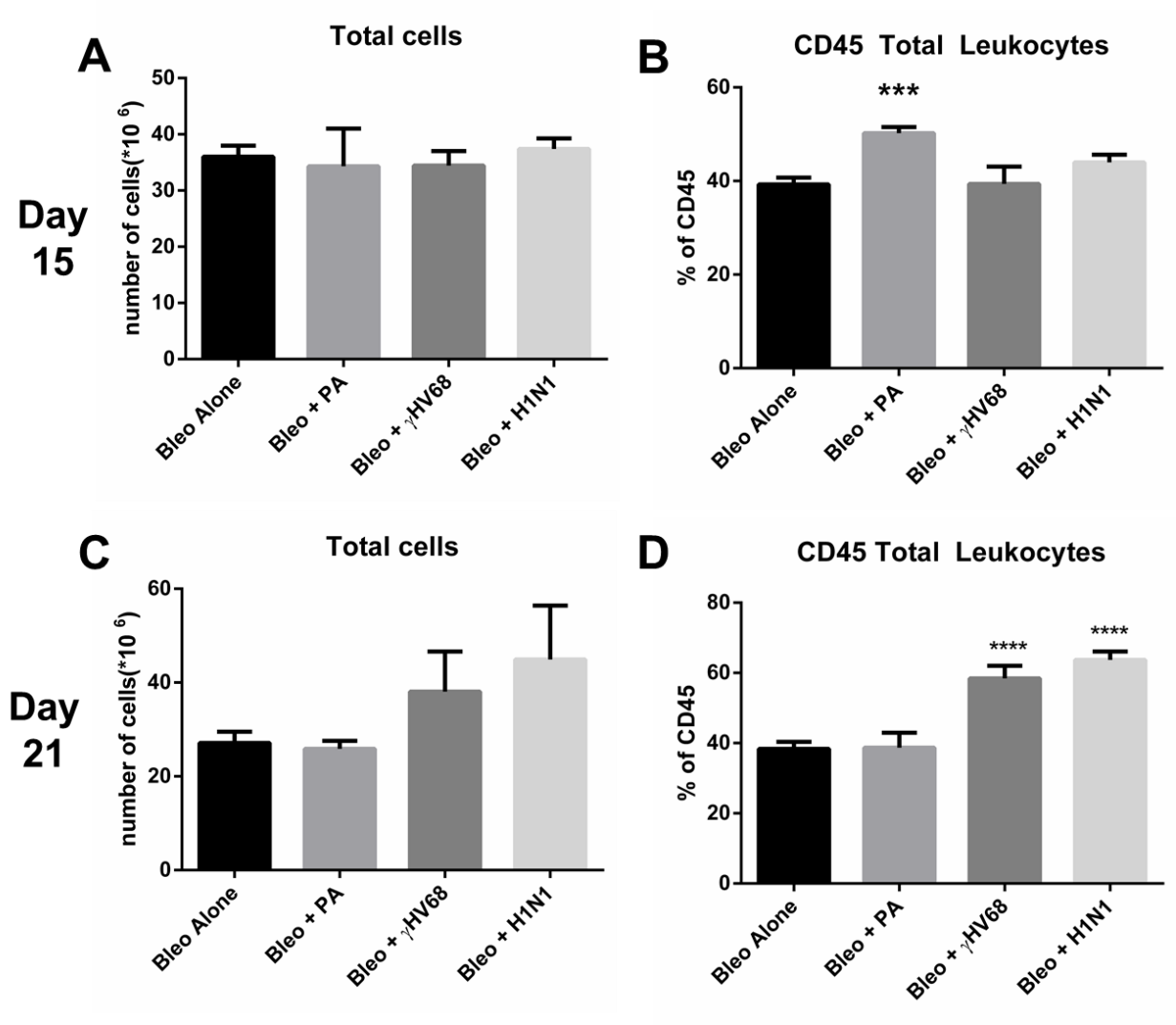

Figure 14: Leukocyte recruitment was enhanced following infection.
Mice were injected with bleomycin on day 0. On day 14, mice were infected with saline, *P. aeruginosa*, H1N1 or γHV-68. Lungs were harvested from n=4 mice each on day 15 or day 21. Total lung leukocytes were enumerated (A and C) and percentage of CD45+ leukocytes were assessed (B and D) by flow cytometry. Data are from one experiment representative of 2.

Because H1N1 infected mice did not exacerbate fibrosis whereas γHV-68 infected mice did, we analyzed the various leukocyte subsets between these two groups. There were no discernable differences in the percentages of CD4, CD8, NK, NK-T, B, monocyte, PMN, or eosinophils between these groups **(Figure 15).** Thus, differential accumulation of leukocyte

subsets could not explain why γHV-68 infection augments fibrotic responses in the lung whereas H1N1 infection did not.

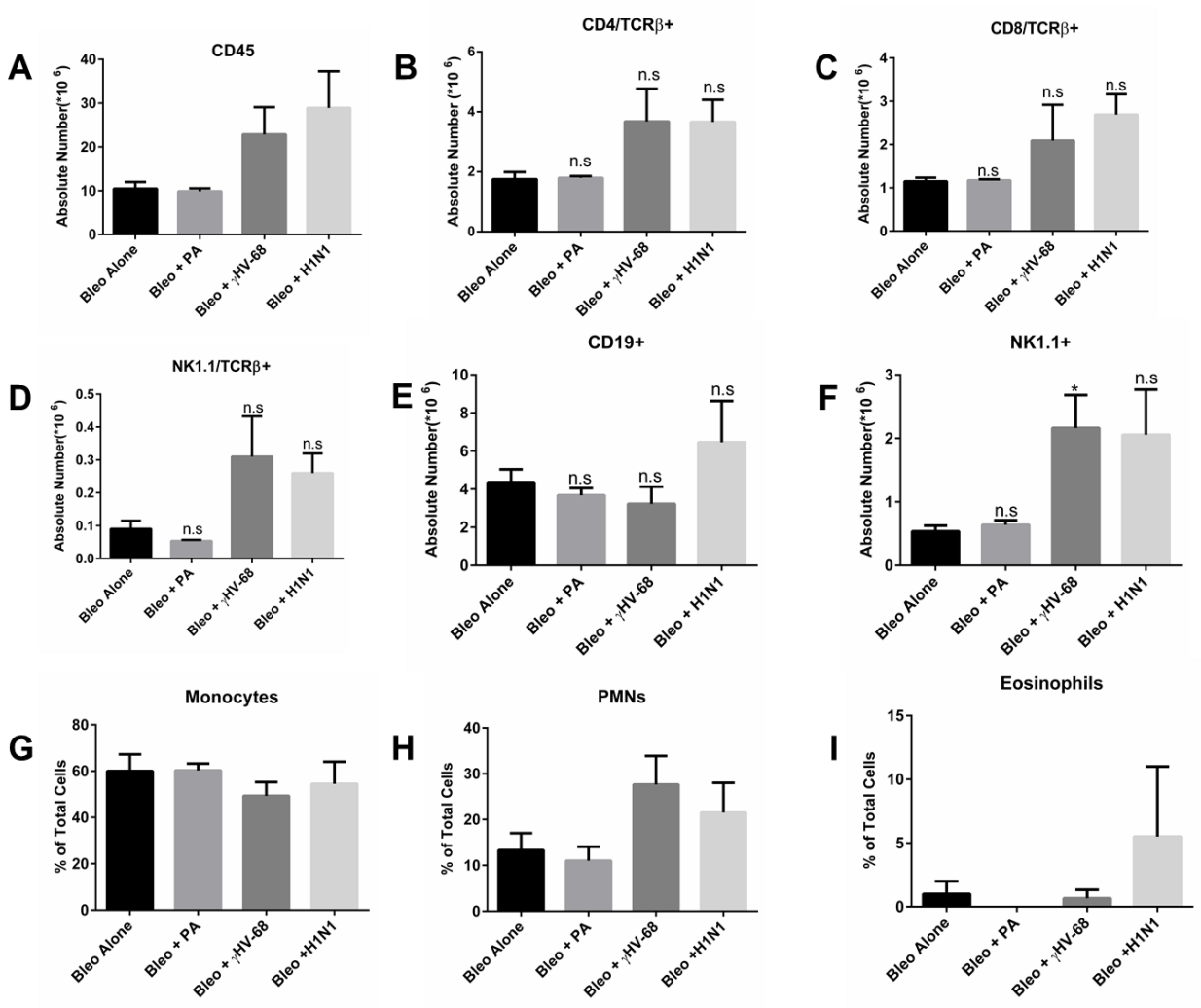

Figure 15: Leukocyte recruitment was enhanced following infection.
Mice were injected with bleomycin on day 0. On day 14, mice were infected with saline, *P. aeruginosa*, H1N1 or γHV-68. Lungs were harvested from n=4 mice each on day 15 or day 21. Total lung leukocytes were enumerated and absolute numbers of A) CD45+, B) CD4 TcRβ, C) CD8 TcRβ, D) Nk1.1 TcRβ E) CD19, and F) NK1 positive cells were determined based on flow cytometry. Differential analysis was done to determine the percentage of G) monocytes/macrophages H) neutrophils and I) eosinophils. Data shown are from one experiment representative of 2.

Differences in profibrotic mediators do not explain the ability of γHV-68, but not H1N1 to exacerbate fibrosis.

The production of several pro- and anti-fibrotic mediators were determined by ELISA. Expression of CCL12 **(Figure 16A)** was elevated in both viral infections, but only reached significance in the H1N1-infected mice. Expression of CCL2 **(Figure 16B)** was decreased post-γHV-68 infection, but was unchanged post-H1N1. Expression of active and total TGFβ **(Figure 16C)** was similar in all groups.

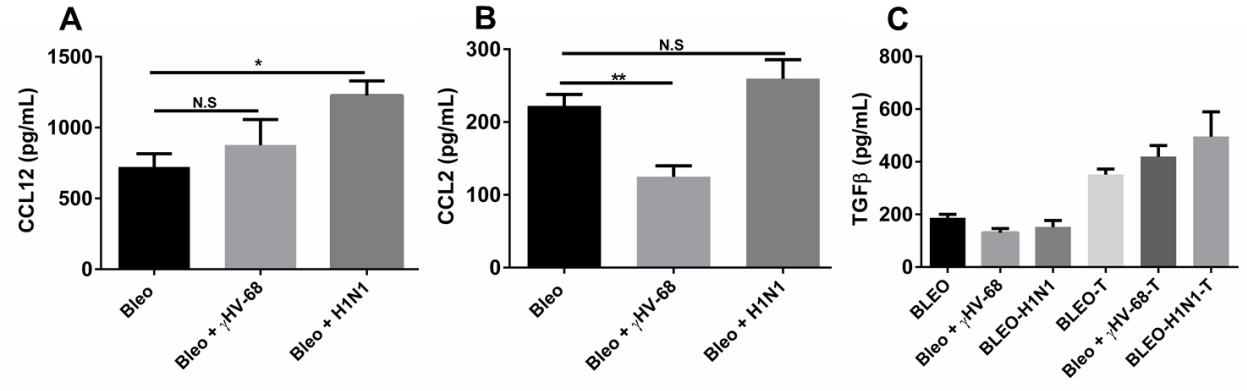

Figure 16: Differences in CCL12, CCL2 and TGFβ could not explain the differential ability of γHV-68, but not H1N1 to exacerbate ECM deposition post-bleomycin.
Mice were treated with bleomycin on day 0 and infected with saline, γHV-68 or H1N1 on day 14. On day 21, lungs were harvested and whole lung homogenates were analyzed by ELISA for CCL12 (A), CCL2 (B), levels of active (Panel C, left side) or acid-activated total TGFβ (panel C, right side). n=3-5 mice/group representative of 2 experiments.

When evaluating Th1, Th2 and Th17 cytokines, IFNγ was elevated in γHV-68-infected mice when compared to bleomycin plus mock infection **(Figure 17A)**, confirming earlier results in FITC and γHV-68-infected mice (129). Interestingly, levels of IFNγ were reduced in H1N1-infected mice, perhaps consistent with the observation that H1N1 replication is resolving at this time point. Levels of IL-13 **(Figure 17B)** and IL-17 **(Figure 17C)** were reduced in both groups of virally infected mice compared to the bleomycin control group, but only reached significance

in γHV-68 infected animals. This is also consistent with the earlier observation that γHV-68 can augment fibrosis in the absence of Th2 cytokines (129). Previous studies have shown that aged mice, which are susceptible to γHV-68-induced fibrosis have elevated levels of TGFβ receptors on lung fibroblasts (122). However, in the present studies, levels of TGFβR1 **(Figure 17D)** were not different, and levels of TGFβRII **(Figure 17E)** were elevated only in H1N1-infected mice when measured in the whole lung.

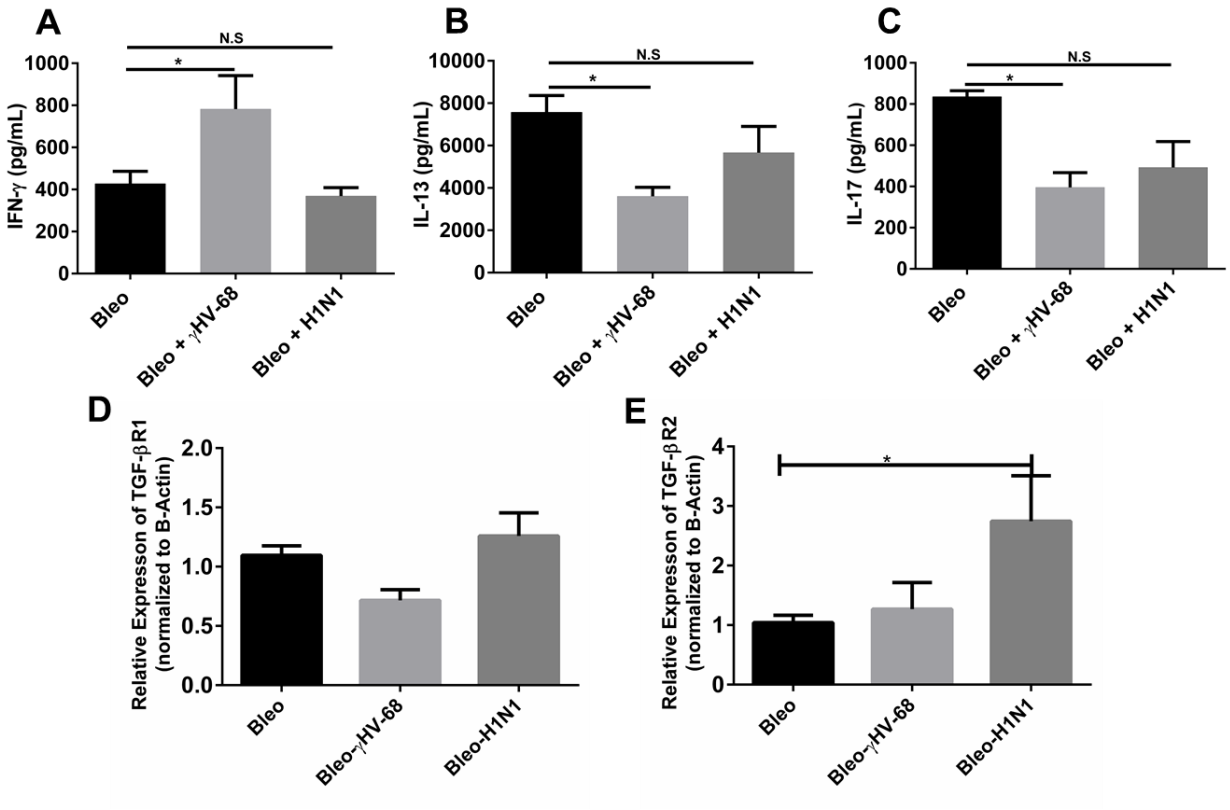

Figure 17: Differences in Th1, Th2, and Th17 and TGFβ receptors in whole lung did not explain the differential ability of γHV-68, but not H1N1 to exacerbate ECM deposition post-bleomycin.
Mice were treated with bleomycin on day 0 and infected with saline, γHV-68 or H1N1 on day 14. On day 21, lungs were harvested and whole lung homogenates were analyzed by ELISA for IFNγ (A), IL-13 (B), and IL-17 (C); n=5 for each group. In panels D and E, whole lung RNA was prepared and analyzed for expression of TGFβRI and II by real-time RT-PCR, n=3-5 for each group; all representative of 2 experiments

Comparing the induction of IFNγ or TNFα in mice treated with either virus alone compared to the amount made in response to viral infection post-bleomycin, it was noted that pre-treatment with bleomycin did not alter levels of either cytokine in response to H1N1 infection significantly. However, the ability of bleomycin-treated mice to produce TNFα was significantly inhibited post-γHV68 infection, and production of IFNγ tended to be lower **(Figure 18).** These results may indicate a sub-optimal anti-viral response to γHV-68 in bleomycin pre-treated mice.

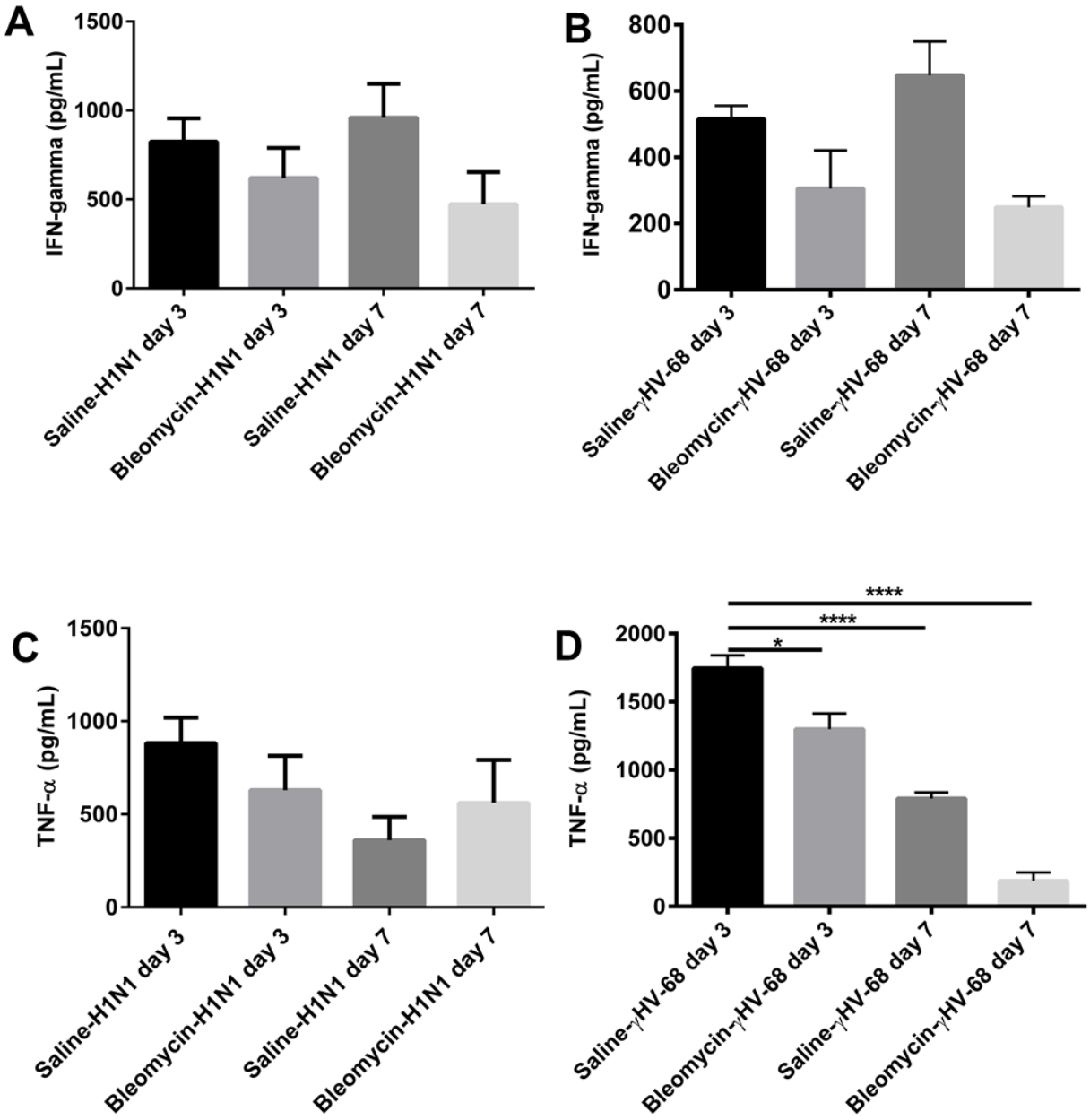

Figure 18: Bleomycin-treated mice showed a defect in the production of TNFα to γHV-68 infection but not H1N1.

Mice were treated with saline or bleomycin on day 0. On day 14 mice from each treatment group were infected with 50PFU H1N1 or 5x 10^4 PFU of γHV-68. On days 17 and 21 (days 3 and 7 post-infection), lungs were harvested and whole lung homogenates were analyzed by ELISA for IFNγ (A and B), TNFα (C and D). Data shown is representative from one experiment n=3-4/mice per group.

Alveolar epithelial cells are more sensitive to TGFβ signaling and show evidence of apoptosis post-γHV-68 infection.

Human studies that have associated exacerbation of lung fibrosis with herpes virus have shown presence of virus in alveolar epithelial cells (AECs), and because latent infection of AECs with γHV-68 have demonstrated elevated production of cysteinyl leukotrienes (346), AECs were isolated from bleomycin + mock infection, bleomycin +H1N1 or bleomycin+γHV-68 infected mice on day 21 and analyzed them for expression of leukotriene synthetic enzymes, expression of TGFβ receptors and analyzed their protein lysates for evidence of SMAD3 phosphorylation and apoptosis via cleaved PARP **(Figure 19)**. Expression of leukotriene synthetic enzymes [5-lipoxygenase (5-LO) and 5-LO activating protein (FLAP)] were increased in response to both infections. However, only infection with γHV-68 resulted in increased expression of TGFβR1, increased evidence of SMAD3 phosphorylation and increased evidence of apoptosis as noted by cleaved PARP.

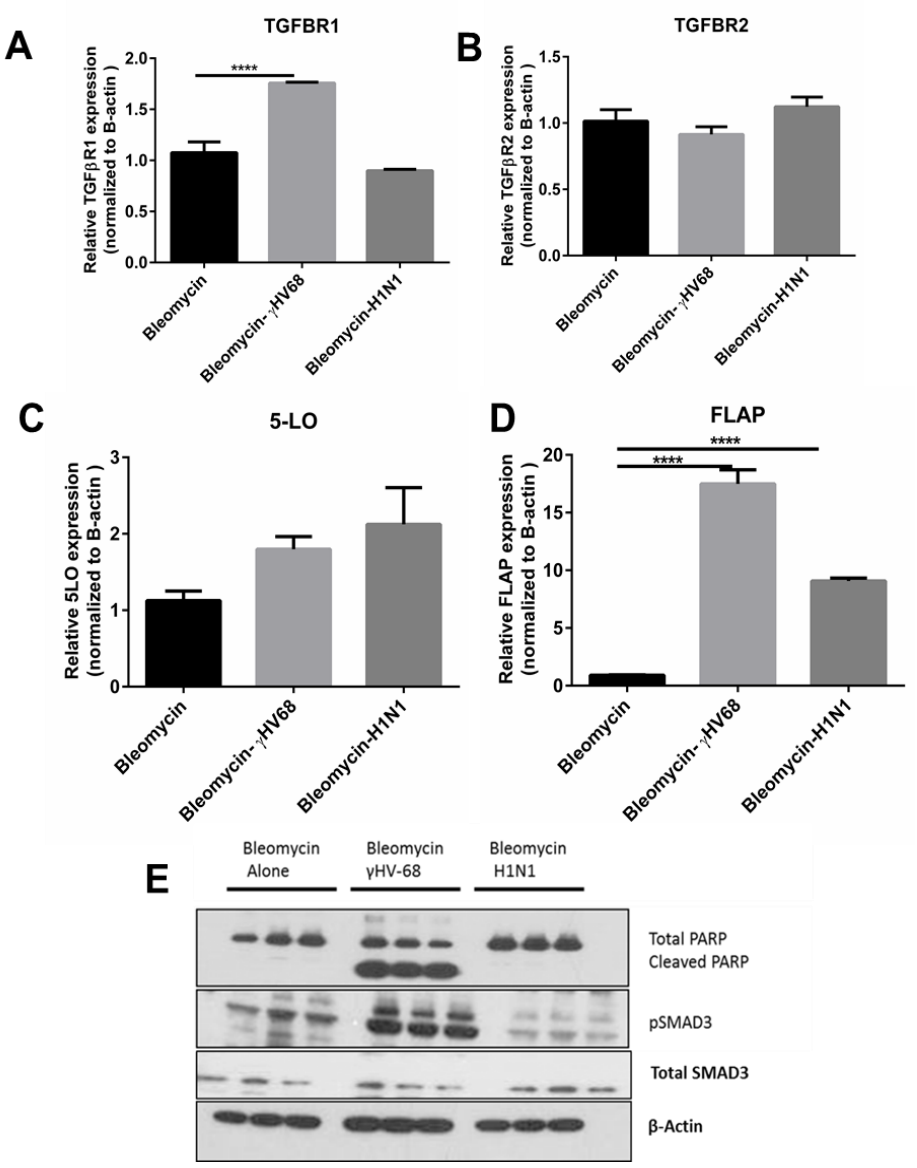

Figure 19: AECs from bleomycin and γHV-68-treated mice showed increased sensitivity to TGFβ signaling, and increased evidence of leukotriene synthesis and apoptosis post- γHV-68 infection.

Mice were treated with bleomycin on day 0. On day 14, some mice were infected with saline, H1N1 or γHV-68. Primary AECs were isolated from the lungs of all groups of mice on day 21. Total RNA was isolated and by real time RT-PCR we measured the expression of TGFβ receptor I/II (A, B), 5-LO (C) and FLAP (D). Phosphorylated SMAD3, total SMAD3, cleaved PARP, total PARP and beta actin were detected by western blotting (E). Data in all panels represent n=3/group

Discussion

The cause of IPF is unknown, yet several lines of evidence have suggested that viral infections may play a role either as initiating or exacerbating agents. Mounting clinical evidence suggests that patients with IPF have T cells with low expression of CD28 (370, 371). This suggests chronic activation of T cells in IPF patients, potentially due to underlying and undiagnosed infections. Thus, the goal of this study was to determine whether both bacterial and viral infections could exacerbate bleomycin-induced fibrosis.

Even though *P. aeruginosa* has the capability of infecting epithelial cells (372) and IPF patients tend to do poorly when they develop bacterial pneumonia (373), *P. aeruginosa* infection was effectively cleared from the lungs and did not exacerbate fibrosis. While our results suggested that this bacteria would not worsen fibrosis due to enhanced ECM deposition, there is caution in extrapolating these results to humans. The progressive nature of IPF is not modeled by bleomycin, thus, it is likely that in humans with chronic disease and more diminished lung capacity, a bacterial infection could be far more devastating, and certainly an influx of inflammatory cells might worsen dyspnea even if it does not alter ECM deposition. A recent study assessing the role of the lung microbiome in IPF demonstrated that the presence of high numbers of the *staphylococcus* and *streptococcus* genera of bacteria was associated with disease progression in IPF (374). So, it is possible that since we saw no exacerbation of disease with *Psuedomonas aeruginosa*, using a different genus of bacteria may show a different phenotype.

Our results using bleomycin verified earlier results using FITC as a fibrotic stimulus (129) and demonstrated that γHV-68 could exacerbate ECM deposition post-bleomycin stimulus. The ability of γHV-68 to do this likely involves ability of the virus to reactivate from latency as the ΔORF72 mutant was not able to do this. Our unpublished observations suggest that the first

three days of replication by ΔORF72 and γHV-68 are similar, but viral gene expression is significantly diminished by 7 days post-infection in ΔORF72-infected mice. Thus, exacerbation of fibrosis likely requires on-going viral replication or spread within the AECs. These data are consistent with earlier studies showing that ongoing viral replication is necessary for fibrosis in Th2-biased mice as well (357). It may also be a unique feature of γHV-68 or perhaps of γ herpesviruses in general since CMV (a β herpesvirus) did not enhance fibrosis. It should be noted that our experiments used the same dose of γHV-68 and CMV; however, C57Bl/6 mice are relatively resistant to CMV infection and we could not plaque infectious CMV from the lungs on day 7 post-infection whereas we could demonstrate infectious virus in γHV-68-infected mice **(Figure 11).** We could demonstrate by RT-PCR that CMV viral RNA was expressed (data not shown), albeit at low levels. However, our earlier finding that murine adenovirus type 1 (MAV1) was also unable to exacerbate fibrosis following FITC challenge (129) and our current results with H1N1 suggest that this is not a feature of all viral infections which can infect AECs. Caution should be used when interpreting these data however since it is clear that the rates of infection are different for all these viruses.

When examining a variety of pro-and anti-fibrotic mediators and the composition of the inflammatory cell influx which followed both infections, no notable differences could explain the discrepancy between the ability of γHV-68, but not H1N1 to exacerbate fibrosis. This prompted us to look at changes that might be specific to AECs, the initial site of infection and viral replication within the lung. We have observed that γHV-68 can replicate in AECs in culture without lytic destruction of all the cells. In contrast, H1N1 may be more likely to ultimately destroy all infected epithelial cells. Our results *in vivo* suggest that γHV-68-infected mice have AECs that are more responsive to TGFβ signaling and show signs of apoptosis. This

is consistent with earlier work showing that γHV-68 infection in aged mice is associated with AEC apoptosis and ER stress (123). One caveat was that our analyses of AECs were done at day 7 post-infection, a time point when H1N1 replication was diminished, but γHV-68 replication was on-going. It is possible that the prolonged replication of γHV-68 at 7 dpi may cause more epithelial stress. We have previously demonstrated that AECs isolated from mice with latent γHV-68 infection overproduce profibrotic factors such as TGFβ and cysteinyl leukotrienes (121, 346).

Our current data confirm that infection with γHV-68 and H1N1 both significantly upregulate FLAP in AECs, enzymatic machinery necessary for cysteinyl leukotriene synthesis, however induction of FLAP was highest with γHV-68. Because cysteinyl leukotrienes can promote fibrocyte proliferation (375) and activation of resident lung fibroblasts (376, 377), this could promote ECM deposition post-viral infection. When we looked for evidence of TGFβ signaling in AECs, we observed elevated TGFβR1 in AECs from γHV-68-infected mice. This resulted in increased evidence of TGFβ activation of these cells at this time point as demonstrated by increased phospho-SMAD3 expression. Ultimately, we believe these AECs may be undergoing apoptosis *in vivo* as there was evidence of cleaved PARP, a marker of apoptosis. Thus, we speculate that the ability of γHV-68 to undergo persistent rounds of reactivation and an enhanced sensitivity of the infected AECs to respond to TGFβ leads to ongoing apoptosis in AECs along with induction of profibrotic factors such as cysteinyl leukotrienes which ultimately promote ECM deposition in these mice. Because H1N1 has also been shown to induce apoptotic machinery in AECs as a way to promote viral replication (378), it is not clear why our results differ with these two viral infections. These results may merely reflect the doses of virus used the extent of ultimate damage to the AECs, alterations in the

ability to repair damaged epithelium following each infection or additional signaling cascades induced by the distinct viruses that we have not yet identified.

While our results in AECs highlight cell-specific increases in susceptibility to TGFβ signaling post-γHV-68 infection, we did not observe differences in total or active TGFβ in the lungs of bleomycin-treated mice infected with γHV-68 or H1N1. As this cytokine is often activated locally on the cell surface, it is likely that measurements in lung homogenates do not accurately reflect levels available during cell-cell communication. However, we were surprised that levels of TGFβRII were actually elevated in H1N1-infected mice within the whole lung. One caveat of these interpretations however is that receptor expression levels were measured in whole lungs, not in isolated fibroblasts. As TGFβ receptors can be expressed on numerous cell types, it is not clear what cells may be overexpressing TGFβRII in H1N1-infected mice. Because TGFβRII can interact with various other cellular proteins such as cyclin B2 (379) endoglin (CD105) (380) or TGFβRIII (381), this may result in differential cell activation of some cell types in the H1N1 infected mice that may further explain the discrepancies between outcomes with H1N1 vs. γHV-68.

Finally, the differences in cell types that are readily infected by each virus may play an additional role. We have demonstrated that γHV-68 is readily found as both lytic and latent infection in lung AECs, fibroblasts, macrophages and B cells (121). However, H1N1 tends to restrict replication predominantly to the epithelial cells within the lung (382) and in our hands does not replicate well in macrophages. It is interesting that one study has suggested that H1N1 can replicate more effectively in type II AECs from IPF patients (383). Additionally, a recent case report noted acute exacerbation of IPF following H1N1 vaccination (384). Thus, as mentioned before, bleomycin may not be effectively modeling all the epithelial changes noted in

patients with IPF. It should also be noted that while H1N1 infection at the doses used in this study do not appear to worsen ECM deposition, that is not to say that H1N1 infection is not detrimental to fibrotic lungs. At higher doses of H1N1 (500 PFU), bleomycin-treated mice were highly susceptible to rapid death, most likely from acute lung injury so we were unable to analyze data from these experiments. However, this dose was also lethal in some control mice.

In summary, γHV-68 was able to exacerbate bleomycin-induced fibrosis or FITC-induced fibrosis (129) and stimulated collagen deposition. Infection with *P. aeruginosa*, H1N1 and CMV did not exacerbate bleomycin-induced fibrosis at the doses tested in our studies. The difference in the ability of γHV-68, but not the other pathogens tested to exacerbate collagen deposition required the ability of γHV-68 to undergo reactivation from latency as demonstrated by our experiments with the ΔORF72 mutant virus. Additionally, we have demonstrated evidence of enhanced sensitivity to TGFβ signaling in AECs from γHV-68-infected mice likely leading to enhanced profibrotic release of cysteinyl leukotrienes, AEC stress and apoptosis.

Chapter 4:

Periostin regulates fibrocyte function to promote myofibroblast differentiation and lung fibrosis

Background

Fibrosis can be triggered by various known insults (e.g., infection, allergens, toxins, or radiation), or can occur for unknown reasons as in the case of idiopathic pulmonary fibrosis (IPF) (348). IPF is a chronic progressive parenchymal lung disease of unknown origin, with mean survival rate of 3-5 years after diagnosis. Prevalence and mortality rates are increasing globally (1, 17, 385). The cellular mechanisms leading to IPF remain unclear but a commonly held paradigm describes continuous cycles of injury to the alveolar epithelium leading to dysregulated repair. Prominent features of this dysregulated repair include fibroblast differentiation, myofibroblast accumulation and excessive collagen deposition in the alveolar space (137, 386, 387). Mediators such as growth factors and cytokines from different cell types contribute to the persistence of activated fibroblasts and myofibroblasts(388). Based on our current knowledge, bone marrow-derived collagen producing cells (e.g. fibrocytes and other collagen producing cells) play a significant role in the development of lung fibrosis ((102, 217, 389-395). Fibrocytes respond to a number of cytokines and chemokines that are typically associated with migration and activation of inflammatory cells(189). Fibrocytes are hematopoietic bone marrow-derived cells that express both mesenchymal and leukocyte markers.

They circulate in the peripheral blood and can be isolated from tissues. Cultured fibrocytes have been shown to express a number of ECM proteins including collagen 1, collagen 3 and fibronectin (97, 189, 191, 192, 396). In addition, fibrocytes also express a number of chemokine receptors, including CXCR4, CCR7 and CCR2 which may contribute to the recruitment and activation of fibrocytes resulting in migration to damaged tissues (25, 94, 98). Although several reports indicate that fibrocytes express type I collagen, others have suggested that uptake of secreted type I collagen by hematopoietic cells characterizes the fibrocyte population (397, 398).

A more recent study demonstrated that cells of hematopoietic origin produce type I collagen but are not a necessary source of type I collagen during experimental lung fibrosis (200). Kleaveland et al. illustrated that fibrocytes can efficiently uptake type I collagen even though the underlying mechanism is not clearly understood (200). Adoptive transfer of fibrocytes leads to augmented fibrosis in a FITC-induced mouse model and several studies have found a correlation between increased numbers of fibrocytes and worse disease progression(94, 187, 396, 399, 400). Recently, fibrocytes were shown to contribute to the progression of pulmonary fibrosis without differentiating to myofibroblasts themselves using a transforming growth factor alpha model of fibrosis (401). Additionally, Garcia de Alba *et al*. also showed that fibrocytes contributed to increased mRNA levels of ECM proteins in both fibrosis and chronic pneumonitis (400). Work from our laboratory demonstrated that fibrocytes in circulation of IPF patients are major producers of the matricellular protein, periostin, and that periostin accumulates in the lung tissue of IPF patients (402).

Periostin, also known as osteoblast-specific factor 2, is a recently characterized matricellular protein that binds to components of the ECM including type I collagen and fibronectin and has been shown to be involved in collagen fibrillogenesis (403). Periostin protein

transmits signals from the ECM to the cell by binding to cellular receptors such as integrins that affect cell adhesion, proliferation, migration and tissue angiogenesis (253). It has been reported that periostin promotes cancer cell invasion and metastasis through the integrin/phosphatidylinositol 3-kinase/AKT pathway, leading to the development of various tumors (404). Work from our laboratory and others have shown that there is an increased circulating periostin level in IPF patients compared to controls (258, 402). Our work further showed that the increased periostin expression in IPF tissues was localized to active areas of fibrosis and that IPF patients also showed increased percentages of periostin-expressing fibrocytes and monocytes in the blood (402).

Chimeric mouse studies showed that both structural and hematopoietic sources of periostin were important in protecting periostin-deficient mice from bleomycin-induced fibrosis (402). Although periostin has diverse functions, it is becoming increasingly clear that periostin is upregulated in lung tissue in the context of several respiratory diseases (256). At present, the precise function of periostin in the lung has not been fully elucidated. In this study we used bleomycin to establish fibrosis in mice, and then analyzed how hematopoietic-derived fibrocytes might signal structural myofibroblast differentiation through their ability to secrete periostin or other soluble mediators in the presence of periostin. We explored the use of periostin-deficient fibrocytes in adoptive transfer experiments as well as the use of integrin blocking antibodies to demonstrate that periostin interacts with different receptors on fibrocytes and fibroblasts and that periostin secretion by fibrocytes is important for the exacerbation of bleomycin-induced lung fibrosis.

Results

Mesenchymal cells increased periostin mRNA expression after bleomycin treatment

To specifically assess the upregulation of periostin expression in lung mesenchymal cells after bleomycin treatment, WT mice were given intratracheal saline or bleomycin on day 0. All lungs were harvested on day 14 and mesenchymal cells were cultured for 14 days then sorted into fibrocytes (CD45 positive) and fibroblasts (CD45 negative). RNA was isolated for real-time RT-PCR analysis. We observed that both fibroblasts and fibrocytes had significant increases in periostin mRNA expression post bleomycin treatment **(Figure 20).**

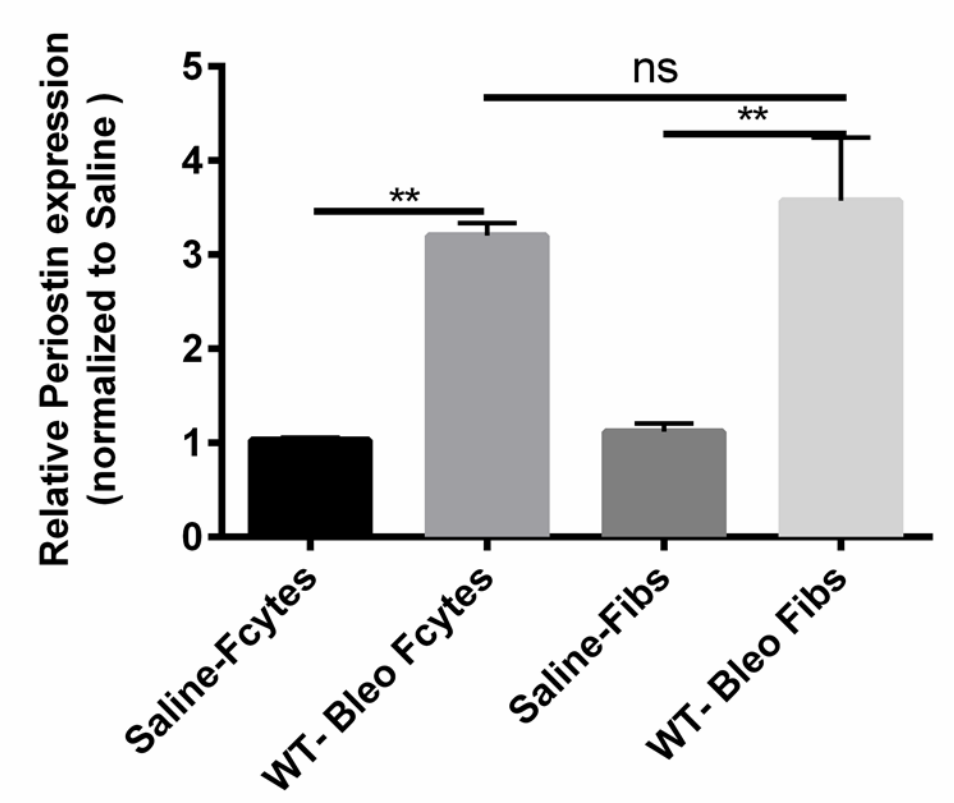

Figure 20: Increased mRNA expression of periostin in lung mesenchymal cells post-bleomycin treatment.
Wild type mice were given 0.25U of bleomycin or saline intratracheally on day 0. On day 14, lung mesenchymal cells were cultured and sorted by Magnetic bead separation for fibroblasts and fibrocytes. Total RNA was isolated and by real time RT-PCR we measured the expression of periostin and β-actin in fibrocytes and fibroblasts. Data represent n=3 per group pooled from multiple mice. **$p < 0.01$, *$p < 0.05$, ns=not significant.

TGFβ and periostin co-regulated each other in lung mesenchymal cells

Previous data from our laboratory demonstrated that treatment of WT mesenchymal cells with TGFβ showed a significant increase in periostin production (402). To assess whether periostin also up-regulated TGFβ1 production in murine mesenchymal cells sorted to separate the fibroblasts and fibrocytes, we isolated these cell types from lung mince cultures from naïve mouse lungs and treated with recombinant periostin (500 ng/mL) in serum-free media. Treatment of WT fibrocytes and fibroblasts with periostin lead to increased TGFβ1 production as measured

by ELISA **(Figure 21A).** In addition, treatment of fibroblasts and fibrocytes with recombinant TGF-β (2ng/mL) increased protein production of periostin as measured by ELISA **(Figure 21B)**, as well as increased mRNA expression of periostin **(Figure 21C-D).**

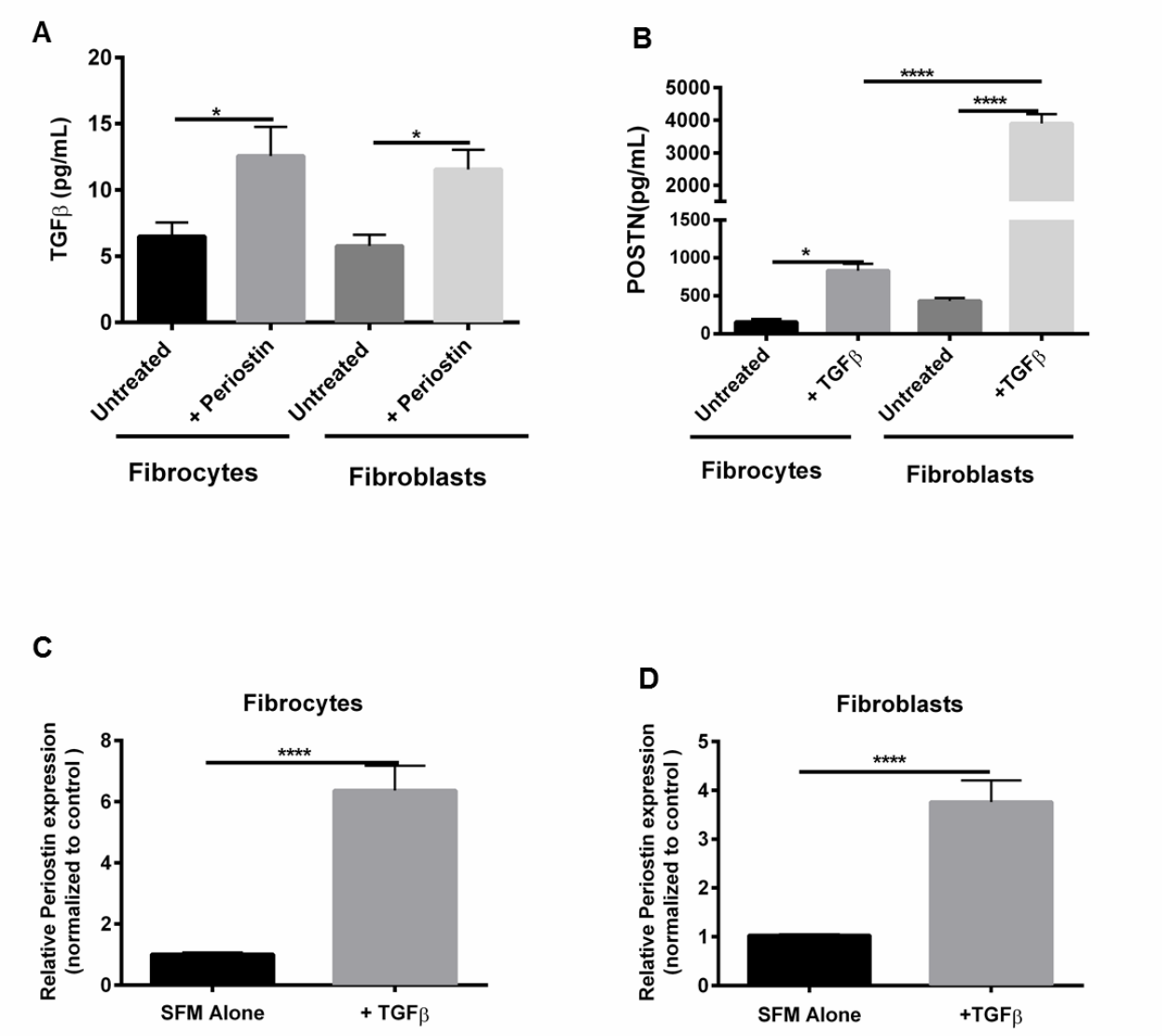

Figure 21: Periostin and TGFβ treatment regulated each other in fibroblasts and fibrocytes. Fibroblasts and fibrocytes from wild-type mice were treated with periostin (500ng/mL) or TGFβ (2ng/mL) for 48 hours. Cell-free supernatants were collected and analyzed by ELISA for TGFβ (A) and periostin (B). Total RNA was isolated and by real time RT-PCR we measured the expression of periostin and β-actin in fibrocytes (C) and fibroblasts (D). Data are representative of mean ±SEM, n=3 wells/treatment per group. *p< 0.05, **p < 0.01 ,****p<0.0001, ns=not significant

Since, periostin and TGFβ1 seemed to be co-regulating each other, we wanted to assess whether the production of collagen I from fibroblasts and fibrocytes was different in the presence of periostin and if this effect was dependent on TGF-β1 signaling. **Figure 22** illustrates that treatment of murine lung mesenchymal cells with periostin for 48hrs led to a significant increase in mRNA expression for collagen I. However, the increase in collagen I expression was independent of TGFβ1 signaling in the fibrocytes compared to the fibroblasts as indicated by treatment with the A8301 TGF-β1 receptor inhibitor. Overall these data suggested that TGFβ1 and periostin are co-regulating each other but periostin can signal to fibrocytes independently of TGFβ1 and that the receptor needed for periostin signaling may be different on fibrocytes compared to fibroblasts.

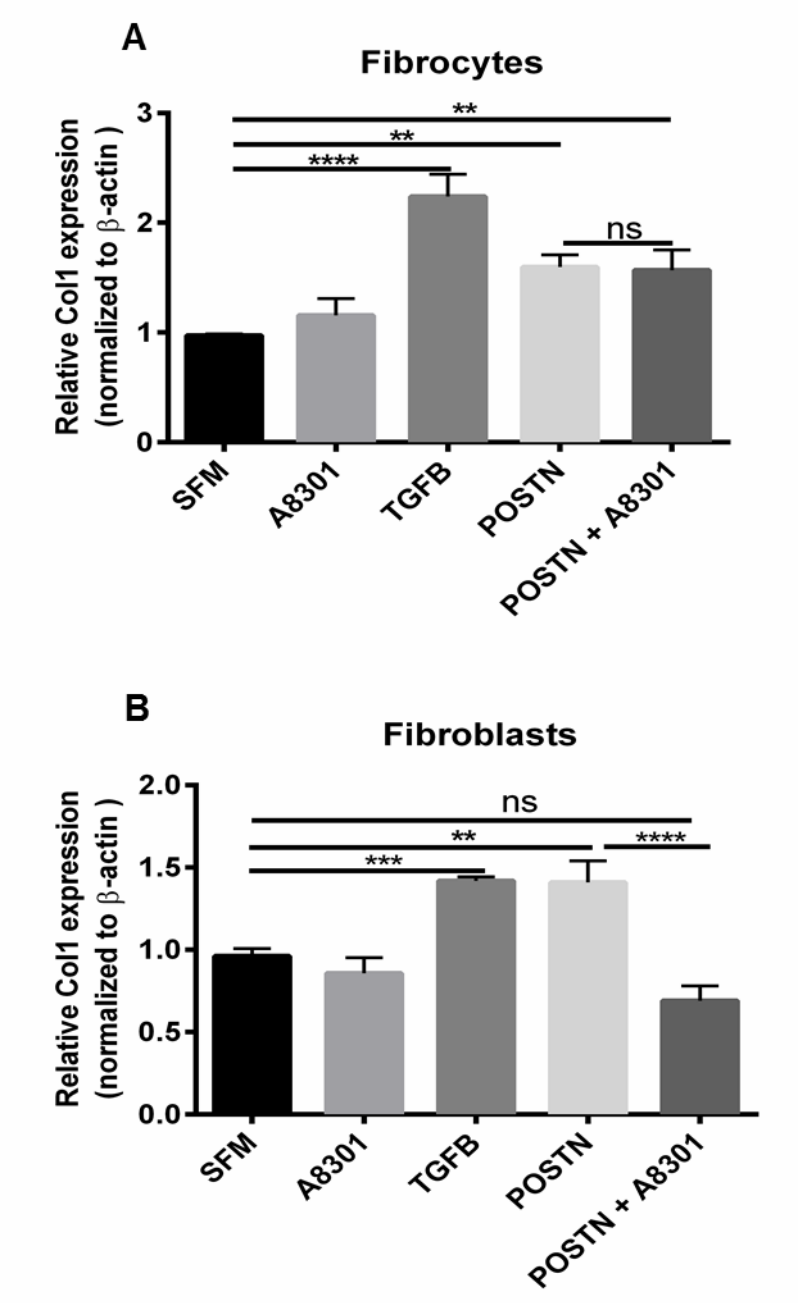

Figure 22: Periostin induced collagen 1 expression in fibrocytes independently of TGFβ signaling.

Mesenchymal cells were cultured in complete media, sorted into fibrocytes and fibroblasts, then switched to serum-free media where they were treated with TGFB (2ng/mL), A8301 (ALK5 inhibitor) or periostin (500ng/mL) for 48hours. Total RNA was isolated and by real time RT-PCR we measured the expression of collagen I and β-actin in fibrocytes (**A**) and fibroblasts (**B**). Data are representative of mean ±SEM, n=3 wells/treatment per group from 2 independent experiments ****p<0.0001, ***p<0.001,**p<0.01, *p<0.05 and ns + not significant

Decreased integrin expression in fibrocytes from periostin$^{-/-}$ mice post-bleomycin treatment

In many cancers, periostin binds to integrins activating the AKT/PKB and FAK-mediated signaling pathways. This leads to increased cell survival, invasion, angiogenesis, metastasis and epithelial-mesenchymal transition (405). Periostin also functions as a ligand for integrin alphaVbeta3 and alphaVbeta 5 to support adhesion and migration of epithelial cells (406). Because our data suggested that periostin might be signaling differently in fibrocytes vs fibroblasts, we wanted to examine the expression levels of integrins in WT and periostin$^{-/-}$ naïve lung mesenchymal cells. As illustrated in **figure 23A-D**, there was no significant difference in the baseline mRNA expression levels of alpha 1, alpha V, beta 1 and beta 5 integrin levels on fibrocytes and fibroblasts from WT or periostin$^{-/-}$ mice, although in most cases, the expression levels of integrins were lower in fibrocytes than fibroblasts. We next treated WT and periostin$^{-/-}$ mice intratracheally with saline or bleomycin for 14 days then cultured lung mesenchymal cells, sorted for fibrocytes and assessed mRNA expression for different integrins post-bleomycin treatment. Alpha 1, alpha V and beta 1 were found to be significantly upregulated in WT fibrocytes post bleomycin treatment but beta 5 expression was not altered. None of the integrins were upregulated post-bleomycin in the periostin$^{-/-}$ cells (**Figure 23E-J).**

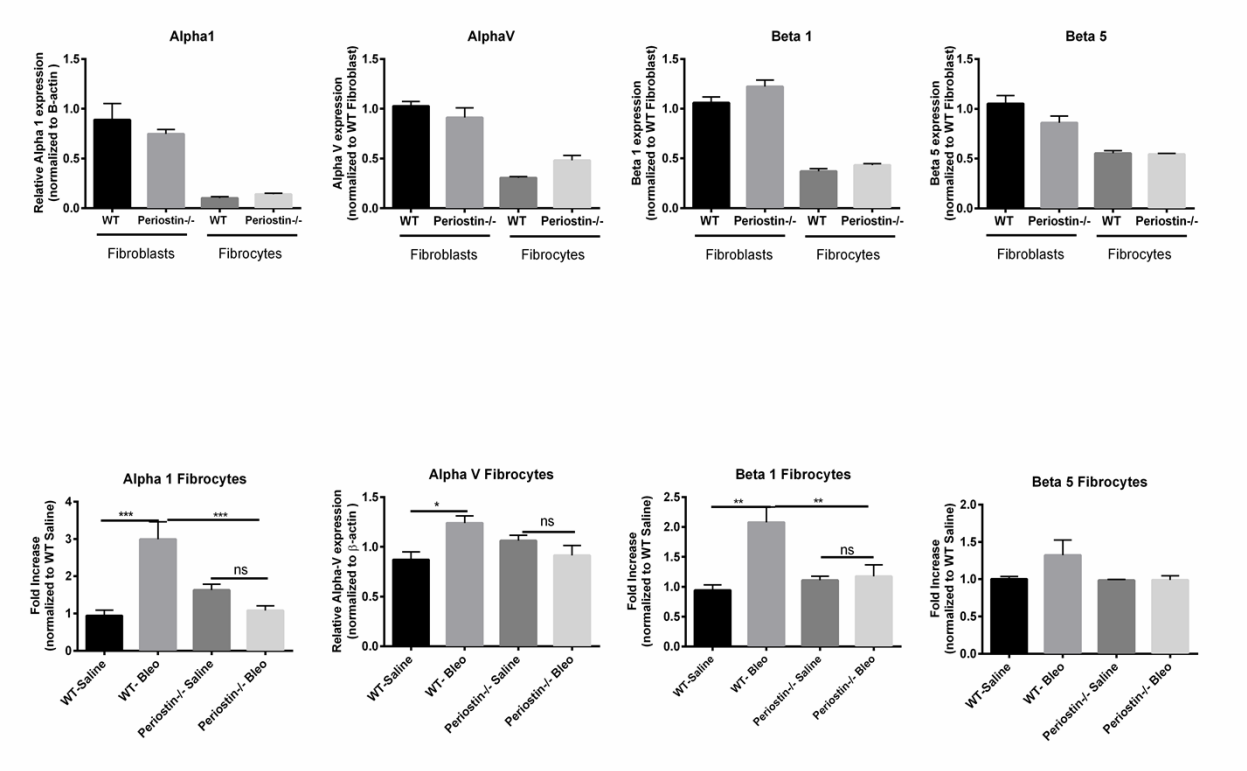

Figure 23: Loss of periostin decreased the expression of integrins post-bleomycin treatment. (A-D) Wild type or periostin-/- mice were given bleomycin or saline intratracheally on day 0. On day 14 lungs were harvested and mesenchymal cells were cultured and sorted as previously described. Total RNA was isolated and by real time RT-PCR we measured the expression of alpha1, alphaV, beta 1 and beta 5 expressions in saline treated (A-D) and bleomycin treated (E-H) fibrocytes. Values are expressed as mean ± SEM, and represent n=3 animals/group from two independent experiments ns=not significant, ***p<0.001,**p<0.01 and *p<0.05.

To determine if the increase in mRNAs for the different integrins correlated with TGFβ1 production, we treated fibrocytes with exogenous TGFβ1 and found increased mRNA expression for alpha V, alpha 1 and beta 5 in wild-type cells **(Figure 24).** Expression of these integrins was similarly increased in the periostin$^{-/-}$ cells treated with TGFβ1. In contrast, TGFβ1 treatment caused modest, but not significant increase in beta 1 expression in WT cells, but did not in periostin$^{-/-}$ cells suggesting that beta 1 integrin expression may be necessary for periostin signaling to fibrocytes in murine lungs **(Figure 24).** Next, WT fibrocytes and fibroblasts were treated with periostin in the presence of a beta 1 integrin-blocking antibody (102209-Biolegend)

and after 48h, collagen1 mRNA expression was assessed as an indication of mesenchymal cell activation. Fibrocytes treated with periostin in the presence of beta 1 blocking antibody had markedly less collagen I mRNA expression compared to samples treated with periostin and isotype control. In contrast, addition of beta 1 integrin blocking antibody to fibroblasts showed no change in collagen I expression **(Figure 25).** Taken together our data suggested periostin signals collagen expression through beta 1 integrin to activate fibrocytes and this is independent of TGFβ signaling.

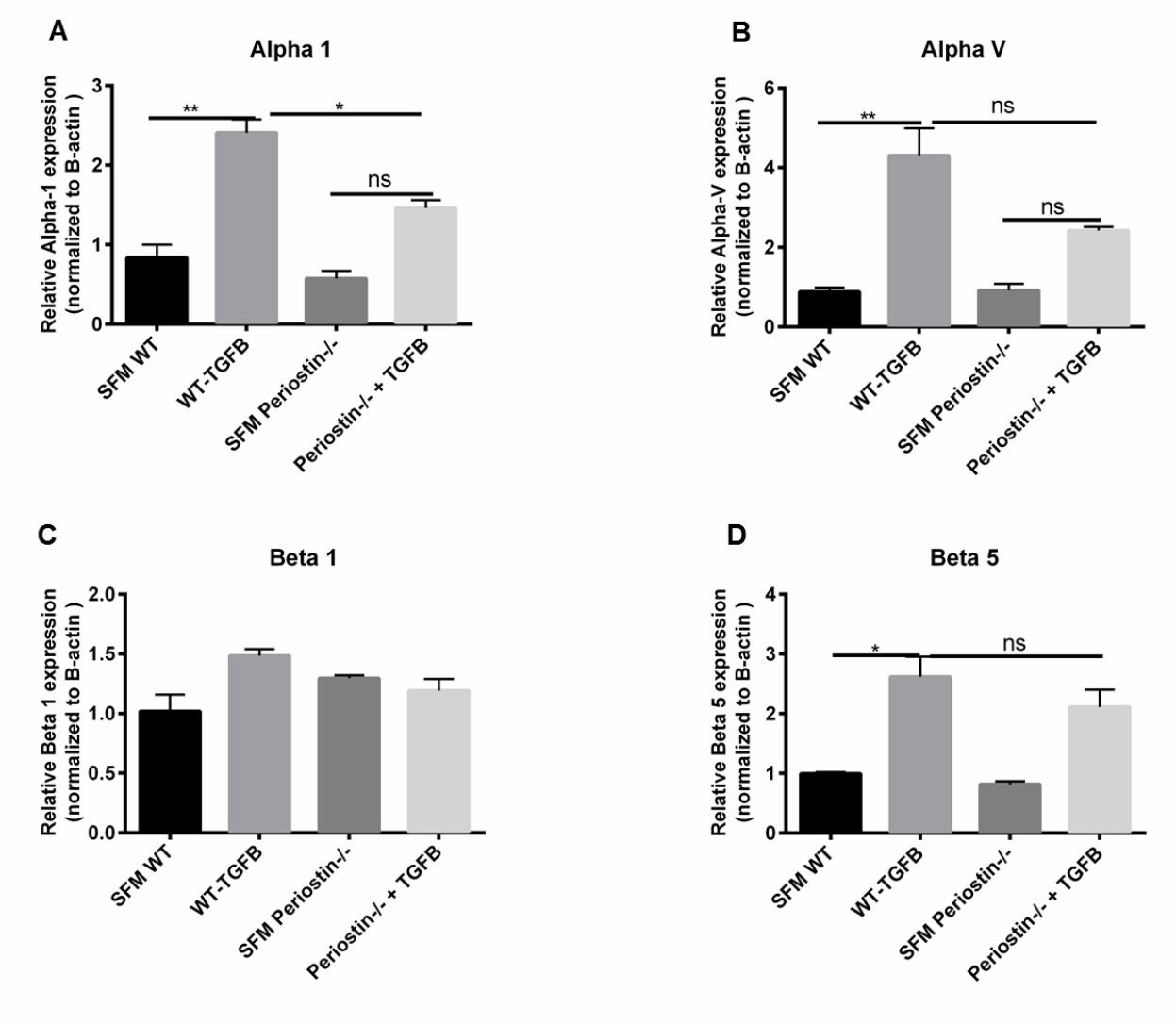

Figure 24:TGFβ treatment did not induce β1 integrin mRNA expression in fibrocytes in the absence of periostin.

Fibrocytes from wild-type and periostin-/- mice were treated with recombinant TGFβ (2ng/mL) for 48 hours. Total RNA was isolated and by real time RT-PCR we measured the expression of different integrins and β-actin in fibrocytes (**A)** Alpha 1, **(B**) AlphaV, (**C)** Beta 1(β1) and **(D**) Beta 5. Data are representative of mean ±SEM, n=3 wells/treatment per group ,**p<0.01, *p<0.05 and ns=not significant.

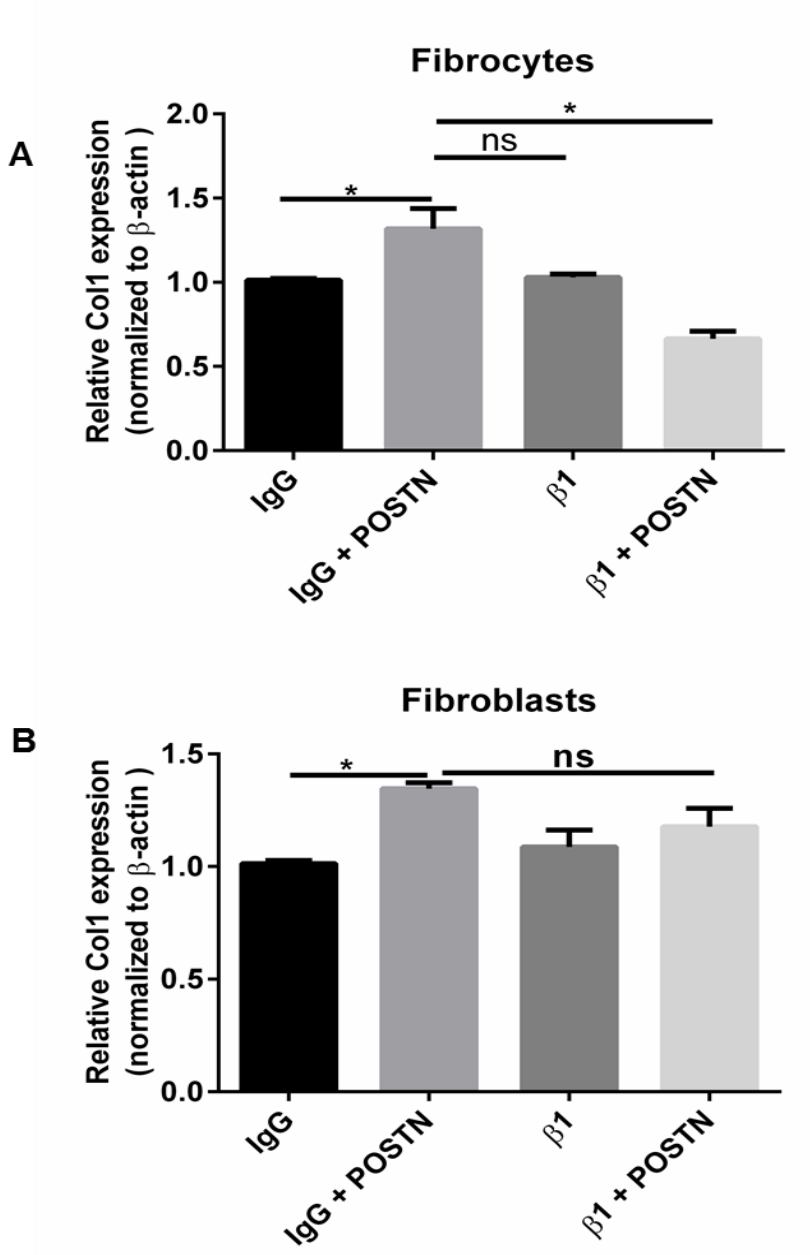

Figure 25: β1 integrin blockade in WT fibrocytes caused decreased Collagen 1 expression with periostin treatment but showed no effect in fibroblasts.
Mesenchymal cells were cultured in complete media, sorted into fibrocytes and fibroblasts, then switched to serum-free media where they were treated with purified rat anti-mouse β1(HMβ1-1, rat CD29) blocking antibody or purified armenian Hamster IgG (400916) isotype control for 30mins, then incubated with or without periostin (500ng/mL) for 48hours. Total RNA was isolated and by real time RT-PCR we measured the expression of collagen 1 and β-actin in fibrocytes (**A**) and fibroblasts (**B**). Data are representative of mean ±SEM, n=3 wells/treatment per group *$p<0.05$ and ns=not significant.

Fibrocytes exacerbated bleomycin-induced fibrosis through paracrine effects and in a periostin-dependent manner

We previously showed that fibrocytes augmented FITC-induced lung fibrosis (94). In addition, fibrocytes and monocytes were the major producers of periostin in circulation and a hematopoietic source of periostin was important for fibrogenesis in the bleomycin model of lung fibrosis (402). To specifically assess the role of periostin produced by fibrocytes in lung fibrogenesis, WT or periostin$^{-/-}$ mice were given intratracheal saline or bleomycin on day 0. On day 4 post-bleomycin, mice were give $5x10^5$ additional cultured WT or periostin$^{-/-}$ lung fibrocytes. Lungs from all mice were harvested on day 21 post-bleomycin and lung collagen content was measured by hydroxyproline assay. As expected, bleomycin-treated WT mice showed a significant increase in collagen content when compared to saline controls but WT mice that received the additional WT fibrocytes had significantly higher amounts of collagen in the lungs compared to bleomycin alone. Interestingly, bleomycin-treated WT mice given the periostin$^{-/-}$ fibrocytes showed similar levels of lung collagen as the bleomycin-treated wild-type mice with no added cells **(Figure 26A). Figure 26B** demonstrates that periostin$^{-/-}$ mice treated with bleomycin then given additional WT lung fibrocytes had significantly more collagen content in the lungs compared to periostin$^{-/-}$ mice treated with bleomycin alone. Additionally, we analyzed the ability of fibrocytes to maintain their CD45 expression post-transfer over time. Using flow cytometry analysis we found that all the labeled PKH26 positive fibrocytes were detected as CD45 positive cells 4-8 days after transfer. These data demonstrate that fibrocytes were not differentiating into CD45-negative fibroblasts after transfer **(Figure 26C)**

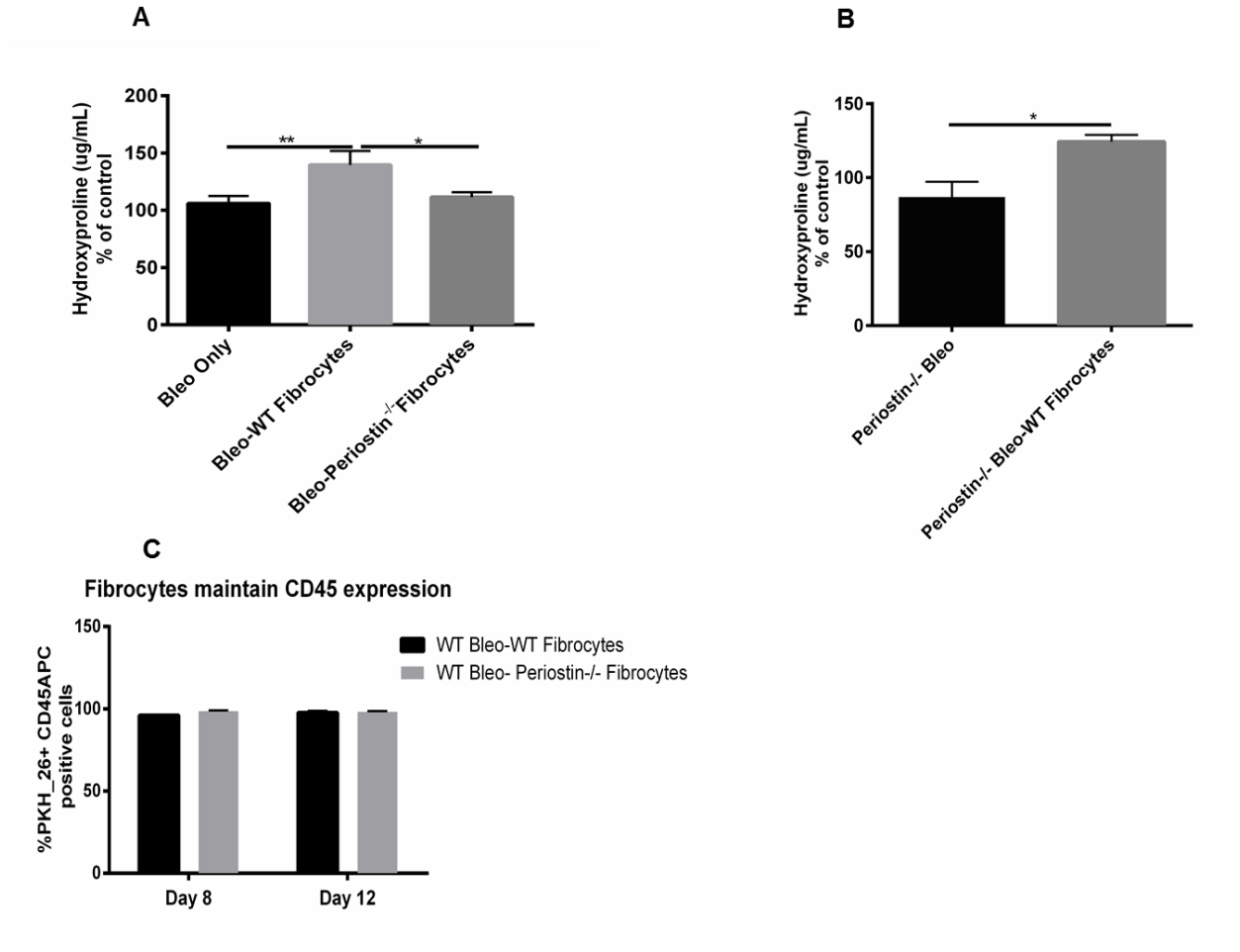

Figure 26: Adoptive transfer of WT but not periostin$^{-/-}$ fibrocytes augmented bleomycin-induced fibrosis but fibrocytes of both genotypes maintained CD45 expression in vivo.
(A) Wild type mice were given 0.25U of bleomycin or PBS intratracheally on day 0. On day 5, post-bleomycin treatment half of each group received $5x10^5$ WT of periostin$^{-/-}$ fibrocytes by intravenous tail vein injection. Lungs were harvested on day 21 post-bleomycin for hydroxyproline quantification. Data shown are pooled from two independent experiments, with n = 4-6 mice per group in each experiment. **$p<0.01$, *$p<0.05$ and ns=not significant **(B)** Periostin$^{-/-}$ mice were given 0.25U of bleomycin intratracheally on day 0. On day 5 post-bleomycin treatment, half of each group received $5x10^5$ WT fibrocytes, lungs were harvested and assessed collagen content on day 21 by hydroxyproline assay *$p<0.05$.
(C) Wild type mice were given 0.25U of bleomycin or PBS intratracheally on day 0. On day 5, post-bleomycin treatment half of each group received $5X10^5$ PKH-26 labeled WT of periostin$^{-/-}$ fibrocytes by intravenous tail vein injection. On day 3 and 7 post-transfer, lungs were then harvested and total lung leukocytes were enumerated and then labeled with CD45 APC to determine the percentages of PKH-26CD45+APC fibrocytes. Data shown represents mean ± SEM, n=3 animals/group, ns, not significant.

Periostin production by fibrocytes promoted their profibrotic effects on myofibroblasts via other mediators

Myofibroblast differentiation is characterized, in part, by induction of αSMA gene expression as well as by increased production of ECM components and fibrogenic cytokines such as TGFβ1 (213, 405, 406). To assess how fibrocyte-derived periostin affected myofibroblast differentiation, we analyzed protein expression of αSMA in WT untreated fibroblasts that were incubated with cell-free supernatants from CD45 positive fibrocytes from bleomycin-treated WT and periostin$^{-/-}$ mice. Cells were incubated in this media for 24h. After 24h we analyzed expression of αSMA by western blot and saw less αSMA expression in WT fibroblasts that were incubated with bleomycin-treated supernatants from periostin$^{-/-}$ cells **(Figure 27A)**. To address whether this effect was solely due to periostin or possibly involved other downstream signaling proteins a microarray analysis using a targeted mouse fibrosis array was performed with the goal of identifying differences between the WT and periostin$^{-/-}$ fibrocytes. A significant decrease in connective tissue growth factor (CTGF) and Lysyl oxidase (LOX) but not platelet-derived growth factor (PDGF) α was seen in periostin$^{-/-}$ fibrocytes. Findings were confirmed by RT-qPCR **(Figure 27B)**. In addition, there was a significant increase in CTGF mRNA expression in fibrocytes treated with exogenous periostin but this increase was diminshed in the presence of a beta1 integrin blocking antibody **(Figure 27C).** There was no change in CTGF mRNA expression in fibroblasts **(Figure 27D)**. Given the importance of CTGF in fibrogenesis, we measured the amount of CTGF protein in the supernatants used in the experiments described in **Figure 27A** by ELISA and saw less CTGF in the periostin$^{-/-}$ fibrocyte supernatants **(Figure 27E)**. Taken together these data suggested that fibrocytes in the presence of periostin secrete additional pro-fibrotic mediators such as CTGF that contributed to myofibroblast differentiation.

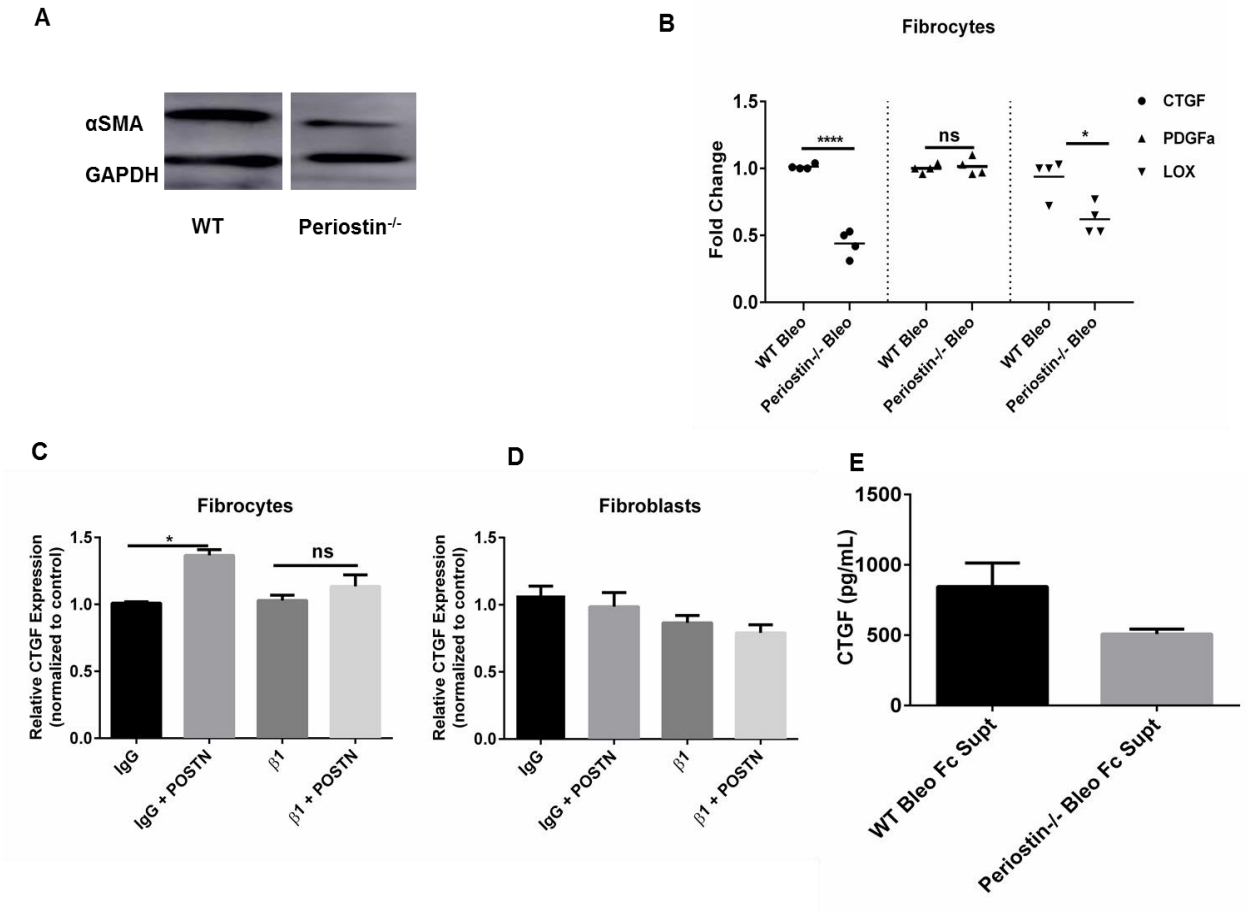

Figure 27: WT fibrocytes secreted CTGF in the presence of periostin and increased αSMA protein expression in fibroblasts in the presence of periostin.
(A) Wild type mice were given 0.25U of bleomycin or PBS intratracheally on day 0. On day 14, post-bleomycin treatment lung mesenchymal cells were cultured for 14 days. After 14 days in culture cells were sorted and CD45 positive fibrocytes were incubated in serum-free media overnight. Cell-free supernatants were collected from both bleomycin-WT and periostin$^{-/-}$ cells and added 1:1 onto WT untreated fibroblasts (CD45 negative) cells for 24h. Cells were lysed in RIPA buffer with protease inhibitor and we assessed the expression of αSMA and GAPDH by western blot. **(B)** Total RNA was isolated from the WT and periostin$^{-/-}$ fibrocytes after overnight incubation in serum-free media and by real time RT-PCR we measured the mRNA expression of CTGF, PDGFα and LOX. Data shown represents mean ± SEM, n=3 wells/group, ns=not significant, ****p<0.0001, **p<0.01 and *p<0.05. **(C-D)** Total RNA was isolated from WT mesenchymal cells treated with periostin (500ng/mL) and by real time RT-PCR we measured the mRNA expression of CTGF. Data shown represents mean ± SEM, n=3 wells/group, ns=not significant and *p<0.05. **(E))** Cell free supernatants were analyzed by ELISA for CTGF

Discussion

Previous studies have shown that periostin $^{-/-}$ mice treated with bleomycin intratracheally had decreased collagen content compared with WT littermates (257, 402). Both monocytes and fibrocytes likely contribute to the pool of circulating periostin in IPF patients and chimeric mouse studies demonstrated that both the hematopoietic-derived and structural sources of periostin contributed similarly to fibrogenesis (402). However, lung fibroblasts secrete more periostin than circulating cells **(Figure 21).** Together these studies suggested that a circulating source of periostin could be playing a significant role in the exacerbation of lung fibrosis, but it was unclear how the lower levels of periostin produced by these cells vs. structural cells (e.g. fibroblasts, **Figure 21B**) were influencing disease. Our current findings *in vivo*, and *in vitro*, suggest that fibrocyte profibrotic function is likely via multiple paracrine mechanisms.

We examined the effects of fibrocytes in the exacerbation of bleomycin-induced fibrosis in WT and periostin$^{-/-}$ mice. Adoptive transfer of WT fibrocytes during established lung fibrosis augmented bleomycin-induced fibrosis in recipient mice, corroborating the earlier studies in a fluorescein isothiocyanate (FITC)-induced model of pulmonary fibrosis (94). Furthermore, in periostin$^{-/-}$ mice receiving WT fibrocytes there was a significant increase in lung hydroxyproline which is evidence of enhanced lung fibrosis relative to the periostin$^{-/-}$ mice that did not receive additional fibrocytes. We first wondered whether there was a defect in migration of periostin$^{-/-}$ fibrocytes to the injured lung. However, Figure 19C shows that periostin$^{-/-}$ fibrocytes could be identified in the lungs as easily as WT fibrocytes. Furthermore, we found no defect in the expression of chemokine receptors on the WT vs the periostin$^{-/-}$ fibrocytes after bleomycin treatment **(Figure 28)**. Therefore, the decrease in fibrosis in mice treated with the periostin$^{-/-}$ fibrocytes could not be attributed to a migration defect. Furthermore, we considered the

possibility that WT fibrocytes might better be able to differentiate into fibroblasts or myofibroblasts once arriving in the injured lung.

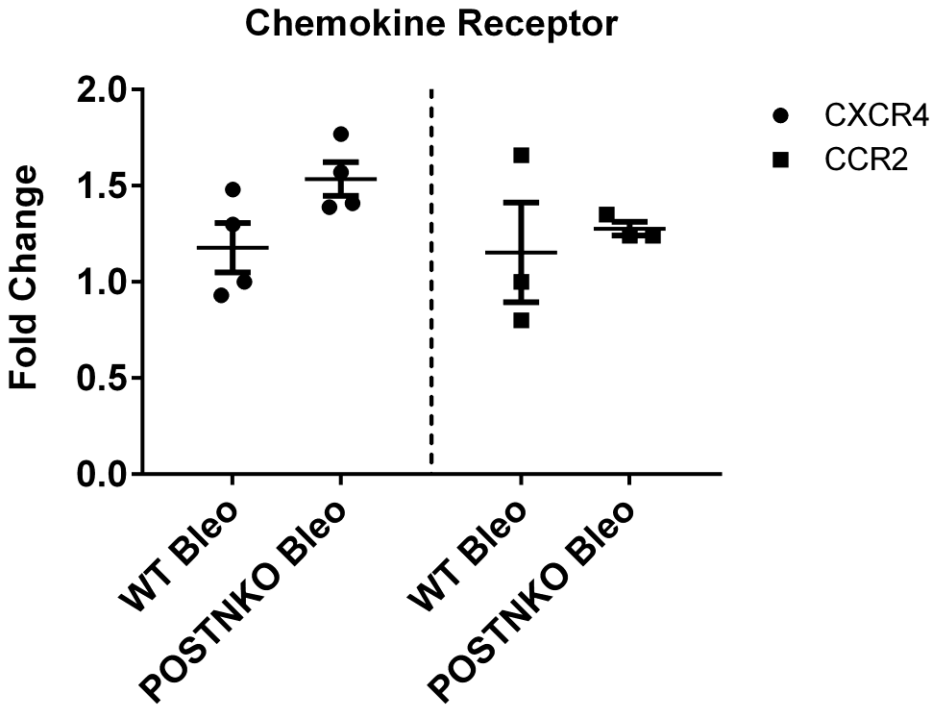

Figure 28: Chemokine receptor expression in WT and periostin knockout fibrocytes post-bleomycin treatment.
Wild type mice were given 0.25U of bleomycin or PBS intratracheally on day 0. On day 14, post-bleomycin treatment lung mesenchymal cells were cultured for 14 days. Total RNA was isolated from the WT and periostin$^{-/-}$ fibrocytes after overnight incubation in serum-free media and by real time RT-PCR we measured the mRNA expression of CCR2 and CXCR4.

While in vitro work has clearly shown that fibrocytes can differentiate into myofibroblasts (98, 186, 407), our *in vivo* work corroborates recent findings in another model system to suggest fibrocytes are not differentiating into myofibroblasts during fibrosis **(Figure 26C)** (401). We also previously showed that fibrocytes migrate to areas in the lungs adjacent to fibroblasts (25). Given that collagen production by circulating cells is also dispensable for

development of lung fibrosis (200), these data, when taken together, suggest that fibrocytes work mostly by paracrine mechanisms to induce fibrogenesis.

It is likely that some of the paracrine effects of periostin-producing fibrocytes are due to periostin itself. We have previously shown that periostin can directly influence ECM deposition and migration of lung fibroblasts (402). Another feature of myofibroblasts is their ability to resist apoptosis, likely due to upregulation of anti-apoptotic proteins such as X-linked inhibitor of apoptosis (XIAP) expression (308). Periostin may directly contribute to myofibroblast resistance to apoptosis via stimulating XIAP protein expression **(Figure 29).** We recently demonstrated that blocking inhibitor of apoptosis family proteins using pharmacologic interventions attenuated bleomycin-induced fibrosis (308, 408). Thus, periostin likely contributes to the exacerbation of bleomycin-induced fibrosis at least in part via direct effects on fibroblasts.

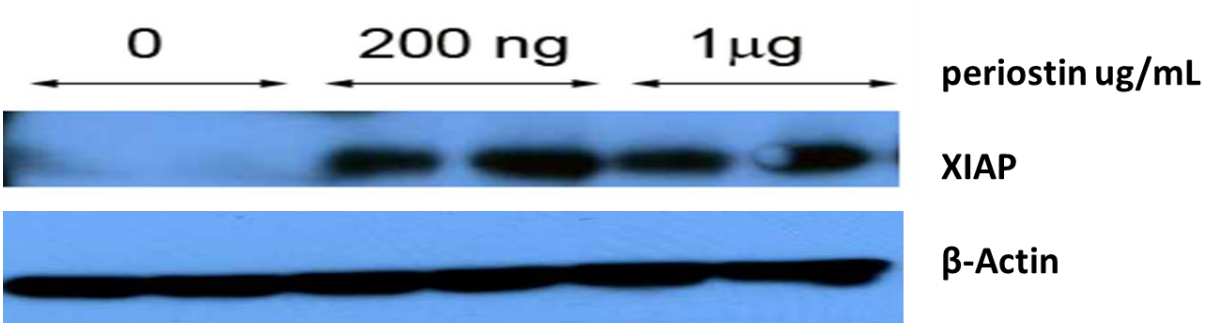

Figure 29: Exogenous periostin treatment increased protein expression of XIAP in lung mesenchymal cells.
WT mesenchymal cells were cultured in complete media for 14 days. Cells were then plated in serum-free media where they were treated with different concentrations of mouse recombinant periostin. Cells were then lysed in RIPA buffer with protease inhibitor and immunoblotted for X-linked inhibitor of apoptosis (XIAP) and β-actin

Another possibility is that periostin signals back to the fibrocytes themselves to influence production of other profibrotic mediators. We demonstrated that treatment with exogenous periostin increased CTGF mRNA expression in fibrocytes **(Figure 27C)** and fibrocytes secreted

less CTGF in the absence of periostin post-bleomycin treatment **(Figure 27D)**. CTGF has previously been described as an activator of mesenchymal cells (274, 275, 409), while LOX is known to promote collagen crosslinking, likely leading to stiffer ECM and more robust matrix-dependent fibroblast activation (259, 403). CTGF can induce a variety of cytokines such as TGFβ and vascular endothelial growth factor [reviewed in (409)], which in turn induce more expression of CTGF, indicating a positive feedback loop involving CTGF expression that can contribute to the progression of fibrosis. It is also likely that a similar feedback loop is occurring with periostin. Inhibiting this positive feedback loop would be ideal for understanding the mechanism by which CTGF from fibrocytes enables persistent lung fibrosis and promotes myofibroblast differentiation in the presence of periostin. However, there is not a specific receptor antagonist for CTGF due to the complex mechanism of CTGF signaling. Treatment of WT untreated fibroblasts with 10μM of an MRTF inhibitor (CCG 203971, shown to inhibit CTGF expression), in the presence of WT bleomycin fibrocyte supernatant resulted in a decrease in αSMA protein expression similar to what was seen with the periostin$^{-/-}$ supernatants demonstrating the importance of autocrine CTGF expression in the fibroblasts **(Figure 30)**.

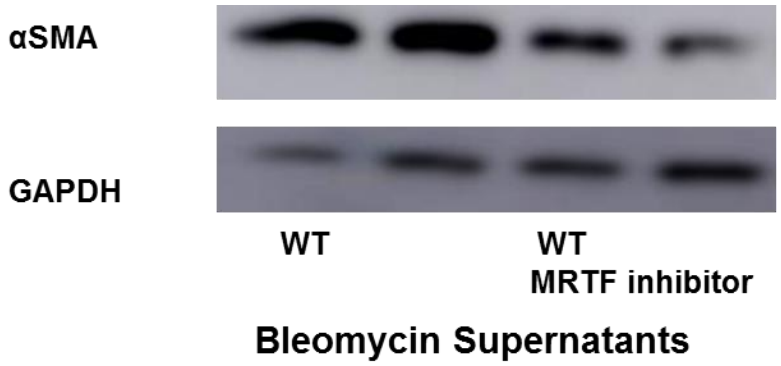

Figure 30: Inhibition of CTGF expression within fibroblasts limited the upregulation of αSMA in these cells when cultured with WT fibrocyte supernatants.
WT mesenchymal cells were cultured in complete media for 14 days. Cells were then sorted in fibroblasts (CD45-) and fibrocytes (CD45+). Fibroblasts were plated in serum-free media overnight. Cell-free supernatants were from both bleomycin-WT fibrocytes was added 1:1 onto WT untreated fibroblasts (CD45 negative) with or without 10μM MRTF inhibitor for 24h. Cells were lysed in RIPA buffer with protease inhibitor and we assessed the expression of αSMA and GAPDH by western blot.

To further examine the effects of periostin on fibrocytes we designed experiments using integrin-blocking antibodies. Our results suggest that periostin signals uniquely to fibrocytes via beta 1 integrin. A recent study by Reed and colleagues (301) suggested that inhibition of the alphaVbeta1 integrin using a small molecule inhibitor significantly attenuated bleomycin-induced pulmonary fibrosis. In that study the authors only looked at lung mesenchymal cells which are a combination of fibroblasts and fibrocytes. Given our findings that beta1 integrins are critical for periostin signaling to fibrocytes, it will be important to determine if the alphav-beta1 heterodimers are responsible for periostin signaling to fibrocytes.

One very interesting experiment would have been to deplete fibrocytes during fibrosis; however this strategy proved technically unsuccessful. We generated a collagenIα2-Cre-DTR transgenic mouse and used these animals to generate bone-marrow chimeras in a CD45.2 mouse so that the bone-marrow derived cells (but not lung resident cells) would only be expressing CD45.1 and the collagenIα2-Cre-DTR transgene. These mice were then given bleomycin and treated with diphtheria toxin on different days over a 3-week period to deplete the recruited collagen I-CRE-DTR expressing cells. Despite excellent chimerism in peripheral organs, surprisingly, there was a high percentage of recipient fibrocytes present in the lung at day 21 post- bleomycin treatment suggesting that either through recruitment from the bone marrow and /or expansion of progenitors upon recruitment to the lung, there remains a population of recipient

cells that expanded as a consequence of the bleomycin-induced lung injury that could not be eliminated by diphtheria toxin treatment **(Figure 31).** We feel it is important for the lung community to know that this strategy to create a fibrocyte-knock-out mouse was not effective. Definitive proof of the role of fibrocytes in lung fibrosis awaits the characterization of a fibrocyte-specific promoter that can be used in future cellular depletion studies.

In conclusion, the current study showed that fibrocyte-derived periostin caused an increase in myofibroblast differentiation. Once recruited to the lungs, fibrocytes did not differentiate into fibroblasts directly, but provided paracrine factors such as CTGF in a periostin-dependent manner to promote myofibroblast differentiation.

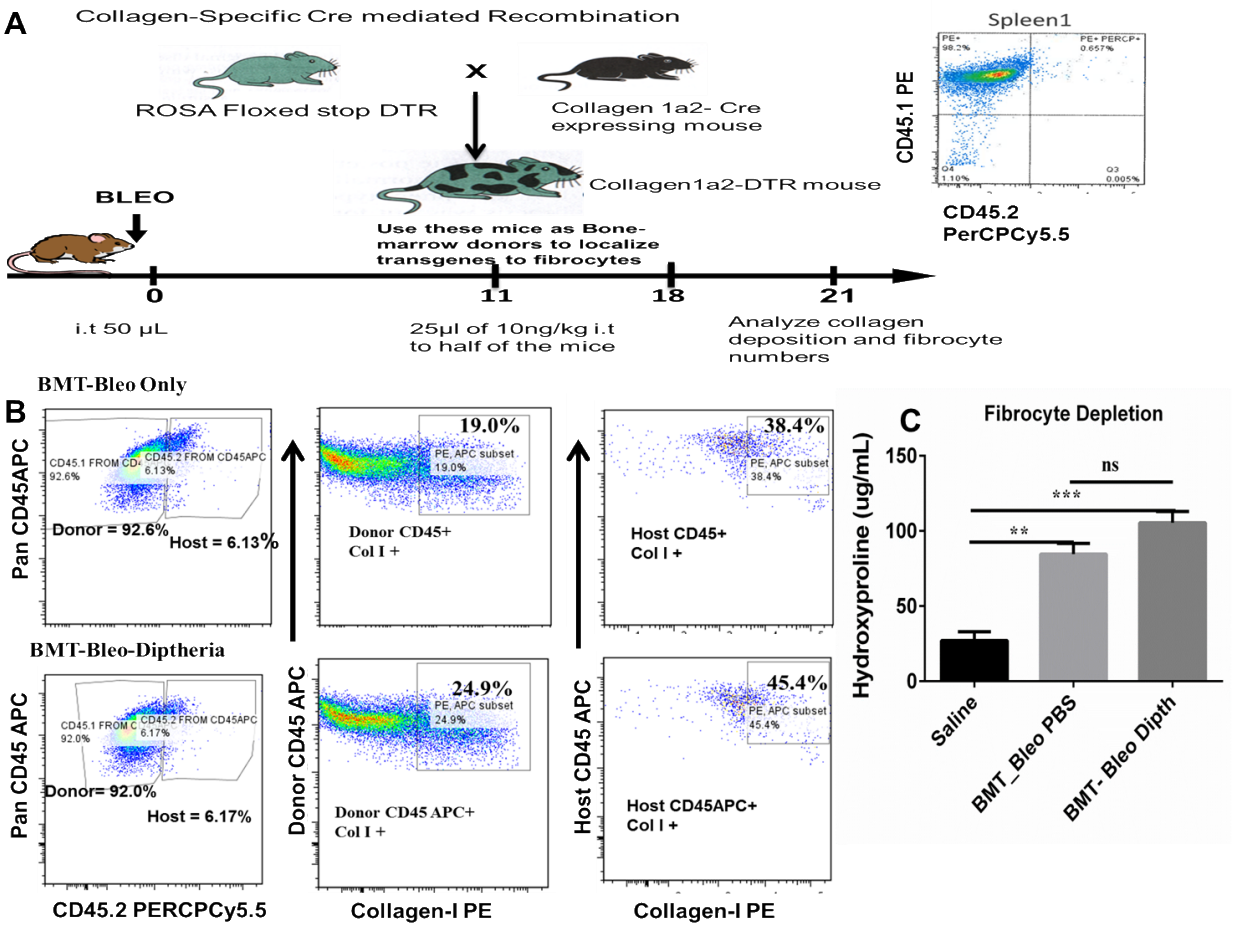

Figure 31- Generation of a Col1a2-Cre DTR mouse to deplete fibrocytes.
(A)Rosa- DTR mice (Jackson labs) were crossed with Col1a2-Cre mice (a gift from Paul Noble's laboratory) to generate Col1a2-Cre-DTR expressing mice.Spleens were analyzed by flow cytometry to demonstrate that the donor mice were CD45.1 **(B)** Bone-marrow chimeras were generated using these mice as donors into WT-C57BL/6 (CD45.2) mice. After 5 weeks, the bone-marrow transplanted mice were given intratracheal bleomycin 0.25U. 10 days post-bleomycin treatment, half of the mice were given 10µg/kg diphtheria toxin in PBS intratracheally to deplete the bone-marrow derived DTR expressing cells that were recruited to the lungs. This dose was repeated twice. Lungs were harvested from these mice on day 21 post-bleomycin treatment. Three lungs from each group was collagenase digested to generate single cell suspension of leukocytes. Cells were stained with a pan-CD45APCCD45.2PERCPCy5.5, collagen-I- PE to assess the percentages of donor derived vs host fibrocytes. **(C)** Remaining lungs were homogenized and collagen content was assessed by hydroxyproline assay.
For the flow cytometry analyses, from left to right. Cells were gated on pan CD45APC+, then from the CD45 + we looked for CD45.2PERCPCy5.5, then 2nd row is CD45.2 negative cells (Donor) that are pan CD45APC+ and Col I PE +(Fibrocytes). 3rd row is CD45.2+ cells(Host) that are pan CD45APC+ and Col I PE (Fibrocytes)

Chapter 5:

Targeting inhibitor of apoptosis proteins protects from bleomycin-induced lung fibrosis

Background

Pulmonary fibrosis is characterized by the accumulation of extracellular matrix resulting in decreased lung compliance and impairment of gas exchange (6). Fibrosis can be triggered by various known insults (e.g., infection, allergens, toxins, or radiation), or can occur for unknown reasons as in the case of idiopathic pulmonary fibrosis (IPF) (348). IPF is a progressive disease with a high mortality rate and a prevalence that is increasing globally (1, 17). The pathogenesis of IPF remains unclear but a commonly held paradigm attributes this pathology to continuous cycles of injury to the alveolar epithelium coupled with a dysregulated repair response. Prominent features of this dysregulated repair include fibroblast differentiation, myofibroblast accumulation and excessive collagen deposition in the alveolar space (137, 386, 387). Regardless of the initial insult, the persistence of myofibroblasts is aided by their acquisition of an apoptosis-resistant phenotype (229, 308, 410-413).

Cell susceptibility to apoptotic stimuli is regulated, in part, by the presence of proteins that can block the propagation and execution of pro-apoptotic signals (414). One example is the inhibitor of apoptosis protein (IAP) family which is composed of eight proteins: XIAP (X-linked IAP), cIAP-1 (cellular IAP1), cIAP-2, LM-IAP (melanoma IAP)/Livin, ILP2 (ILAPlike protein-2), NAIP (neuronal apoptosis-inhibitory protein), Bruce/Apollon and survivin (415). Each IAP

family member contains at least one baculovirus IAP repeat (BIR) domain which allows these proteins to bind caspases and, in some cases, prevent apoptosis by directly blocking caspase activation (415-417). The most studied IAP, XIAP, is well known to inhibit the intrinsic and extrinsic apoptotic pathways through both direct mechanisms (blocking activation of caspases 3, 7 and 9) and indirect mechanisms involving its RING domain (418-424). cIAP-1 and cIAP-2 contain a similar domain structure to XIAP. While these cIAPs do not directly inhibit caspase activation, they can impair apoptosis through alternative mechanisms (e.g. by promoting NF_kB-induced activation of anti-apoptotic proteins) and they have been shown to function cooperatively with XIAP (419, 425-427). The anti-apoptotic function of XIAP and the two cIAPs can be blocked by second mitochondria-derived activator of caspases (Smac) / direct IAP-binding protein with low PI (DIABLO), an IAP-binding protein released from mitochondria during apoptosis (428).

Recent reports indicate that XIAP is important in the pathogenesis of IPF. For example, XIAP is highly expressed within fibroblastic foci in IPF lungs (229). Also, fibroblasts from IPF lung tissue are apoptosis-resistant and show increased XIAP expression (308). Both TGF-β1 and another profibrotic mediator, endothelin (ET)-1, induce XIAP protein expression in normal human fibroblasts while knockdown of XIAP sensitizes lung fibroblasts to Fas-mediated apoptosis (308). XIAP also plays a role in TGFβ-mediated signaling that is distinct from its direct anti-apoptotic functions (429). Consistent with a pro-fibrotic role for XIAP, treatment of lung mesenchymal cells with the anti-fibrotic lipid mediator prostaglandin E_2 suppresses XIAP expression and enhances Fas-mediated apoptosis (229). Although much less is known about the role of cIAPs in lung fibrosis, based on their structural overlap with XIAP we speculate that these proteins may also influence fibroblast apoptosis resistance. We hypothesized that XIAP,

and potentially the cIAPs, are critical to the pathogenesis of lung fibrosis. To address this hypothesis, we employed a murine model of lung fibrosis and antagonized the IAPs with AT-406 (an orally active mimetic of Smac/DIABLO with activity against XIAP, cIAP1 and cIAP2) and specifically disrupted XIAP via gene deletion (345).

Results

Murine mesenchymal cells had a significant increase in XIAP, cIAP-1 and cIAP-2 mRNA after treatment with TGFβ1

TGFβ1, the central profibrotic mediator in pulmonary fibrosis, induces an apoptosis resistant phenotype in mesenchymal cells and significantly increases XIAP expression in normal human lung fibroblasts (308). To assess whether TGFβ1 also up-regulateed IAP expression in murine mesenchymal cells, fibroblasts and fibrocytes were isolated from naïve mouse lungs and treated with TGFβ1 (2 ng/mL) in serum-free media. RNA was then isolated for real-time RT-PCR analysis. We observed that both fibroblasts and fibrocytes had significantly increased levels of XIAP, cIAP-1 and cIAP-2 mRNA in response to TGFβ1 stimulation **(Figure 32).**

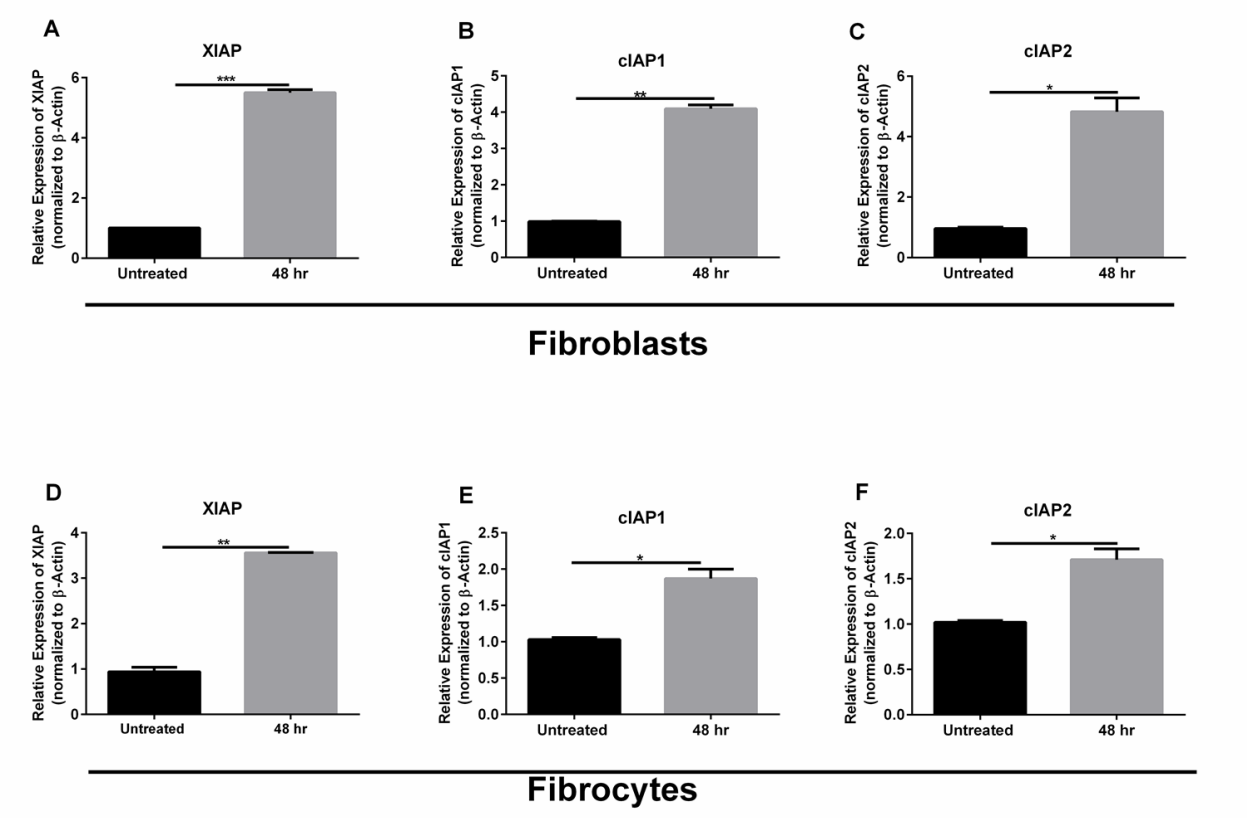

Figure 32: TGFβ treatment increased the expression of XIAP and cIAPs in fibroblasts and fibrocytes.
Fibroblasts and fibrocytes from wild-type mice were treated with TGFβ (2ng/mL) for 48 hours. Total RNA was isolated and by real time RT-PCR we measured the expression of XIAP, cIAP-1 and cIAP-2 and β-actin in fibroblasts (**A-C**) and fibrocytes (**B-D**). Data represent cells collected from n=3 mice total from 2 different experiments. ***p<0.001,**p<0.01 and *p<0.05.

Functional inhibition of IAPs with AT-406 protected wild type mice from bleomycin-induced lung fibrosis

To examine the role of IAPs on lung fibrosis *in vivo,* an orally bioavailable IAP antagonist AT-406 (100 mg/kg by oral gavage) or vehicle control was administered from days 0-6 (for assessment of inflammation) or 0-20 (for assessment of fibrosis) to wild-type mice treated with intratracheal PBS or bleomycin on day 0. AT-406 significantly decreased remodeling of lung architecture and fibrosis as determined on day 21 by hydroxyproline quantification **(Figure 33A)** and histology, including analysis of Picrosirius Red stained sections to elucidate collagen

deposition in the lungs **(Figure 33B).** To determine whether AT-406 treatment impacted the recruitment of inflammatory cells, we determined the number and composition of the inflammatory cell infiltrate at day 7 post-bleomycin. Figure 26C demonstrates that the total inflammatory cell number was not different with AT-406 treatment. The differential analysis showed modest reductions in the percentage of monocyte/macrophages and small increases in lymphocytes and neutrophils **(Figure 33D).** Taken together, these data demonstrated that inhibition of XIAP together with cIAP1 and cIAP2 limited the development of fibrosis following bleomycin-induced injury without major effects on inflammation.

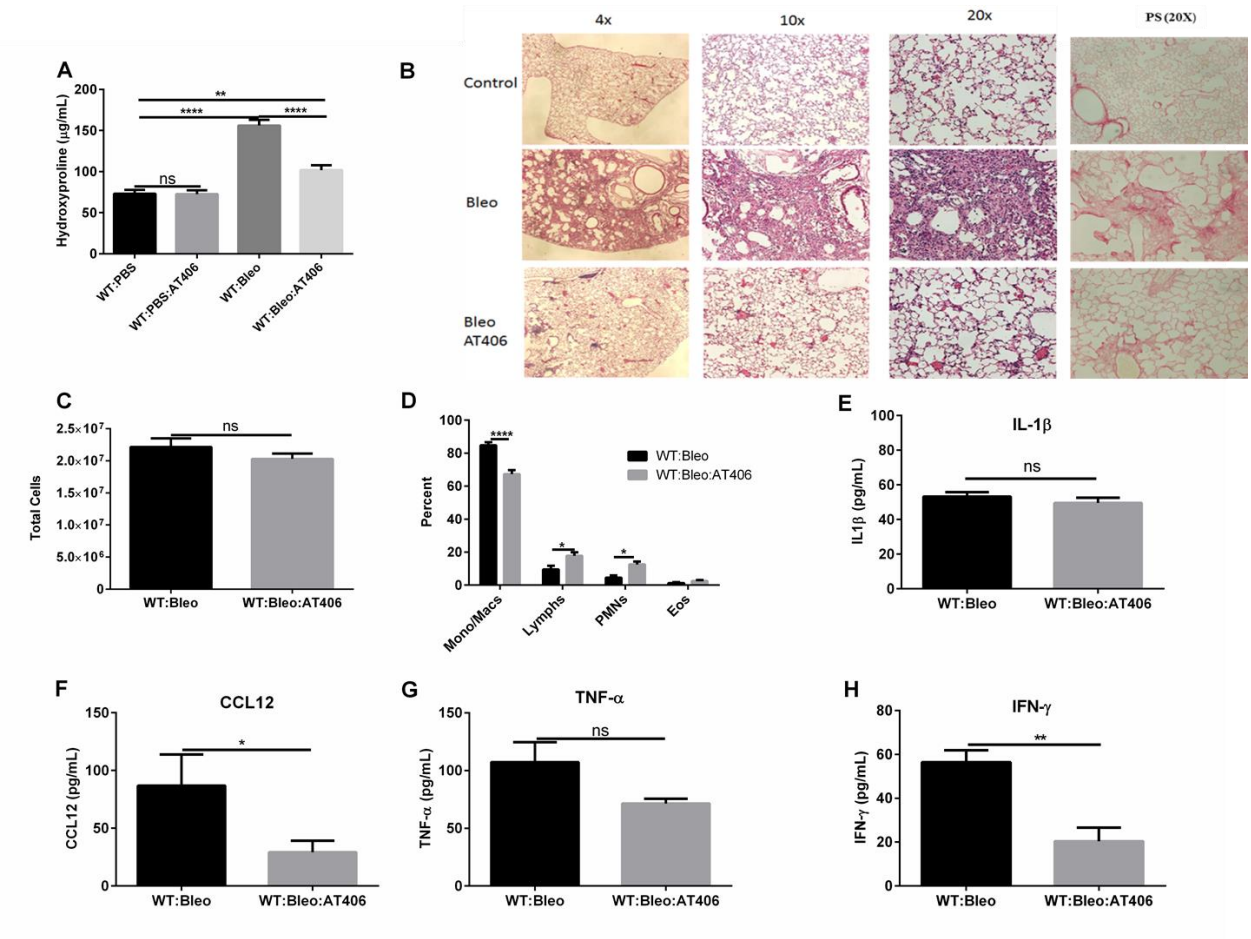

Figure 33: Blockade of IAPs with AT-406 inhibited lung collagen accumulation on day 21 post-bleomycin treatment and decreases lung levels of CCL12.

(A) Wild type mice were given 1.15 U/Kg of bleomycin or PBS intratracheally on day 0. AT-406 (100 mg/kg by oral gavage) was administered daily through day 20 to half of the mice and vehicle control (PBS) was administered to the other half. Lungs were harvested on day 21 for hydroxyproline quantification. **(B)** Histochemical staining showing representative lungs of mice treated with vehicle control (PBS), bleomycin or bleomycin with AT-406. Shown are hematoxylin and eosin (H&E) and Picrosirius Red (PS). Magnification is via the 4x, 10x and 20x objectives from left to right. **(C)** On day 7, lungs were harvested, digested and total lung leukocytes were enumerated. **(D)** Differential analysis of leukocytes was done to determine the percentage of monocytes/macrophages, lymphocytes, neutrophils, and eosinophils. Data shown represents mean ± SEM, n=3 animals/group, ns=not significant. (**E**) Leukocytes were plated at $3x10^6$ cells/mL in serum free media overnight. Cell-free supernatants were analyzed by ELISA for IL1β, **(F)** CCL12, (**G**) TNF-α and (**H**) IFNγ. Data shown are pooled from two independent experiments, with n = 4-6 mice per group in each experiment. ****p<0.0001, **p < 0.01, *p< 0.05, ns=not significant.

AT-406 treatment diminishes CCL12 and IFNγ

To determine the impact of AT-406 treatment on lung cytokine levels, lung homogenates collected on day 7 were analyzed for the expression of IL-1β, TNFα, CCL12 and IFNγ. Figures 26E-H demonstrates that AT-406-treated mice showed significant inhibition of both CCL12 and IFNγ, but no alteration in IL-1β. There was a trend towards reduction of TNFα.

Delayed administration of AT-406 has therapeutic benefit

To determine whether inhibition of IAP proteins could have an anti-fibrotic effect during the post-inflammatory phase of bleomycin-induced fibrosis, we next administered AT-406 using a treatment protocol. Wild type mice were given bleomycin or PBS on day 0, daily treatments with AT-406 (or vehicle) were given from days 10-20 and lungs were harvested for analysis on day 21. Supporting an anti-fibrotic effect that is independent of the early inflammatory phase, the therapeutic dosing regimen of AT-406 maintained efficacy with reductions in lung collagen to similar levels as observed with the preventive strategy as indicated by hydroxyproline quantification **(Figure 34A)**, histology and Picrosirius Red staining **(Figure 34B).**

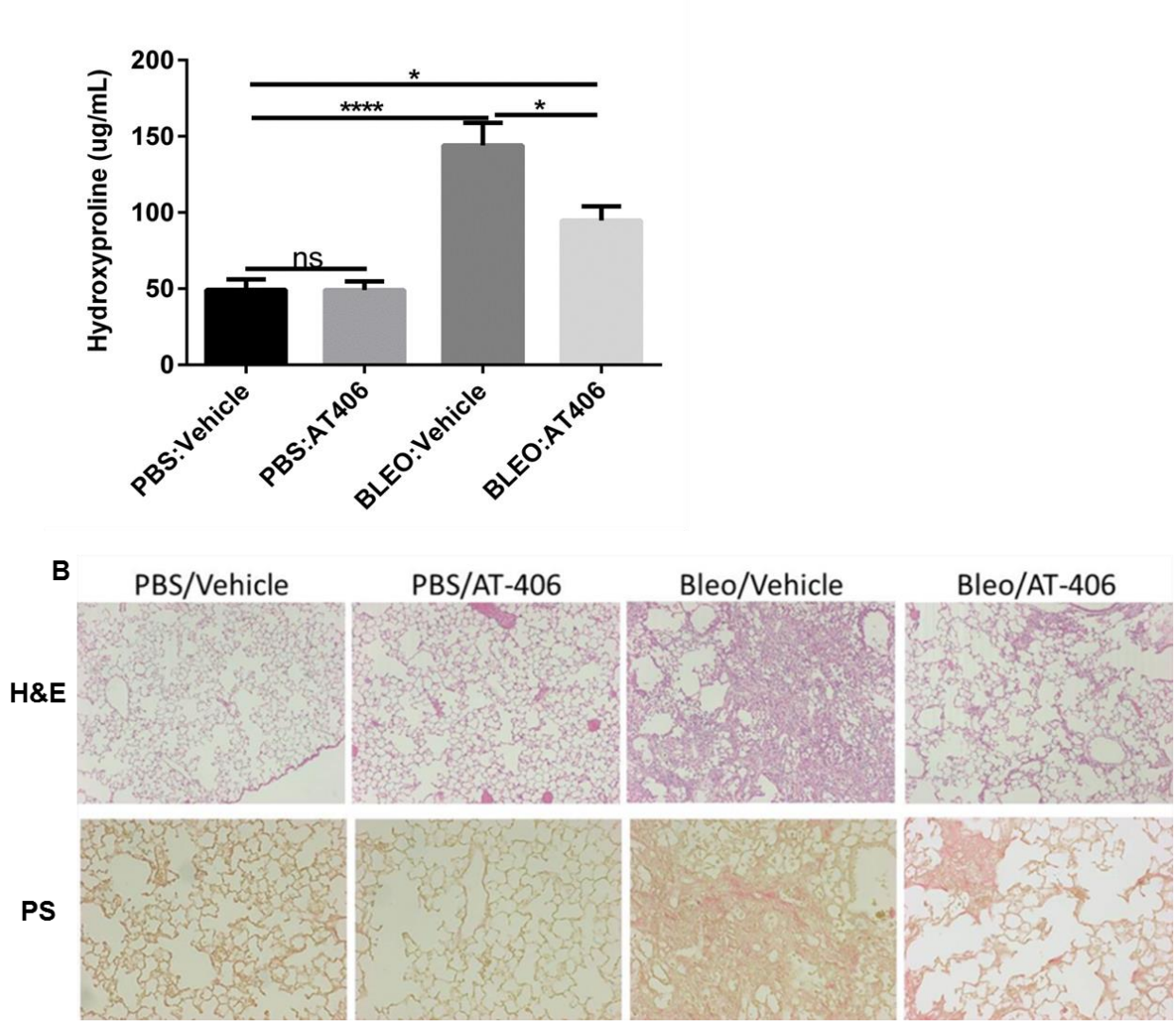

Figure 34: Therapeutic administration of AT-406 limits lung fibrosis.
(A) Wild type mice were given 1.15 U/Kg of bleomycin or PBS intratracheally on day 0. Half of each group received 100 mg of AT-406 (100 mg/kg) by oral gavage daily starting on Day 10 through day 20 and lungs were harvested on day 21 for hydroxyproline quantification. **(B)** Histochemical staining showing representative lungs of mice treated with intratracheal PBS and vehicle control (PBS), intratracheal bleomycin and AT-406, intratracheal bleomycin and vehicle control or intratracheal bleomycin and AT-406. Shown are hematoxylin and eosin (H&E) and Picrosirius Red staining. Magnification is via the 20x objective. Data shown represents mean ± SEM, represent n=4-6 mice/group, ns,=not significant. ****$p<0.0001$ and *$p<0.05$.

Therapeutic administration of AT-406 enhanced mesenchymal cell apoptosis in vivo

To determine whether therapeutic AT-406 treatment enhanced apoptosis *in vivo,* AT-406 was administered beginning on day 11 post-bleomycin and apoptosis was assessed on day 13.

First, the total level of caspase 3/7 activity was measured in lung homogenates. AT-406 treatment showed a trend towards increasing caspase activity in the lung compared to the activity measured in lungs from mice treated with bleomycin and vehicle control **(Figure 35A).** To assess apoptosis within the myofibroblast population (α-SMA expressing mesenchymal cells), lung sections were co-stained with α-SMA and TUNEL **(Figures 35B-H).** Enumeration of apoptotic myofibroblasts in stained sections revealed significantly increased myofibroblast apoptosis in the bleomycin-injured AT-406-treated mice **(Figure 35B)**.

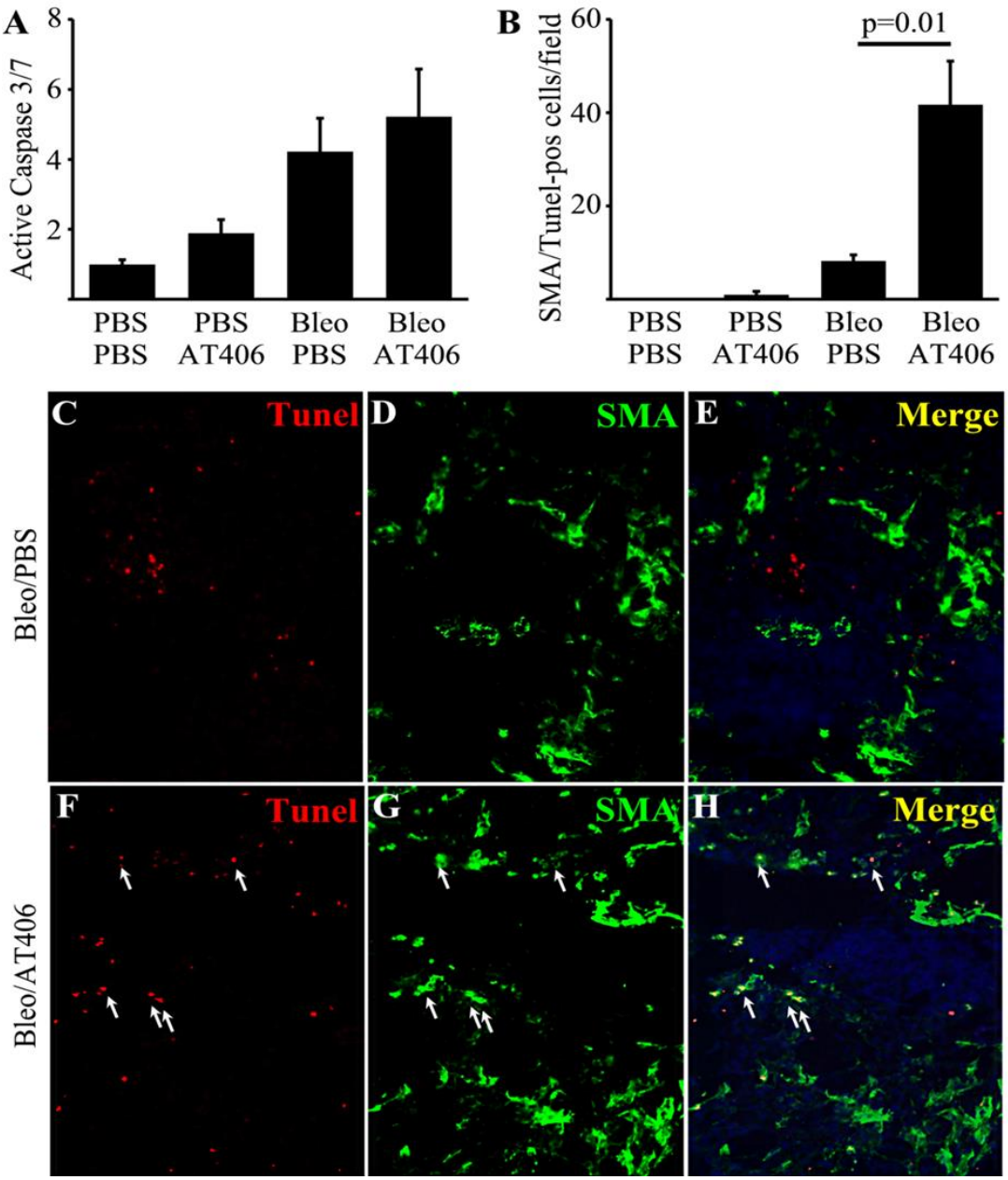

Figure 35: AT-406 augmented myofibroblast apoptosis in vivo after bleomycin injury. Wild type mice were given 1.15 U/Kg of bleomycin or PBS intratracheally on day 0. On days 11, 12 and 13 half of each group was administered AT-406 (100 mg/kg via oral gavage) and the lungs were harvested on day 13. **(A)** Whole lung homogenates were assessed for activation of caspase 3/7. $p < 0.01$for Bleo/AT-406 compared to controls. (**B-H).** Lung sections were co-stained for TUNEL (C and F) and α-smooth muscle actin (SMA; D and G). Cells that were positive for both TUNEL and α-SMA were quantified using merged images (E and H) in four random 20x objective fields by an investigator who was blinded to the treatment groups. This quantification **(B)** demonstrated significantly more co-positive cells in bleomycin/AT-406 lung sections compared to bleomycin/PBS lung sections. p=0.01. Co-stained cells in representative merged images (**E and H**) are indicated by arrows

Genetic deficiency of XIAP did not protect against bleomycin-induced lung fibrosis

To specifically assess the role of XIAP in lung fibrogenesis, wild-type ($XIAP^{+/+}$) and $XIAP^{-/y}$ mice were given intratracheal PBS or bleomycin on day 0. On day 7, lungs were collected and XIAP expression was assessed from cultured lung mesenchymal cells. These results demonstrated the upregulation of XIAP in mesenchymal cells from the lungs of wild-type mice following intratracheal bleomycin **(Figure 36A).** As expected, mesenchymal cells from the lungs of $XIAP^{-/y}$ mice had undetectable levels of XIAP (data not shown). The remaining lungs were harvested on day 21 and lung collagen content was measured by hydroxyproline assay in $XIAP^{+/+}$ and $XIAP^{-/y}$ mice treated with PBS or bleomycin. As expected, bleomycin-treated wild type mice showed a significant increase in collagen content when compared to PBS controls. However, in contrast to the results with AT-406 treatment, bleomycin-treated $XIAP^{-/y}$ mice showed similar levels of lung collagen as the bleomycin-treated wild-type mice **(Figure 36B).** Representative histology also showed similar levels of remodeling and cellular infiltration between the two strains **(Figure 36C)**. XIAP deficiency had no significant effect on total inflammatory cell recruitment **(Figure 36D)** or inflammatory cell composition **(Figure 36E)** at day 7 following bleomycin.

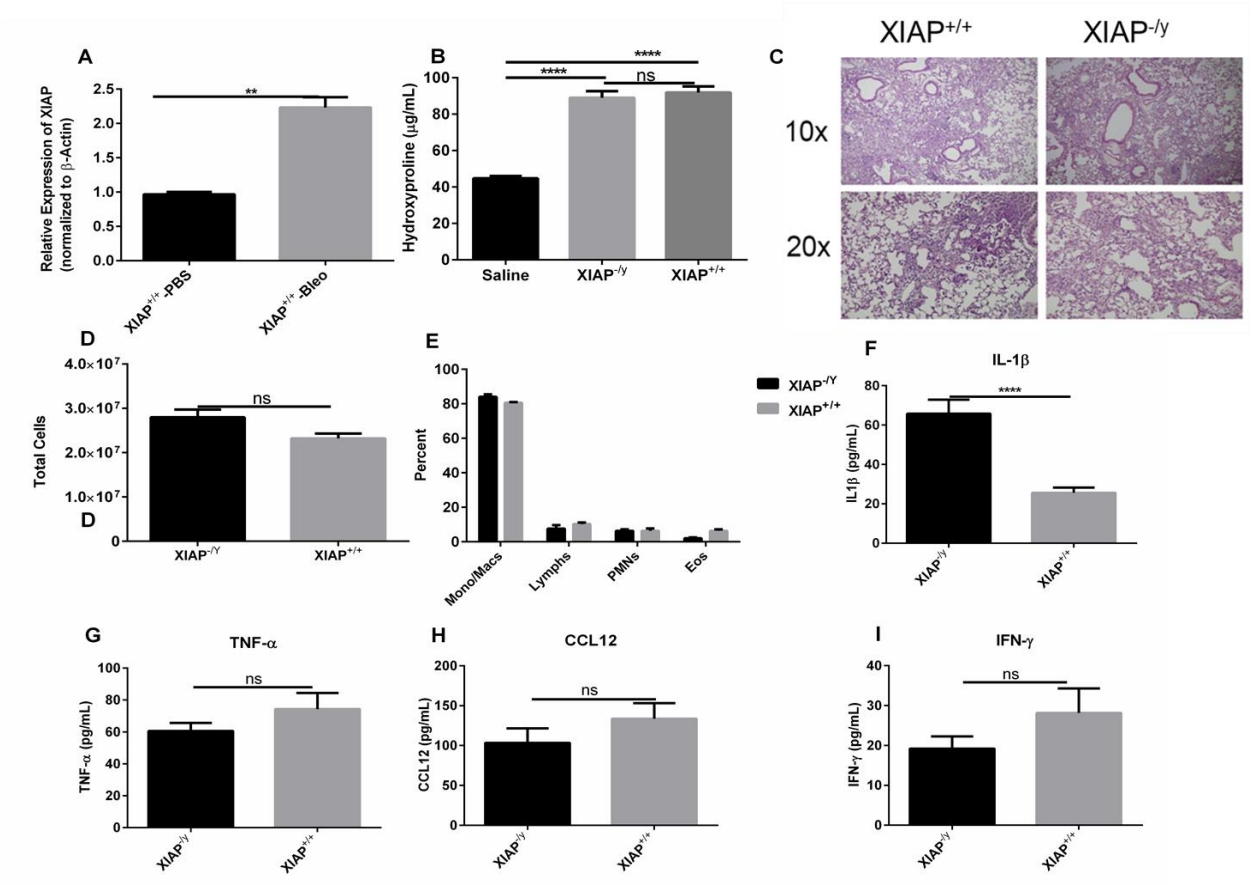

Figure 36: XIAP deficient mice were not protected from bleomycin-induced pulmonary fibrosis and show elevated levels of IL-1β.
Wild-type littermate ($XIAP^{+/+}$) or $XIAP^{-/y}$ mice were given bleomycin or PBS intratracheally on day 0. Lungs were harvested on day 7. Lung minces were then digested in collagenase and total lung leukocytes were enumerated and lung mesenchymal cells were cultured. **(A)** XIAP mRNA expression was assessed in cultured lung mesenchymal cells by RT-PCR. **(B)** On day 21 lungs were harvested for hydroxyproline quantification. **(C).** Representative hematoxylin and eosin staining from day 21. Magnification is through the 10x (top) and 20X (bottom) objectives. Representative of n=4 mice examined. **(D)** Total lung leukocytes from day 7 lung minces were enumerated. **(E)** Differential analysis was done to determine the percentage of monocytes/macrophages, lymphocytes, neutrophils, and eosinophils. Data shown represent n = 6–10 mice per group pooled from 3 independent experiments. Cells were plated at $3X10^6$ cells/ml in serum free media overnight and cell free supernatants were analyzed by ELISA for IL1β **(F)**, TNFα **(G),** CCL12 **(H),** and IFNγ (**I**). Data shown represents mean ± SEM, represent n=4-6 mice/group, ns, not significant. ****p<0.0001, ***p<0.001

XIAP$^{-/y}$ mice expressed more IL-1β post-bleomycin treatment

In contrast to the changes observed in wild-type mice treated with AT-406, the XIAP$^{-/y}$ mice had no significant changes in TNFα, CCL12 or IFNγ. The XIAP$^{-/y}$ mice did show enhanced production of IL-1β **(Figure 36F-I).** However, this increase in IL-1β did not seem to impact the levels of fibrosis when compared to wild-type mice.

XIAP$^{-/y}$ mesenchymal cells are resistant to Fas-mediated apoptosis

Because mesenchymal cell accumulation is a critical feature of lung fibrosis, we next sought to determine how the loss of XIAP impacted mesenchymal cell apoptosis. Lung mesenchymal cells (a mixture of both fibroblasts and fibrocytes) from wild-type and XIAP$^{-/y}$ mice were treated with a Fas-activating antibody and apoptosis was assessed over time as indicated by caspase 3/7-mediated cleavage of a fluorogenic substrate. In contrast to our findings in normal human lung fibroblasts in which XIAP was silenced with siRNA (308), we observed that murine lung mesenchymal cells congenitally lacking XIAP had increased resistance to Fas-mediated apoptosis when compared to wild-type cells **(Figure 37A).** This finding suggested that alternative anti-apoptotic mechanisms might provide functional compensation for the genetic deficiency in XIAP$^{-/y}$ mice, and offered a potential explanation for why these mice remained susceptible to bleomycin-induced fibrosis.

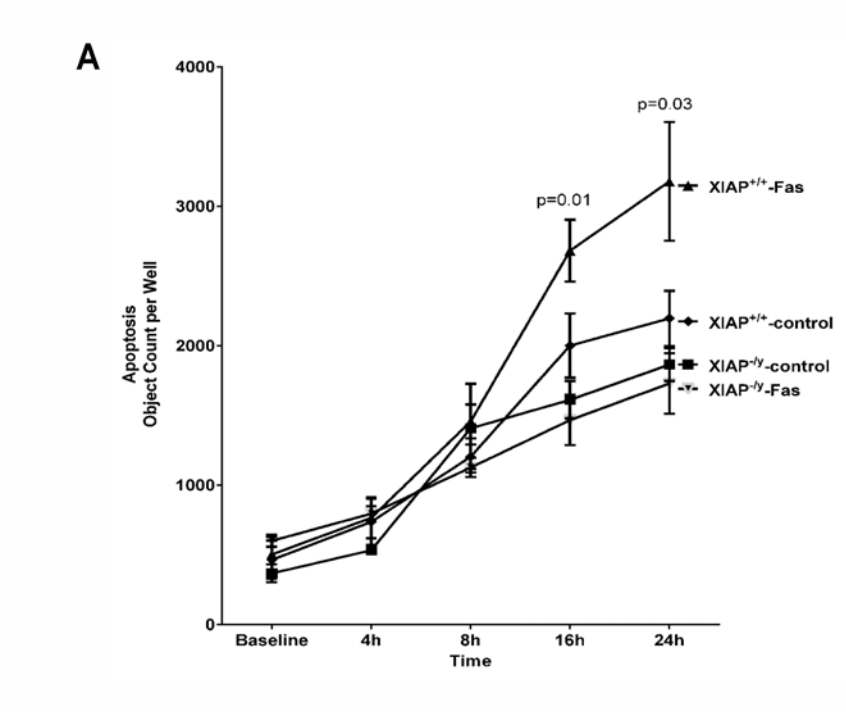

cIAPs expression was increased in XIAP gene-targeted mice

Initial characterization of the XIAP$^{-/y}$ mice demonstrated that the expression of cIAP-1 and 2 proteins was increased, suggesting that in the congenital absence of XIAP, there exists a mechanism by which the increased production of other IAP family members may contribute to functional compensation (338)**.** The expression of cIAP-1 and 2 in lung homogenates and in lung mesenchymal cells cultured from XIAP$^{+/+}$ and XIAP$^{-/y}$ mice treated with bleomycin were analyzed by qRT-PCR. In the lung homogenates, levels of cIAP-1 were significantly elevated following intratracheal bleomycin in wild type and XIAP deficient mice and cIAP-2 showed a non-statistically significant increase in XIAP$^{-/y}$ mice **(Figure 37B and C).** In isolated mesenchymal cells from untreated mice however, the opposite result was seen with basal levels of cIAP-1 being unchanged **(Figure 37D)** while cIAP-2 mRNA expression was significantly increased in XIAP$^{-/y}$ cells when compared to wild type **(Figure 37E).** These data support the possibility of a functional compensation at baseline by cIAPs in the XIAP$^{-/y}$ mice.

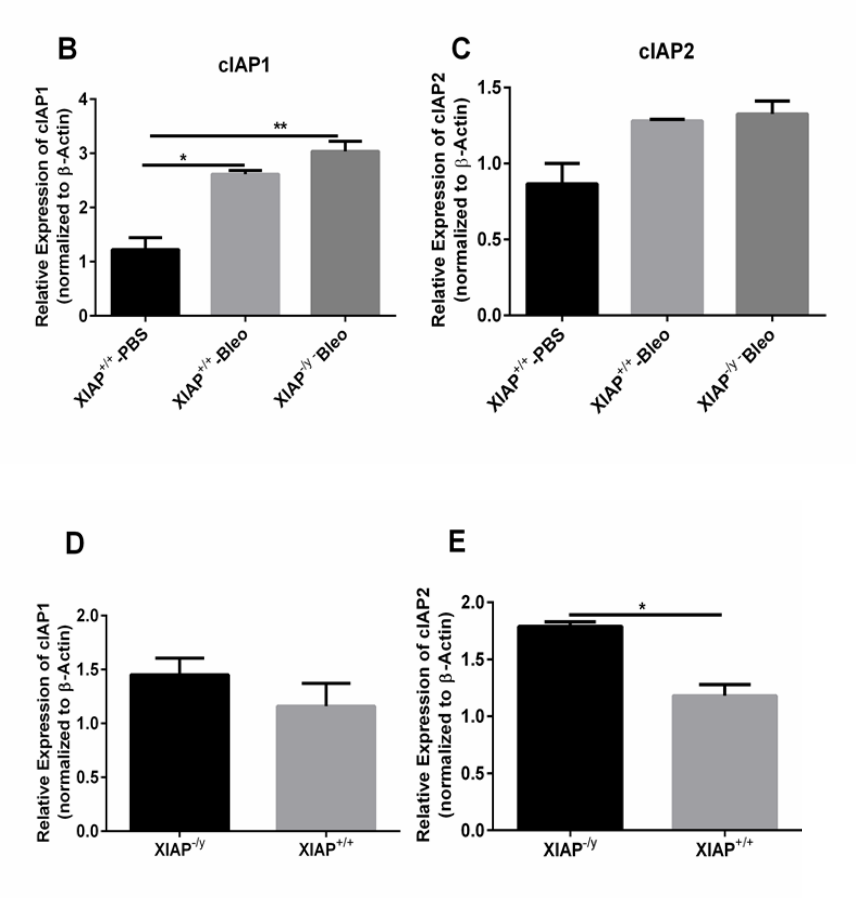

Figure 37: XIAP$^{-/y}$ mesenchymal cells have increased cIAP expression associated with decreased susceptibility to Fas-mediated apoptosis and inhibition of cIAPs enhanced their apoptosis.

(A) Lung fibroblasts from wild type and XIAP$^{-/y}$ mice were treated with/without Fas-activating antibody (250 ng/mL) along with Cellplayer^{TM} kinetic caspase 3/7 reagent. Plates were loaded into the IncuCyte incubator and photographed every 2 hours for 24 hours. Apoptosis was quantified by automated counting "objects per well" (object = green fluorescence indicating cleavage of a fluorogenic substrate by caspase 3/7). **(B-C)** Total RNA was isolated from fibroblasts cultured form the lungs of XIAP$^{+/+}$ and XIAP$^{-/y}$ mice treated with/without bleomycin and expression of cIAP-1, cIAP-2 and β-actin was measured by real time RT-PCR. Data represent n=3 per group pooled from multiple mice. *P<0.01. **(D-E)** RNA isolated from lung homogenates of untreated XIAP$^{+/+}$ and XIAP$^{-/y}$ mice were assessed for cIAP-1 and cIAP-2. Data represent n=3 per group pooled from multiple mice. *P<0.01. **(F)** Lung fibroblasts from XIAP$^{-/y}$ were treated with/without Fas-activating antibody (250 ng/mL) and/or AT-406 (1.0 μM). Apoptosis was evaluated as described above with n=3 wells/group. * $p < 0.05$ vs. control and AT-406, $p < 0.01$ vs. Fas treatment. Data are representative of mean ±SEM, n=3 wells/treatment per group, with 9 images per well at each time point.

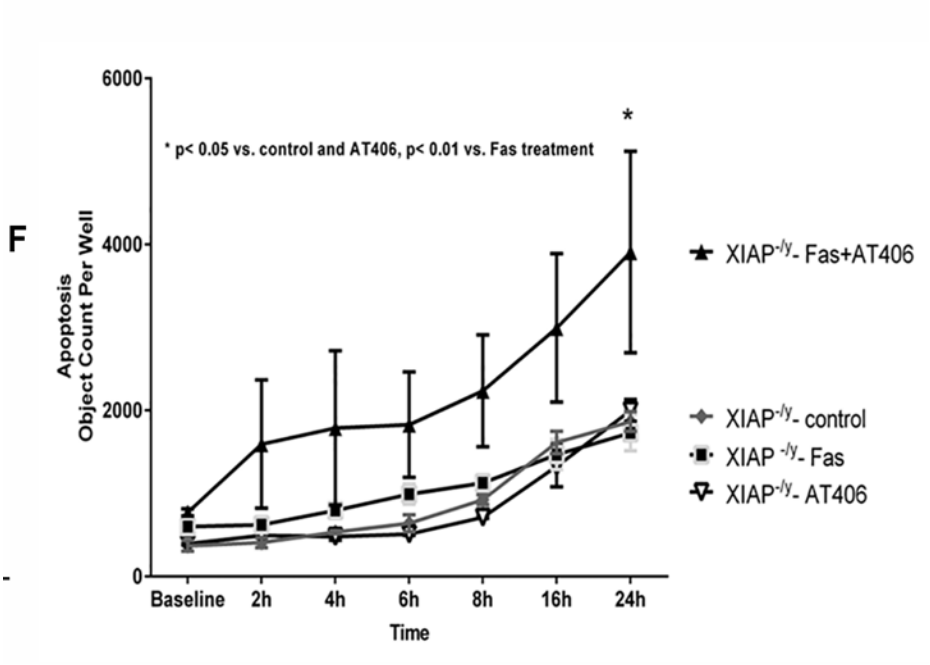

AT-406 sensitized XIAP$^{-/y}$ mesenchymal cells to Fas-mediated apoptosis

To determine if increased cIAP expression provided functional compensation for the deficiency of XIAP in lung mesenchymal cells, we determined whether inhibition of cIAP-1 and cIAP-2 would restore sensitivity to Fas-induced apoptosis in XIAP$^{-/y}$ mesenchymal cells. XIAP$^{-/y}$ cells were treated with the IAP antagonist, AT-406, and susceptibility to Fas-mediated apoptosis was assessed over 24 hours. Supporting the hypothesis of functional compensation by cIAPs, inhibition of cIAP-1 and cIAP-2 with AT-406 enhanced the apoptotic sensitivity of the XIAP-deficient mesenchymal cells **(Figure 37F).** Of note, treatment of XIAP deficient mesenchymal cells with AT-406 alone did not increase apoptosis in the absence of Fas-activation, suggesting that the increased apoptosis was not a non-specific effect of the compound.

AT-406 treatment limited fibrosis in XIAP$^{-/y}$ mice

To verify that AT-406 treatment could reduce bleomycin-induced fibrosis in vivo, XIAP$^{-/y}$ mice or XIAP$^{+/+}$ mice were treated with intratracheal PBS or bleomycin and AT-406 or vehicle control beginning on day 0. There was an unexpected early toxicity of AT-406 treatment that was observed during the acute inflammatory phase of the model (between days 4-7) in the cohort of XIAP$^{-/y}$ mice that had received intratracheal bleomycin. This effect was observed in multiple experiments and reduced the n value for these experiments. However, in the mice that did survive the inflammatory phase of the model, there was a trend towards reduced levels of collagen accumulation in the lungs as measured by hydroxyproline assay **(Figure 38A)**. Analysis of accumulated inflammatory cells and cytokines at day 7 showed no changes other than increased neutrophils in the XIAP$^{-/y}$ mice that received bleomycin which was accentuated in the XIAP$^{-/y}$ mice that received the bleomycin and AT-406, suggesting that toxicity in this group might be related to alterations in the acute response to injury **(Figures 38B-E)**. In addition, AT-406 treatment was associated with a trend for decreased elaboration of IL-1β and CCL12 from leukocytes isolated from the XIAP deficient mice on day 7 after bleomycin **(Figures 38F and G)**.

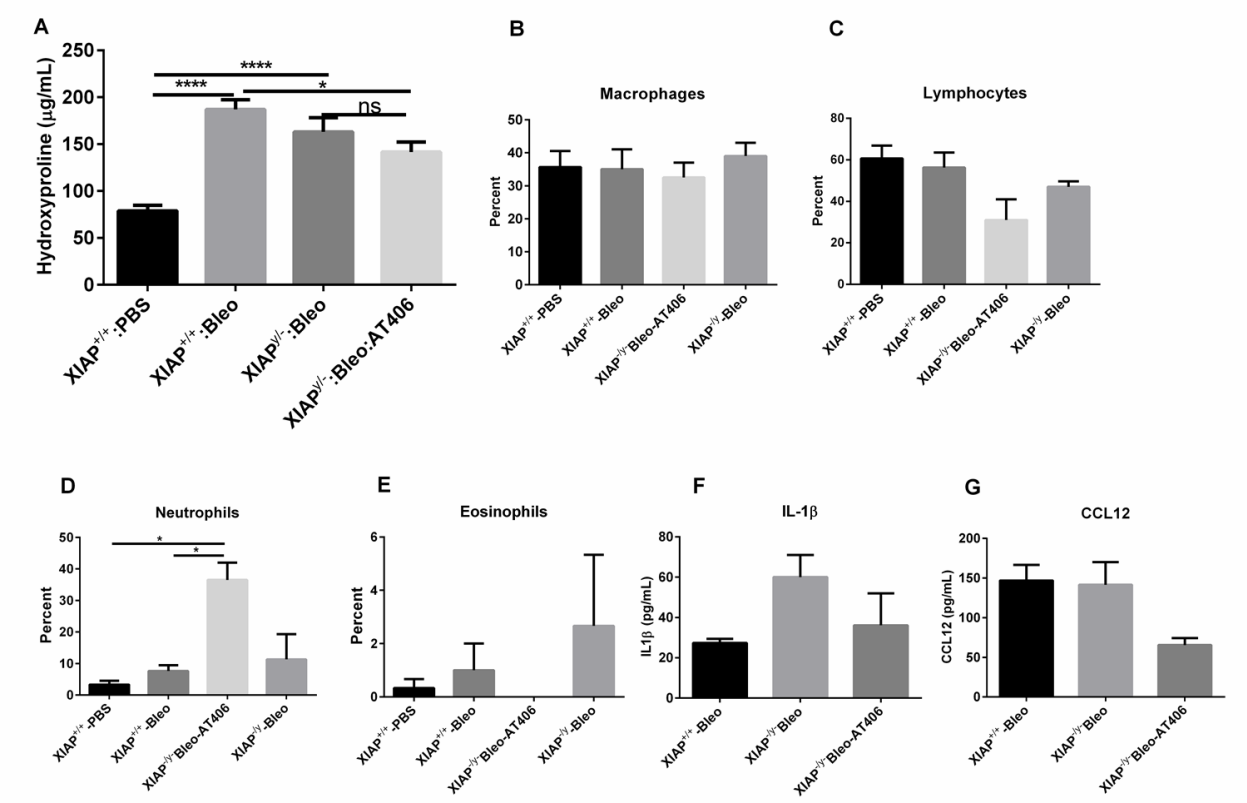

Figure 38: AT-406 decreased bleomycin-induced lung fibrosis in XIAP$^{-/y}$ mice.
(A-I) XIAP$^{+/+}$ or XIAP$^{-/y}$ mice were given bleomycin or PBS intratracheally on day 0. Lungs were harvested and assessed for inflammation on day 7 and fibrosis on day 21 as described in Figure 5. **(A)** Hydroxyproline quantification at day 21. Data shown represents mean ± SEM. n = 7-11 mice/group. ns, not significant. ****p<0.0001, ***p<0.001, * p<0.05. **(B-E)** Leukocyte differentials in lung collagenase digest on day 7. n = 3 lungs per group. * p<0.05. **(F-G)** Cytokines in cell-free supernatants from day 7 leukocytes.

Discussion

Previous studies have shown that fibroblastic foci, but not the epithelial cells in IPF tissues, express high levels of XIAP (229, 430), that PGE_2 suppresses XIAP expression while increasing fibroblast susceptibility to apoptosis, that the pro-fibrotic mediators TGFβ1 and ET-1 increase XIAP expression in normal fibroblasts and that XIAP (but not cIAP-1 or cIAP-2) expression is increased in lung fibroblasts from patients with IPF (229, 308). Together, these studies suggested XIAP might contribute to the accumulation of myofibroblasts and extracellular

matrix in IPF and that targeting XIAP could represent a therapeutic approach for lung fibrosis. Testing this hypothesis in a murine model of experimental lung fibrosis using pharmacologic and genetic approaches led to discordant findings *in vivo*, and our subsequent studies suggested other IAP family members (i.e. the cIAPs) may contribute to mesenchymal cell apoptosis resistance and fibrogenesis.

Consistent with our findings in human lung fibroblasts, we found that the profibrotic mediator, TGFβ1, enhanced expression of XIAP in murine mesenchymal cells. Importantly, TGFβ1 also increased the expression of cIAPs (cIAP-1 and cIAP-2) in these cells. Similarly, bleomycin treatment upregulated both XIAP and cIAP-l. Treatment of mice with the IAP antagonist, AT-406 substantially decreased lung fibrosis in vivo, establishing a causal role for the IAPs in lung fibrogenesis. In contrast to the broad inhibition of the IAPs with AT-406, the specific targeting of XIAP by transgenic deletion did not protect against bleomycin-induced fibrosis. Assessment of early inflammatory responses to bleomycin-treated mice showed no differences in total inflammatory cell recruitment in the mice treated with AT-406 or in $XIAP^{-/y}$ mice compared to wild-type mice treated with bleomycin. Differential cell counts showed no difference between inflammatory cell populations in wild-type and XIAP-deficient mice which were not protected from fibrosis; in contrast, mice receiving AT-406 did have a small, but statistically significant decrease in the monocyte/macrophage population coupled with increases in the lymphocyte and neutrophil populations. Thus, it seems unlikely that the protection from fibrosis seen by AT-406 administration is due to decreased lung injury and inflammation. In fact, we were surprised to find that AT-406 treatment in the $XIAP^{-/y}$ mice actually showed some toxicity and enhanced neutrophil recruitment.

When analyzing the cytokine profiles of XIAP$^{-/y}$ or AT-406-treated mice, the XIAP$^{-/y}$ mice showed increases in IL-1β, but this did not alter levels of lung fibrosis. In contrast, the AT-406 treated mice had equivalent levels of IL-1β, but did show reduced expression of CCL12, IFNγ and, a trend for decreased TNFα. Certainly CCL12 has been shown to promote fibrotic responses in the lung by mediating fibrocyte recruitment (94), so reduced levels of CCL12 may limit fibrocyte accumulation. Similarly, the CCL12 receptor CCR2 has been shown to be critical for the recruitment of exudate macrophages to the lung, and decreased recruitment of exudate macrophages was associated with decreased fibrosis in a model of targeted type II alveolar epithelial injury (395). The impact of IFNγ on lung fibrogenesis is controversial, and clinical trials have failed to demonstrate a significant therapeutic benefit for IFNγ as a treatment for IPF (431, 432). However, as these clinical trials were predicated on the multitude of anti-fibrotic actions of IFNγ in pre-clinical models, it seems unlikely that the decline in IFNγ observed with AT-406 treatment accounted for the decreased fibrosis observed in our experiments. Thus, while acknowledging that differences in the accumulation of monocyte/macrophages and fibrocytes, or decreased levels of CCL12 or IFNγ might contribute to the discordant fibrotic outcomes in these two approaches, we went on to investigate the apoptotic susceptibility of murine lung mesenchymal cells.

Studies increasingly support the hypothesis that impaired apoptosis contributes to myofibroblast accumulation in lung fibrosis (55, 229, 308, 412, 413, 433, 434). Consistent with the initial characterization of XIAP deficient mice (338), our investigation revealed that mesenchymal cells from the XIAP-deficient mice did not demonstrate increased susceptibility to Fas-mediated apoptosis. Indeed, the cells lacking XIAP actually had a significant decrease in apoptotic susceptibility. Because XIAP$^{-/y}$ mesenchymal cells maintained expression of cIAP-1

and displayed enhanced expression of cIAP-2, we interpreted these results to suggest that alternative anti-apoptotic mechanisms, including the increase in cIAP protein expression, might provide a functional compensation for the genetic loss of XIAP. Consistent with this hypothesis, treatment of $XIAP^{-/y}$ mesenchymal cells with AT-406 restored the anticipated apoptotic susceptibility to $XIAP^{-/y}$ cells *in vitro*, and treatment of the bleomycin-treated mice with AT-406 increased myofibroblast apoptosis *in vivo*. Because resistance to apoptosis contributes to the persistence of myofibroblasts, we speculate that the different outcomes to bleomycin-induced lung injury are related to the differential apoptotic susceptibility of mesenchymal cells in these different genetic and pharmacologic models. If true, it is encouraging that AT-406 was able to limit fibrosis following bleomcyin challenge. IAP antagonist compounds are already being tested in clinical trials as cancer therapeutics (418, 435-439), such therapies could potentially be adopted quickly in IPF.

The fact that AT-406 exerted beneficial effects that were not mirrored by XIAP deficiency, and the fact that cIAP proteins do not antagonize caspase activation (420, 440, 441), raises the question of how the cIAP proteins may be functioning to promote bleomycin-induced fibrosis. Certainly, this family of proteins functions through a variety of mechanisms involving TGFβ signaling, NFκB activation, and E3 ligase activity (427, 429, 442). cIAP1 and -2 have been shown to be important in TNF-α mediated NF_kB activation (443); however, we did not observe a significant difference in TNFα *in vivo*. Thus, it is likely that cIAP-1 and cIAP-2 contribute to the anti-apoptotic phenotype via induction of other anti-apoptotic proteins or via modulation of cell signaling pathways yet to be determined. Importantly, AT-406 acts to promote degradation of cIAP-1 and cIAP-2, raising additional mechanistic possibilities for the anti-fibrotic actions of this approach (444-446).

XIAP is expressed in the fibroblastic foci of IPF tissues and is increased in IPF fibroblasts, but cIAP-1 and cIAP-2 are not increased in IPF fibroblasts (229, 308). This suggests that in human IPF fibroblasts, there may be less compensation than is occurring in $XIAP^{-/y}$ mice or that cIAP protein function is sufficient at levels present in IPF cells. The potential for cIAPs to compensate for the post-natal loss or inhibition of XIAP in adults has yet to be explored. Regardless, it is encouraging that AT-406 has previously been shown to restore apoptotic sensitivity of IPF fibroblasts to Fas-mediated apoptosis (308) and that our murine studies show benefit of AT-406 when given therapeutically during the fibroproliferative phase of the disease.

.

Chapter 6:

Six-SOMAmer index relating to immune, protease and angiogenic functions predicts progression in IPF

Background

Clinical, radiographic and pathologic features differentiate idiopathic interstitial pneumonias. However, the most common and deadly diagnosis is idiopathic pulmonary fibrosis (IPF). IPF is diagnosed using clinical and laboratory features corroborated by characteristic high-resolution computed tomography (CT) or by presence of usual interstitial pneumonia histopathology on lung biopsy (447). Natural course of IPF can vary significantly with some patients experiencing relative stability, while others experience more rapid disease progression (448). Well-validated biomarkers from peripheral blood could have tremendous impact if they differentiate diagnosis of IPF from other more-treatable forms of interstitial lung disease or if they provide accurate prognostic information.

IPF biomarkers have been identified using approaches like transcriptomic profiling, microbiome analyses and candidate biomarker analyses in blood and lung (134, 374, 449, 450). These data along with findings that IPF patients treated with the immunosuppressive prednisone, azathioprine and N-acetylcysteine (451) do worse; have led to speculation that occult immune insults may drive some IPF progression. This is underscored by studies showing progressive disease in IPF associated with overall bacterial burden and certain classes of organisms (134,

374). Such biomarker analyses have provided potential insight into pathogenic mechanisms for IPF progression.

Studies have explored angiogenesis in fibrosis with mixed results. Some IPF studies showed elevations in angiogenesis inhibitors (452) or reduced angiogenic factors (453, 454). Another study reports mixed phenotypes measuring higher levels of both angiogenic and angiostatic factors (455). These variations suggest angiogenesis is important for both pathogenesis and repair. Regarding protease imbalances, alterations in metalloproteases are common (456), but proteasomal processing is also implicated in fibrotic lungs (457).

The slow-off rate-modified aptamer (SOMAmer) SOMAscan panel (337)-based proteomics platform measures 1129 analytes with increased sensitivity for low-abundance biomarkers. Using this assay proteins are measured using a modified aptamer reagent and measured quantitatively in relative fluorescence units (RFU'S) on a custom Agilent hybridization chip. Using this unbiased approach, we analyzed plasma from 60 IPF patients enrolled in the observational study, *COMET* (Correlating Outcome Measures to Estimate Time to progression in IPF. Biomarkers were correlated with measures of disease progression and identified a six-SOMAmer index that predicted IPF progression.

Results

Patient demographics were similar in progressor and non-progressor groups

Sixty IPF patients enrolled in COMET with longitudinal plasma samples collected at weeks 0, 48 and 80 were selected for analysis. Within this cohort, 35 (58%) met criteria for disease progression at some time over 80 weeks follow-up while 25 (42%) did not. There were no statistical differences in age, gender, and smoking history or baseline lung physiology between patients when categorized by progressor status (**Table 2**).

Table 2: IPF Patient Characteristics for N=60 COMET patients by 80-week Progression Status*; Continuous Variables Reported as Mean (Standard Deviation), Categorical Variables Reported as N (%)*

	All (N=60)	Progressor (N=35)	Non-progressor (N=25)	P-value
Age in Years	64.6 (7.7)	65.2 (8.3)	63.7 (6.9)	0.48
Male	41 (68.3)	22 (62.9)	19(76.0)	0.28
Smoker				0.58*
Never	19 (31.7)	12 (34.3)	7 (28.00)	0.61**
Past	40 (66.7)	23 (65.7)	17 (68.00)	0.85**
Current	1 (1.7)	0	1 (4.00)	0.42**
FVC, % pred	70.0 (16.2)	71.2 (16.3)	68.2 (16.3)	0.50
DLCO, %pred	46.1 (13.1)	46.9 (12.9)	44.8 (13.8)	0.56

*Overall Chi-square comparison; **Comparisons of corresponding category vs others.

Nine analytes predicted progression in IPF

Out of 1129 biomarkers analyzed, only 9 biomarkers satisfied criteria for estimated AUC > 0.7 from ROC analysis of the biomarker as a binary variable (above versus below its threshold); these were carbonic anhydrase 13, Cath-S, FCN2, GRN, ICOS, LGMN, nascent polypeptide-associated complex subunit alpha (NACA), TRY3 and VEGFsR2. Univariate ROC analysis for these 9 biomarkers is shown in **Table 3**, along with odds ratios (ORs) for progression for those above versus below their biomarker thresholds. Above threshold values of VEGFsR2, LGMN, FCN2, Cath-S and GRN were associated with lack of progression during follow-up ($OR < 1.0$, $p < 0.05$), and above threshold values for ICOS, TRY3, carbonic anhydrase 13 and NACA were associated with progression during follow-up ($OR > 1.0$, $p < 0.05$) in both adjusted and unadjusted analyses.

Table 3: Biomarker Threshold Values in RFU, Corresponding Sensitivity and Specificity for Predicting 80-week Progression Status and Univariate Odds Ratios *(Unadjusted and Adjusted) for Progression When Above Versus Below the Threshold.*

Biomarker	Better Prognosis Threshold (RFU)	Sensitivity	Specificity	AUC	OR	95% CI	P	OR	95% CI	P
					(Unadjusted)			(Adjusted*)		
VEGF sR2	>9559.30	0.71	0.80	0.74	0.11	0.03-0.39	0.001	0.07	0.01-0.33	0.001
LGMN	>5173.33	0.54	0.96	0.74	0.04	0.005-0.32	0.003	0.04	0.00-0.38	0.005
FCN2	>2015.33	0.74	0.72	0.73	0.13	0.04-0.43	0.001	0.12	0.03-0.50	0.003
Cathepsin S	>1451.44	0.54	0.88	0.71	0.11	0.03-0.46	0.002	0.08	0.02-0.46	0.004
ICOS	<8031.61	0.77	0.64	0.71	6.00	1.93-18.68	0.002	13.5	2.88-62.88	0.001
TRY3	<928.22	0.77	0.64	0.71	6.00	1.93-18.68	0.002	6.1	1.65-22.82	0.007
Carbonic_an-hydrase_XIII	<8738.54	0.69	0.76	0.72	6.91	2.16-22.10	0.001	5.9	1.64-20.98	0.007
GRN	>32046.22	0.69	0.72	0.70	0.18	0.06-0.55	0.003	0.11	0.03-0.50	0.004
NACA	<17976.83	0.69	0.72	0.70	5.61	1.82-17.33	0.003	7.5	1.57-35.88	0.012

Thresholds were chosen to maximize sensitivity plus specificity in separate ROC curve analyses. Odds ratios greater than 1.0 indicate higher risk of progression when above threshold; Odds ratios less than 1.0 indicate lower risk of progression when above threshold. Nine biomarkers met screening criteria of (1) AUC > 0.7, (2) unadjusted and adjusted P-values <0.05.

*Adjusted logistic models were adjusted by age, gender, smoking status, baseline FVC % predicted and DLCO % predicted.
**Abbreviations: AUC=Area under the ROC curve based on biomarker threshold variable binary threshold version of biomarkers; OR: Odds ratio; VEGFsR2= soluble vascular endothelial growth factor receptor-2; LGMN=legumain; FCN2=ficolin 2; ICOS= inducible T cell costimulator; TRY3=trypsin 3; GRN=granulin; NACA= nascent polypeptide-associated complex subunit alpha.

Determining analytes for scoring index

The top 4 biomarkers used to predict progression in 2 complementary multivariable model paradigms are shown in **Tables 4A-B**, where biomarkers in Table 3A were selected using multivariable logistic regression model for 80-week progression status and biomarkers in Table

3B were selected using a multivariable Cox proportional hazards model for time to progression over the 80-week follow-up. Logistic regression model identified the 4 best binary biomarkers as FCN2, VEGFsR2, Cath-S and TRY3. Cox proportional hazard regression model also placed FCN2 and TRY3 in its model along with ICOS and LGMN. Of the 6 unique biomarkers selected from the two multivariable progression model paradigms, values above identified thresholds were associated with lack of progression during the 80-week follow-up period in 4 cases (FCN2, VEGFsR2, Cath-S, LGMN) and progression in 2 cases (ICOS and TRY3).

Table 4A: Best logistic regression model based on 4 binary biomarkers

	Odds ratio	**95% CI**	**P**
FCN2	0.03	0.002-0.47	0.012
VEGF sR2	0.02	0.001-0.30	0.005
Cathepsin S	0.003	0.000-0.16	0.005
TRY3	50.10	2.93-857.24	0.007

Table 4B: Best Cox proportional hazard regression model based on 4 binary biomarkers

	Hazard ratio	**95% CI**	**P**
LGMN	0.27	0.13-0.56	0.0003
FCN2	0.49	0.22-1.08	0.076
ICOS	2.32	1.02-5.24	0.044
TRY3	2.32	1.03-5.20	0.042

6-analytes created a weighted scoring index to predict IPF progression

All 6 binary biomarkers identified for the scoring index had different time-to-progression profiles for the 80-week follow-up, suggesting different weights should be used for each in predicting progression within the index. Kaplan-Meier curves in **Figure 39** display progression-free survival for those above (black dashes) and below (red dashes) their corresponding threshold values. ICOS, LGMN, FCN2 and TRY3 progression-free profiles diverged quickly following

baseline threshold measurements, while differences in progression-free survival diverged later, after 40-weeks of follow-up, for those above and below Cath-S or VEGFsR2 thresholds at baseline. **Figure 40** shows progression-free survival curves for 3 biomarkers not selected for use in the index.

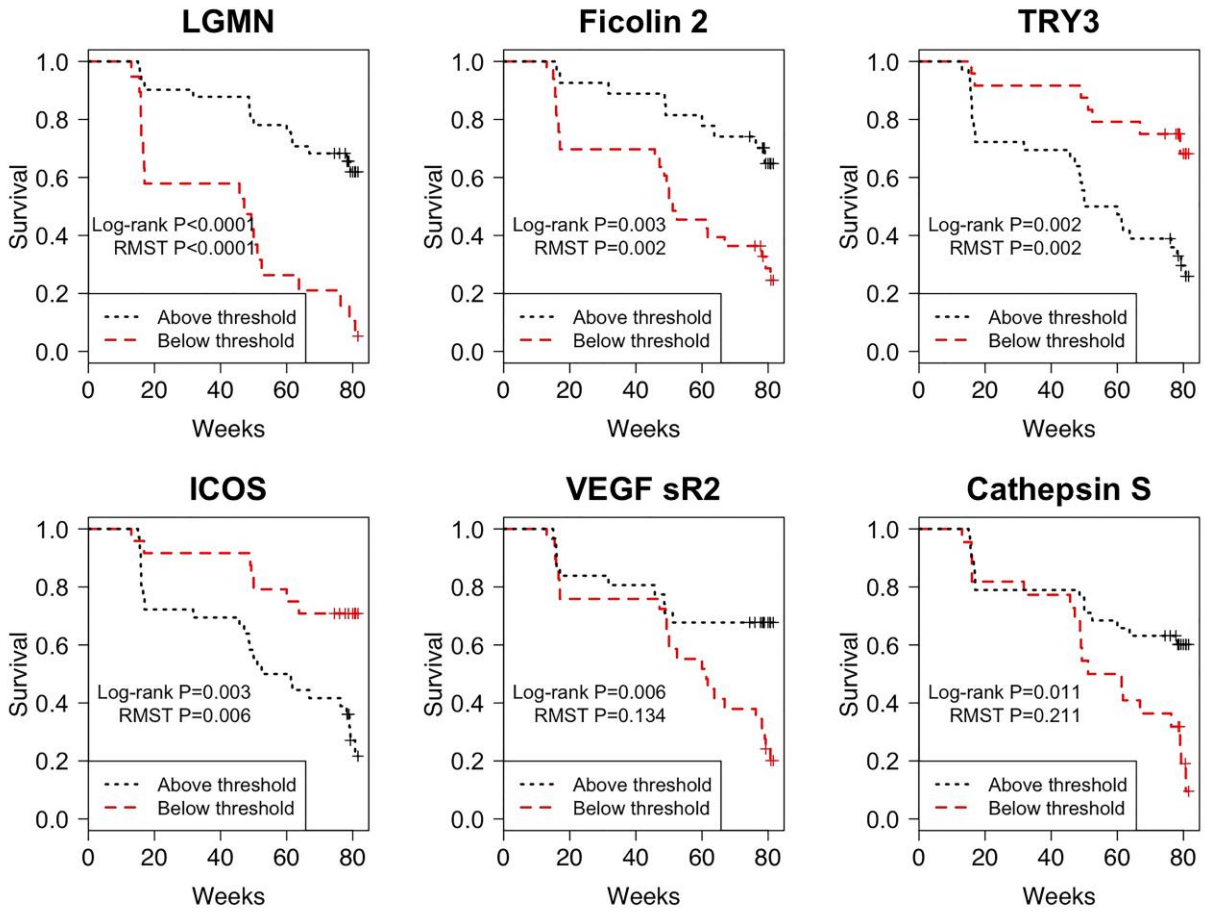

Figure 39: Kaplan-Meier curves showing progression free survival for IPF patients related to markers of immune activation or angiogenesis.
ICOS stands for inducible T cell co-stimulator, VEGF sR2 stands for soluble vascular endothelial growth factor receptor 2, TRY3 is trypsin 3 and LGMN is legumain

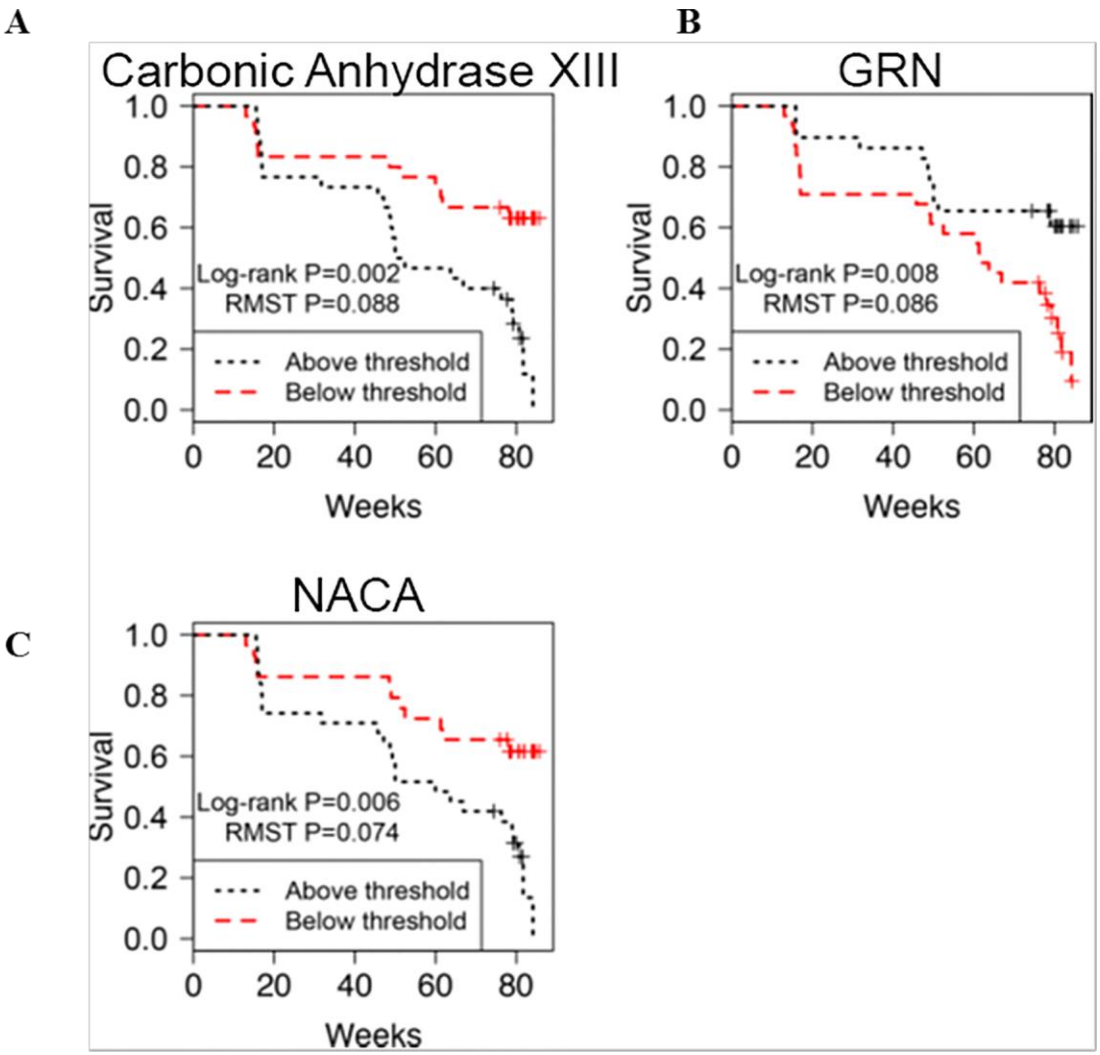

Figure 40: Kaplan-Meier curves showing progression free survival for IPF patients with baseline biomarker levels above or below the identified thresholds.
Thresholds for analytes (A)Carbonic Anhydrase XIII, (B) Granulin(GRN) and (C) Nascent polypeptide-associated complex subunit alpha (NACA).

Weighted index scores were created based on AUC. Kaplan-Meier estimates for each biomarker were generated individually to calculate the restricted mean survival (AUC) by 571 follow-up days, which was the minimum number of follow-up days for which we had data in different groups (**Table 5**). Based on differences between AUC for each biomarker, a score was created to provide weight to each biomarker consistent with its AUC, and determined

assignments on the basis of the OR direction. Therefore, the lowest AUC differences (Cath-S at 58 days and VEGFsR2 at 69 days) were assigned a value of 1. AUC differences for the next three biomarkers (ICOS, TRY3 and FCN2) were approximately 2-fold that of Cath-S and VEGFsR2, so those biomarkers were given a score of 2.

Finally LGMN AUC difference was approximately 3-fold Cath-S and VEGFsR2, so that biomarker was given a score of 3 in the index. For each patient a composite score was generated (scale of 0 to 11) based on whether their baseline values for the 6 biomarkers were above or below the identified thresholds. **Table 6A** shows distribution of scores for progressors vs. non-progressors. **Table 6B** shows distribution of scores assigned to 3 unique groups. Group level 1 included scores 0-2. Group level 2 consisted of scores 3-6. Group level 3 contained scores 7-11. Analyzing the ROC curve for this model, we determined this scoring index has an AUC=0.91 (**Figure 41**). A score ≥3 on this index had 56% specificity and 97% sensitivity for predicting progression-free survival in IPF while a score of ≥7 had 66% sensitivity and 100% specificity for predicting progression-free survival in IPF.

Figure 42 shows Kaplan-Meier curves for this scoring index by groups 1, 2 and 3. After adjusting for age, gender, smoking status, baseline FVC percent predicted and baseline DL_{CO} percent predicted, Group 2 [scores 3-6] and Group 3 [scores 7-11] have 9.7 and 32.3 times the hazard of Group 1 [scores 0-2] (95% CI for Groups 2 vs 1: 1.2, 76.9; p= 0.03; 95% CI for Groups 3 vs 1: 4.2, 250; p= 0.0008). A group level ≥ 2 [index score ≥ 3] had an adjusted hazard 18.7 times higher than group 1, (95% CI 2.5 -140.7), P=0.005. Bootstrap distribution of area between Kaplan Meier curves for groups 2 and 3 compared to 1 is shown in Figure 37. There is an estimated 131 days (18.7 weeks) lived longer during the 590 days (84.3 weeks) of follow-up comparing Group1 to Group2 (95% CI: 48-215 days, P=0.002) and an estimated 246

days (35.1 weeks) lived longer during 589 days (84.1 weeks) of follow-up comparing Group1 to Group3 (95% CI: 168-325 days, P<0.001). Bootstrap distribution of ROC curve shown in **Figure 43**, with our cohort's observed ROC overlaid, is displayed in Figure 44. These results demonstrate the index performed well in these random sampling analyses.

Table 5: Restricted mean survival (AUC) using Kaplan-Meier estimates for each biomarker individually over 571 days of follow up utilized to generate a standardized score.

Biomarker	Marker prognosis good	Marker prognosis bad	Difference	Score
LGMN	481	296	185	3
FCN2	495	363	132	2
TRY3	501	370	131	2
ICOS	493	376	117	2
VEGF sR2	456	387	69	1
Cathepsin S	444	386	58	1

Table 6A: Distribution of scores for patients meeting the definition for progressor or non-progressor

Frequency **Row Pct** **Col Pct**	**Score**												
	0	**1**	**2**	**3**	**4**	**5**	**6**	**7**	**8**	**9**	**10**	**11**	**Total**
Non-progressor	5 20 100	2 8 100	7 28 87.5	4 16 66.7	4 16 80	1 4 25	2 8 28.6	0	0	0	0	0	25
Progressor	0	0	1 2.9 12.5	2 5.7 33.3	1 2.9 20	3 8.6 75	5 14.3 71.4	5 14.3 100	7 20 100	3 8.6 100.	6 17.1 100	2 5.7 100	35
Total	5	2	8	6	5	4	7	5	7	3	6	2	60

Table 6B: Distribution of group scores among progressors and non-progressors

	Score group			
Frequency **Row Pct** **Col Pct**	**1** **[0,2]**	**2** **[3,6]**	**3** **[7,11]**	**Total**
Non-progressor	14 56 93.3	11 44 50	0	25
Progressor	1 2.9 6.7	11 31.4 50	23 65.7 100	35
Total	15	22	23	60

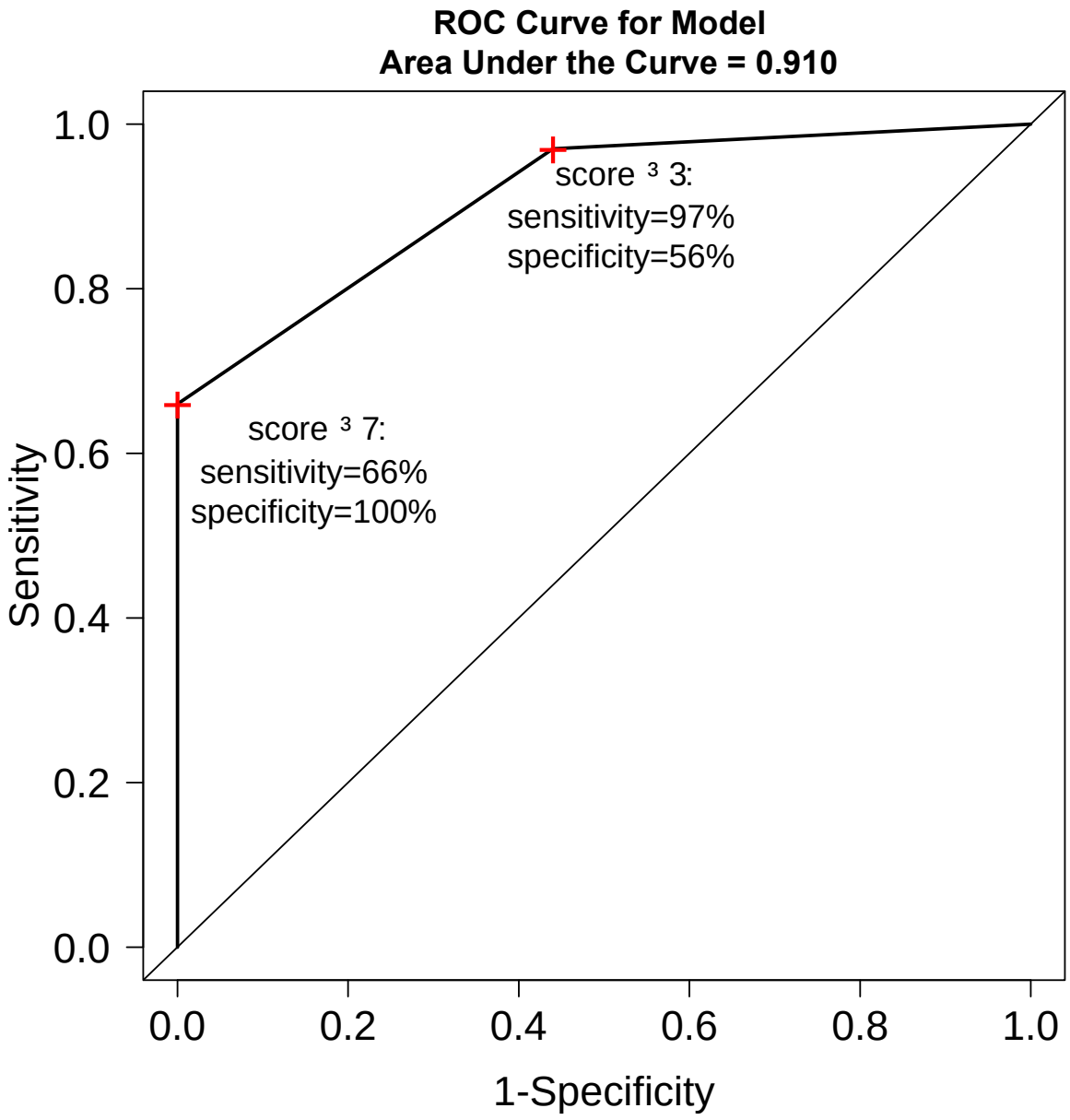

Figure 41: Receiver operating characteristic (ROC) curve using two prognostic index thresholds (corresponding to groups shown in Figure 42.
Higher areas under the curve indicate better overall classification, where AUC = 0.5 indicates a useless classification tool and AUC=1.0 indicates a perfect classification tool. Our prognostic index score AUC = 0.91 indicates an extremely useful prognostic index score.

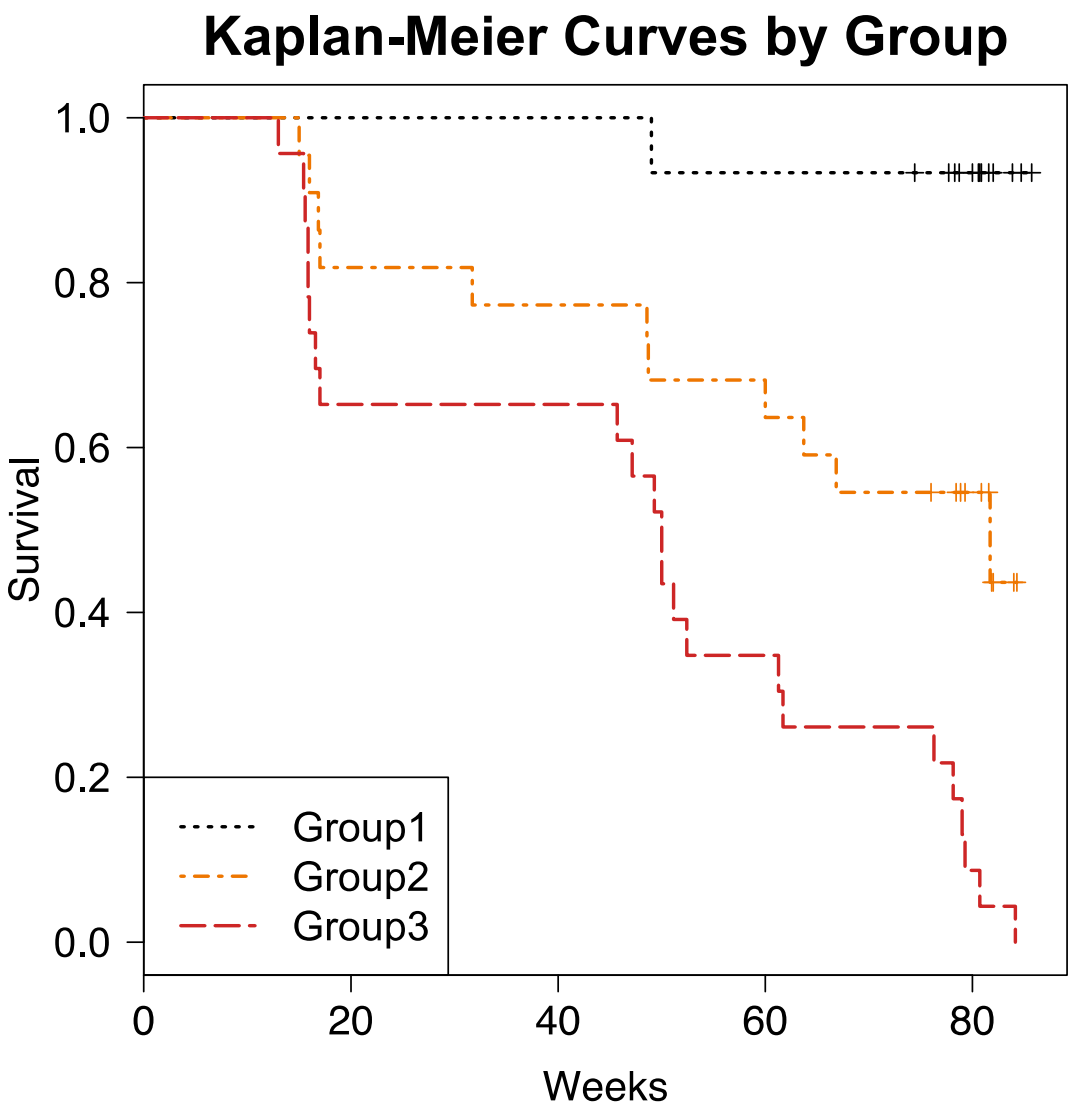

Figure 42: Kaplan-Meier curve showing progression free survival for patients according to the different groups in our weighted index score.
In unadjusted analyses, A group level **increasing by 1** using this index has a hazard ratio=4.02, (95%CI 2.28-7.10), P<0.0001 for predicting IPF progression by univariate Cox regression model. In adjusted analyses, a group level **increasing by 1** using this index has a hazard ratio=4.27, (95%CI 2.30-7.96), P<0.0001 for predicting IPF progression by Cox regression model after being adjusted by age, gender, smoking status, baseline FVC percent predicted and baseline DLCO percent predicted

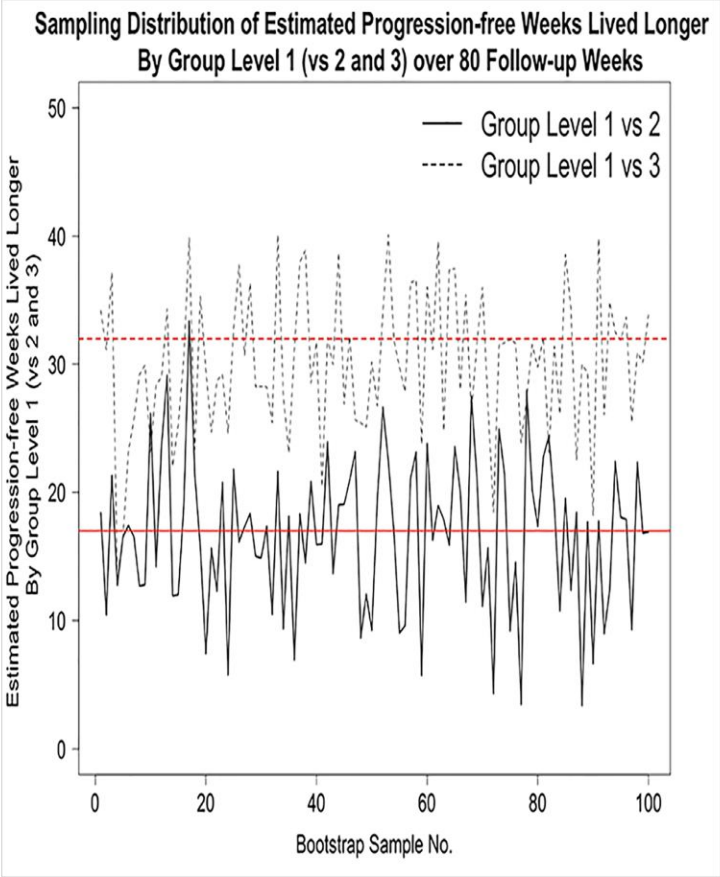

	Minimum	1st Quartile	Median	3rd Quartile	Maximum
Group Level 1 vs 2	2.6	12.6	15.7	19.6	29.5
Group Level 1 vs 3	13.8	26.1	30.0	33.4	43.5

Figure 43: Sampling distribution of the number of progression-free weeks that group level 1 lived longer than group levels 2 and 3 over 80 follow-up weeks.
(Calculated via bootstrap methodology.) Our cohort estimates are superimposed in red.

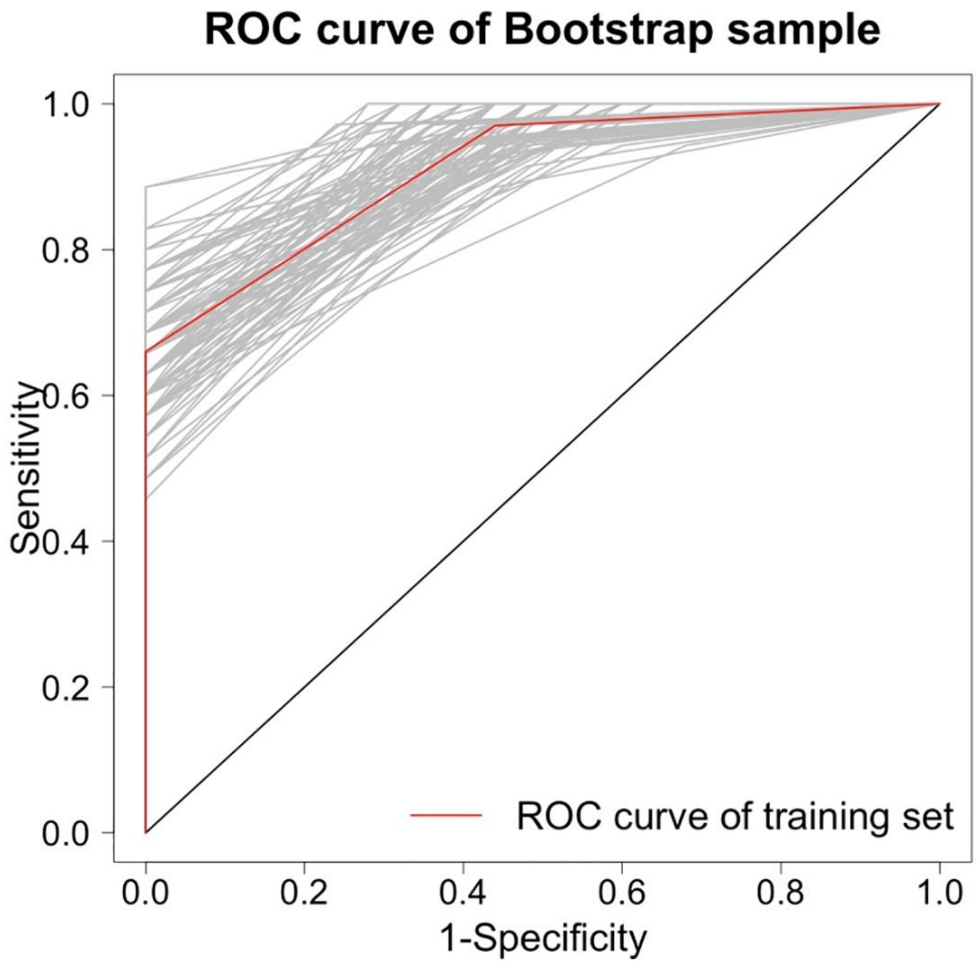

Figure 44: Bootstrapped distribution of receiver operating characteristic (ROC) curves, with observed curve from our cohort superimposed in red.

Discussion

Blood-based biomarker analysis could be useful if it provides prognostic information for IPF patients. IPF natural history can vary considerably with some patients experiencing relative disease stability, while others experience rapid progression (448). While there are two FDA-approved drugs available to treat IPF (pirfenidone and nintedanib), costs of these medications are prohibitive for many, and benefit is limited to slowing disease progression over an ~6 month time frame in patients with mild to moderate functional impairment (458, 459). Thus, the ability

to accurately predict patients who are likely to progress could help focus treatment to patients at highest risk for functional decline.

Biomarkers may also determine aberrant signaling pathways associated with disease progression. Interestingly, some of our predictive analytes are associated with processes already known to be aberrant in IPF, namely immune dysfunction, angiogenesis and proteolysis. Accumulating evidence suggests IPF is characterized by immunologic alteration, with studies showing either activated leukocytes or impaired immunologic responses. Peripheral blood gene expression analysis demonstrated IPF patients are characterized by activated leukocyte phenotypes (333). Similarly, CD4 T cells in IPF patients have activated phenotypes characterized by lower levels of CD28(53), but elevated levels of MHC class II , CD154 and oligoclonal Vβ gene expression (174). Additionally, CXCR3+ CD8 cells which represent activated cytotoxic T cells also correlate with progression in IPF when found in increased percentages in peripheral blood (460). A correlation between increased percentages of CD14hi, CD16hi monocytes in circulation and IPF progression in COMET IPF patients was previously shown (460) and these cells corresponded to intermediate monocytes(461). Thus, it is interesting that 3 of the SOMAmer analytes identified have known roles in immunologic functions namely, ICOS, FCN-2 and Cath-S.

ICOS is a CD28-superfamily costimulatory molecule upregulated on CD4+ T cells following antigenic stimulation. This molecule intensifies CD28 signaling during established immune responses and induces T cell effector functions (462). ICOS may also regulate lung mucosal inflammatory responses (463). In bleomycin-induced lung and skin fibrosis, ICOS-deficiency attenuated fibrosis (464). Conversely, in IPF peripheral blood mononuclear cells (PBMCs), decreased expression of ICOS, CD28 and lymphocyte-specific protein tyrosine kinase

(LCK) led to more severe IPF (333). In our studies, elevated levels of ICOS measured in plasma correlated with worse IPF. While seemingly contradictory, these human measurements were made in different compartments. We tested if ICOS is shed from T cells after activation. **Figure 45** demonstrates activation of murine T cells releaseed ICOS into supernatant, suggesting elevated ICOS in circulation could indicate leukocyte activation. Certainly there is evidence for shedding of ICOS ligand induced by ICOS itself (465). Thus, we hypothesize ICOS is released either by shedding or via exosomes upon cellular activation, and this may explain why lower levels of ICOS mRNA in PBMCs (333), but higher levels of ICOS in plasma could both be associated with IPF progression.

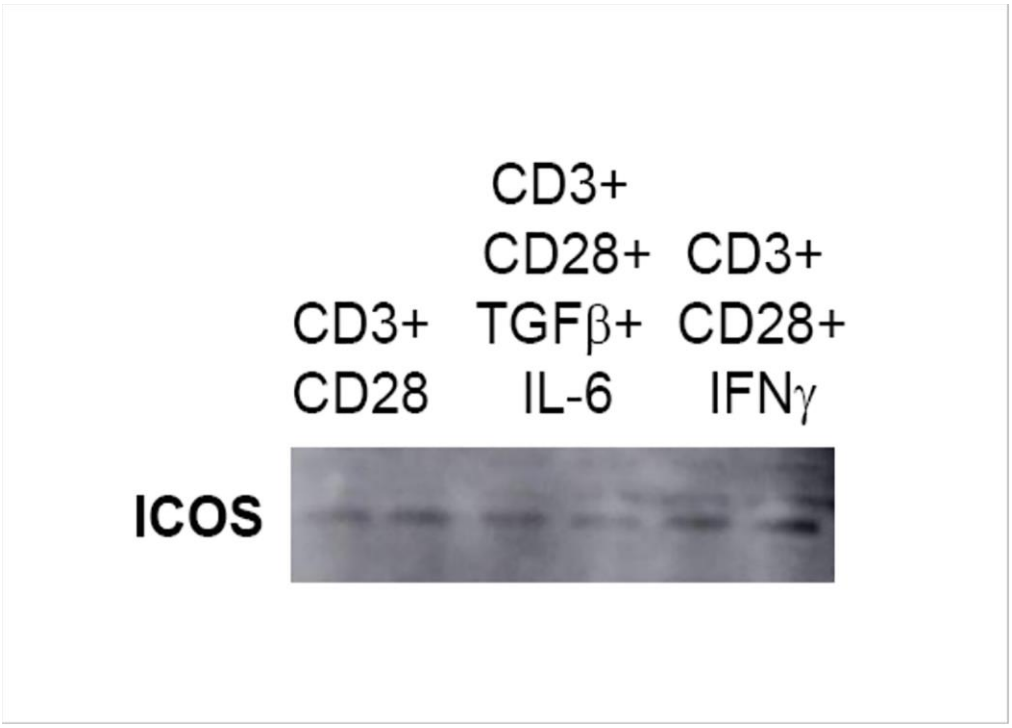

Figure 45: ICOS is shed by activated T cells.
A million CD4 positive splenocytes were stimulated with CD3 + CD28(T cell markers) then (TGFβ, 2ng/mL+ IL-6, 20ng/mL cytokines) or TH1 (IFNγ, 10ng/mL) for 24 hr. Cell free supernatants were collected and concentrated using Amicon Ultra Centrifugal filters (Millipore, Billerica, MA). Equal amounts of protein from each sample were separated on a 4-20% gradient SDS-polyacrylamide gel and transferred to a PVDF membrane (Amersham/GE Healthcare, Pittsburgh, PA). PVDF membrane was probed with rabbit monoclonal ICOS (Abcam).

Another factor believed to contribute to IPF pathogenesis is the presence of pathogens, both viral and bacterial. Studies in both IPF patients and animal models have shown viral infections, particularly herpesviral infections may promote fibrogenesis [reviewed in (351)]; however, bacterial burden may also predict worse outcomes (134, 374). FCN-2 reductions correlate with IPF progression. Human L-Ficolin (FCN 2) is synthesized in liver and secreted into the bloodstream where it's a major pattern recognition receptor (466). FCN2 can opsonize several species of bacteria, in a manner similar to mannose-binding lectin (MBL) (467). FCN2 and MBL activate the lectin complement pathway and studies have linked this pathway to fibrotic organ manifestations in Scleroderma, including ILD (468). Furthermore, FCN2-deficiency may predispose patients to development of bronchiectasis (469). Common variable immunodeficiency (CVID) patients with bronchiectasis also demonstrate low levels of FCN2 (470). FCN2 binds to *S.pneumoniae* activating the lectin pathway of complement (471) and mice lacking ficolin-A, the murine homolog of FCN2 showed increased mortality in a model of *S. pneumoniae* pneumonia (472, 473). It is particularly noteworthy that microbiome analyses also conducted in COMET IPF patients suggest *Streptococcus* species are overabundant in progressive IPF patients (374). Lower levels of FCN2 may contribute to overabundance of these bacterial species, which may, in-turn promote disease pathogenesis. *S. pneumoniae* promotes fibrogenesis through pneumolysin-mediated destruction of lung epithelial cells in animal models (474), suggesting a mechanism whereby bacterial burden may promote lung injury and fibrosis.

Cath-S is a single chain, non-glycosylated cysteine protease ubiquitously distributed in the lysosome. It is expressed mainly in lymphatic tissues and is characterized as a key enzyme in class II-mediated antigen presentation (475). LGMN is a cysteine peptidase existing in a number of mammalian tissues, such as kidney, placenta, spleen, liver and testis. Interestingly, LGMN

acts as a primary regulator of cysteine cathepsins (476). Our study identified an association between high circulating levels of both proteases and improved progression free survival in IPF, suggesting impaired endo-lysosomal function may directly promote disease progression. Or, the lower levels of Cath -S in circulation could indicate IPF patients have defective antigen presentation or aberrant cell survival pathways. Cath -S also promotes tumor cell invasion, metastasis and angiogenesis once secreted into the extracellular milieu it causes degradation of extracellular matrix proteins including laminin, fibronectin, elastin, and some collagens (477-479). Thus, it's not surprising that Cath -S levels are reduced in progressive IPF patients. Additionally, LGMN was identified as a diagnostic and prognostic liver fibrosis biomarker (480). Our study is the first to correlate lower levels of LGMN with poor outcomes in IPF, and we speculate LGMN may be important for degrading provisional matrix following injury.

TRY3/mesotrypsin is a serine protease, encoded by the PRSS3 gene. Mesotrypsin/PRSS3 is overexpressed in human primary pancreatic cancer tissues and is associated with metastasis and poor prognosis of pancreatic (481), prostate, and non-small cell lung cancer (482, 483). Alternative splicing produces four isoforms of human trypsinogen protein. How TRY3 influences IPF is unknown.

VEGF is a potent and specific endothelial cell mitogen that regulates blood and lymphatic vessel development and homeostasis. The VEGF receptor family consists of three members, VEGFR1 (FLT1), VEGFR2 (KDR/FLK1) and VEGFR3 (FLT4) (484). Among these, VEGFR1 binds strongly to VEGF, VEGFR2 binds more weakly, and VEGFR3 shows essentially no binding, although it does bind to other members of the VEGF family. Soluble forms (VEGFsR1 and VEGsFR2) have been studied as potential biomarkers for a number of diseases but most of the data available is about VEGFsR1, not VEGFsR2 (485-487). VEGFsR2 was first

reported as a truncated 160KDa protein detected both in mouse and human plasma (488). An inverse correlation between the levels of VEGFsR2 and increasing tumor size has been observed (489). The SOMAmer reagent was selected against VEGFsR2 and our analysis indicates lower levels of this protein correlated with disease progression. It is unknown how circulating VEGFsR2 may correlate with endothelial cell activation or protective vs. pathologic angiogenesis in IPF, but we speculate lower levels of circulating VEGFsR2 would predict less ability to inhibit VEGF actions, potentially enhancing angiogenesis associated with disease progression.

Our study was the first to analyze IPF patients using SOMAmers, and a limitation is small sample size and the lack of a validation cohort. Given the expense of Somascan validation, sensitivity and specificity of the index was addressed using a bootstrap analysis. The index performed well across all 100 different bootstrap analyses performed (Fig. E4) implying the index should perform well in other patient cohorts. Future studies are needed to determine whether smaller analyte panels could be cost-effective or if ELISA measurements for these markers show similar or divergent results. Periostin levels were measured in the same patient samples using an ELISA developed by Abbott Pharmaceuticals. There was a good correlation between measures made by SOMAmer and ELISA for this biomarker with a Spearman correlation of $r=0.44$, $p<0.0001$ (**Figure. 46**).

Together, our results demonstrated a 6-analyte SOMAmer panel measuring circulating markers of immune function; proteolysis and angiogenesis could be used to create a simple index with excellent sensitivity and specificity for predicting progression-free survival in IPF. Use of this index on easily-accessible plasma should be further validated to offer a simple way of predicting IPF patient outcomes.

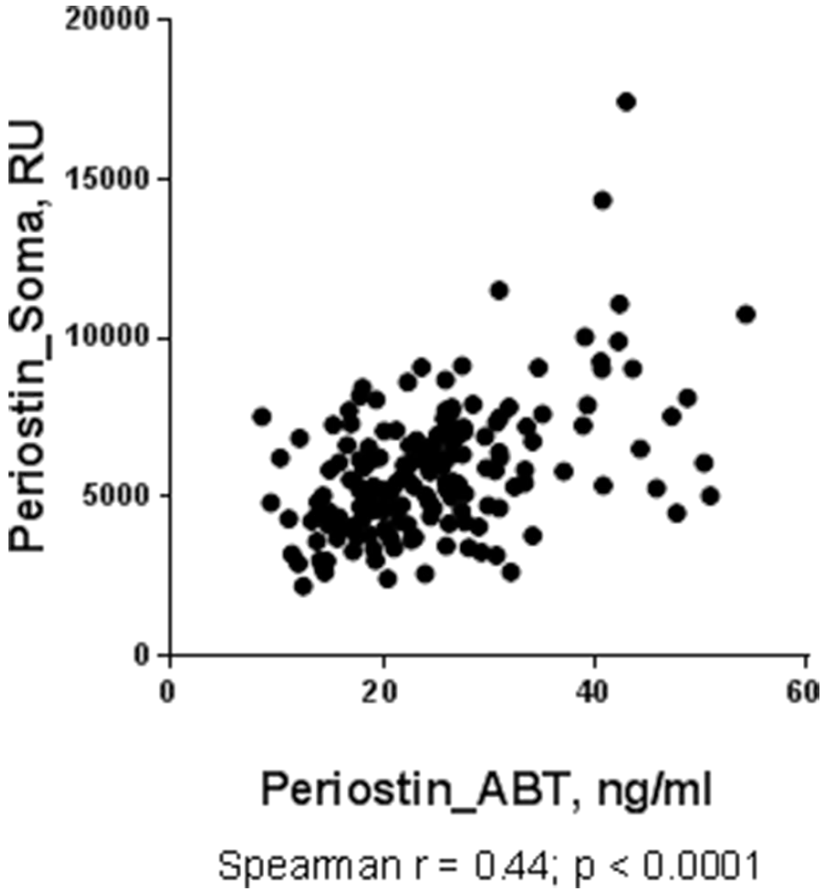

Figure 46: Periostin levels in IPF patients correlate by SOMAscan and ELISA.
The same plasma samples were run on a periostin ELISA developed by Abbot Pharmaceuticals and were compared to measures of periostin made by SOMAmer. The correlation was significant, Spearman r=0.44; p<0.0001.

Chapter 7:

Conclusions

Viral and Bacterial Exacerbation Studies

Previous work from our lab illustrated that either short term or long term γ-herpesvirus latency in the lung could significantly enhance the response to fibrotic challenge. It was demonstrated that latent γHV-68 infection could augment a subsequent fibrotic challenge and that the worsened fibrosis was not associated with substantial reactivation of the lytic phase of the virus (346). Based on these observations we wanted to further expand our studies to examine whether the exacerbation of established fibrosis was only limited to γ-herpesvirus or whether other pathogens could also have a similar effect.

It was shown that γHV-68 exacerbated bleomycin-induced fibrosis and stimulated collagen deposition. Once lung fibrosis was established, infection with Influenza (H1N1), CMV or the Gram-negative bacterium, *P. aeruginosa* did not exacerbate fibrosis at the doses tested. γHV-68 augmented established fibrosis as previously published, and the use of the ΔORF-72 mutant virus did not, further demonstrating that the ability of γHV-68 to exacerbate bleomycin-induced fibrosis and enhance collagen deposition required the ability of γHV-68 to undergo reactivation from latency.

In addition, there was a cell-specific increase in susceptibility to TGFβ signaling post-γHV-68 infection with no observed difference in the active or total TGFβ in the lungs of bleomycin-treated mice infected with H1N1 or γHV-68. Interestingly, herpesviruses have

received the most attention as either a causal or exacerbating agent of IPF [reviewed in (490)],but it was assumed that other agents which may be able to damage lung epithelium could have similar effects. Thus, it was very surprising that we did not see similar results in the infection studies with γHV-68 and H1N1 infection after established fibrosis, since both viruses can infect epithelial cells. These results seem to suggest that the critical feature for the ability to exacerbate fibrosis by a pathogen is the ability to maintain replication and or sensitize AECs to the induction of apoptosis, a feature that was only seen following γHV-68 infection in our studies. H1N1 infection can activate TGFβ signaling and increase apoptosis in AECs, yet in our model it caused no change in collagen deposition. Potentially, this could reflect dose differences or the intense pathogenicity of H1N1 in mice. A 1000-fold lower dose of H1N1 was given to the mice to keep them alive long enough to analyze fibrotic outcomes. When higher doses of H1N1 were given, the mice died of acute lung injury. Extrapolating to humans, this would obviously be a severe exacerbation, but it is likely that patients (and rodents) in this case die of lung injury before the fibrotic response can be manifested (perhaps in an attempt to provide lung repair). Why murine CMV did not exacerbate may reflect the propensity of this virus to migrate to the CNS rather than establish robust infection in the respiratory tract.

When put in the context of our other studies in this dissertation, it is interesting to speculate that γHV-68 infection leads to epithelial cell apoptosis, recruitment of periostin-expressing fibrocytes and that fibrosis may propagate due to the paracrine effects of these cells on the resident fibroblasts.

Fibrocyte and Periostin Studies

Our laboratory and others have reported increased circulating levels of periostin in patients with IPF (258, 402). In our study high levels of periostin in plasma at diagnosis

predicted disease progression as defined by a relative change of 10% FVC, a 15% drop in DL_{CO}, acute exacerbation, lung transplant or death in a 48 week follow-up (122). In addition, circulating fibrocytes cultured from the peripheral blood of IPF patients expressed higher mRNA levels of periostin compared to normal volunteers (122). In our BM-chimera studies we showed that periostin production by both structural and hematopoietic cell types was critical for development of bleomycin-induced fibrosis (122). These observations propelled our studies to determine the contribution of fibrocytes and fibrocyte-derived periostin in the development of lung fibrosis. Our first thought was to generate a mouse where we could conditionally deplete fibrocytes. We generated a collagenIa2-Cre-DTR mouse (CD45.1), and used these mice as bone marrow donors into WT (CD45.2) mice to localize the transgene for deletion to just the circulating mesenchymal cells (i.e. fibrocytes) as opposed to using the full-body deletion which would also target resident and structural fibroblasts throughout the body. After full hematopoietic reconstitution mice were treated with bleomycin and then given diphtheria toxin via oropharyngeal aspiration. On day 21 we assessed the percentage of fibrocytes by comparing CD45.1 and CD45.2 positive cells; despite great reconstitution we were not successful at depleting fibrocytes regardless of whether we gave DT systemically or locally. The depletion of fibrocytes using our Col1a2-Cre-ROSA-DTR mice as donors was not very successful as there was an increase in recipient fibrocytes over time. The host continued to regenerate new fibrocytes while we were depleting donor-derived cells. These results may indicate that there is either a lung-resident stem cell that can regenerate circulating fibrocytes in addition to a bone marrow-derived stem cell or that there was a radio-resistant host-derived population that could be stimulated to proliferate following lung injury.

The role of fibrocytes in exacerbating bleomycin-induced fibrosis was further explored by performing adoptive transfer experiments with WT and periostin$^{-/-}$ fibrocytes. It was shown that both WT and periostin$^{-/-}$ fibrocytes are capable of effectively migrating to the lungs after transfer, as we saw no difference in the mRNA expression of the chemokine receptors CCR2 and CXCR4, suggesting no defect in trafficking of fibrocytes in the absence of periostin. Additionally, fibrocytes recruited to the lungs both in the presence and absence of periostin did not differentiate into other cell types as they maintained their CD45 expression over time. Thus, these studies showed that the ability of fibrocytes to augment bleomycin-induced fibrosis was through paracrine function. Our studies corroborate another in vivo study suggesting that fibrocytes do not differentiate into myofibroblasts in the lung during fibrogenesis (401). This is an important contribution to the literature in this field as the dominantly held belief in the lung fibrosis community has been that fibrocytes contribute to fibrogenesis via direct differentiation into myofibroblasts. Further support for this view comes from work from Dr. Kim's laboratory here at the University of Michigan showing that the ability of fibrocytes to produce collagen is irrelevant to the development of fibrosis, (200) again suggesting that paracrine functions other than collagen secretion and myofibroblast differentiation are critical.

Using PCR array analysis, we assayed for the differences in gene expression in bleomycin-treated fibrocytes from WT and periostin$^{-/-}$ mice. The data demonstrated that fibrocytes from perisotin$^{-/-}$ mice had a significant decrease in mRNA expression of LOX and CTGF but no difference in PDGFα mRNA expression. Conditioned medium collected from bleomycin-treated fibrocytes and added back to WT untreated fibroblasts caused an increase in αSMA protein expression in fibroblasts that received supernatant from WT bleomycin-treated cells. Using ELISA we measured higher amounts of CTGF in the condition medium from WT

bleomycin-treated fibrocytes. Furthermore, using a MRTF inhibitor to block expression of CTGF in the WT untreated fibroblasts also resulted in less αSMA production by fibroblasts after addition of conditioned medium. This was the first data to demonstrate that production of one matricellular protein (periostin) could influence the production of other matricellular proteins like CTGF in circulating fibrocytes. Given that fibrocytes are just one source of periostin in the lung, it is perhaps surprising that deletion of periostin just from hematopoietic sources or deletion of periostin from just the adoptively transferred fibrocytes could have such a large impact on fibrosis. We speculate that this is likely because the fibrocytes have the ability via their chemokine receptors to migrate to the exact sites of tissue injury. In this way, they may be uniquely positioned to deliver the paracrine signals to the injured epithelium and underlying mesenchymal cells.

Targeting Inhibitor of Apoptosis Studies

Work from Ajayi et al. showed that fibroblasts isolated from IPF patients express increased levels of the anti-apoptotic protein XIAP. To determine whether this anti-apoptotic protein is responsive to periostin stimulation, we treated normal lung murine mesenchymal cells with periostin and measured induction of XIAP by western blot. These results suggested that periostin may be partially responsible for changes in lung fibroblasts causing them to be resistant to apoptosis during the course of fibrogenesis. To further characterize the role of IAPs in promoting lung fibrosis, we assessed the effects of TGFβ on increasing the mRNA expression of IAPs (XIAP, cIAP1 and -2) and saw significant increases in the expression of these genes. Additionally, the inhibition of IAPs using a bioavailable IAP anatgonist, AT-406, limited bleomycin-induced lung fibrosis but had no effect on inflammation. Therapeutic administration of AT-406, at day 10 after the initiation of lung fibrosis caused a decrease in the fibrotic outcome

by day 21 suggesting that AT-406 displayed anti-fibrotic effects independently of the early phase inflammation. This indicated that the beneficial effects occurred during the stage of disease associated with fibroblast accumulation. It was also demonstrated that within 48hrs after in vivo AT-406 treatment, there was an increase in caspase-3 activity, in isolated murine lung mesenchymal cells. Taken together, these results indicate that IAPs play a role in the pathogenesis of lung fibrosis and that loss of one IAP, XIAP, was not sufficient to attenuate bleomycin-induced lung fibrosis. However, broad functional inhibition of IAPs may be an effective strategy for treatment of lung fibrosis by promoting mesenchymal cell apoptosis.

Our overall results for these projects demonstrated that γ-herpesvirus but not H1N1, CMV or *P. aeruginosa* couls exacerbate bleomycin-induced fibrosis via effects on AECs and likely via induction of chemokines to recruit fibrocytes. In turn, the paracrine activity of fibrocytes was dependent on periostin and had direct effects on resident mesenchymal cells. Perisotin can upregulate anti-apoptotic genes such as XIAP in fibroblasts and through the upregulation of other profibrotic mediators such as CTGF can promote the differentiation of myofibroblasts and ultimately enhance the fibrotic response. The anti-apoptotic effects of XIAP can be inhibited through treatment with a bioavailable IAP antagonist AT-406. This drug had no effect on inflammation but caused changes in the fibroproliferative phase attenuating bleomycin-induced lung fibrosis (**Figure 47).**

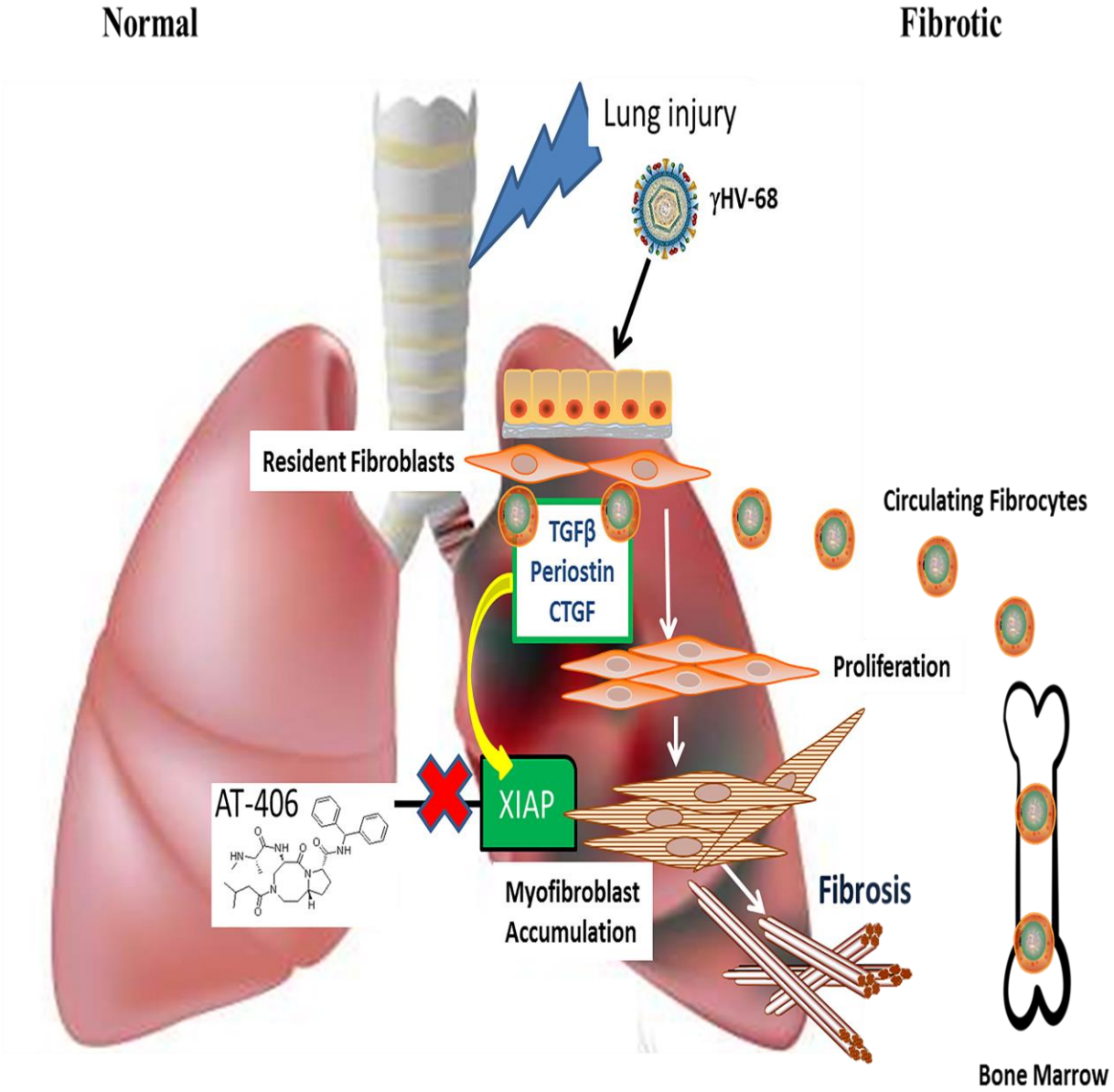

Figure 47: A model of how virus and recruited fibrocytes promote fibrosis.
Damage to the lung epithelial cells by bleomycin or viral infection leads to production of cytokines/chemokines and profibrotic mediators such as TGFβ, periostin and CTGF. The profibrotic mediators cause fibroblast proliferation; periostin causes upregulation of XIAP. XIAP expression in myofibroblasts leads the accumulation of apoptosis-resistant myofibroblasts leading to accumulation of ECM proteins and fibrosis. Therapeutic administration of AT-406 (SMAC mimetic) blocks XIAP leading the attenuation of fibrosis.

IPF Biomarker Studies

Biomarkers in accessible compartments like peripheral blood that can predict disease progression in idiopathic pulmonary fibrosis (IPF) would be clinically useful regarding clinical trial participation or treatment decisions. For these studies we screened for biomarkers in the plasma of IPF patients. Plasma from IPF patients was measured using an 1129 analyte slow off-rate modified aptamer (SOMAmer) array and patient outcomes were followed over the next 80 weeks. The ability of each continuous biomarker to predict IPF progression over an 80 week period was assessed. ROC curves were constructed and a biomarker threshold was chosen to maximize the combined sensitivity and specificity. An estimated AUC of 0.7 from the ROC analysis was chosen for further consideration of each biomarker. To further screen the biomarker threshold values, adjusted and unadjusted odds ratios were generated through logistic regression adjusting for age, gender, smoking status, baseline percent predicted FVC and baseline predicted DL_{CO}. To be considered for the IPF progression index, biomarker threshold variables had to maintain a statistical significance of 0.05 levels in both the adjusted and unadjusted analyses.

In order to ensure independent prognostic ability of the biomarkers both multivariable logistic and COX regression models were investigated. Using a multivariable logistic regression predicting 80-week progression status and a multivariable COX proportional hazard regression predicting time to progression over the 80-week follow-up period, we identified six unique biomarkers with p values less than 0.05 for predicting either 80 week progression status or time to progression. Overall these biomarkers corresponded to changes in immune response, angiogenesis or protease activity. Using Kaplan-Meier estimates of progression-free survival for those above and below their threshold we showed that legumain, FCN2, VEGFsR2 and cathepsin S below threshold and ICOS and TRY3 above threshold predicted IPF progression over a 80

week follow-up. In light of our murine data suggesting that infection can exacerbate fibrosis, and that recruitment of fibrocytes via the vasculature are important events to exacerbate fibrosis, we were gratified to find that the functional categories that these biomarkers represent seem to fit well with what we understand about the pathogenesis of lung fibrosis using our animal models.

Chapter 8:

Final Thoughts and Future Directions

In summary, we constructed a mouse model to further our understanding about some essential players in bleomycin-induced lung fibrosis. Our results demonstrate that only a DNA virus that can establish latency can augment established fibrosis. We speculate that the model could be explored further to better understand the specific cell types that are critical for the virus-induced augmentation of lung fibrosis. Additionally, since this is a "two hit model", we would like to explore the effects of infection with H1N1 or other pathogens before bleomycin treatment. We are interested in investigating if the damage induced by bleomycin before the viral infection caused defects in toll-like receptor (TLR) signaling. TLRs detect pathogens such as bacteria and viruses. TLR3 is located in endosomal membrane compartments and recognizes dsRNA, an intermediate product from replicating RNA viruses such as Influenza (491). The synthetic double stranded RNA (dsRNA) analog poly (I:C) has been shown to activate RhoA in small airway epithelial cells (492), suggesting a possibility that influenza might be able to activate TGFβ through TLR3. We speculate that this might lead to downstream activation of an integrins that may be interacting with TGFβ but we have not explored these experiments yet. Also, it would be very interesting to isolate different cell types from bleomycin-treated H1N1 compared to γHV-68 infected mice to understand the Th1 and Th2 cytokines in these microenvironments. Another potential reason why the H1N1 infections did not exacerbate bleomycin-induced

fibrosis may be that the bleomycin-injured epithelium was just too damaged to support robust H1N1 replication. This is another reason why studying the response in the reverse order of exposure could be interesting. As mentioned before, H1N1 infection at higher doses lead to animal death due to acute lung injury. This is also a clinically relevant problem and future studies could attempt to understand exactly how H1N1 and γHV-68 differ in their induction of acute lung injury and could attempt to find therapeutic targets. This could also improve outcomes for patients who develop influenza infections often with precipitous declines in lung function.

Our description of the role of fibrocyte and fibrocyte-derived periostin in promoting lung fibrosis suggests that fibrocytes in the presence of periostin secrete other profibrotic mediators leading to increased myofibroblast differentiation as shown by the increase in αSMA production. We also showed that TGFβ and periostin were coregulating each other and that perisotin binds to different integrins on fibrocytes compared to fibroblasts.

It will be very interesting to test whether CTGF and periostin were coregulating each other in fibrocytes or if they can function independent of each other. Loss of periostin did not totally abolish the secretion of CTGF from the fibrocytes suggesting a necessary role for CTGF and the possibility that other mediators such as TGFβ could be contributing to the production of CTGF. Performing experiments with CTGF knockdown to see if it inhibits persiotin-dependent effects on fibrocytes or if knockdown of CTGF affects the ability of fibrocyte supernatant to induce myofibroblast differentiation are now warranted. Furthermore, we could explore the impact of CTGF on proliferation in lung mesenchymal cells (fibroblasts and fibrocytes). Since beta 1 integrin is shown to be important for persiotin to interact with fibrocytes we want to identify the site on periostin that is binding to this integrin. These experiments can be performed

through the development of domain specific periostin mutants. Knowledge of this site would be an initial step towards developing specific drugs that block periostin during lung disease, while potentially preserving beneficial functions of periostin in other contexts (like prevention of myocardial infarction).

Integrins are known to regulate collagen expression, usually by modulating members of the TGFβ1 signaling pathway. In our data we showed that blocking beta 1 integrin decreased collagen I mRNA expression in fibrocytes after treatment with periostin. One pathway linking activation of collagen expression involves increased activity of Rac1 (a small Rho GTPase) and ERK (493). Activation of ERK appears to be a common pathway for non-canonical expression of collagen 1. Fibrocytes would be treated with periostin with or without beta1 integrin blocking antibody then assessed for the presence of ERK phosphorylation by western blot. To determine the role of Rac, cell free supernatants will be collected from fibrocytes treated as mentioned above and Rac1 activity will be measured with a commercially available ELISA kit. We also know that there is a small molecule available that inhibits alphaVbeta1 function (301), and it would be interesting to assess the importance of alphaVbeta1 in fibrocyte function in vivo. In collaboration with Dean Sheppard's group at University of California at San Francisco, we will incubate WT fibrocytes with this small molecule then adoptively transfer these cells into WT mice after bleomycin treatment to demonstrate an in vivo role for fibrocytes interacting with periostin to enhance the fibrotic response. Another formal possibility is that many alpha integrin partners may be able to interact with beta 1 to promote periostin effects on fibrocytes. This would be best explored in the future through siRNA knock-downs of particular integrin chains.

Several studies have documented a role for microRNAs in fibroblast biology [reviewed in (494)]. Conditioned medium from WT bleomycin-treated fibrocytes led to an increase in αSMA

production by fibroblasts; some of which is accounted for by the presence of CTGF and periostin in these supernatants. However, the differential signaling of periostin in fibrocytes compared to fibroblasts suggests that microRNAs might be playing a role in the ability of fibrocytes to exacerbate lung fibrosis. MicroRNAs are small single stranded ribonucleic acids functioning as posttranscriptional regulators of gene expression (495). Many studies have characterized these small molecules as important regulators of cell proliferation and tissue repair, tissue development and differentiation (496, 497). A number of microRNAs have been shown to be upregulated in IPF [(reviewed in (494)]. We would like to examine the microRNA profiling in fibrocytes from WT and periostin$^{-/-}$ bleomycin-treated mice. Once different microRNAs have been identified we will perform studies directed at how these microRNAs promote the profibrotic response of fibrocytes to periostin. It is also possible that the presence of periostin results in the release of exosomes containing different arrays of miRNA in fibrocytes from WT vs. periostin$^{-/-}$ mice. Future studies could determine whether there are differential effects of fibrocyte exosomes from WT vs. periostin$^{-/-}$ mice on fibroblasts.

In the apoptosis studies we showed that loss XIAP alone was not sufficient to attenuate bleomycin -induced fibrosis but blockade of all IAPs with a small molecule early or late caused a decrease in the fibrotic outcome. Overall, these data suggest that in the absence of XIAP there is a compensatory effect by the other IAPs thus enhancing an anti-apoptotic response of lung mesenchymal cells during bleomycin-induced fibrosis.

We did not evaluate how conditional deletion of XIAP expressing cells would affect bleomycin-induced fibrosis. It might be nice to create a transgenic mouse that could be induced to delete XIAP in the post-natal mouse. This mouse may more faithfully recapitulate the phenotype of fibroblasts from IPF lung. We would also like to investigate the role of apoptosis

in the exacerbation model of fibrosis by infecting XIAP conditionally- deficient mice or mice treated with AT-406 with γHV-68, H1N1 or *P. aeruginosa* to assess inflammation and fibrosis. It is interesting that lung leukocytes isolated from XIAP deficient mice post-bleomycin treatment secreted higher levels of IL1β production but showed no difference in lung fibrosis. Even, though the role of IL1β in fibrosis is controversial, the increased production of IL1β could also suggest a role for inflammasomes, which we could also assess in this model. It is likely that inflammasome activation could play a larger role in the pathogen-exacerbated fibrosis models than it does in the sterile bleomycin-injury model.

In the biomarker studies we used Slow Off-rate modified aptamer array to analyze plasma samples from 60 IPF patients. We identified 1129 analytes from these samples, constructed ROC curves for all candidate biomarker and chose a threshold to maximize sensitivity and specificity. Overall we identified a six-analyte panel that included legumain, FCN2, cathespin S, TRY3, VEGFsR2 and ICOS that correlated to progression of IPF. ICOS and TRY3 were above threshold, while legumain, Cathespin S, FCN2 and VEGFsR2 were below threshold.

To further assess the role of these proteins in lung fibrosis we would like to evaluate the role of legumain and FCN2 in our mouse model of bleomycin-induced fibrosis. Legumain has been shown to degrade fibronectin causing changes in the ECM in interstitial renal fibrosis (498). Legumain deficient mice showed worse fibrosis in unilateral ureteral obstruction (UUO)-induced renal fibrosis and significant accumulation of fibronectin (498). We would like to treat legumain deficient mice with bleomycin and assess inflammation and fibrosis post-bleomycin treatment. Additionally, we will validate our SOMAmer array data using ELISA to analyze our six analytes. Given that the SOMAmer array is prohibitively expensive and ELISA-based array measuring

these same factors could be more cost effective. The most important future direction for our biomarker work in humans will be to repeat these analyses in a validation cohort of patients. Finally we will also assess the role of ficolin in bleomycin-induced fibrosis by instilling lung fibrosis in ficoln $2^{-/-}$ mice. FCN2 was recently shown to bind to Streptococcus, and it would be interesting to expand our studies to understand how different viral or bacterial pathogens affect the fibrotic response in ficolin $2^{-/-}$ mice.

Concluding Remarks

We recognize that IPF is a multifactorial disease and that patients suffering from the disease may have alterations in genetic or environmental factors or both. Our mouse models have allowed us to investigate the potential of both environmental factors (infections) and host factors (periostin) that can contribute to lung fibrogenesis and have uncovered important signaling responses in both epithelial cells and fibroblasts. We have also performed translational studies to determine whether biomarkers can be identified that provide prognostic information as well as insight into disease pathogenesis. We hope that this work may help lead to new therapeutic interventions for patients suffering from this devastating disease.

References

1. King TE, Jr., Pardo A, and Selman M. Idiopathic pulmonary fibrosis. *Lancet.* 2011;378(9807):1949-61.
2. Travis WD, Costabel U, Hansell DM, King TE, Jr., Lynch DA, Nicholson AG, Ryerson CJ, Ryu JH, Selman M, Wells AU, et al. An official American Thoracic Society/European Respiratory Society statement: Update of the international multidisciplinary classification of the idiopathic interstitial pneumonias. *Am J Respir Crit Care Med.* 2013;188(6):733-48.
3. Bonella F, Stowasser S, and Wollin L. Idiopathic pulmonary fibrosis: current treatment options and critical appraisal of nintedanib. *Drug Des Devel Ther.* 2015;9(6407-19.
4. Thomeer M, Demedts M, Vandeurzen K, and Diseases VWGoIL. Registration of interstitial lung diseases by 20 centres of respiratory medicine in Flanders. *Acta Clin Belg.* 2001;56(3):163-72.
5. Tinelli C, De Silvestri A, Richeldi L, and Oggionni T. The Italian register for diffuse infiltrative lung disorders (RIPID): a four-year report. *Sarcoidosis Vasc Diffuse Lung Dis.* 2005;22 Suppl 1(S4-8.
6. American Thoracic Society. Idiopathic pulmonary fibrosis: diagnosis and treatment. International consensus statement. American Thoracic Society (ATS), and the European Respiratory Society (ERS). *Am J Respir Crit Care Med.* 2000;161(2 Pt 1):646-64.
7. Hutchinson J, Fogarty A, Hubbard R, and McKeever T. Global incidence and mortality of idiopathic pulmonary fibrosis: a systematic review. *Eur Respir J.* 2015;46(3):795-806.
8. Raghu G, Chen SY, Yeh WS, Maroni B, Li Q, Lee YC, and Collard HR. Idiopathic pulmonary fibrosis in US Medicare beneficiaries aged 65 years and older: incidence, prevalence, and survival, 2001-11. *The Lancet Respiratory medicine.* 2014;2(7):566-72.
9. Gribbin J, Hubbard RB, Le Jeune I, Smith CJ, West J, and Tata LJ. Incidence and mortality of idiopathic pulmonary fibrosis and sarcoidosis in the UK. *Thorax.* 2006;61(11):980-5.
10. Navaratnam V, Fleming KM, West J, Smith CJ, Jenkins RG, Fogarty A, and Hubbard RB. The rising incidence of idiopathic pulmonary fibrosis in the U.K. *Thorax.* 2011;66(6):462-7.
11. Natsuizaka M, Chiba H, Kuronuma K, Otsuka M, Kudo K, Mori M, Bando M, Sugiyama Y, and Takahashi H. Epidemiologic survey of Japanese patients with idiopathic pulmonary fibrosis and investigation of ethnic differences. *Am J Respir Crit Care Med.* 2014;190(7):773-9.

12. Raghu G, Collard HR, Egan JJ, Martinez FJ, Behr J, Brown KK, Colby TV, Cordier JF, Flaherty KR, Lasky JA, et al. An official ATS/ERS/JRS/ALAT statement: idiopathic pulmonary fibrosis: evidence-based guidelines for diagnosis and management. *Am J Respir Crit Care Med.* 2011;183(6):788-824.
13. Bjoraker JA, Ryu JH, Edwin MK, Myers JL, Tazelaar HD, Schroeder DR, and Offord KP. Prognostic significance of histopathologic subsets in idiopathic pulmonary fibrosis. *Am J Respir Crit Care Med.* 1998;157(1):199-203.
14. Ohshimo S, Bonella F, Cui A, Beume M, Kohno N, Guzman J, and Costabel U. Significance of bronchoalveolar lavage for the diagnosis of idiopathic pulmonary fibrosis. *Am J Respir Crit Care Med.* 2009;179(11):1043-7.
15. Casoni GL, Tomassetti S, Cavazza A, Colby TV, Dubini A, Ryu JH, Carretta E, Tantalocco P, Piciucchi S, Ravaglia C, et al. Transbronchial lung cryobiopsy in the diagnosis of fibrotic interstitial lung diseases. *PloS one.* 2014;9(2):e86716.
16. Kropski JA, Pritchett JM, Mason WR, Sivarajan L, Gleaves LA, Johnson JE, Lancaster LH, Lawson WE, Blackwell TS, Steele MP, et al. Bronchoscopic cryobiopsy for the diagnosis of diffuse parenchymal lung disease. *PloS one.* 2013;8(11):e78674.
17. Hutchinson JP, McKeever TM, Fogarty AW, Navaratnam V, and Hubbard RB. Increasing global mortality from idiopathic pulmonary fibrosis in the twenty-first century. *Ann Am Thorac Soc.* 2014;11(8):1176-85.
18. Martinez FJ, Safrin S, Weycker D, Starko KM, Bradford WZ, King TE, Jr., Flaherty KR, Schwartz DA, Noble PW, Raghu G, et al. The clinical course of patients with idiopathic pulmonary fibrosis. *Ann Intern Med.* 2005;142(12 Pt 1):963-7.
19. Gross TJ, and Hunninghake GW. Idiopathic pulmonary fibrosis. *N Engl J Med.* 2001;345(7):517-25.
20. Furuie H, Yamasaki H, Suga M, and Ando M. Altered accessory cell function of alveolar macrophages: a possible mechanism for induction of Th2 secretory profile in idiopathic pulmonary fibrosis. *Eur Respir J.* 1997;10(4):787-94.
21. Hancock A, Armstrong L, Gama R, and Millar A. Production of interleukin 13 by alveolar macrophages from normal and fibrotic lung. *Am J Respir Cell Mol Biol.* 1998;18(1):60-5.
22. Kunkel SL, Lukacs NW, Strieter RM, and Chensue SW. Th1 and Th2 responses regulate experimental lung granuloma development. *Sarcoidosis Vasc Diffuse Lung Dis.* 1996;13(2):120-8.
23. Martinez JA, King TE, Jr., Brown K, Jennings CA, Borish L, Mortenson RL, Khan TZ, Bost TW, and Riches DW. Increased expression of the interleukin-10 gene by alveolar macrophages in interstitial lung disease. *Am J Physiol.* 1997;273(3 Pt 1):L676-83.
24. Romagnani S. Th1/Th2 cells. *Inflammatory bowel diseases.* 1999;5(4):285-94.
25. Moore BB, Kolodsick JE, Thannickal VJ, Cooke K, Moore TA, Hogaboam C, Wilke CA, and Toews GB. CCR2-mediated recruitment of fibrocytes to the alveolar space after fibrotic injury. *Am J Pathol.* 2005;166(3):675-84.
26. Liu T, Jin H, Ullenbruch M, Hu B, Hashimoto N, Moore B, McKenzie A, Lukacs NW, and Phan SH. Regulation of found in inflammatory zone 1 expression in

bleomycin-induced lung fibrosis: role of IL-4/IL-13 and mediation via STAT-6. *J Immunol.* 2004;173(5):3425-31.
27. Selman M, and Pardo A. Stochastic age-related epigenetic drift in the pathogenesis of idiopathic pulmonary fibrosis. *Am J Respir Crit Care Med.* 2014;190(12):1328-30.
28. Selman M, and Pardo A. Revealing the pathogenic and aging-related mechanisms of the enigmatic idiopathic pulmonary fibrosis. an integral model. *Am J Respir Crit Care Med.* 2014;189(10):1161-72.
29. Spagnolo P, Grunewald J, and du Bois RM. Genetic determinants of pulmonary fibrosis: evolving concepts. *The Lancet Respiratory medicine.* 2014;2(5):416-28.
30. Sasaki J, Rafigul AC, Lu CL, and Tamagake T. [Distribution of human alpha-fetoprotein in animal tumor cells]. *Gan To Kagaku Ryoho.* 1988;15(12):3305-8.
31. Idiopathic Pulmonary Fibrosis Clinical Research N, Martinez FJ, de Andrade JA, Anstrom KJ, King TE, Jr., and Raghu G. Randomized trial of acetylcysteine in idiopathic pulmonary fibrosis. *N Engl J Med.* 2014;370(22):2093-101.
32. Idiopathic Pulmonary Fibrosis Clinical Research N, Raghu G, Anstrom KJ, King TE, Jr., Lasky JA, and Martinez FJ. Prednisone, azathioprine, and N-acetylcysteine for pulmonary fibrosis. *N Engl J Med.* 2012;366(21):1968-77.
33. King TE, Jr., Bradford WZ, Castro-Bernardini S, Fagan EA, Glaspole I, Glassberg MK, Gorina E, Hopkins PM, Kardatzke D, Lancaster L, et al. A phase 3 trial of pirfenidone in patients with idiopathic pulmonary fibrosis. *N Engl J Med.* 2014;370(22):2083-92.
34. Richeldi L, du Bois RM, Raghu G, Azuma A, Brown KK, Costabel U, Cottin V, Flaherty KR, Hansell DM, Inoue Y, et al. Efficacy and safety of nintedanib in idiopathic pulmonary fibrosis. *N Engl J Med.* 2014;370(22):2071-82.
35. Raghu G, Rochwerg B, Zhang Y, Garcia CA, Azuma A, Behr J, Brozek JL, Collard HR, Cunningham W, Homma S, et al. An Official ATS/ERS/JRS/ALAT Clinical Practice Guideline: Treatment of Idiopathic Pulmonary Fibrosis. An Update of the 2011 Clinical Practice Guideline. *Am J Respir Crit Care Med.* 2015;192(2):e3-19.
36. Xaubet A, Ancochea J, Bollo E, Fernandez-Fabrellas E, Franquet T, Molina-Molina M, Montero MA, Serrano-Mollar A, and Sociedad Espanola de Neumologia y Cirugia Toracica Research Group on Diffuse Pulmonary D. Guidelines for the diagnosis and treatment of idiopathic pulmonary fibrosis. Sociedad Espanola de Neumologia y Cirugia Toracica (SEPAR) Research Group on Diffuse Pulmonary Diseases. *Arch Bronconeumol.* 2013;49(8):343-53.
37. de la Fuente M, Hernanz A, Guayerbas N, Alvarez P, and Alvarado C. Changes with age in peritoneal macrophage functions. Implication of leukocytes in the oxidative stress of senescence. *Cell Mol Biol (Noisy-le-grand).* 2004;50 Online Pub(OL683-90.
38. Elder AC, Gelein R, Finkelstein JN, Cox C, and Oberdorster G. Pulmonary inflammatory response to inhaled ultrafine particles is modified by age, ozone exposure, and bacterial toxin. *Inhal Toxicol.* 2000;12 Suppl 4(227-46.
39. Pawelec G, and Larbi A. Immunity and ageing in man: Annual Review 2006/2007. *Exp Gerontol.* 2008;43(1):34-8.

40. Meyer KC, Rosenthal NS, Soergel P, and Peterson K. Neutrophils and low-grade inflammation in the seemingly normal aging human lung. *Mech Ageing Dev.* 1998;104(2):169-81.
41. Plackett TP, Schilling EM, Faunce DE, Choudhry MA, Witte PL, and Kovacs EJ. Aging enhances lymphocyte cytokine defects after injury. *FASEB J.* 2003;17(6):688-9.
42. Xu J, Mora AL, LaVoy J, Brigham KL, and Rojas M. Increased bleomycin-induced lung injury in mice deficient in the transcription factor T-bet. *Am J Physiol Lung Cell Mol Physiol.* 2006;291(4):L658-67.
43. Saadat M. Change in sex ratio at birth in Sardasht (north west of Iran) after chemical bombardment. *J Epidemiol Community Health.* 2006;60(2):183.
44. Murray LA, Argentieri RL, Farrell FX, Bracht M, Sheng H, Whitaker B, Beck H, Tsui P, Cochlin K, Evanoff HL, et al. Hyper-responsiveness of IPF/UIP fibroblasts: interplay between TGFbeta1, IL-13 and CCL2. *Int J Biochem Cell Biol.* 2008;40(10):2174-82.
45. Raghu G, Weycker D, Edelsberg J, Bradford WZ, and Oster G. Incidence and prevalence of idiopathic pulmonary fibrosis. *Am J Respir Crit Care Med.* 2006;174(7):810-6.
46. Lopez-Otin C, Blasco MA, Partridge L, Serrano M, and Kroemer G. The hallmarks of aging. *Cell.* 2013;153(6):1194-217.
47. Moskalev AA, Shaposhnikov MV, Plyusnina EN, Zhavoronkov A, Budovsky A, Yanai H, and Fraifeld VE. The role of DNA damage and repair in aging through the prism of Koch-like criteria. *Ageing Res Rev.* 2013;12(2):661-84.
48. Park CB, and Larsson NG. Mitochondrial DNA mutations in disease and aging. *J Cell Biol.* 2011;193(5):809-18.
49. Demopoulos K, Arvanitis DA, Vassilakis DA, Siafakas NM, and Spandidos DA. MYCL1, FHIT, SPARC, p16(INK4) and TP53 genes associated to lung cancer in idiopathic pulmonary fibrosis. *J Cell Mol Med.* 2002;6(2):215-22.
50. Alder JK, Chen JJ, Lancaster L, Danoff S, Su SC, Cogan JD, Vulto I, Xie M, Qi X, Tuder RM, et al. Short telomeres are a risk factor for idiopathic pulmonary fibrosis. *Proc Natl Acad Sci U S A.* 2008;105(35):13051-6.
51. Araya J, Kojima J, Takasaka N, Ito S, Fujii S, Hara H, Yanagisawa H, Kobayashi K, Tsurushige C, Kawaishi M, et al. Insufficient autophagy in idiopathic pulmonary fibrosis. *Am J Physiol Lung Cell Mol Physiol.* 2013;304(1):L56-69.
52. Kuwano K, Hagimoto N, Maeyama T, Fujita M, Yoshimi M, Inoshima I, Nakashima N, Hamada N, Watanabe K, and Hara N. Mitochondria-mediated apoptosis of lung epithelial cells in idiopathic interstitial pneumonias. *Lab Invest.* 2002;82(12):1695-706.
53. Gilani SR, Vuga LJ, Lindell KO, Gibson KF, Xue J, Kaminski N, Valentine VG, Lindsay EK, George MP, Steele C, et al. CD28 down-regulation on circulating CD4 T-cells is associated with poor prognoses of patients with idiopathic pulmonary fibrosis. *PloS one.* 2010;5(1):e8959.
54. Seshadri M, and Mazi-Kotwal N. A copyright-free alternative to the mini-mental state examination is needed. *BMJ.* 2012;345(e8589.

55. Hecker L, Logsdon NJ, Kurundkar D, Kurundkar A, Bernard K, Hock T, Meldrum E, Sanders YY, and Thannickal VJ. Reversal of persistent fibrosis in aging by targeting Nox4-Nrf2 redox imbalance. *Sci Transl Med.* 2014;6(231):231ra47.
56. Mays PK, Bishop JE, and Laurent GJ. Age-related changes in the proportion of types I and III collagen. *Mech Ageing Dev.* 1988;45(3):203-12.
57. Huang K, Mitzner W, Rabold R, Schofield B, Lee H, Biswal S, and Tankersley CG. Variation in senescent-dependent lung changes in inbred mouse strains. *J Appl Physiol (1985).* 2007;102(4):1632-9.
58. Roman J, Ritzenthaler JD, Bechara R, Brown LA, and Guidot D. Ethanol stimulates the expression of fibronectin in lung fibroblasts via kinase-dependent signals that activate CREB. *Am J Physiol Lung Cell Mol Physiol.* 2005;288(5):L975-87.
59. Muro AF, Moretti FA, Moore BB, Yan M, Atrasz RG, Wilke CA, Flaherty KR, Martinez FJ, Tsui JL, Sheppard D, et al. An essential role for fibronectin extra type III domain A in pulmonary fibrosis. *Am J Respir Crit Care Med.* 2008;177(6):638-45.
60. McDonald JA, Kelley DG, and Broekelmann TJ. Role of fibronectin in collagen deposition: Fab' to the gelatin-binding domain of fibronectin inhibits both fibronectin and collagen organization in fibroblast extracellular matrix. *J Cell Biol.* 1982;92(2):485-92.
61. Bitterman PB, Rennard SI, Adelberg S, and Crystal RG. Role of fibronectin as a growth factor for fibroblasts. *J Cell Biol.* 1983;97(6):1925-32.
62. Sueblinvong V, Neujahr DC, Mills ST, Roser-Page S, Ritzenthaler JD, Guidot D, Rojas M, and Roman J. Predisposition for disrepair in the aged lung. *Am J Med Sci.* 2012;344(1):41-51.
63. Umezawa H, Ishizuka M, Maeda K, and Takeuchi T. Studies on bleomycin. *Cancer.* 1967;20(5):891-5.
64. Muggia FM, Louie AC, and Sikic BI. Pulmonary toxicity of antitumor agents. *Cancer Treat Rev.* 1983;10(4):221-43.
65. Phan SH, Thrall RS, and Williams C. Bleomycin-induced pulmonary fibrosis. Effects of steroid on lung collagen metabolism. *Am Rev Respir Dis.* 1981;124(4):428-34.
66. Schmieder RE. Hypertensive heart disease--significance of left ventricular hypertrophy. *J Cardiovasc Pharmacol.* 1992;20 Suppl 6(S50-5.
67. Gharaee-Kermani M, Hatano K, Nozaki Y, and Phan SH. Gender-based differences in bleomycin-induced pulmonary fibrosis. *Am J Pathol.* 2005;166(6):1593-606.
68. Lawson WE, Polosukhin VV, Stathopoulos GT, Zoia O, Han W, Lane KB, Li B, Donnelly EF, Holburn GE, Lewis KG, et al. Increased and prolonged pulmonary fibrosis in surfactant protein C-deficient mice following intratracheal bleomycin. *Am J Pathol.* 2005;167(5):1267-77.
69. Chua F, Gauldie J, and Laurent GJ. Pulmonary fibrosis: searching for model answers. *Am J Respir Cell Mol Biol.* 2005;33(1):9-13.
70. Limjunyawong N, Mitzner W, and Horton MR. A mouse model of chronic idiopathic pulmonary fibrosis. *Physiol Rep.* 2014;2(2):e00249.

71. Hao H, Cohen DA, Jennings CD, Bryson JS, and Kaplan AM. Bleomycin-induced pulmonary fibrosis is independent of eosinophils. *J Leukoc Biol.* 2000;68(4):515-21.
72. Peng R, Sridhar S, Tyagi G, Phillips JE, Garrido R, Harris P, Burns L, Renteria L, Woods J, Chen L, et al. Bleomycin induces molecular changes directly relevant to idiopathic pulmonary fibrosis: a model for "active" disease. *PloS one.* 2013;8(4):e59348.
73. Izbicki G, Segel MJ, Christensen TG, Conner MW, and Breuer R. Time course of bleomycin-induced lung fibrosis. *Int J Exp Pathol.* 2002;83(3):111-9.
74. Janick-Buckner D, Ranges GE, and Hacker MP. Alteration of bronchoalveolar lavage cell populations following bleomycin treatment in mice. *Toxicol Appl Pharmacol.* 1989;100(3):465-73.
75. Phan SH, Armstrong G, Sulavik MC, Schrier D, Johnson KJ, and Ward PA. A comparative study of pulmonary fibrosis induced by bleomycin and an O2 metabolite producing enzyme system. *Chest.* 1983;83(5 Suppl):44S-5S.
76. Schrier DJ, Kunkel RG, and Phan SH. The role of strain variation in murine bleomycin-induced pulmonary fibrosis. *Am Rev Respir Dis.* 1983;127(1):63-6.
77. Crystal RG. Lung collagen: definition, diversity and development. *Fed Proc.* 1974;33(11):2248-55.
78. Sleijfer S. Bleomycin-induced pneumonitis. *Chest.* 2001;120(2):617-24.
79. Harrison JH, Jr., and Lazo JS. High dose continuous infusion of bleomycin in mice: a new model for drug-induced pulmonary fibrosis. *J Pharmacol Exp Ther.* 1987;243(3):1185-94.
80. Chandler DB. Possible mechanisms of bleomycin-induced fibrosis. *Clin Chest Med.* 1990;11(1):21-30.
81. Siddiqui R, Jarroll EL, and Khan NA. Balamuthia mandrillaris: role of galactose in encystment and identification of potential inhibitory targets. *Exp Parasitol.* 2010;126(1):22-7.
82. Sheppard D. Integrin-mediated activation of transforming growth factor-beta(1) in pulmonary fibrosis. *Chest.* 2001;120(1 Suppl):49S-53S.
83. Dhainaut JF, Charpentier J, and Chiche JD. Transforming growth factor-beta: a mediator of cell regulation in acute respiratory distress syndrome. *Crit Care Med.* 2003;31(4 Suppl):S258-64.
84. Yoshida M, Sakuma J, Hayashi S, Abe K, Saito I, Harada S, Sakatani M, Yamamoto S, Matsumoto N, Kaneda Y, et al. A histologically distinctive interstitial pneumonia induced by overexpression of the interleukin 6, transforming growth factor beta 1, or platelet-derived growth factor B gene. *Proc Natl Acad Sci U S A.* 1995;92(21):9570-4.
85. Merkus D, Kajiya F, Vink H, Vergroesen I, Dankelman J, Goto M, and Spaan JA. Prolonged diastolic time fraction protects myocardial perfusion when coronary blood flow is reduced. *Circulation.* 1999;100(1):75-81.
86. Moore BB, and Hogaboam CM. Murine models of pulmonary fibrosis. *American Journal of Physiology - Lung Cellular and Molecular Physiology.* 2008;294(2):L152-L60.

87. Spence J, Krings T, terBrugge KG, da Costa LB, and Agid R. Percutaneous sclerotherapy for facial venous malformations: subjective clinical and objective MR imaging follow-up results. *AJNR Am J Neuroradiol.* 2010;31(5):955-60.
88. Jules-Elysee K, and White DA. Bleomycin-induced pulmonary toxicity. *Clin Chest Med.* 1990;11(1):1-20.
89. O'Sullivan JM, Huddart RA, Norman AR, Nicholls J, Dearnaley DP, and Horwich A. Predicting the risk of bleomycin lung toxicity in patients with germ-cell tumours. *Ann Oncol.* 2003;14(1):91-6.
90. White DA, Kris MG, and Stover DE. Bronchoalveolar lavage cell populations in bleomycin lung toxicity. *Thorax.* 1987;42(7):551-2.
91. Roberts SN, Howie SE, Wallace WA, Brown DM, Lamb D, Ramage EA, and Donaldson K. A novel model for human interstitial lung disease: hapten-driven lung fibrosis in rodents. *The Journal of pathology.* 1995;176(3):309-18.
92. Christensen PJ, Goodman RE, Pastoriza L, Moore B, and Toews GB. Induction of lung fibrosis in the mouse by intratracheal instillation of fluorescein isothiocyanate is not T-cell-dependent. *Am J Pathol.* 1999;155(5):1773-9.
93. Moore BB, Paine R, 3rd, Christensen PJ, Moore TA, Sitterding S, Ngan R, Wilke CA, Kuziel WA, and Toews GB. Protection from pulmonary fibrosis in the absence of CCR2 signaling. *J Immunol.* 2001;167(8):4368-77.
94. Moore BB, Murray L, Das A, Wilke CA, Herrygers AB, and Toews GB. The role of CCL12 in the recruitment of fibrocytes and lung fibrosis. *Am J Respir Cell Mol Biol.* 2006;35(2):175-81.
95. Korfhagen TR, Swantz RJ, Wert SE, McCarty JM, Kerlakian CB, Glasser SW, and Whitsett JA. Respiratory epithelial cell expression of human transforming growth factor-alpha induces lung fibrosis in transgenic mice. *J Clin Invest.* 1994;93(4):1691-9.
96. Fisher CE, Ahmad SA, Fitch PM, Lamb JR, and Howie SE. FITC-induced murine pulmonary inflammation: CC10 up-regulation and concurrent Shh expression. *Cell Biol Int.* 2005;29(10):868-76.
97. Bucala R, Spiegel LA, Chesney J, Hogan M, and Cerami A. Circulating fibrocytes define a new leukocyte subpopulation that mediates tissue repair. *Mol Med.* 1994;1(1):71-81.
98. Phillips RJ, Burdick MD, Hong K, Lutz MA, Murray LA, Xue YY, Belperio JA, Keane MP, and Strieter RM. Circulating fibrocytes traffic to the lungs in response to CXCL12 and mediate fibrosis. *J Clin Invest.* 2004;114(3):438-46.
99. Pierce EM, Carpenter K, Jakubzick C, Kunkel SL, Flaherty KR, Martinez FJ, and Hogaboam CM. Therapeutic targeting of CC ligand 21 or CC chemokine receptor 7 abrogates pulmonary fibrosis induced by the adoptive transfer of human pulmonary fibroblasts to immunodeficient mice. *Am J Pathol.* 2007;170(4):1152-64.
100. Bergers G, and Song S. The role of pericytes in blood-vessel formation and maintenance. *Neuro Oncol.* 2005;7(4):452-64.
101. Armulik A, Genove G, and Betsholtz C. Pericytes: developmental, physiological, and pathological perspectives, problems, and promises. *Dev Cell.* 2011;21(2):193-215.

102. Hung C, Linn G, Chow YH, Kobayashi A, Mittelsteadt K, Altemeier WA, Gharib SA, Schnapp LM, and Duffield JS. Role of lung pericytes and resident fibroblasts in the pathogenesis of pulmonary fibrosis. *Am J Respir Crit Care Med.* 2013;188(7):820-30.
103. Rock JR, Barkauskas CE, Cronce MJ, Xue Y, Harris JR, Liang J, Noble PW, and Hogan BL. Multiple stromal populations contribute to pulmonary fibrosis without evidence for epithelial to mesenchymal transition. *Proc Natl Acad Sci U S A.* 2011;108(52):E1475-83.
104. Collard HR, Moore BB, Flaherty KR, Brown KK, Kaner RJ, King TE, Jr., Lasky JA, Loyd JE, Noth I, Olman MA, et al. Acute exacerbations of idiopathic pulmonary fibrosis. *Am J Respir Crit Care Med.* 2007;176(7):636-43.
105. Ashley SL, Jegal Y, Moore TA, van Dyk LF, Laouar Y, and Moore BB. gamma-Herpes virus-68, but not Pseudomonas aeruginosa or influenza A (H1N1), exacerbates established murine lung fibrosis. *Am J Physiol Lung Cell Mol Physiol.* 2014;307(3):L219-30.
106. Luckhardt TR, Coomes SM, Trujillo G, Stoolman JS, Vannella KM, Bhan U, Wilke CA, Moore TA, Toews GB, Hogaboam C, et al. TLR9-induced interferon beta is associated with protection from gammaherpesvirus-induced exacerbation of lung fibrosis. *Fibrogenesis Tissue Repair.* 2011;4(18.
107. Golden A, and Bronk TT. Diffuse interstitial fibrosis of lungs; a form of diffuse interstitial angiosis and reticulosis of the lungs. *AMA Arch Intern Med.* 1953;92(5):106-14.
108. Ueda T, Ohta K, Suzuki N, Yamaguchi M, Hirai K, Horiuchi T, Watanabe J, Miyamoto T, and Ito K. Idiopathic pulmonary fibrosis and high prevalence of serum antibodies to hepatitis C virus. *Am Rev Respir Dis.* 1992;146(1):266-8.
109. Irving WL, Day S, and Johnston ID. Idiopathic pulmonary fibrosis and hepatitis C virus infection. *Am Rev Respir Dis.* 1993;148(6 Pt 1):1683-4.
110. Meliconi R, Andreone P, Fasano L, Galli S, Pacilli A, Miniero R, Fabbri M, Solforosi L, and Bernardi M. Incidence of hepatitis C virus infection in Italian patients with idiopathic pulmonary fibrosis. *Thorax.* 1996;51(3):315-7.
111. Vergnon JM, Vincent M, de The G, Mornex JF, Weynants P, and Brune J. Cryptogenic fibrosing alveolitis and Epstein-Barr virus: an association? *Lancet.* 1984;2(8406):768-71.
112. Cullen B. Roles for the WOC nurse in a disaster. *J Wound Ostomy Continence Nurs.* 2008;35(3):282-6.
113. Stewart JP, Egan JJ, Ross AJ, Kelly BG, Lok SS, Hasleton PS, and Woodcock AA. The detection of Epstein-Barr virus DNA in lung tissue from patients with idiopathic pulmonary fibrosis. *Am J Respir Crit Care Med.* 1999;159(4 Pt 1):1336-41.
114. Kelly BG, Lok SS, Hasleton PS, Egan JJ, and Stewart JP. A rearranged form of Epstein-Barr virus DNA is associated with idiopathic pulmonary fibrosis. *Am J Respir Crit Care Med.* 2002;166(4):510-3.
115. Calabrese F, Kipar A, Lunardi F, Balestro E, Perissinotto E, Rossi E, Nannini N, Marulli G, Stewart JP, and Rea F. Herpes virus infection is associated with vascular remodeling and pulmonary hypertension in idiopathic pulmonary fibrosis. *PloS one.* 2013;8(2):e55715.

116. Tang YW, Johnson JE, Browning PJ, Cruz-Gervis RA, Davis A, Graham BS, Brigham KL, Oates JA, Jr., Loyd JE, and Stecenko AA. Herpesvirus DNA is consistently detected in lungs of patients with idiopathic pulmonary fibrosis. *J Clin Microbiol.* 2003;41(6):2633-40.
117. Kropski JA, Lawson WE, and Blackwell TS. Right place, right time: the evolving role of herpesvirus infection as a "second hit" in idiopathic pulmonary fibrosis. *Am J Physiol Lung Cell Mol Physiol.* 2012;302(5):L441-4.
118. Guillaume JC, Escudier B, Espagne E, Roujeau JC, Prost C, Domart P, Nitenberg G, and Avril MF. [Bullous dermatosis with linear IgA deposits along the basement membrane during treatment with gamma interferon and interleukin-2]. *Ann Dermatol Venereol.* 1990;117(11):899-902.
119. Lok SS, Haider Y, Howell D, Stewart JP, Hasleton PS, and Egan JJ. Murine gammaherpes virus as a cofactor in the development of pulmonary fibrosis in bleomycin resistant mice. *Eur Respir J.* 2002;20(5):1228-32.
120. Mora AL, Woods CR, Garcia A, Xu J, Rojas M, Speck SH, Roman J, Brigham KL, and Stecenko AA. Lung infection with gamma-herpesvirus induces progressive pulmonary fibrosis in Th2-biased mice. *Am J Physiol Lung Cell Mol Physiol.* 2005;289(5):L711-21.
121. Stoolman JS, Vannella KM, Coomes SM, Wilke CA, Sisson TH, Toews GB, and Moore BB. Latent infection by gammaherpesvirus stimulates profibrotic mediator release from multiple cell types. *Am J Physiol Lung Cell Mol Physiol.* 2011;300(2):L274-85.
122. Naik PN, Horowitz JC, Moore TA, Wilke CA, Toews GB, and Moore BB. Pulmonary fibrosis induced by gamma-herpesvirus in aged mice is associated with increased fibroblast responsiveness to transforming growth factor-beta. *J Gerontol A Biol Sci Med Sci.* 2012;67(7):714-25.
123. Torres-Gonzalez E, Bueno M, Tanaka A, Krug LT, Cheng DS, Polosukhin VV, Sorescu D, Lawson WE, Blackwell TS, Rojas M, et al. Role of endoplasmic reticulum stress in age-related susceptibility to lung fibrosis. *Am J Respir Cell Mol Biol.* 2012;46(6):748-56.
124. Isler JA, Skalet AH, and Alwine JC. Human cytomegalovirus infection activates and regulates the unfolded protein response. *J Virol.* 2005;79(11):6890-9.
125. Lawson WE, Crossno PF, Polosukhin VV, Roldan J, Cheng DS, Lane KB, Blackwell TR, Xu C, Markin C, Ware LB, et al. Endoplasmic reticulum stress in alveolar epithelial cells is prominent in IPF: association with altered surfactant protein processing and herpesvirus infection. *Am J Physiol Lung Cell Mol Physiol.* 2008;294(6):L1119-26.
126. Egan JJ, Adamali HI, Lok SS, Stewart JP, and Woodcock AA. Ganciclovir antiviral therapy in advanced idiopathic pulmonary fibrosis: an open pilot study. *Pulm Med.* 2011;2011(240805.
127. Judge EP, Fabre A, Adamali HI, and Egan JJ. Acute exacerbations and pulmonary hypertension in advanced idiopathic pulmonary fibrosis. *Eur Respir J.* 2012;40(1):93-100.
128. Huie TJ, Olson AL, Cosgrove GP, Janssen WJ, Lara AR, Lynch DA, Groshong SD, Moss M, Schwarz MI, Brown KK, et al. A detailed evaluation of acute

respiratory decline in patients with fibrotic lung disease: aetiology and outcomes. *Respirology.* 2010;15(6):909-17.
129. McMillan TR, Moore BB, Weinberg JB, Vannella KM, Fields WB, Christensen PJ, van Dyk LF, and Toews GB. Exacerbation of established pulmonary fibrosis in a murine model by gammaherpesvirus. *Am J Respir Crit Care Med.* 2008;177(7):771-80.
130. Wootton SC, Kim DS, Kondoh Y, Chen E, Lee JS, Song JW, Huh JW, Taniguchi H, Chiu C, Boushey H, et al. Viral infection in acute exacerbation of idiopathic pulmonary fibrosis. *Am J Respir Crit Care Med.* 2011;183(12):1698-702.
131. Richter AG, Stockley RA, Harper L, and Thickett DR. Pulmonary infection in Wegener granulomatosis and idiopathic pulmonary fibrosis. *Thorax.* 2009;64(8):692-7.
132. Shulgina L, Cahn AP, Chilvers ER, Parfrey H, Clark AB, Wilson EC, Twentyman OP, Davison AG, Curtin JJ, Crawford MB, et al. Treating idiopathic pulmonary fibrosis with the addition of co-trimoxazole: a randomised controlled trial. *Thorax.* 2013;68(2):155-62.
133. Friaza V, la Horra C, Rodriguez-Dominguez MJ, Martin-Juan J, Canton R, Calderon EJ, and Del Campo R. Metagenomic analysis of bronchoalveolar lavage samples from patients with idiopathic interstitial pneumonia and its antagonic relation with Pneumocystis jirovecii colonization. *J Microbiol Methods.* 2010;82(1):98-101.
134. Molyneaux PL, Cox MJ, Willis-Owen SA, Mallia P, Russell KE, Russell AM, Murphy E, Johnston SL, Schwartz DA, Wells AU, et al. The role of bacteria in the pathogenesis and progression of idiopathic pulmonary fibrosis. *Am J Respir Crit Care Med.* 2014;190(8):906-13.
135. Han MK, Zhou Y, Murray S, Tayob N, Noth I, Lama VN, Moore BB, White ES, Flaherty KR, Huffnagle GB, et al. Lung microbiome and disease progression in idiopathic pulmonary fibrosis: an analysis of the COMET study. *The Lancet Respiratory medicine.* 2014;2(7):548-56.
136. Wynn TA. Integrating mechanisms of pulmonary fibrosis. *The Journal of experimental medicine.* 2011;208(7):1339-50.
137. Fernandez IE, and Eickelberg O. New cellular and molecular mechanisms of lung injury and fibrosis in idiopathic pulmonary fibrosis. *Lancet.* 2012;380(9842):680-8.
138. Todd NW, Luzina IG, and Atamas SP. Molecular and cellular mechanisms of pulmonary fibrosis. *Fibrogenesis Tissue Repair.* 2012;5(1):11.
139. Brieland JK, Flory CM, Jones ML, Miller GR, Remick DG, Warren JS, and Fantone JC. Regulation of monocyte chemoattractant protein-1 gene expression and secretion in rat pulmonary alveolar macrophages by lipopolysaccharide, tumor necrosis factor-alpha, and interleukin-1 beta. *Am J Respir Cell Mol Biol.* 1995;12(1):104-9.
140. Mora AL, Torres-Gonzalez E, Rojas M, Corredor C, Ritzenthaler J, Xu J, Roman J, Brigham K, and Stecenko A. Activation of alveolar macrophages via the alternative pathway in herpesvirus-induced lung fibrosis. *Am J Respir Cell Mol Biol.* 2006;35(4):466-73.
141. Willems S, Verleden SE, Vanaudenaerde BM, Wynants M, Dooms C, Yserbyt J, Somers J, Verbeken EK, Verleden GM, and Wuyts WA. Multiplex protein profiling

of bronchoalveolar lavage in idiopathic pulmonary fibrosis and hypersensitivity pneumonitis. *Ann Thorac Med.* 2013;8(1):38-45.
142. Mantovani A, Sica A, Sozzani S, Allavena P, Vecchi A, and Locati M. The chemokine system in diverse forms of macrophage activation and polarization. *Trends Immunol.* 2004;25(12):677-86.
143. Prasse A, Pechkovsky DV, Toews GB, Jungraithmayr W, Kollert F, Goldmann T, Vollmer E, Muller-Quernheim J, and Zissel G. A vicious circle of alveolar macrophages and fibroblasts perpetuates pulmonary fibrosis via CCL18. *Am J Respir Crit Care Med.* 2006;173(7):781-92.
144. Sun L, Louie MC, Vannella KM, Wilke CA, LeVine AM, Moore BB, and Shanley TP. New concepts of IL-10-induced lung fibrosis: fibrocyte recruitment and M2 activation in a CCL2/CCR2 axis. *Am J Physiol Lung Cell Mol Physiol.* 2011;300(3):L341-53.
145. Gibbons MA, MacKinnon AC, Ramachandran P, Dhaliwal K, Duffin R, Phythian-Adams AT, van Rooijen N, Haslett C, Howie SE, Simpson AJ, et al. Ly6Chi monocytes direct alternatively activated profibrotic macrophage regulation of lung fibrosis. *Am J Respir Crit Care Med.* 2011;184(5):569-81.
146. Murray LA, Chen Q, Kramer MS, Hesson DP, Argentieri RL, Peng X, Gulati M, Homer RJ, Russell T, van Rooijen N, et al. TGF-beta driven lung fibrosis is macrophage dependent and blocked by Serum amyloid P. *Int J Biochem Cell Biol.* 2011;43(1):154-62.
147. Migliaccio CT, Buford MC, Jessop F, and Holian A. The IL-4Ralpha pathway in macrophages and its potential role in silica-induced pulmonary fibrosis. *J Leukoc Biol.* 2008;83(3):630-9.
148. Murray LA, Rosada R, Moreira AP, Joshi A, Kramer MS, Hesson DP, Argentieri RL, Mathai S, Gulati M, Herzog EL, et al. Serum amyloid P therapeutically attenuates murine bleomycin-induced pulmonary fibrosis via its effects on macrophages. *PloS one.* 2010;5(3):e9683.
149. Pechkovsky DV, Prasse A, Kollert F, Engel KM, Dentler J, Luttmann W, Friedrich K, Muller-Quernheim J, and Zissel G. Alternatively activated alveolar macrophages in pulmonary fibrosis-mediator production and intracellular signal transduction. *Clin Immunol.* 2010;137(1):89-101.
150. Border WA, and Noble NA. Transforming growth factor beta in tissue fibrosis. *N Engl J Med.* 1994;331(19):1286-92.
151. Thiery JP, and Sleeman JP. Complex networks orchestrate epithelial-mesenchymal transitions. *Nat Rev Mol Cell Biol.* 2006;7(2):131-42.
152. Chapman HA. Epithelial-mesenchymal interactions in pulmonary fibrosis. *Annu Rev Physiol.* 2011;73(413-35.
153. Xu J, Lamouille S, and Derynck R. TGF-beta-induced epithelial to mesenchymal transition. *Cell Res.* 2009;19(2):156-72.
154. Rispoli M. The mosaic acquisition of grammatical relations. *J Child Lang.* 1991;18(3):517-51.
155. Travis MA, and Sheppard D. TGF-beta activation and function in immunity. *Annu Rev Immunol.* 2014;32(51-82.
156. Fernandez IE, and Eickelberg O. The impact of TGF-beta on lung fibrosis: from targeting to biomarkers. *Proc Am Thorac Soc.* 2012;9(3):111-6.

157. Kampf C, Relova AJ, Sandler S, and Roomans GM. Effects of TNF-alpha, IFN-gamma and IL-beta on normal human bronchial epithelial cells. *Eur Respir J.* 1999;14(1):84-91.
158. Burgess JK, Blake AE, Boustany S, Johnson PR, Armour CL, Black JL, Hunt NH, and Hughes JM. CD40 and OX40 ligand are increased on stimulated asthmatic airway smooth muscle. *J Allergy Clin Immunol.* 2005;115(2):302-8.
159. Hughes JM, Stringer RS, Black JL, and Armour CL. The effects of tumour necrosis factor alpha on mediator release from human lung. *Pulm Pharmacol.* 1995;8(1):31-6.
160. Wagner EM. TNF-alpha induced bronchial vasoconstriction. *Am J Physiol Heart Circ Physiol.* 2000;279(3):H946-51.
161. Choi IW, Sun K, Kim YS, Ko HM, Im SY, Kim JH, You HJ, Lee YC, Lee JH, Park YM, et al. TNF-alpha induces the late-phase airway hyperresponsiveness and airway inflammation through cytosolic phospholipase A(2) activation. *J Allergy Clin Immunol.* 2005;116(3):537-43.
162. Grashoff WF, Sont JK, Sterk PJ, Hiemstra PS, de Boer WI, Stolk J, Han J, and van Krieken JM. Chronic obstructive pulmonary disease: role of bronchiolar mast cells and macrophages. *Am J Pathol.* 1997;151(6):1785-90.
163. O'Shaughnessy TC, Ansari TW, Barnes NC, and Jeffery PK. Inflammation in bronchial biopsies of subjects with chronic bronchitis: inverse relationship of CD8+ T lymphocytes with FEV1. *Am J Respir Crit Care Med.* 1997;155(3):852-7.
164. Mannino DM. COPD: epidemiology, prevalence, morbidity and mortality, and disease heterogeneity. *Chest.* 2002;121(5 Suppl):121S-6S.
165. Barnes PJ. New treatments for COPD. *Nat Rev Drug Discov.* 2002;1(6):437-46.
166. Niederman MS, and Fein AM. Sepsis syndrome, the adult respiratory distress syndrome, and nosocomial pneumonia. A common clinical sequence. *Clin Chest Med.* 1990;11(4):633-56.
167. Lee WL, and Downey GP. Neutrophil activation and acute lung injury. *Curr Opin Crit Care.* 2001;7(1):1-7.
168. Leeper-Woodford SK, Carey PD, Byrne K, Jenkins JK, Fisher BJ, Blocher C, Sugerman HJ, and Fowler AA, 3rd. Tumor necrosis factor. Alpha and beta subtypes appear in circulation during onset of sepsis-induced lung injury. *Am Rev Respir Dis.* 1991;143(5 Pt 1):1076-82.
169. Sheridan BC, McIntyre RC, Meldrum DR, and Fullerton DA. Pentoxifylline treatment attenuates pulmonary vasomotor dysfunction in acute lung injury. *J Surg Res.* 1997;71(2):150-4.
170. Lundblad LK, Thompson-Figueroa J, Leclair T, Sullivan MJ, Poynter ME, Irvin CG, and Bates JH. Tumor necrosis factor-alpha overexpression in lung disease: a single cause behind a complex phenotype. *Am J Respir Crit Care Med.* 2005;171(12):1363-70.
171. Redente EF, Keith RC, Janssen W, Henson PM, Ortiz LA, Downey GP, Bratton DL, and Riches DW. Tumor necrosis factor-alpha accelerates the resolution of established pulmonary fibrosis in mice by targeting profibrotic lung macrophages. *Am J Respir Cell Mol Biol.* 2014;50(4):825-37.
172. Distler JH, Schett G, Gay S, and Distler O. The controversial role of tumor necrosis factor alpha in fibrotic diseases. *Arthritis Rheum.* 2008;58(8):2228-35.

173. Sime PJ, Marr RA, Gauldie D, Xing Z, Hewlett BR, Graham FL, and Gauldie J. Transfer of tumor necrosis factor-alpha to rat lung induces severe pulmonary inflammation and patchy interstitial fibrogenesis with induction of transforming growth factor-beta1 and myofibroblasts. *Am J Pathol.* 1998;153(3):825-32.
174. Feghali-Bostwick CA, Tsai CG, Valentine VG, Kantrow S, Stoner MW, Pilewski JM, Gadgil A, George MP, Gibson KF, Choi AM, et al. Cellular and humoral autoreactivity in idiopathic pulmonary fibrosis. *J Immunol.* 2007;179(4):2592-9.
175. Piguet PF, Collart MA, Grau GE, Kapanci Y, and Vassalli P. Tumor necrosis factor/cachectin plays a key role in bleomycin-induced pneumopathy and fibrosis. *The Journal of experimental medicine.* 1989;170(3):655-63.
176. Ortiz LA, Lasky J, Hamilton RF, Jr., Holian A, Hoyle GW, Banks W, Peschon JJ, Brody AR, Lungarella G, and Friedman M. Expression of TNF and the necessity of TNF receptors in bleomycin-induced lung injury in mice. *Exp Lung Res.* 1998;24(6):721-43.
177. Kalderen C, Stadler C, Forsgren M, Kvastad L, Johansson E, Sydow-Backman M, and Svensson Gelius S. CCL2 mediates anti-fibrotic effects in human fibroblasts independently of CCR2. *Int Immunopharmacol.* 2014;20(1):66-73.
178. Baran CP, Opalek JM, McMaken S, Newland CA, O'Brien JM, Jr., Hunter MG, Bringardner BD, Monick MM, Brigstock DR, Stromberg PC, et al. Important roles for macrophage colony-stimulating factor, CC chemokine ligand 2, and mononuclear phagocytes in the pathogenesis of pulmonary fibrosis. *Am J Respir Crit Care Med.* 2007;176(1):78-89.
179. Hartl D, Griese M, Nicolai T, Zissel G, Prell C, Reinhardt D, Schendel DJ, and Krauss-Etschmann S. A role for MCP-1/CCR2 in interstitial lung disease in children. *Respir Res.* 2005;6(93.
180. Capelli A, Di Stefano A, Gnemmi I, and Donner CF. CCR5 expression and CC chemokine levels in idiopathic pulmonary fibrosis. *Eur Respir J.* 2005;25(4):701-7.
181. Shinoda H, Tasaka S, Fujishima S, Yamasawa W, Miyamoto K, Nakano Y, Kamata H, Hasegawa N, and Ishizaka A. Elevated CC chemokine level in bronchoalveolar lavage fluid is predictive of a poor outcome of idiopathic pulmonary fibrosis. *Respiration.* 2009;78(3):285-92.
182. Deng X, Xu M, Yuan C, Yin L, Chen X, Zhou X, Li G, Fu Y, Feghali-Bostwick CA, and Pang L. Transcriptional regulation of increased CCL2 expression in pulmonary fibrosis involves nuclear factor-kappaB and activator protein-1. *Int J Biochem Cell Biol.* 2013;45(7):1366-76.
183. Gharaee-Kermani M, McCullumsmith RE, Charo IF, Kunkel SL, and Phan SH. CC-chemokine receptor 2 required for bleomycin-induced pulmonary fibrosis. *Cytokine.* 2003;24(6):266-76.
184. Liu X, Das AM, Seideman J, Griswold D, Afuh CN, Kobayashi T, Abe S, Fang Q, Hashimoto M, Kim H, et al. The CC chemokine ligand 2 (CCL2) mediates fibroblast survival through IL-6. *Am J Respir Cell Mol Biol.* 2007;37(1):121-8.
185. Ekert JE, Murray LA, Das AM, Sheng H, Giles-Komar J, and Rycyzyn MA. Chemokine (C-C motif) ligand 2 mediates direct and indirect fibrotic responses in human and murine cultured fibrocytes. *Fibrogenesis Tissue Repair.* 2011;4(1):23.

186. Abe R, Donnelly SC, Peng T, Bucala R, and Metz CN. Peripheral blood fibrocytes: differentiation pathway and migration to wound sites. *J Immunol.* 2001;166(12):7556-62.
187. Xu J, Cong M, Park TJ, Scholten D, Brenner DA, and Kisseleva T. Contribution of bone marrow-derived fibrocytes to liver fibrosis. *Hepatobiliary Surg Nutr.* 2015;4(1):34-47.
188. Strieter RM, Keeley EC, Hughes MA, Burdick MD, and Mehrad B. The role of circulating mesenchymal progenitor cells (fibrocytes) in the pathogenesis of pulmonary fibrosis. *J Leukoc Biol.* 2009;86(5):1111-8.
189. Kleaveland KR, Moore BB, and Kim KK. Paracrine functions of fibrocytes to promote lung fibrosis. *Expert Rev Respir Med.* 2014;8(2):163-72.
190. Quan TE, Cowper S, Wu SP, Bockenstedt LK, and Bucala R. Circulating fibrocytes: collagen-secreting cells of the peripheral blood. *Int J Biochem Cell Biol.* 2004;36(4):598-606.
191. Chesney J, Bacher M, Bender A, and Bucala R. The peripheral blood fibrocyte is a potent antigen-presenting cell capable of priming naive T cells in situ. *Proc Natl Acad Sci U S A.* 1997;94(12):6307-12.
192. Chesney J, Metz C, Stavitsky AB, Bacher M, and Bucala R. Regulated production of type I collagen and inflammatory cytokines by peripheral blood fibrocytes. *J Immunol.* 1998;160(1):419-25.
193. Gomperts BN, and Strieter RM. Fibrocytes in lung disease. *J Leukoc Biol.* 2007;82(3):449-56.
194. Bellini A, and Mattoli S. The role of the fibrocyte, a bone marrow-derived mesenchymal progenitor, in reactive and reparative fibroses. *Lab Invest.* 2007;87(9):858-70.
195. Hong KM, Belperio JA, Keane MP, Burdick MD, and Strieter RM. Differentiation of human circulating fibrocytes as mediated by transforming growth factor-beta and peroxisome proliferator-activated receptor gamma. *J Biol Chem.* 2007;282(31):22910-20.
196. Kisseleva T, and Brenner DA. Fibrogenesis of parenchymal organs. *Proc Am Thorac Soc.* 2008;5(3):338-42.
197. Moeller A, Gilpin SE, Ask K, Cox G, Cook D, Gauldie J, Margetts PJ, Farkas L, Dobranowski J, Boylan C, et al. Circulating fibrocytes are an indicator of poor prognosis in idiopathic pulmonary fibrosis. *Am J Respir Crit Care Med.* 2009;179(7):588-94.
198. Naik PK, Bozyk PD, Bentley JK, Popova AP, Birch CM, Wilke CA, Fry CD, White ES, Sisson TH, Tayob N, et al. Periostin promotes fibrosis and predicts progression in patients with idiopathic pulmonary fibrosis. *Am J Physiol Lung Cell Mol Physiol.* 2012;303(12):L1046-56.
199. Garibaldi BT, D'Alessio FR, Mock JR, Files DC, Chau E, Eto Y, Drummond MB, Aggarwal NR, Sidhaye V, and King LS. Regulatory T cells reduce acute lung injury fibroproliferation by decreasing fibrocyte recruitment. *Am J Respir Cell Mol Biol.* 2013;48(1):35-43.
200. Kleaveland KR, Velikoff M, Yang J, Agarwal M, Rippe RA, Moore BB, and Kim KK. Fibrocytes are not an essential source of type I collagen during lung fibrosis. *J Immunol.* 2014;193(10):5229-39.

201. Pilling D, Vakil V, Cox N, and Gomer RH. TNF-alpha-stimulated fibroblasts secrete lumican to promote fibrocyte differentiation. *Proc Natl Acad Sci U S A.* 2015;112(38):11929-34.
202. Shiota M, Heike T, Haruyama M, Baba S, Tsuchiya A, Fujino H, Kobayashi H, Kato T, Umeda K, Yoshimoto M, et al. Isolation and characterization of bone marrow-derived mesenchymal progenitor cells with myogenic and neuronal properties. *Exp Cell Res.* 2007;313(5):1008-23.
203. Meran S, and Steadman R. Fibroblasts and myofibroblasts in renal fibrosis. *Int J Exp Pathol.* 2011;92(3):158-67.
204. Liu J, Wang Y, Pan Q, Su Y, Zhang Z, Han J, Zhu X, Tang C, and Hu D. Wnt/beta-catenin pathway forms a negative feedback loop during TGF-beta1 induced human normal skin fibroblast-to-myofibroblast transition. *J Dermatol Sci.* 2012;65(1):38-49.
205. Hu B, Gharaee-Kermani M, Wu Z, and Phan SH. Epigenetic regulation of myofibroblast differentiation by DNA methylation. *Am J Pathol.* 2010;177(1):21-8.
206. George SJ. Regulation of myofibroblast differentiation by convergence of the Wnt and TGF-beta1/Smad signaling pathways. *J Mol Cell Cardiol.* 2009;46(5):610-1.
207. Dees C, Tomcik M, Zerr P, Akhmetshina A, Horn A, Palumbo K, Beyer C, Zwerina J, Distler O, Schett G, et al. Notch signalling regulates fibroblast activation and collagen release in systemic sclerosis. *Ann Rheum Dis.* 2011;70(7):1304-10.
208. Liu T, Hu B, Choi YY, Chung M, Ullenbruch M, Yu H, Lowe JB, and Phan SH. Notch1 signaling in FIZZ1 induction of myofibroblast differentiation. *Am J Pathol.* 2009;174(5):1745-55.
209. Horn A, Palumbo K, Cordazzo C, Dees C, Akhmetshina A, Tomcik M, Zerr P, Avouac J, Gusinde J, Zwerina J, et al. Hedgehog signaling controls fibroblast activation and tissue fibrosis in systemic sclerosis. *Arthritis Rheum.* 2012;64(8):2724-33.
210. Mitchell J, Woodcock-Mitchell J, Reynolds S, Low R, Leslie K, Adler K, Gabbiani G, and Skalli O. Alpha-smooth muscle actin in parenchymal cells of bleomycin-injured rat lung. *Lab Invest.* 1989;60(5):643-50.
211. Kuhn C, and McDonald JA. The roles of the myofibroblast in idiopathic pulmonary fibrosis. Ultrastructural and immunohistochemical features of sites of active extracellular matrix synthesis. *Am J Pathol.* 1991;138(5):1257-65.
212. Pache JC, Christakos PG, Gannon DE, Mitchell JJ, Low RB, and Leslie KO. Myofibroblasts in diffuse alveolar damage of the lung. *Mod Pathol.* 1998;11(11):1064-70.
213. Phan SH. The myofibroblast in pulmonary fibrosis. *Chest.* 2002;122(6 Suppl):286S-9S.
214. Epperly MW, Guo H, Gretton JE, and Greenberger JS. Bone marrow origin of myofibroblasts in irradiation pulmonary fibrosis. *Am J Respir Cell Mol Biol.* 2003;29(2):213-24.
215. Willis BC, duBois RM, and Borok Z. Epithelial origin of myofibroblasts during fibrosis in the lung. *Proc Am Thorac Soc.* 2006;3(4):377-82.

216. Kasai H, Allen JT, Mason RM, Kamimura T, and Zhang Z. TGF-beta1 induces human alveolar epithelial to mesenchymal cell transition (EMT). *Respir Res.* 2005;6(56.
217. Kalluri R, and Weinberg RA. The basics of epithelial-mesenchymal transition. *J Clin Invest.* 2009;119(6):1420-8.
218. Desmouliere A, Geinoz A, Gabbiani F, and Gabbiani G. Transforming growth factor-beta 1 induces alpha-smooth muscle actin expression in granulation tissue myofibroblasts and in quiescent and growing cultured fibroblasts. *J Cell Biol.* 1993;122(1):103-11.
219. McAnulty RJ. Fibroblasts and myofibroblasts: their source, function and role in disease. *Int J Biochem Cell Biol.* 2007;39(4):666-71.
220. Micallef L, Vedrenne N, Billet F, Coulomb B, Darby IA, and Desmouliere A. The myofibroblast, multiple origins for major roles in normal and pathological tissue repair. *Fibrogenesis Tissue Repair.* 2012;5(Suppl 1):S5.
221. Horowitz JC, and Thannickal VJ. Idiopathic pulmonary fibrosis : new concepts in pathogenesis and implications for drug therapy. *Treat Respir Med.* 2006;5(5):325-42.
222. King TE, Jr., Schwarz MI, Brown K, Tooze JA, Colby TV, Waldron JA, Jr., Flint A, Thurlbeck W, and Cherniack RM. Idiopathic pulmonary fibrosis: relationship between histopathologic features and mortality. *Am J Respir Crit Care Med.* 2001;164(6):1025-32.
223. Makinde T, Murphy RF, and Agrawal DK. The regulatory role of TGF-beta in airway remodeling in asthma. *Immunol Cell Biol.* 2007;85(5):348-56.
224. Hardie WD, Glasser SW, and Hagood JS. Emerging concepts in the pathogenesis of lung fibrosis. *Am J Pathol.* 2009;175(1):3-16.
225. Fallowfield JA. Therapeutic targets in liver fibrosis. *American journal of physiology Gastrointestinal and liver physiology.* 2011;300(5):G709-15.
226. Horowitz JC, Rogers DS, Sharma V, Vittal R, White ES, Cui Z, and Thannickal VJ. Combinatorial activation of FAK and AKT by transforming growth factor-beta1 confers an anoikis-resistant phenotype to myofibroblasts. *Cell Signal.* 2007;19(4):761-71.
227. Huang SK, White ES, Wettlaufer SH, Grifka H, Hogaboam CM, Thannickal VJ, Horowitz JC, and Peters-Golden M. Prostaglandin E(2) induces fibroblast apoptosis by modulating multiple survival pathways. *FASEB J.* 2009;23(12):4317-26.
228. Kulasekaran P, Scavone CA, Rogers DS, Arenberg DA, Thannickal VJ, and Horowitz JC. Endothelin-1 and transforming growth factor-beta1 independently induce fibroblast resistance to apoptosis via AKT activation. *Am J Respir Cell Mol Biol.* 2009;41(4):484-93.
229. Maher TM, Evans IC, Bottoms SE, Mercer PF, Thorley AJ, Nicholson AG, Laurent GJ, Tetley TD, Chambers RC, and McAnulty RJ. Diminished prostaglandin E2 contributes to the apoptosis paradox in idiopathic pulmonary fibrosis. *Am J Respir Crit Care Med.* 2010;182(1):73-82.
230. Kolodsick JE, Peters-Golden M, Larios J, Toews GB, Thannickal VJ, and Moore BB. Prostaglandin E2 inhibits fibroblast to myofibroblast transition via E.

prostanoid receptor 2 signaling and cyclic adenosine monophosphate elevation. *Am J Respir Cell Mol Biol.* 2003;29(5):537-44.
231. Huang SK, Scruggs AM, Donaghy J, McEachin RC, Fisher AS, Richardson BC, and Peters-Golden M. Prostaglandin E(2) increases fibroblast gene-specific and global DNA methylation via increased DNA methyltransferase expression. *FASEB J.* 2012;26(9):3703-14.
232. Bornstein P. Diversity of function is inherent in matricellular proteins: an appraisal of thrombospondin 1. *J Cell Biol.* 1995;130(3):503-6.
233. Bornstein P. Matricellular proteins: an overview. *J Cell Commun Signal.* 2009;3(3-4):163-5.
234. Raugi GJ, Mumby SM, Abbott-Brown D, and Bornstein P. Thrombospondin: synthesis and secretion by cells in culture. *J Cell Biol.* 1982;95(1):351-4.
235. Murphy-Ullrich JE, Schultz-Cherry S, and Hook M. Transforming growth factor-beta complexes with thrombospondin. *Mol Biol Cell.* 1992;3(2):181-8.
236. Schultz-Cherry S, and Murphy-Ullrich JE. Thrombospondin causes activation of latent transforming growth factor-beta secreted by endothelial cells by a novel mechanism. *J Cell Biol.* 1993;122(4):923-32.
237. Crawford SE, Stellmach V, Murphy-Ullrich JE, Ribeiro SM, Lawler J, Hynes RO, Boivin GP, and Bouck N. Thrombospondin-1 is a major activator of TGF-beta1 in vivo. *Cell.* 1998;93(7):1159-70.
238. Tan K, and Lawler J. The interaction of Thrombospondins with extracellular matrix proteins. *J Cell Commun Signal.* 2009;3(3-4):177-87.
239. Tucker RP, and Chiquet-Ehrismann R. The regulation of tenascin expression by tissue microenvironments. *Biochim Biophys Acta.* 2009;1793(5):888-92.
240. Xia Y, Lee K, Li N, Corbett D, Mendoza L, and Frangogiannis NG. Characterization of the inflammatory and fibrotic response in a mouse model of cardiac pressure overload. *Histochem Cell Biol.* 2009;131(4):471-81.
241. Frangogiannis NG, Shimoni S, Chang SM, Ren G, Dewald O, Gersch C, Shan K, Aggeli C, Reardon M, Letsou GV, et al. Active interstitial remodeling: an important process in the hibernating human myocardium. *J Am Coll Cardiol.* 2002;39(9):1468-74.
242. Paivaniemi OE, Maasilta PK, Alho HS, Vainikka TL, and Salminen US. Epithelial tenascin predicts obliterative airway disease. *J Heart Lung Transplant.* 2008;27(4):400-7.
243. Carey WA, Taylor GD, Dean WB, and Bristow JD. Tenascin-C deficiency attenuates TGF-ss-mediated fibrosis following murine lung injury. *Am J Physiol Lung Cell Mol Physiol.* 2010;299(6):L785-93.
244. Chlenski A, and Cohn SL. Modulation of matrix remodeling by SPARC in neoplastic progression. *Semin Cell Dev Biol.* 2010;21(1):55-65.
245. Strandjord TP, Madtes DK, Weiss DJ, and Sage EH. Collagen accumulation is decreased in SPARC-null mice with bleomycin-induced pulmonary fibrosis. *Am J Physiol.* 1999;277(3 Pt 1):L628-35.
246. Sangaletti S, Tripodo C, Cappetti B, Casalini P, Chiodoni C, Piconese S, Santangelo A, Parenza M, Arioli I, Miotti S, et al. SPARC oppositely regulates inflammation and fibrosis in bleomycin-induced lung damage. *Am J Pathol.* 2011;179(6):3000-10.

247. Chang W, Wei K, Jacobs SS, Upadhyay D, Weill D, and Rosen GD. SPARC suppresses apoptosis of idiopathic pulmonary fibrosis fibroblasts through constitutive activation of beta-catenin. *J Biol Chem.* 2010;285(11):8196-206.
248. Lo Bello S. [Dental transplants or biological implants]. *Dent Press.* 1975;11(2):11-5.
249. Yokosaki Y, Tanaka K, Higashikawa F, Yamashita K, and Eboshida A. Distinct structural requirements for binding of the integrins alphavbeta6, alphavbeta3, alphavbeta5, alpha5beta1 and alpha9beta1 to osteopontin. *Matrix Biol.* 2005;24(6):418-27.
250. Wang KX, and Denhardt DT. Osteopontin: role in immune regulation and stress responses. *Cytokine Growth Factor Rev.* 2008;19(5-6):333-45.
251. Vetrone SA, Montecino-Rodriguez E, Kudryashova E, Kramerova I, Hoffman EP, Liu SD, Miceli MC, and Spencer MJ. Osteopontin promotes fibrosis in dystrophic mouse muscle by modulating immune cell subsets and intramuscular TGF-beta. *J Clin Invest.* 2009;119(6):1583-94.
252. Takeshita S, Kikuno R, Tezuka K, and Amann E. Osteoblast-specific factor 2: cloning of a putative bone adhesion protein with homology with the insect protein fasciclin I. *The Biochemical journal.* 1993;294 (Pt 1)(271-8.
253. Horiuchi K, Amizuka N, Takeshita S, Takamatsu H, Katsuura M, Ozawa H, Toyama Y, Bonewald LF, and Kudo A. Identification and characterization of a novel protein, periostin, with restricted expression to periosteum and periodontal ligament and increased expression by transforming growth factor beta. *J Bone Miner Res.* 1999;14(7):1239-49.
254. Wen W, Chau E, Jackson-Boeters L, Elliott C, Daley TD, and Hamilton DW. TGF-ss1 and FAK regulate periostin expression in PDL fibroblasts. *J Dent Res.* 2010;89(12):1439-43.
255. Sidhu SS, Yuan S, Innes AL, Kerr S, Woodruff PG, Hou L, Muller SJ, and Fahy JV. Roles of epithelial cell-derived periostin in TGF-beta activation, collagen production, and collagen gel elasticity in asthma. *Proc Natl Acad Sci U S A.* 2010;107(32):14170-5.
256. Izuhara K, Conway SJ, Moore BB, Matsumoto H, Holweg CT, Matthews JG, and Arron JR. Roles of Periostin in Respiratory Disorders. *Am J Respir Crit Care Med.* 2016.
257. Uchida M, Shiraishi H, Ohta S, Arima K, Taniguchi K, Suzuki S, Okamoto M, Ahlfeld SK, Ohshima K, Kato S, et al. Periostin, a matricellular protein, plays a role in the induction of chemokines in pulmonary fibrosis. *Am J Respir Cell Mol Biol.* 2012;46(5):677-86.
258. Okamoto M, Hoshino T, Kitasato Y, Sakazaki Y, Kawayama T, Fujimoto K, Ohshima K, Shiraishi H, Uchida M, Ono J, et al. Periostin, a matrix protein, is a novel biomarker for idiopathic interstitial pneumonias. *Eur Respir J.* 2011;37(5):1119-27.
259. Maruhashi T, Kii I, Saito M, and Kudo A. Interaction between periostin and BMP-1 promotes proteolytic activation of lysyl oxidase. *J Biol Chem.* 2010;285(17):13294-303.
260. Chen CC, and Lau LF. Functions and mechanisms of action of CCN matricellular proteins. *Int J Biochem Cell Biol.* 2009;41(4):771-83.

261. Leask A, and Abraham DJ. All in the CCN family: essential matricellular signaling modulators emerge from the bunker. *J Cell Sci.* 2006;119(Pt 23):4803-10.
262. Bradham DM, Igarashi A, Potter RL, and Grotendorst GR. Connective tissue growth factor: a cysteine-rich mitogen secreted by human vascular endothelial cells is related to the SRC-induced immediate early gene product CEF-10. *J Cell Biol.* 1991;114(6):1285-94.
263. Pennica D, Swanson TA, Welsh JW, Roy MA, Lawrence DA, Lee J, Brush J, Taneyhill LA, Deuel B, Lew M, et al. WISP genes are members of the connective tissue growth factor family that are up-regulated in wnt-1-transformed cells and aberrantly expressed in human colon tumors. *Proc Natl Acad Sci U S A.* 1998;95(25):14717-22.
264. Jun JI, and Lau LF. Taking aim at the extracellular matrix: CCN proteins as emerging therapeutic targets. *Nat Rev Drug Discov.* 2011;10(12):945-63.
265. Weston BS, Wahab NA, and Mason RM. CTGF mediates TGF-beta-induced fibronectin matrix deposition by upregulating active alpha5beta1 integrin in human mesangial cells. *J Am Soc Nephrol.* 2003;14(3):601-10.
266. Segarini PR, Nesbitt JE, Li D, Hays LG, Yates JR, 3rd, and Carmichael DF. The low density lipoprotein receptor-related protein/alpha2-macroglobulin receptor is a receptor for connective tissue growth factor. *J Biol Chem.* 2001;276(44):40659-67.
267. Wahab NA, Weston BS, and Mason RM. Connective tissue growth factor CCN2 interacts with and activates the tyrosine kinase receptor TrkA. *J Am Soc Nephrol.* 2005;16(2):340-51.
268. Riser BL, Denichilo M, Cortes P, Baker C, Grondin JM, Yee J, and Narins RG. Regulation of connective tissue growth factor activity in cultured rat mesangial cells and its expression in experimental diabetic glomerulosclerosis. *J Am Soc Nephrol.* 2000;11(1):25-38.
269. Liu FY, Xiao L, Peng YM, Duan SB, Liu H, Liu YH, Ling GH, Yuan F, Chen JX, Fu X, et al. Inhibition effect of small interfering RNA of connective tissue growth factor on the expression of vascular endothelial growth factor and connective tissue growth factor in cultured human peritoneal mesothelial cells. *Chinese medical journal.* 2007;120(3):231-6.
270. Riser BL, Najmabadi F, Perbal B, Rambow JA, Riser ML, Sukowski E, Yeger H, Riser SC, and Peterson DR. CCN3/CCN2 regulation and the fibrosis of diabetic renal disease. *J Cell Commun Signal.* 2010;4(1):39-50.
271. Gore-Hyer E, Shegogue D, Markiewicz M, Lo S, Hazen-Martin D, Greene EL, Grotendorst G, and Trojanowska M. TGF-beta and CTGF have overlapping and distinct fibrogenic effects on human renal cells. *Am J Physiol Renal Physiol.* 2002;283(4):F707-16.
272. Grotendorst GR, Rahmanie H, and Duncan MR. Combinatorial signaling pathways determine fibroblast proliferation and myofibroblast differentiation. *FASEB J.* 2004;18(3):469-79.
273. Lee CH, Shah B, Moioli EK, and Mao JJ. CTGF directs fibroblast differentiation from human mesenchymal stem/stromal cells and defines connective tissue healing in a rodent injury model. *J Clin Invest.* 2010;120(9):3340-9.

274. Yang J, Velikoff M, Canalis E, Horowitz JC, and Kim KK. Activated alveolar epithelial cells initiate fibrosis through autocrine and paracrine secretion of connective tissue growth factor. *Am J Physiol Lung Cell Mol Physiol.* 2014;306(8):L786-96.
275. Lipson KE, Wong C, Teng Y, and Spong S. CTGF is a central mediator of tissue remodeling and fibrosis and its inhibition can reverse the process of fibrosis. *Fibrogenesis Tissue Repair.* 2012;5(Suppl 1):S24.
276. Riser BL, Najmabadi F, Perbal B, Peterson DR, Rambow JA, Riser ML, Sukowski E, Yeger H, and Riser SC. CCN3 (NOV) is a negative regulator of CCN2 (CTGF) and a novel endogenous inhibitor of the fibrotic pathway in an in vitro model of renal disease. *Am J Pathol.* 2009;174(5):1725-34.
277. Riser BL, Najmabadi F, Garchow K, Barnes JL, Peterson DR, and Sukowski EJ. Treatment with the matricellular protein CCN3 blocks and/or reverses fibrosis development in obesity with diabetic nephropathy. *Am J Pathol.* 2014;184(11):2908-21.
278. Colston JT, de la Rosa SD, Koehler M, Gonzales K, Mestril R, Freeman GL, Bailey SR, and Chandrasekar B. Wnt-induced secreted protein-1 is a prohypertrophic and profibrotic growth factor. *Am J Physiol Heart Circ Physiol.* 2007;293(3):H1839-46.
279. Li X, Chen Y, Ye W, Tao X, Zhu J, Wu S, and Lou L. Blockade of CCN4 attenuates CCl4-induced liver fibrosis. *Arch Med Sci.* 2015;11(3):647-53.
280. Konigshoff M, Kramer M, Balsara N, Wilhelm J, Amarie OV, Jahn A, Rose F, Fink L, Seeger W, Schaefer L, et al. WNT1-inducible signaling protein-1 mediates pulmonary fibrosis in mice and is upregulated in humans with idiopathic pulmonary fibrosis. *J Clin Invest.* 2009;119(4):772-87.
281. Yoon PO, Lee MA, Cha H, Jeong MH, Kim J, Jang SP, Choi BY, Jeong D, Yang DK, Hajjar RJ, et al. The opposing effects of CCN2 and CCN5 on the development of cardiac hypertrophy and fibrosis. *J Mol Cell Cardiol.* 2010;49(2):294-303.
282. Zhang L, Li Y, Liang C, and Yang W. CCN5 overexpression inhibits profibrotic phenotypes via the PI3K/Akt signaling pathway in lung fibroblasts isolated from patients with idiopathic pulmonary fibrosis and in an in vivo model of lung fibrosis. *International journal of molecular medicine.* 2014;33(2):478-86.
283. Batmunkh R, Nishioka Y, Aono Y, Azuma M, Kinoshita K, Kishi J, Makino H, Kishi M, Takezaki A, and Sone S. CCN6 as a profibrotic mediator that stimulates the proliferation of lung fibroblasts via the integrin beta1/focal adhesion kinase pathway. *J Med Invest.* 2011;58(3-4):188-96.
284. Cepek KL, Shaw SK, Parker CM, Russell GJ, Morrow JS, Rimm DL, and Brenner MB. Adhesion between epithelial cells and T lymphocytes mediated by E-cadherin and the alpha E beta 7 integrin. *Nature.* 1994;372(6502):190-3.
285. Munger JS, Huang X, Kawakatsu H, Griffiths MJ, Dalton SL, Wu J, Pittet JF, Kaminski N, Garat C, Matthay MA, et al. The integrin alpha v beta 6 binds and activates latent TGF beta 1: a mechanism for regulating pulmonary inflammation and fibrosis. *Cell.* 1999;96(3):319-28.
286. Brooks PC, Stromblad S, Sanders LC, von Schalscha TL, Aimes RT, Stetler-Stevenson WG, Quigley JP, and Cheresh DA. Localization of matrix

metalloproteinase MMP-2 to the surface of invasive cells by interaction with integrin alpha v beta 3. *Cell.* 1996;85(5):683-93.
287. Hynes RO. Integrins: bidirectional, allosteric signaling machines. *Cell.* 2002;110(6):673-87.
288. Sheppard D. The role of integrins in pulmonary fibrosis. *European Respiratory Review.* 2008;17(109):157-62.
289. Ruoslahti E, and Pierschbacher MD. New perspectives in cell adhesion: RGD and integrins. *Science.* 1987;238(4826):491-7.
290. Busk M, Pytela R, and Sheppard D. Characterization of the integrin alpha v beta 6 as a fibronectin-binding protein. *J Biol Chem.* 1992;267(9):5790-6.
291. Prieto AL, Edelman GM, and Crossin KL. Multiple integrins mediate cell attachment to cytotactin/tenascin. *Proc Natl Acad Sci U S A.* 1993;90(21):10154-8.
292. Huang XZ, Wu JF, Cass D, Erle DJ, Corry D, Young SG, Farese RV, Jr., and Sheppard D. Inactivation of the integrin beta 6 subunit gene reveals a role of epithelial integrins in regulating inflammation in the lung and skin. *J Cell Biol.* 1996;133(4):921-8.
293. Horan GS, Wood S, Ona V, Li DJ, Lukashev ME, Weinreb PH, Simon KJ, Hahm K, Allaire NE, Rinaldi NJ, et al. Partial inhibition of integrin alpha(v)beta6 prevents pulmonary fibrosis without exacerbating inflammation. *Am J Respir Crit Care Med.* 2008;177(1):56-65.
294. Mu D, Cambier S, Fjellbirkeland L, Baron JL, Munger JS, Kawakatsu H, Sheppard D, Broaddus VC, and Nishimura SL. The integrin alpha(v)beta8 mediates epithelial homeostasis through MT1-MMP-dependent activation of TGF-beta1. *J Cell Biol.* 2002;157(3):493-507.
295. Kitamura H, Cambier S, Somanath S, Barker T, Minagawa S, Markovics J, Goodsell A, Publicover J, Reichardt L, Jablons D, et al. Mouse and human lung fibroblasts regulate dendritic cell trafficking, airway inflammation, and fibrosis through integrin alphavbeta8-mediated activation of TGF-beta. *J Clin Invest.* 2011;121(7):2863-75.
296. Asano Y, Ihn H, Yamane K, Jinnin M, Mimura Y, and Tamaki K. Increased expression of integrin alpha(v)beta3 contributes to the establishment of autocrine TGF-beta signaling in scleroderma fibroblasts. *J Immunol.* 2005;175(11):7708-18.
297. Asano Y, Ihn H, Yamane K, Jinnin M, and Tamaki K. Increased expression of integrin alphavbeta5 induces the myofibroblastic differentiation of dermal fibroblasts. *Am J Pathol.* 2006;168(2):499-510.
298. Wipff PJ, Rifkin DB, Meister JJ, and Hinz B. Myofibroblast contraction activates latent TGF-beta1 from the extracellular matrix. *J Cell Biol.* 2007;179(6):1311-23.
299. Chattopadhyay N, Wang Z, Ashman LK, Brady-Kalnay SM, and Kreidberg JA. alpha3beta1 integrin-CD151, a component of the cadherin-catenin complex, regulates PTPmu expression and cell-cell adhesion. *J Cell Biol.* 2003;163(6):1351-62.
300. Kim KK, Wei Y, Szekeres C, Kugler MC, Wolters PJ, Hill ML, Frank JA, Brumwell AN, Wheeler SE, Kreidberg JA, et al. Epithelial cell alpha3beta1 integrin links beta-catenin and Smad signaling to promote myofibroblast formation and pulmonary fibrosis. *J Clin Invest.* 2009;119(1):213-24.

301. Reed NI, Jo H, Chen C, Tsujino K, Arnold TD, DeGrado WF, and Sheppard D. The alphavbeta1 integrin plays a critical in vivo role in tissue fibrosis. *Sci Transl Med.* 2015;7(288):288ra79.
302. Puthawala K, Hadjiangelis N, Jacoby SC, Bayongan E, Zhao Z, Yang Z, Devitt ML, Horan GS, Weinreb PH, Lukashev ME, et al. Inhibition of integrin alpha(v)beta6, an activator of latent transforming growth factor-beta, prevents radiation-induced lung fibrosis. *Am J Respir Crit Care Med.* 2008;177(1):82-90.
303. Hahm K, Lukashev ME, Luo Y, Yang WJ, Dolinski BM, Weinreb PH, Simon KJ, Chun Wang L, Leone DR, Lobb RR, et al. Alphav beta6 integrin regulates renal fibrosis and inflammation in Alport mouse. *Am J Pathol.* 2007;170(1):110-25.
304. Ma LJ, Yang H, Gaspert A, Carlesso G, Barty MM, Davidson JM, Sheppard D, and Fogo AB. Transforming growth factor-beta-dependent and -independent pathways of induction of tubulointerstitial fibrosis in beta6(-/-) mice. *Am J Pathol.* 2003;163(4):1261-73.
305. Humphries JD, Byron A, and Humphries MJ. Integrin ligands at a glance. *J Cell Sci.* 2006;119(Pt 19):3901-3.
306. Desmouliere A, Redard M, Darby I, and Gabbiani G. Apoptosis mediates the decrease in cellularity during the transition between granulation tissue and scar. *Am J Pathol.* 1995;146(1):56-66.
307. Thannickal VJ, and Horowitz JC. Evolving concepts of apoptosis in idiopathic pulmonary fibrosis. *Proc Am Thorac Soc.* 2006;3(4):350-6.
308. Ajayi IO, Sisson TH, Higgins PD, Booth AJ, Sagana RL, Huang SK, White ES, King JE, Moore BB, and Horowitz JC. X-linked inhibitor of apoptosis regulates lung fibroblast resistance to Fas-mediated apoptosis. *Am J Respir Cell Mol Biol.* 2013;49(1):86-95.
309. Selman M, Rojas M, Mora AL, and Pardo A. Aging and interstitial lung diseases: unraveling an old forgotten player in the pathogenesis of lung fibrosis. *Semin Respir Crit Care Med.* 2010;31(5):607-17.
310. Hagimoto N, Kuwano K, Nomoto Y, Kunitake R, and Hara N. Apoptosis and expression of Fas/Fas ligand mRNA in bleomycin-induced pulmonary fibrosis in mice. *Am J Respir Cell Mol Biol.* 1997;16(1):91-101.
311. Lee CG, Cho SJ, Kang MJ, Chapoval SP, Lee PJ, Noble PW, Yehualaeshet T, Lu B, Flavell RA, Milbrandt J, et al. Early growth response gene 1-mediated apoptosis is essential for transforming growth factor beta1-induced pulmonary fibrosis. *The Journal of experimental medicine.* 2004;200(3):377-89.
312. Lee HC, and Wei YH. Oxidative stress, mitochondrial DNA mutation, and apoptosis in aging. *Exp Biol Med (Maywood).* 2007;232(5):592-606.
313. Beere HM. "The stress of dying": the role of heat shock proteins in the regulation of apoptosis. *J Cell Sci.* 2004;117(Pt 13):2641-51.
314. Tanaka K, Tanaka Y, Namba T, Azuma A, and Mizushima T. Heat shock protein 70 protects against bleomycin-induced pulmonary fibrosis in mice. *Biochem Pharmacol.* 2010;80(6):920-31.
315. Biomarkers Definitions Working G. Biomarkers and surrogate endpoints: preferred definitions and conceptual framework. *Clinical pharmacology and therapeutics.* 2001;69(3):89-95.

316. Fleming TR, and Powers JH. Biomarkers and surrogate endpoints in clinical trials. *Stat Med.* 2012;31(25):2973-84.
317. Bossuyt PM, Reitsma JB, Bruns DE, Gatsonis CA, Glasziou PP, Irwig LM, Lijmer JG, Moher D, Rennie D, de Vet HC, et al. Towards complete and accurate reporting of studies of diagnostic accuracy: The STARD Initiative. *Ann Intern Med.* 2003;138(1):40-4.
318. McShane LM, Altman DG, Sauerbrei W, Taube SE, Gion M, Clark GM, and Statistics Subcommittee of the NCIEWGoCD. Reporting recommendations for tumor marker prognostic studies. *J Clin Oncol.* 2005;23(36):9067-72.
319. Selman M, King TE, Pardo A, American Thoracic S, European Respiratory S, and American College of Chest P. Idiopathic pulmonary fibrosis: prevailing and evolving hypotheses about its pathogenesis and implications for therapy. *Ann Intern Med.* 2001;134(2):136-51.
320. Boon K, Bailey NW, Yang J, Steel MP, Groshong S, Kervitsky D, Brown KK, Schwarz MI, and Schwartz DA. Molecular phenotypes distinguish patients with relatively stable from progressive idiopathic pulmonary fibrosis (IPF). *PloS one.* 2009;4(4):e5134.
321. Ishii H, Mukae H, Kadota J, Kaida H, Nagata T, Abe K, Matsukura S, and Kohno S. High serum concentrations of surfactant protein A in usual interstitial pneumonia compared with non-specific interstitial pneumonia. *Thorax.* 2003;58(1):52-7.
322. Ohnishi H, Yokoyama A, Kondo K, Hamada H, Abe M, Nishimura K, Hiwada K, and Kohno N. Comparative study of KL-6, surfactant protein-A, surfactant protein-D, and monocyte chemoattractant protein-1 as serum markers for interstitial lung diseases. *Am J Respir Crit Care Med.* 2002;165(3):378-81.
323. Stuart BD, Lee JS, Kozlitina J, Noth I, Devine MS, Glazer CS, Torres F, Kaza V, Girod CE, Jones KD, et al. Effect of telomere length on survival in patients with idiopathic pulmonary fibrosis: an observational cohort study with independent validation. *The Lancet Respiratory medicine.* 2014;2(7):557-65.
324. O'Dwyer DN, Armstrong ME, Trujillo G, Cooke G, Keane MP, Fallon PG, Simpson AJ, Millar AB, McGrath EE, Whyte MK, et al. The Toll-like receptor 3 L412F polymorphism and disease progression in idiopathic pulmonary fibrosis. *Am J Respir Crit Care Med.* 2013;188(12):1442-50.
325. Hodgson U, Pulkkinen V, Dixon M, Peyrard-Janvid M, Rehn M, Lahermo P, Ollikainen V, Salmenkivi K, Kinnula V, Kere J, et al. ELMOD2 is a candidate gene for familial idiopathic pulmonary fibrosis. *Am J Hum Genet.* 2006;79(1):149-54.
326. Pulkkinen V, Bruce S, Rintahaka J, Hodgson U, Laitinen T, Alenius H, Kinnula VL, Myllarniemi M, Matikainen S, and Kere J. ELMOD2, a candidate gene for idiopathic pulmonary fibrosis, regulates antiviral responses. *FASEB J.* 2010;24(4):1167-77.
327. Noth I, Zhang Y, Ma SF, Flores C, Barber M, Huang Y, Broderick SM, Wade MS, Hysi P, Scuirba J, et al. Genetic variants associated with idiopathic pulmonary fibrosis susceptibility and mortality: a genome-wide association study. *The Lancet Respiratory medicine.* 2013;1(4):309-17.

328. Mukae H, Iiboshi H, Nakazato M, Hiratsuka T, Tokojima M, Abe K, Ashitani J, Kadota J, Matsukura S, and Kohno S. Raised plasma concentrations of alpha-defensins in patients with idiopathic pulmonary fibrosis. *Thorax.* 2002;57(7):623-8.
329. Furuhashi K, Suda T, Nakamura Y, Inui N, Hashimoto D, Miwa S, Hayakawa H, Kusagaya H, Nakano Y, Nakamura H, et al. Increased expression of YKL-40, a chitinase-like protein, in serum and lung of patients with idiopathic pulmonary fibrosis. *Respiratory medicine.* 2010;104(8):1204-10.
330. Korthagen NM, van Moorsel CH, Barlo NP, Ruven HJ, Kruit A, Heron M, van den Bosch JM, and Grutters JC. Serum and BALF YKL-40 levels are predictors of survival in idiopathic pulmonary fibrosis. *Respiratory medicine.* 2011;105(1):106-13.
331. Kahloon RA, Xue J, Bhargava A, Csizmadia E, Otterbein L, Kass DJ, Bon J, Soejima M, Levesque MC, Lindell KO, et al. Patients with idiopathic pulmonary fibrosis with antibodies to heat shock protein 70 have poor prognoses. *Am J Respir Crit Care Med.* 2013;187(7):768-75.
332. Vuga LJ, Tedrow JR, Pandit KV, Tan J, Kass DJ, Xue J, Chandra D, Leader JK, Gibson KF, Kaminski N, et al. C-X-C motif chemokine 13 (CXCL13) is a prognostic biomarker of idiopathic pulmonary fibrosis. *Am J Respir Crit Care Med.* 2014;189(8):966-74.
333. Herazo-Maya JD, Noth I, Duncan SR, Kim S, Ma SF, Tseng GC, Feingold E, Juan-Guardela BM, Richards TJ, Lussier Y, et al. Peripheral blood mononuclear cell gene expression profiles predict poor outcome in idiopathic pulmonary fibrosis. *Sci Transl Med.* 2013;5(205):205ra136.
334. Jenkins RG, Simpson JK, Saini G, Bentley JH, Russell AM, Braybrooke R, Molyneaux PL, McKeever TM, Wells AU, Flynn A, et al. Longitudinal change in collagen degradation biomarkers in idiopathic pulmonary fibrosis: an analysis from the prospective, multicentre PROFILE study. *The Lancet Respiratory medicine.* 2015;3(6):462-72.
335. Saini G, Porte J, Weinreb PH, Violette SM, Wallace WA, McKeever TM, and Jenkins G. alphavbeta6 integrin may be a potential prognostic biomarker in interstitial lung disease. *Eur Respir J.* 2015;46(2):486-94.
336. Gold L, Ayers D, Bertino J, Bock C, Bock A, Brody EN, Carter J, Dalby AB, Eaton BE, Fitzwater T, et al. Aptamer-based multiplexed proteomic technology for biomarker discovery. *PloS one.* 2010;5(12):e15004.
337. Rohloff JC, Gelinas AD, Jarvis TC, Ochsner UA, Schneider DJ, Gold L, and Janjic N. Nucleic Acid Ligands With Protein-like Side Chains: Modified Aptamers and Their Use as Diagnostic and Therapeutic Agents. *Molecular therapy Nucleic acids.* 2014;3(e201.
338. Harlin H, Reffey SB, Duckett CS, Lindsten T, and Thompson CB. Characterization of XIAP-deficient mice. *Mol Cell Biol.* 2001;21(10):3604-8.
339. Coomes SM, Wilke CA, Moore TA, and Moore BB. Induction of TGF-beta 1, not regulatory T cells, impairs antiviral immunity in the lung following bone marrow transplant. *J Immunol.* 2010;184(9):5130-40.
340. Mancuso P, Standiford TJ, Marshall T, and Peters-Golden M. 5-Lipoxygenase reaction products modulate alveolar macrophage phagocytosis of Klebsiella pneumoniae. *Infect Immun.* 1998;66(11):5140-6.

341. Ojielo CI, Cooke K, Mancuso P, Standiford TJ, Olkiewicz KM, Clouthier S, Corrion L, Ballinger MN, Toews GB, Paine R, 3rd, et al. Defective phagocytosis and clearance of Pseudomonas aeruginosa in the lung following bone marrow transplantation. *J Immunol.* 2003;171(8):4416-24.
342. Ballinger MN, Aronoff DM, McMillan TR, Cooke KR, Olkiewicz K, Toews GB, Peters-Golden M, and Moore BB. Critical role of prostaglandin E2 overproduction in impaired pulmonary host response following bone marrow transplantation. *J Immunol.* 2006;177(8):5499-508.
343. Hubbard LL, Ballinger MN, Thomas PE, Wilke CA, Standiford TJ, Kobayashi KS, Flavell RA, and Moore BB. A role for IL-1 receptor-associated kinase-M in prostaglandin E2-induced immunosuppression post-bone marrow transplantation. *J Immunol.* 2010;184(11):6299-308.
344. Serezani CH, Aronoff DM, Jancar S, Mancuso P, and Peters-Golden M. Leukotrienes enhance the bactericidal activity of alveolar macrophages against Klebsiella pneumoniae through the activation of NADPH oxidase. *Blood.* 2005;106(3):1067-75.
345. Cai Q, Sun H, Peng Y, Lu J, Nikolovska-Coleska Z, McEachern D, Liu L, Qiu S, Yang CY, Miller R, et al. A potent and orally active antagonist (SM-406/AT-406) of multiple inhibitor of apoptosis proteins (IAPs) in clinical development for cancer treatment. *J Med Chem.* 2011;54(8):2714-26.
346. Vannella KM, Luckhardt TR, Wilke CA, van Dyk LF, Toews GB, and Moore BB. Latent herpesvirus infection augments experimental pulmonary fibrosis. *Am J Respir Crit Care Med.* 2010;181(5):465-77.
347. Sisson TH, Ajayi IO, Subbotina N, Dodi AE, Rodansky ES, Chibucos LN, Kim KK, Keshamouni VG, White ES, Zhou Y, et al. Inhibition of myocardin-related transcription factor/serum response factor signaling decreases lung fibrosis and promotes mesenchymal cell apoptosis. *Am J Pathol.* 2015;185(4):969-86.
348. Wilson MS, and Wynn TA. Pulmonary fibrosis: pathogenesis, etiology and regulation. *Mucosal Immunol.* 2009;2(2):103-21.
349. Adkins JM, and Collard HR. Idiopathic pulmonary fibrosis. *Semin Respir Crit Care Med.* 2012;33(5):433-9.
350. Harari S, and Caminati A. IPF: new insight on pathogenesis and treatment. *Allergy.* 2010;65(5):537-53.
351. Naik PK, and Moore BB. Viral infection and aging as cofactors for the development of pulmonary fibrosis. *Expert Rev Respir Med.* 2010;4(6):759-71.
352. Lasithiotaki I, Antoniou KM, Vlahava VM, Karagiannis K, Spandidos DA, Siafakas NM, and Sourvinos G. Detection of herpes simplex virus type-1 in patients with fibrotic lung diseases. *PLoS One.* 2011;6(12):e27800. doi: 10.1371/journal.pone.0027800. Epub 2011 Dec 20.
353. Wangoo A, Shaw RJ, Diss TC, Farrell PJ, du Bois RM, and Nicholson AG. Cryptogenic fibrosing alveolitis: lack of association with Epstein-Barr virus infection. *Thorax.* 1997;52(10):888-91.
354. Zamo A, Poletti V, Reghellin D, Montagna L, Pedron S, Piccoli P, and Chilosi M. HHV-8 and EBV are not commonly found in idiopathic pulmonary fibrosis. *Sarcoidosis Vasc Diffuse Lung Dis.* 2005;22(2):123-8.

355. Efstathiou S, Ho YM, Hall S, Styles CJ, Scott SD, and Gompels UA. Murine herpesvirus 68 is genetically related to the gammaherpesviruses Epstein-Barr virus and herpesvirus saimiri. *J Gen Virol.* 1990;71 (Pt 6)(1365-72.
356. Gangadharan B, Hoeve MA, Allen JE, Ebrahimi B, Rhind SM, Dutia BM, and Nash AA. Murine gammaherpesvirus-induced fibrosis is associated with the development of alternatively activated macrophages. *J Leukoc Biol.* 2008;84(1):50-8.
357. Mora AL, Torres-Gonzalez E, Rojas M, Xu J, Ritzenthaler J, Speck SH, Roman J, Brigham K, and Stecenko A. Control of virus reactivation arrests pulmonary herpesvirus-induced fibrosis in IFN-gamma receptor-deficient mice. *Am J Respir Crit Care Med.* 2007;175(11):1139-50.
358. Van Delden C, and Iglewski BH. Cell-to-cell signaling and Pseudomonas aeruginosa infections. *Emerg Infect Dis.* 1998;4(4):551-60.
359. Lovewell RR, Patankar YR, and Berwin BL. Mechanisms of Phagocytosis and Host Clearance of Pseudomonas aeruginosa. *Am J Physiol Lung Cell Mol Physiol.* 2014.
360. Kumagai Y, Takeuchi O, Kato H, Kumar H, Matsui K, Morii E, Aozasa K, Kawai T, and Akira S. Alveolar macrophages are the primary interferon-alpha producer in pulmonary infection with RNA viruses. *Immunity.* 2007;27(2):240-52.
361. GeurtsvanKessel CH, Willart MA, van Rijt LS, Muskens F, Kool M, Baas C, Thielemans K, Bennett C, Clausen BE, Hoogsteden HC, et al. Clearance of influenza virus from the lung depends on migratory langerin+CD11b- but not plasmacytoid dendritic cells. *J Exp Med.* 2008;205(7):1621-34.
362. Sanders CJ, Doherty PC, and Thomas PG. Respiratory epithelial cells in innate immunity to influenza virus infection. *Cell Tissue Res.* 2011;343(1):13-21.
363. McGill J, Heusel JW, and Legge KL. Innate immune control and regulation of influenza virus infections. *J Leukoc Biol.* 2009;86(4):803-12.
364. Banchereau J, and Steinman RM. Dendritic cells and the control of immunity. *Nature.* 1998;392(6673):245-52.
365. Stewart JP, Usherwood EJ, Ross A, Dyson H, and Nash T. Lung epithelial cells are a major site of murine gammaherpesvirus persistence. *J Exp Med.* 1998;187(12):1941-51.
366. Weslow-Schmidt JL, Jewell NA, Mertz SE, Simas JP, Durbin JE, and Flano E. Type I interferon inhibition and dendritic cell activation during gammaherpesvirus respiratory infection. *J Virol.* 2007;81(18):9778-89.
367. Tsai CY, Hu Z, Zhang W, and Usherwood EJ. Strain-dependent requirement for IFN-gamma for respiratory control and immunotherapy in murine gammaherpesvirus infection. *Viral Immunol.* 2011;24(4):273-80.
368. Sparks-Thissen RL, Braaten DC, Hildner K, Murphy TL, Murphy KM, and Virgin HWt. CD4 T cell control of acute and latent murine gammaherpesvirus infection requires IFNgamma. *Virology.* 2005;338(2):201-8.
369. van Dyk LF, Virgin HWt, and Speck SH. The murine gammaherpesvirus 68 v-cyclin is a critical regulator of reactivation from latency. *J Virol.* 2000;74(16):7451-61.
370. Gilani SR, Vuga LJ, Lindell KO, Gibson KF, Xue J, Kaminski N, Valentine VG, Lindsay EK, George MP, Steele C, et al. CD28 down-regulation on circulating

CD4 T-cells is associated with poor prognoses of patients with idiopathic pulmonary fibrosis. *PLoS One.* 2010;5(1):e8959. doi: 10.1371/journal.pone.0008959.
371. Herazo-Maya JD, Noth I, Duncan SR, Kim S, Ma SF, Tseng GC, Feingold E, Juan-Guardela BM, Richards TJ, Lussier Y, et al. Peripheral Blood Mononuclear Cell Gene Expression Profiles Predict Poor Outcome in Idiopathic Pulmonary Fibrosis. *Sci Transl Med.* 2013;5(205):205ra136.
372. Schmiedl A, Kerber-Momot T, Munder A, Pabst R, and Tschernig T. Bacterial distribution in lung parenchyma early after pulmonary infection with Pseudomonas aeruginosa. *Cell Tissue Res.* 2010;342(1):67-73. doi: 10.1007/s00441-010-1036-y. Epub 2010 Sep 14.
373. Rangappa P, and Moran JL. Outcomes of patients admitted to the intensive care unit with idiopathic pulmonary fibrosis. *Crit Care Resusc.* 2009;11(2):102-9.
374. Han MK, Zhou Y, Murray S, Tayob N, Noth I, Lama VN, Moore BB, White ES, Flaherty KR, Huffnagle GB, et al. Lung microbiome and disease progression in idiopathic pulmonary fibrosis: an analysis of the COMET study. *The Lancet Respiratory medicine.* 2014;2(7):548-56.
375. Vannella KM, McMillan TR, Charbeneau RP, Wilke CA, Thomas PE, Toews GB, Peters-Golden M, and Moore BB. Cysteinyl leukotrienes are autocrine and paracrine regulators of fibrocyte function. *J Immunol.* 2007;179(11):7883-90.
376. Baud L, Perez J, Denis M, and Ardaillou R. Modulation of fibroblast proliferation by sulfidopeptide leukotrienes: effect of indomethacin. *J Immunol.* 1987;138(4):1190-5.
377. Phan SH, McGarry BM, Loeffler KM, and Kunkel SL. Binding of leukotriene C4 to rat lung fibroblasts and stimulation of collagen synthesis in vitro. *Biochemistry.* 1988;27(8):2846-53.
378. Wang X, Tan J, Zoueva O, Zhao J, Ye Z, and Hewlett I. Novel pandemic influenza A (H1N1) virus infection modulates apoptotic pathways that impact its replication in A549 cells. *Microbes Infect.* 2013.
379. Liu JH, Wei S, Burnette PK, Gamero AM, Hutton M, and Djeu JY. Functional association of TGF-beta receptor II with cyclin B. *Oncogene.* 1999;18(1):269-75.
380. Barbara NP, Wrana JL, and Letarte M. Endoglin is an accessory protein that interacts with the signaling receptor complex of multiple members of the transforming growth factor-beta superfamily. *J Biol Chem.* 1999;274(2):584-94.
381. Henis YI, Moustakas A, Lin HY, and Lodish HF. The types II and III transforming growth factor-beta receptors form homo-oligomers. *J Cell Biol.* 1994;126(1):139-54.
382. Weinheimer VK, Becher A, Tonnies M, Holland G, Knepper J, Bauer TT, Schneider P, Neudecker J, Ruckert JC, Szymanski K, et al. Influenza A viruses target type II pneumocytes in the human lung. *J Infect Dis.* 2012;206(11):1685-94. doi: 10.093/infdis/jis455. Epub 2012 Jul 24.
383. Fujino N, Kubo H, Ota C, Suzuki T, Takahashi T, Yamada M, Suzuki S, Kondo T, Nagatomi R, Tando Y, et al. Increased severity of 2009 pandemic influenza A virus subtype H1N1 infection in alveolar type II cells from patients with pulmonary fibrosis. *J Infect Dis.* 2013;207(4):692-3. doi: 10.1093/infdis/jis739. Epub 2012 Nov 29.

384. Umeda Y, Morikawa M, Anzai M, Sumida Y, Kadowaki M, Ameshima S, and Ishizaki T. Acute exacerbation of idiopathic pulmonary fibrosis after pandemic influenza A (H1N1) vaccination. *Intern Med.* 2010;49(21):2333-6. Epub 010 Nov 1.
385. Martinez FJ, Safrin S, Weycker D, Starko KM, Bradford WZ, King TE, Jr., Flaherty KR, Schwartz DA, Noble PW, Raghu G, et al. The clinical course of patients with idiopathic pulmonary fibrosis. *Ann Intern Med.* 2005;142(12 Pt 1):963-7.
386. Antoniou KM, Pataka A, Bouros D, and Siafakas NM. Pathogenetic pathways and novel pharmacotherapeutic targets in idiopathic pulmonary fibrosis. *Pulm Pharmacol Ther.* 2007;20(5):453-61.
387. Blackwell TS, Tager AM, Borok Z, Moore BB, Schwartz DA, Anstrom KJ, Bar-Joseph Z, Bitterman P, Blackburn MR, Bradford W, et al. Future directions in idiopathic pulmonary fibrosis research. An NHLBI workshop report. *American journal of respiratory and critical care medicine.* 2014;189(2):214-22.
388. Scotton CJ, and Chambers RC. Molecular targets in pulmonary fibrosis: the myofibroblast in focus. *Chest.* 2007;132(4):1311-21.
389. Kalluri R, and Neilson EG. Epithelial-mesenchymal transition and its implications for fibrosis. *J Clin Invest.* 2003;112(12):1776-84.
390. Zeisberg EM, Tarnavski O, Zeisberg M, Dorfman AL, McMullen JR, Gustafsson E, Chandraker A, Yuan X, Pu WT, Roberts AB, et al. Endothelial-to-mesenchymal transition contributes to cardiac fibrosis. *Nature medicine.* 2007;13(8):952-61.
391. Selman M, and Pardo A. Role of epithelial cells in idiopathic pulmonary fibrosis: from innocent targets to serial killers. *Proc Am Thorac Soc.* 2006;3(4):364-72.
392. Hashimoto N, Phan SH, Imaizumi K, Matsuo M, Nakashima H, Kawabe T, Shimokata K, and Hasegawa Y. Endothelial-mesenchymal transition in bleomycin-induced pulmonary fibrosis. *Am J Respir Cell Mol Biol.* 2010;43(2):161-72.
393. Humphreys BD, Lin SL, Kobayashi A, Hudson TE, Nowlin BT, Bonventre JV, Valerius MT, McMahon AP, and Duffield JS. Fate tracing reveals the pericyte and not epithelial origin of myofibroblasts in kidney fibrosis. *Am J Pathol.* 2010;176(1):85-97.
394. LeBleu VS, Taduri G, O'Connell J, Teng Y, Cooke VG, Woda C, Sugimoto H, and Kalluri R. Origin and function of myofibroblasts in kidney fibrosis. *Nature medicine.* 2013;19(8):1047-53.
395. Osterholzer JJ, Olszewski MA, Murdock BJ, Chen GH, Erb-Downward JR, Subbotina N, Browning K, Lin Y, Morey RE, Dayrit JK, et al. Implicating exudate macrophages and Ly-6C(high) monocytes in CCR2-dependent lung fibrosis following gene-targeted alveolar injury. *J Immunol.* 2013;190(7):3447-57.
396. Moore BB, and Kolb M. Fibrocytes and progression of fibrotic lung disease. Ready for showtime? *Am J Respir Crit Care Med.* 2014;190(12):1338-9.
397. Madsen DH, Ingvarsen S, Jurgensen HJ, Melander MC, Kjoller L, Moyer A, Honore C, Madsen CA, Garred P, Burgdorf S, et al. The non-phagocytic route of collagen uptake: a distinct degradation pathway. *J Biol Chem.* 2011;286(30):26996-7010.

398. Bianchetti L, Barczyk M, Cardoso J, Schmidt M, Bellini A, and Mattoli S. Extracellular matrix remodelling properties of human fibrocytes. *J Cell Mol Med.* 2012;16(3):483-95.
399. Xu J, and Kisseleva T. Bone marrow-derived fibrocytes contribute to liver fibrosis. *Exp Biol Med (Maywood).* 2015;240(6):691-700.
400. Garcia de Alba C, Buendia-Roldan I, Salgado A, Becerril C, Ramirez R, Gonzalez Y, Checa M, Navarro C, Ruiz V, Pardo A, et al. Fibrocytes contribute to inflammation and fibrosis in chronic hypersensitivity pneumonitis through paracrine effects. *Am J Respir Crit Care Med.* 2015;191(4):427-36.
401. Madala SK, Edukulla R, Schmidt S, Davidson C, Ikegami M, and Hardie WD. Bone marrow-derived stromal cells are invasive and hyperproliferative and alter transforming growth factor-alpha-induced pulmonary fibrosis. *Am J Respir Cell Mol Biol.* 2014;50(4):777-86.
402. Naik PK, Bozyk PD, Bentley JK, Popova AP, Birch CM, Wilke CA, Fry CD, White ES, Sisson TH, Tayob N, et al. Periostin promotes fibrosis and predicts progression in patients with idiopathic pulmonary fibrosis. *American journal of physiology Lung cellular and molecular physiology.* 2012;303(12):L1046-56.
403. Kudo A. Periostin in fibrillogenesis for tissue regeneration: periostin actions inside and outside the cell. *Cell Mol Life Sci.* 2011;68(19):3201-7.
404. Ruan K, Bao S, and Ouyang G. The multifaceted role of periostin in tumorigenesis. *Cell Mol Life Sci.* 2009;66(14):2219-30.
405. Bonner JC. Mesenchymal cell survival in airway and interstitial pulmonary fibrosis. *Fibrogenesis Tissue Repair.* 2010;3(15.
406. Hinz B, Phan SH, Thannickal VJ, Galli A, Bochaton-Piallat ML, and Gabbiani G. The myofibroblast: one function, multiple origins. *Am J Pathol.* 2007;170(6):1807-16.
407. Schmidt M, Sun G, Stacey MA, Mori L, and Mattoli S. Identification of circulating fibrocytes as precursors of bronchial myofibroblasts in asthma. *J Immunol.* 2003;171(1):380-9.
408. Ashley SL, Sisson TH, Wheaton AK, Kim KK, Wilke CA, Ajayi IO, Subbotina N, Wang S, Duckett CS, Moore BB, et al. Targeting Inhibitor of Apoptosis Proteins Protects from Bleomycin-induced Lung Fibrosis. *Am J Respir Cell Mol Biol.* 2015.
409. Leask A. Potential therapeutic targets for cardiac fibrosis: TGFbeta, angiotensin, endothelin, CCN2, and PDGF, partners in fibroblast activation. *Circulation research.* 2010;106(11):1675-80.
410. Lepparanta O, Pulkkinen V, Koli K, Vahatalo R, Salmenkivi K, Kinnula VL, Heikinheimo M, and Myllarniemi M. Transcription factor GATA-6 is expressed in quiescent myofibroblasts in idiopathic pulmonary fibrosis. *Am J Respir Cell Mol Biol.* 2010;42(5):626-32.
411. Korfei M, Ruppert C, Mahavadi P, Henneke I, Markart P, Koch M, Lang G, Fink L, Bohle RM, Seeger W, et al. Epithelial endoplasmic reticulum stress and apoptosis in sporadic idiopathic pulmonary fibrosis. *Am J Respir Crit Care Med.* 2008;178(8):838-46.
412. Sisson TH, Maher TM, Ajayi IO, King JE, Higgins PD, Booth AJ, Sagana RL, Huang SK, White ES, Moore BB, et al. Increased survivin expression contributes

to apoptosis-resistance in IPF fibroblasts. *Adv Biosci Biotechnol.* 2012;3(6A):657-64.
413. Thannickal VJ, Henke CA, Horowitz JC, Noble PW, Roman J, Sime PJ, Zhou Y, Wells RG, White ES, and Tschumperlin DJ. Matrix biology of idiopathic pulmonary fibrosis: a workshop report of the national heart, lung, and blood institute. *Am J Pathol.* 2014;184(6):1643-51.
414. Kaufmann T, Strasser A, and Jost PJ. Fas death receptor signalling: roles of Bid and XIAP. *Cell death and differentiation.* 2012;19(1):42-50.
415. Salvesen GS, and Duckett CS. IAP proteins: blocking the road to death's door. *Nat Rev Mol Cell Biol.* 2002;3(6):401-10.
416. Eckelman BP, Salvesen GS, and Scott FL. Human inhibitor of apoptosis proteins: why XIAP is the black sheep of the family. *EMBO Rep.* 2006;7(10):988-94.
417. Leulier F, Lhocine N, Lemaitre B, and Meier P. The Drosophila inhibitor of apoptosis protein DIAP2 functions in innate immunity and is essential to resist gram-negative bacterial infection. *Mol Cell Biol.* 2006;26(21):7821-31.
418. Gyrd-Hansen M, and Meier P. IAPs: from caspase inhibitors to modulators of NF-kappaB, inflammation and cancer. *Nat Rev Cancer.* 2010;10(8):561-74.
419. Jin HS, Lee DH, Kim DH, Chung JH, Lee SJ, and Lee TH. cIAP1, cIAP2, and XIAP act cooperatively via nonredundant pathways to regulate genotoxic stress-induced nuclear factor-kappaB activation. *Cancer Res.* 2009;69(5):1782-91.
420. Silke J, Ekert PG, Day CL, Hawkins CJ, Baca M, Chew J, Pakusch M, Verhagen AM, and Vaux DL. Direct inhibition of caspase 3 is dispensable for the anti-apoptotic activity of XIAP. *EMBO J.* 2001;20(12):3114-23.
421. Huang Y, Park YC, Rich RL, Segal D, Myszka DG, and Wu H. Structural basis of caspase inhibition by XIAP: differential roles of the linker versus the BIR domain. *Cell.* 2001;104(5):781-90.
422. Suzuki Y, Nakabayashi Y, and Takahashi R. Ubiquitin-protein ligase activity of X-linked inhibitor of apoptosis protein promotes proteasomal degradation of caspase-3 and enhances its anti-apoptotic effect in Fas-induced cell death. *Proc Natl Acad Sci U S A.* 2001;98(15):8662-7.
423. Chai J, Shiozaki E, Srinivasula SM, Wu Q, Datta P, Alnemri ES, and Shi Y. Structural basis of caspase-7 inhibition by XIAP. *Cell.* 2001;104(5):769-80.
424. Riedl SJ, Renatus M, Schwarzenbacher R, Zhou Q, Sun C, Fesik SW, Liddington RC, and Salvesen GS. Structural basis for the inhibition of caspase-3 by XIAP. *Cell.* 2001;104(5):791-800.
425. Eckelman BP, and Salvesen GS. The human anti-apoptotic proteins cIAP1 and cIAP2 bind but do not inhibit caspases. *J Biol Chem.* 2006;281(6):3254-60.
426. Sessler T, Healy S, Samali A, and Szegezdi E. Structural determinants of DISC function: new insights into death receptor-mediated apoptosis signalling. *Pharmacology & therapeutics.* 2013;140(2):186-99.
427. Bertrand MJ, Milutinovic S, Dickson KM, Ho WC, Boudreault A, Durkin J, Gillard JW, Jaquith JB, Morris SJ, and Barker PA. cIAP1 and cIAP2 facilitate cancer cell survival by functioning as E3 ligases that promote RIP1 ubiquitination. *Molecular cell.* 2008;30(6):689-700.
428. Shiozaki EN, and Shi Y. Caspases, IAPs and Smac/DIABLO: mechanisms from structural biology. *Trends in biochemical sciences.* 2004;29(9):486-94.

429. Birkey Reffey S, Wurthner JU, Parks WT, Roberts AB, and Duckett CS. X-linked inhibitor of apoptosis protein functions as a cofactor in transforming growth factor-beta signaling. *J Biol Chem.* 2001;276(28):26542-9.
430. Tanaka T, Yoshimi M, Maeyama T, Hagimoto N, Kuwano K, and Hara N. Resistance to Fas-mediated apoptosis in human lung fibroblast. *Eur Respir J.* 2002;20(2):359-68.
431. King TE, Jr., Albera C, Bradford WZ, Costabel U, Hormel P, Lancaster L, Noble PW, Sahn SA, Szwarcberg J, Thomeer M, et al. Effect of interferon gamma-1b on survival in patients with idiopathic pulmonary fibrosis (INSPIRE): a multicentre, randomised, placebo-controlled trial. *Lancet.* 2009;374(9685):222-8.
432. Raghu G. Idiopathic pulmonary fibrosis: guidelines for diagnosis and clinical management have advanced from consensus-based in 2000 to evidence-based in 2011. *Eur Respir J.* 2011;37(4):743-6.
433. Huang WT, Akhter H, Jiang C, MacEwen M, Ding Q, Antony V, Thannickal VJ, and Liu RM. Plasminogen activator inhibitor 1, fibroblast apoptosis resistance, and aging-related susceptibility to lung fibrosis. *Exp Gerontol.* 2014;61C(62-75.
434. Zhou Y, Huang X, Hecker L, Kurundkar D, Kurundkar A, Liu H, Jin TH, Desai L, Bernard K, and Thannickal VJ. Inhibition of mechanosensitive signaling in myofibroblasts ameliorates experimental pulmonary fibrosis. *J Clin Invest.* 2013;123(3):1096-108.
435. Vaux DL. Inhibitor of Apoptosis (IAP) proteins as drug targets for the treatment of cancer. *F1000 Biol Rep.* 2009;1(79.
436. Saleem M, Qadir MI, Perveen N, Ahmad B, Saleem U, and Irshad T. Inhibitors of apoptotic proteins: new targets for anticancer therapy. *Chem Biol Drug Des.* 2013;82(3):243-51.
437. Flygare JA, and Fairbrother WJ. Small-molecule pan-IAP antagonists: a patent review. *Expert Opin Ther Pat.* 2010;20(2):251-67.
438. Wright CW, and Duckett CS. Reawakening the cellular death program in neoplasia through the therapeutic blockade of IAP function. *J Clin Invest.* 2005;115(10):2673-8.
439. Wang S. Design of small-molecule Smac mimetics as IAP antagonists. *Curr Top Microbiol Immunol.* 2011;348(89-113.
440. Suzuki Y, Nakabayashi Y, Nakata K, Reed JC, and Takahashi R. X-linked inhibitor of apoptosis protein (XIAP) inhibits caspase-3 and -7 in distinct modes. *J Biol Chem.* 2001;276(29):27058-63.
441. Takahashi R, Deveraux Q, Tamm I, Welsh K, Assa-Munt N, Salvesen GS, and Reed JC. A single BIR domain of XIAP sufficient for inhibiting caspases. *J Biol Chem.* 1998;273(14):7787-90.
442. Kenneth NS, and Duckett CS. IAP proteins: regulators of cell migration and development. *Current opinion in cell biology.* 2012;24(6):871-5.
443. Mahoney DJ, Cheung HH, Mrad RL, Plenchette S, Simard C, Enwere E, Arora V, Mak TW, Lacasse EC, Waring J, et al. Both cIAP1 and cIAP2 regulate TNFalpha-mediated NF-kappaB activation. *Proc Natl Acad Sci U S A.* 2008;105(33):11778-83.
444. Varfolomeev E, Blankenship JW, Wayson SM, Fedorova AV, Kayagaki N, Garg P, Zobel K, Dynek JN, Elliott LO, Wallweber HJ, et al. IAP antagonists induce

autoubiquitination of c-IAPs, NF-kappaB activation, and TNFalpha-dependent apoptosis. *Cell.* 2007;131(4):669-81.
445. Gaither A, Porter D, Yao Y, Borawski J, Yang G, Donovan J, Sage D, Slisz J, Tran M, Straub C, et al. A Smac mimetic rescue screen reveals roles for inhibitor of apoptosis proteins in tumor necrosis factor-alpha signaling. *Cancer Res.* 2007;67(24):11493-8.
446. Petersen SL, Wang L, Yalcin-Chin A, Li L, Peyton M, Minna J, Harran P, and Wang X. Autocrine TNFalpha signaling renders human cancer cells susceptible to Smac-mimetic-induced apoptosis. *Cancer Cell.* 2007;12(5):445-56.
447. Spagnolo P, Sverzellati N, Rossi G, Cavazza A, Tzouvelekis A, Crestani B, and Vancheri C. Idiopathic pulmonary fibrosis: an update. *Annals of medicine.* 2015;47(1):15-27.
448. Kim HJ, Perlman D, and Tomic R. Natural history of idiopathic pulmonary fibrosis. *Respiratory medicine.* 2015.
449. Zhang Y, and Kaminski N. Biomarkers in idiopathic pulmonary fibrosis. *Current opinion in pulmonary medicine.* 2012;18(5):441-6.
450. Fingerlin TE, Murphy E, Zhang W, Peljto AL, Brown KK, Steele MP, Loyd JE, Cosgrove GP, Lynch D, Groshong S, et al. Genome-wide association study identifies multiple susceptibility loci for pulmonary fibrosis. *Nature genetics.* 2013;45(6):613-20.
451. Raghu G, Anstrom KJ, King TE, Jr., Lasky JA, and Martinez FJ. Prednisone, azathioprine, and N-acetylcysteine for pulmonary fibrosis. *N Engl J Med.* 2012;366(21):1968-77.
452. Sumi M, Satoh H, Kagohashi K, Ishikawa H, and Sekizawa K. Increased serum levels of endostatin in patients with idiopathic pulmonary fibrosis. *Journal of clinical laboratory analysis.* 2005;19(4):146-9.
453. Antoniou KM, Soufla G, Lymbouridou R, Economidou F, Lasithiotaki I, Manousakis M, Drositis I, Spandidos DA, and Siafakas NM. Expression analysis of angiogenic growth factors and biological axis CXCL12/CXCR4 axis in idiopathic pulmonary fibrosis. *Connective tissue research.* 2010;51(1):71-80.
454. Margaritopoulos GA, Antoniou KM, Karagiannis K, Vassalou E, Lasithiotaki I, Lambiri I, and Siafakas NM. Investigation of angiogenetic axis Angiopoietin-1 and -2/Tie-2 in fibrotic lung diseases: a bronchoalveolar lavage study. *International journal of molecular medicine.* 2010;26(6):919-23.
455. Smadja DM, Nunes H, Juvin K, Bertil S, Valeyre D, Gaussem P, and Israel-Biet D. Increase in both angiogenic and angiostatic mediators in patients with idiopathic pulmonary fibrosis. *Pathologie-biologie.* 2014;62(6):391-4.
456. Dancer RC, Wood AM, and Thickett DR. Metalloproteinases in idiopathic pulmonary fibrosis. *Eur Respir J.* 2011;38(6):1461-7.
457. Weiss CH, Budinger GR, Mutlu GM, and Jain M. Proteasomal regulation of pulmonary fibrosis. *Proc Am Thorac Soc.* 2010;7(1):77-83.
458. King TE, Jr., Bradford WZ, Castro-Bernardini S, Fagan EA, Glaspole I, Glassberg MK, Gorina E, Hopkins PM, Kardatzke D, Lancaster L, et al. A phase 3 trial of pirfenidone in patients with idiopathic pulmonary fibrosis. *N Engl J Med.* 2014;370(22):2083-92.

459. Richeldi L, du Bois RM, Raghu G, Azuma A, Brown KK, Costabel U, Cottin V, Flaherty KR, Hansell DM, Inoue Y, et al. Efficacy and safety of nintedanib in idiopathic pulmonary fibrosis. *N Engl J Med.* 2014;370(22):2071-82.
460. Moore BB, Fry C, Zhou Y, Murray S, Han MK, Martinez FJ, and Flaherty KR. Inflammatory leukocyte phenotypes correlate with disease progression in idiopathic pulmonary fibrosis. *Frontiers of medicine.* 2014;1(56).
461. Ziegler-Heitbrock L, and Hofer TP. Toward a refined definition of monocyte subsets. *Frontiers in immunology.* 2013;4(23.
462. Tesciuba AG, Subudhi S, Rother RP, Faas SJ, Frantz AM, Elliot D, Weinstock J, Matis LA, Bluestone JA, and Sperling AI. Inducible costimulator regulates Th2-mediated inflammation, but not Th2 differentiation, in a model of allergic airway disease. *J Immunol.* 2001;167(4):1996-2003.
463. Gonzalo JA, Tian J, Delaney T, Corcoran J, Rottman JB, Lora J, Al-garawi A, Kroczek R, Gutierrez-Ramos JC, and Coyle AJ. ICOS is critical for T helper cell-mediated lung mucosal inflammatory responses. *Nat Immunol.* 2001;2(7):597-604.
464. Tanaka C, Fujimoto M, Hamaguchi Y, Sato S, Takehara K, and Hasegawa M. Inducible costimulator ligand regulates bleomycin-induced lung and skin fibrosis in a mouse model independently of the inducible costimulator/inducible costimulator ligand pathway. *Arthritis Rheum.* 2010;62(6):1723-32.
465. Marczynska J, Ozga A, Wlodarczyk A, Majchrzak-Gorecka M, Kulig P, Banas M, Michalczyk-Wetula D, Majewski P, Hutloff A, Schwarz J, et al. The role of metalloproteinase ADAM17 in regulating ICOS ligand-mediated humoral immune responses. *J Immunol.* 2014;193(6):2753-63.
466. Kilpatrick DC, and Chalmers JD. Human L-ficolin (ficolin-2) and its clinical significance. *J Biomed Biotechnol.* 2012;2012(138797.
467. Lynch NJ, Roscher S, Hartung T, Morath S, Matsushita M, Maennel DN, Kuraya M, Fujita T, and Schwaeble WJ. L-ficolin specifically binds to lipoteichoic acid, a cell wall constituent of Gram-positive bacteria, and activates the lectin pathway of complement. *J Immunol.* 2004;172(2):1198-202.
468. Osthoff M, Ngian GS, Dean MM, Nikpour M, Stevens W, Proudman S, Eisen DP, and Sahhar J. Potential role of the lectin pathway of complement in the pathogenesis and disease manifestations of systemic sclerosis: a case-control and cohort study. *Arthritis research & therapy.* 2014;16(6):480.
469. Kilpatrick DC, Chalmers JD, MacDonald SL, Murray M, Mohammed A, Hart SP, Matsushita M, and Hill A. Stable bronchiectasis is associated with low serum L-ficolin concentrations. *Clin Respir J.* 2009;3(1):29-33.
470. Metzger ML, Michelfelder I, Goldacker S, Melkaoui K, Litzman J, Guzman D, Grimbacher B, and Salzer U. Low ficolin-2 levels in common variable immunodeficiency patients with bronchiectasis. *Clin Exp Immunol.* 2015;179(2):256-64.
471. Krarup A, Sorensen UB, Matsushita M, Jensenius JC, and Thiel S. Effect of capsulation of opportunistic pathogenic bacteria on binding of the pattern recognition molecules mannan-binding lectin, L-ficolin, and H-ficolin. *Infect Immun.* 2005;73(2):1052-60.

472. Endo Y, Takahashi M, Iwaki D, Ishida Y, Nakazawa N, Kodama T, Matsuzaka T, Kanno K, Liu Y, Tsuchiya K, et al. Mice deficient in ficolin, a lectin complement pathway recognition molecule, are susceptible to Streptococcus pneumoniae infection. *J Immunol.* 2012;189(12):5860-6.
473. Ali YM, Lynch NJ, Haleem KS, Fujita T, Endo Y, Hansen S, Holmskov U, Takahashi K, Stahl GL, Dudler T, et al. The lectin pathway of complement activation is a critical component of the innate immune response to pneumococcal infection. *PLoS Pathog.* 2012;8(7):e1002793.
474. Knippenberg S, Ueberberg B, Maus R, Bohling J, Ding N, Tort Tarres M, Hoymann HG, Jonigk D, Izykowski N, Paton JC, et al. Streptococcus pneumoniae triggers progression of pulmonary fibrosis through pneumolysin. *Thorax.* 2015;70(7):636-46.
475. Kos J, Sekirnik A, Kopitar G, Cimerman N, Kayser K, Stremmer A, Fiehn W, and Werle B. Cathepsin S in tumours, regional lymph nodes and sera of patients with lung cancer: relation to prognosis. *Br J Cancer.* 2001;85(8):1193-200.
476. Brix K, McInnes J, Al-Hashimi A, Rehders M, Tamhane T, and Haugen MH. Proteolysis mediated by cysteine cathepsins and legumain-recent advances and cell biological challenges. *Protoplasma.* 2015;252(3):755-74.
477. Gormley JA, Hegarty SM, O'Grady A, Stevenson MR, Burden RE, Barrett HL, Scott CJ, Johnston JA, Wilson RH, Kay EW, et al. The role of Cathepsin S as a marker of prognosis and predictor of chemotherapy benefit in adjuvant CRC: a pilot study. *Br J Cancer.* 2011;105(10):1487-94.
478. Levicar N, Strojnik T, Kos J, Dewey RA, Pilkington GJ, and Lah TT. Lysosomal enzymes, cathepsins in brain tumour invasion. *J Neurooncol.* 2002;58(1):21-32.
479. Ward C, Kuehn D, Burden RE, Gormley JA, Jaquin TJ, Gazdoiu M, Small D, Bicknell R, Johnston JA, Scott CJ, et al. Antibody targeting of cathepsin S inhibits angiogenesis and synergistically enhances anti-VEGF. *PloS one.* 2010;5(9).
480. AbdulHameed MD, Tawa GJ, Kumar K, Ippolito DL, Lewis JA, Stallings JD, and Wallqvist A. Systems level analysis and identification of pathways and networks associated with liver fibrosis. *PloS one.* 2014;9(11):e112193.
481. Jiang G, Cao F, Ren G, Gao D, Bhakta V, Zhang Y, Cao H, Dong Z, Zang W, Zhang S, et al. PRSS3 promotes tumour growth and metastasis of human pancreatic cancer. *Gut.* 2010;59(11):1535-44.
482. Marsit CJ, Okpukpara C, Danaee H, and Kelsey KT. Epigenetic silencing of the PRSS3 putative tumor suppressor gene in non-small cell lung cancer. *Molecular carcinogenesis.* 2005;44(2):146-50.
483. Hockla A, Miller E, Salameh MA, Copland JA, Radisky DC, and Radisky ES. PRSS3/mesotrypsin is a therapeutic target for metastatic prostate cancer. *Mol Cancer Res.* 2012;10(12):1555-66.
484. Mustonen T, and Alitalo K. Endothelial receptor tyrosine kinases involved in angiogenesis. *J Cell Biol.* 1995;129(4):895-8.
485. Toi M, Bando H, Ogawa T, Muta M, Hornig C, and Weich HA. Significance of vascular endothelial growth factor (VEGF)/soluble VEGF receptor-1 relationship in breast cancer. *Int J Cancer.* 2002;98(1):14-8.

486. Harris AL, Reusch P, Barleon B, Hang C, Dobbs N, and Marme D. Soluble Tie2 and Flt1 extracellular domains in serum of patients with renal cancer and response to antiangiogenic therapy. *Clin Cancer Res.* 2001;7(7):1992-7.
487. Lamszus K, Ulbricht U, Matschke J, Brockmann MA, Fillbrandt R, and Westphal M. Levels of soluble vascular endothelial growth factor (VEGF) receptor 1 in astrocytic tumors and its relation to malignancy, vascularity, and VEGF-A. *Clin Cancer Res.* 2003;9(4):1399-405.
488. Ebos JM, Bocci G, Man S, Thorpe PE, Hicklin DJ, Zhou D, Jia X, and Kerbel RS. A naturally occurring soluble form of vascular endothelial growth factor receptor 2 detected in mouse and human plasma. *Mol Cancer Res.* 2004;2(6):315-26.
489. Ebos JM, Lee CR, Bogdanovic E, Alami J, Van Slyke P, Francia G, Xu P, Mutsaers AJ, Dumont DJ, and Kerbel RS. Vascular endothelial growth factor-mediated decrease in plasma soluble vascular endothelial growth factor receptor-2 levels as a surrogate biomarker for tumor growth. *Cancer Res.* 2008;68(2):521-9.
490. Moore BB, and Moore TA. Viruses in Idiopathic Pulmonary Fibrosis. Etiology and Exacerbation. *Ann Am Thorac Soc.* 2015;12 Suppl 2(S186-92.
491. Le Goffic R, Pothlichet J, Vitour D, Fujita T, Meurs E, Chignard M, and Si-Tahar M. Cutting Edge: Influenza A virus activates TLR3-dependent inflammatory and RIG-I-dependent antiviral responses in human lung epithelial cells. *J Immunol.* 2007;178(6):3368-72.
492. Manukyan M, Nalbant P, Luxen S, Hahn KM, and Knaus UG. RhoA GTPase activation by TLR2 and TLR3 ligands: connecting via Src to NF-kappa B. *J Immunol.* 2009;182(6):3522-9.
493. Vial E, Sahai E, and Marshall CJ. ERK-MAPK signaling coordinately regulates activity of Rac1 and RhoA for tumor cell motility. *Cancer Cell.* 2003;4(1):67-79.
494. Pandit KV, and Milosevic J. MicroRNA regulatory networks in idiopathic pulmonary fibrosis. *Biochem Cell Biol.* 2015;93(2):129-37.
495. Yates LA, Norbury CJ, and Gilbert RJ. The long and short of microRNA. *Cell.* 2013;153(3):516-9.
496. Hwang HW, and Mendell JT. MicroRNAs in cell proliferation, cell death, and tumorigenesis. *Br J Cancer.* 2006;94(6):776-80.
497. Lau NC, Lim LP, Weinstein EG, and Bartel DP. An abundant class of tiny RNAs with probable regulatory roles in Caenorhabditis elegans. *Science.* 2001;294(5543):858-62.
498. Morita Y, Araki H, Sugimoto T, Takeuchi K, Yamane T, Maeda T, Yamamoto Y, Nishi K, Asano M, Shirahama-Noda K, et al. Legumain/asparaginyl endopeptidase controls extracellular matrix remodeling through the degradation of fibronectin in mouse renal proximal tubular cells. *FEBS letters.* 2007;581(7):1417-24.